

APPENDIX V

Regional Modeling Evaluation

List of Tables

Table V-1 - Locations of the MATES II Toxic Monitoring Network	3
Table V-2 - Toxic Compounds Measured and Modeled at the 10 MATES- II Sites	4
Table V-3 - CALMET Vertical Layers	11
Table V-4 - Boundary Concentrations used for the MATES II modeling	13
Table V-5a - Performance Statistics for Methyl Chloride ($\mu\text{g}/\text{m}^3$)	29
Table V-5b - Performance Statistics for Vinyl Chloride ($\mu\text{g}/\text{m}^3$)	30
Table V-5c - Performance Statistics for 1,3 Butadiene ($\mu\text{g}/\text{m}^3$)	31
Table V-5d - Performance Statistics for Methylene Chloride ($\mu\text{g}/\text{m}^3$)	32
Table V-5e - Performance Statistics for 1,1 Dichloroethane ($\mu\text{g}/\text{m}^3$)	33
Table V-5f - Performance Statistics for Chloroform ($\mu\text{g}/\text{m}^3$)	34
Table V-5g - Performance Statistics for Ethylene Dichloride ($\mu\text{g}/\text{m}^3$)	35
Table V-5h - Performance Statistics for Benzene ($\mu\text{g}/\text{m}^3$)	36
Table V-5i - Performance Statistics for Carbon Tetrachloride ($\mu\text{g}/\text{m}^3$)	37
Table V-5j - Performance Statistics for Trichloroethene ($\mu\text{g}/\text{m}^3$)	38
Table V-5k - Performance Statistics for Toluene ($\mu\text{g}/\text{m}^3$)	39
Table V-5l - Performance Statistics for Ethylene Dibromide ($\mu\text{g}/\text{m}^3$)	40
Table V-5m - Performance Statistics for Perchloroethylene ($\mu\text{g}/\text{m}^3$)	41
Table V-5n - Performance Statistics for Styrene ($\mu\text{g}/\text{m}^3$)	42
Table V-5o - Performance Statistics for P-Dichlorobenzene ($\mu\text{g}/\text{m}^3$)	43
Table V-5p - Performance Statistics for Formaldehyde ($\mu\text{g}/\text{m}^3$)	44
Table V-5q - Performance Statistics for Acetaldehydes ($\mu\text{g}/\text{m}^3$)	45
Table V-5r - Performance Statistics for Acetone ($\mu\text{g}/\text{m}^3$)	46
Table V-5s - Performance Statistics for Methyl Ethyl Ketone ($\mu\text{g}/\text{m}^3$)	47
Table V-5t - Performance Statistics for Organic Carbon ($\mu\text{g}/\text{m}^3$)	48
Table V-5u - Performance Statistics for Elemental Carbon ($\mu\text{g}/\text{m}^3$)	49
Table V-5v - Performance Statistics for Hexavalent Chromium ($\eta\text{g}/\text{m}^3$)	50
Table V-5w - Performance Statistics for Arsenic ($\eta\text{g}/\text{m}^3$)	51
Table V-5x - Performance Statistics for Chromium ($\eta\text{g}/\text{m}^3$)	52
Table V-5y - Performance Statistics Lead - Point Source ($\eta\text{g}/\text{m}^3$)	53
Table V-5z - Performance Statistics for Lead – Total ($\eta\text{g}/\text{m}^3$)	54
Table V-5aa - Performance Statistics for Nickel ($\eta\text{g}/\text{m}^3$)	55
Table V-5ab - Performance Statistics for Selenium ($\eta\text{g}/\text{m}^3$)	56
Table V-5ac - Performance Statistics for Cadmium ($\eta\text{g}/\text{m}^3$)	57
Table V-6 - Toxic Compounds Simulated and Measured at the 10 MATES-II Sites	145
Table V-7 - South Coast Air Basin Modeled Risk	164
Table V-8 - Comparison of the Network Averaged Modeled Risk to Measured Risk at the Ten MATES-II Sites	165
Table V-9 - Modeled Risk at the Fourteen MATES-II Microscale Monitoring Sites	165

List of Figures

Figure V-1 - UAM MATES II regional modeling domain	1
Figure V-2 - Locations of surface meteorological monitoring sites	5
Figure V-3a - January 0600 PST average surface CALMET wind field	7
Figure V-3b - January 1600 PST average surface CALMET wind field	7
Figure V-3c - July 0600 PST average surface CALMET wind field	8
Figure V-3d - July 1600 PST average surface CALMET wind field.....	8
Figure V-4 - Locations of upper air meteorological monitoring sites	9
Figure V-5a - Diurnal variation of mixing at Wilmington (April 1998 - March 1999)	14
Figure V-5b - Diurnal variation of mixing at Central LA (April 1998 - March 1999)	15
Figure V-5c - Diurnal variation of mixing at Burbank (April 1998 - March 1999).....	16
Figure V-5d - Diurnal variation of mixing at Wilmington (April 1998 - March 1999).....	17
Figure V-6a - January 1999 average 1600 PST spatial variation of mixing in the Basin	18
Figure V-6b - July 1998 average 1600 PST spatial variation of mixing in the Basin	18
Figure V-7a - Comparison between UAM-TOX predicted (solid line) and measured (points) 1-hour average ozone concentrations (pphm) at Hawthorne (April 1, 1998 – March 31, 1999)	20
Figure V-7b - Comparison between UAM-TOX predicted (solid line) and measured (points) 1-hour average ozone concentrations (pphm) at Central LA (April 1, 1998 – March 31, 1999)	21
Figure V-7c - Comparison between UAM-TOX predicted (solid line) and measured (points) 1-hour average ozone concentrations (pphm) at Azusa (April 1, 1998 – March 31, 1999)	22
Figure V-7d - Comparison between UAM-TOX predicted (solid line) and measured (points) 1-hour average ozone concentrations (pphm) at Pomona (April 1, 1998 – March 31, 1999)	23
Figure V-7e - Comparison between UAM-TOX predicted (solid line) and measured (points) 1-hour average ozone concentrations (pphm) at Upland (April 1, 1998 – March 31, 1999)	24
Figure V-7f - Comparison between UAM-TOX predicted (solid line) and measured (points) 1-hour average ozone concentrations (pphm) at San Bernardino (April 1, 1998 – March 31, 1999)	25
Figure V-7g - Comparison between UAM-TOX predicted (solid line) and measured (points) 1-hour average ozone concentrations (pphm) at Rubidoux (April 1, 1998 – March 31, 1999).	26
Figure V-7h - Comparison between UAM-TOX predicted (solid line) and measured (points) 1-hour average ozone concentrations (pphm) at Crestline (April 1, 1998 – March 31, 1999).	27
Figure V-8a - Time-series of simulated methyl chloride (solid line) verses measurements (squares and stars).	58
Figure V-8b - Time-series of simulated vinyl chloride (solid line) verses measurements (squares).	59
Figure V-8c - Time-series of simulated 1,3 butadiene (solid line) verses measurements (squares and stars).	60
Figure V-8d - Time-series of simulated methylene chloride (solid line) verses measurements (squares and stars).	61
Figure V-8e - Time-series of simulated 1,2 dichloroethane (solid line) verses measurements (squares and stars).	62
Figure V-8f - Time-series of simulated chloroform (solid line) verses measurements (squares and stars)	63
Figure V-8g - Time-series of simulated ethylene dichloride (solid line) verses measurements (squares and stars).	64

Figure V-8h - Time-series of simulated carbon tetrachloride (solid line) verses measurements (squares and stars)	65
Figure V-8i - Time-series of simulated benzene (solid line) verses measurements (squares and stars)	66
Figure V-8j - Time-series of simulated trichloroethene (solid line) verses measurements (squares and stars)	67
Figure V-8k - Time-series of simulated toluene (solid line) verses measurements (squares and stars)	68
Figure V-8l - Time-series of simulated ethylene dibromide (solid line) verses measurements (squares and stars)	69
Figure V-8m - Time-series of simulated perchloroethylene (solid line) verses measurements (squares and stars)	70
Figure V-8n - Time-series of simulated styrene (solid line) verses measurements (squares and stars)	71
Figure V-8o - Time-series of simulated p-dichlorobenzene (solid line) verses measurements (squares and stars)	72
Figure V-8p - Time-series of simulated formaldehyde (solid line) verses measurements (squares and stars)	73
Figure V-8q - Time-series of simulated acetaldehyde (solid line) verses measurements (squares and stars)	74
Figure V-8r - Time-series of simulated acetone (solid line) verses measurements (squares and stars)	75
Figure V-8s - Time-series of simulated methyl ethyl ketone (solid line) verses measurements (squares and stars)	76
Figure V-8t - Time-series of simulated organic carbon (solid line) verses measurements (squares and stars)	77
Figure V-8u - Time-series of simulated elemental carbon (solid line) verses measurements (squares and stars)	78
Figure V-8v - Time-series of simulated hexavalent chromium (solid line) verses measurements (squares and stars)	79
Figure V-8w - Time-series of simulated arsenic (solid line) verses measurements (squares and stars)	80
Figure V-8x - Time-series of simulated chromium (solid line) verses measurements (squares and stars)	81
Figure V-8y - Time-series of simulated point source lead (solid line) verses measurements (squares and stars)	82
Figure V-8z - Time-series of simulated total lead (solid line) verses measurements (squares and stars)	83
Figure V-8aa - Time-series of simulated nickel (solid line) verses measurements (squares and stars)	84
Figure V-8ab - Time-series of simulated selenium (solid line) verses measurements (squares and stars)	85
Figure V-8ac - Time-series of simulated cadmium (solid line) verses measurements (squares and stars)	86
Figure V-9a - Time-series plot of the residuals between simulated and measured concentrations of methyl chloride)	87
Figure V-9b - Time-series plot of the residuals between simulated and measured concentrations of vinyl chloride.	88
Figure V-9c - Time-series plot of the residuals between simulated and measured concentrations of 1,3 butadiene	89
Figure V-9d - Time-series plot of the residuals between simulated and measured concentrations of methylene chloride	90

Figure V-9e - Time-series plot of the residuals between simulated and measured concentrations of 1,2 dichloroethane	91
Figure V-9f - Time-series plot of the residuals between simulated and measured concentrations of chloroform.	92
Figure V-9g - Time-series plot of the residuals between simulated and measured concentrations of ethylene dichloride	93
Figure V-9h - Time-series plot of the residuals between simulated and measured concentrations of carbon tetrachloride	94
Figure V-9i - Time-series plot of the residuals between simulated and measured concentrations of Benzene	95
Figure V-9j - Time-series plot of the residuals between simulated and measured concentrations of trichloroethene	96
Figure V-9k - Time-series plot of the residuals between simulated and measured concentrations of toluene	97
Figure V-9l - Time-series plot of the residuals between simulated and measured concentrations of ethylene dibromide	98
Figure V-9m - Time-series plot of the residuals between simulated and measured concentrations of perchloroethylene	99
Figure V-9n - Time-series plot of the residuals between simulated and measured concentrations of styrene	100
Figure V-9o - Time-series plot of the residuals between simulated and measured concentrations of p-dichlorobenzene	101
Figure V-9p - Time-series plot of the residuals between simulated and measured concentrations of formaldehyde	102
Figure V-9q - Time-series plot of the residuals between simulated and measured concentrations of acetaldehyde	103
Figure V-9r - Time-series plot of the residuals between simulated and measured concentrations of acetone	104
Figure V-9s - Time-series plot of the residuals between simulated and measured concentrations of methyl ethyl ketone	105
Figure V-9t - Time-series plot of the residuals between simulated and measured concentrations of organic carbon	106
Figure V-9u - Time-series plot of the residuals between simulated and measured concentrations of elemental carbon	107
Figure V-9v - Time-series plot of the residuals between simulated and measured concentrations of hexavalent chromium	108
Figure V-9w - Time-series plot of the residuals between simulated and measured concentrations of arsenic	109
Figure V-9x - Time-series plot of the residuals between simulated and measured concentrations of chromium	110
Figure V-9y - Time-series plot of the residuals between simulated and measured concentrations of point source lead	111
Figure V-9z - Time-series plot of the residuals between simulated and measured concentrations of total lead	112
Figure V-9aa - Time-series plot of the residuals between simulated and measured concentrations of nickel	113
Figure V-9ab - Time-series plot of the residuals between simulated and measured concentrations of selenium	114
Figure V-9ac - Time-series plot of the residuals between simulated and measured concentrations of cadmium	115
Figure V-10a - Scatter and residual plots of simulated and measured concentrations of methyl chloride	116

Figure V-10b - Scatter and residual plots of simulated and measured concentrations of vinyl chloride	117
Figure V-10c - Scatter and residual plots of simulated and measured concentrations of 1,3 butadiene	118
Figure V-10d - Scatter and residual plots of simulated and measured concentrations of methylene chloride	119
Figure V-10e - Scatter and residual plots of simulated and measured concentrations of 1,2 dichloroethane	120
Figure V-10f - Scatter and residual plots of simulated and measured concentrations of chloroform	121
Figure V-10g - Scatter and residual plots of simulated and measured concentrations of ethylene dichloride	122
Figure V-10h - Scatter and residual plots of simulated and measured concentrations of carbon tetrachloride	123
Figure V-10I - Scatter and residual plots of simulated and measured concentrations of benzene	124
Figure V-10j - Scatter and residual plots of simulated and measured concentrations of trichloroethylene	125
Figure V-10k. - Scatter and residual plots of simulated and measured concentrations of toluene	126
Figure V-10l - Scatter and residual plots of simulated and measured concentrations of ethylene dibromide	127
Figure V-10m - Scatter and residual plots of simulated and measured concentrations of perchloroethylene	128
Figure V-10n - Scatter and residual plots of simulated and measured concentrations of styrene	129
Figure V-10o - Scatter and residual plots of simulated and measured concentrations of p-dichlorobenzene	130
Figure V-10p - Scatter and residual plots of simulated and measured concentrations of formaldehyde	131
Figure V-10q - Scatter and residual plots of simulated and measured concentrations of acetaldehyde	132
Figure V-10r - Scatter and residual plots of simulated and measured concentrations of acetone	133
Figure V-10s - Scatter and residual plots of simulated and measured concentrations of methyl ethyl ketone	134
Figure V-10t - Scatter and residual plots of simulated and measured concentrations of organic carbon	135
Figure V-10u - Scatter and residual plots of simulated and measured concentrations of elemental carbon	136
Figure V-10v - Scatter and residual plots of simulated and measured concentrations of hexavalent chromium	137
Figure V-10w - Scatter and residual plots of simulated and measured concentrations of arsenic	138
Figure V-10x - Scatter and residual plots of simulated and measured concentrations of chromium	139
Figure V-10y - Scatter and residual plots of simulated and measured concentrations of point source lead	140
Figure V-10z - Scatter and residual plots of simulated and measured concentrations of total lead	141
Figure V-10aa - Scatter and residual plots of simulated and measured concentrations of nickel	142

Figure V-10ab - Scatter and residual plots of simulated and measured concentrations of selenium	143
Figure V-10ac - Scatter and residual plots of simulated and measured concentrations of cadmium	144
Figure V-11a. - Annual average methyl chloride concentrations simulated for the Basin ($\mu\text{g}/\text{m}^3$)	147
Figure V-11b - Annual average vinyl chloride concentrations simulated for the Basin ($\mu\text{g}/\text{m}^3$)	147
Figure V-11c - Annual average 1,3 butadiene concentrations simulated for the Basin ($\mu\text{g}/\text{m}^3$)	148
Figure V-11d - Annual average methylene chloride concentrations simulated for the Basin ($\mu\text{g}/\text{m}^3$)	148
Figure V-11e - Annual average 1,2 dichloroethane concentrations simulated for the Basin ($\mu\text{g}/\text{m}^3$)	149
Figure V-11f - Annual average chloroform concentrations simulated for the Basin ($\mu\text{g}/\text{m}^3$)	149
Figure V-11g - Annual average ethylene dichloride concentrations simulated for the Basin ($\mu\text{g}/\text{m}^3$)	150
Figure V-11h - Annual average carbon tetrachloride concentrations simulated for the Basin ($\mu\text{g}/\text{m}^3$)	150
Figure V-11i - Annual average benzene concentrations simulated for the Basin ($\mu\text{g}/\text{m}^3$)	151
Figure V-11j - Annual average trichloroethene concentrations simulated for the Basin ($\mu\text{g}/\text{m}^3$)	151
Figure V-11k - Annual average toluene concentrations simulated for the Basin ($\mu\text{g}/\text{m}^3$)	152
Figure V-11l - Annual average ethylene dibromide concentrations simulated for the Basin ($\mu\text{g}/\text{m}^3$)	152
Figure V-11m - Annual average perchloroethylene concentrations simulated for the Basin ($\mu\text{g}/\text{m}^3$)	153
Figure V-11n - Annual average styrene concentrations simulated for the Basin ($\mu\text{g}/\text{m}^3$)	153
Figure V-11o - Annual average p-dichlorobenzene concentrations simulated for the Basin ($\mu\text{g}/\text{m}^3$)	154
Figure V-11p - Annual average formaldehyde concentrations simulated for the Basin ($\mu\text{g}/\text{m}^3$)	154
Figure V-11q - Annual average acetaldehyde concentrations simulated for the Basin ($\mu\text{g}/\text{m}^3$)	155
Figure V-11r - Annual average acetone concentrations simulated for the Basin ($\mu\text{g}/\text{m}^3$)	155
Figure V-11s - Annual average methyl ethyl ketone concentrations simulated for the Basin ($\mu\text{g}/\text{m}^3$)	156
Figure V-11t - Annual average organic carbon concentrations simulated for the Basin ($\mu\text{g}/\text{m}^3$)	156
Figure V-11u - Annual average elemental carbon concentrations simulated for the Basin ($\mu\text{g}/\text{m}^3$)	157
Figure V-11v - Annual average hexavalent chromium concentrations simulated for the Basin (ng/m^3)	157
Figure V-11w - Annual average arsenic concentrations simulated for the Basin (ng/m^3)	158
Figure V-11x - Annual average chromium concentrations simulated for the Basin (ng/m^3)	158

Figure V-11y - Annual average point source lead concentrations simulated for the Basin ($\mu\text{g}/\text{m}^3$)	159
Figure V-11z - Annual average total lead concentrations simulated for the Basin ($\mu\text{g}/\text{m}^3$)	159
Figure V-11aa - Annual average nickel concentrations simulated for the Basin ($\mu\text{g}/\text{m}^3$)	160
Figure V-11ab - Annual average selenium concentrations simulated for the Basin ($\mu\text{g}/\text{m}^3$)	160
Figure V-11ac - Annual average cadmium concentrations simulated for the Basin ($\mu\text{g}/\text{m}^3$)	161
Figure V-11ad - Annual average diesel particulate concentrations simulated for the Basin ($\mu\text{g}/\text{m}^3$)	161
Figure V-12 - Model estimated risk for the Basin. (Number in a million, all sources)	163
Figure V-13 - Model estimated risk for the Basin. (Number in a million, without diesel sources)	164

Introduction

As a tool, regional modeling, using state-of-science 3-dimensional computer models, has historically simulated the dispersion and chemical transformation of the criteria pollutants for the South Coast Air Basin (Basin). The results of these modeling analyses have been the cornerstones of control strategy development for the Air Quality Management Plan (AQMP). One of the main objectives of the Multiple Air Toxics Exposure Study II (MATES-II) program has been to determine if the state of computer simulation modeling is adequate to simulate measured concentrations of toxic compounds and provide a means for estimating spatially resolved risk to the community.

As part of MATES-II program, the challenge of the modeling the dispersion, transport and transformation of the emissions of toxic compounds in the Basin was undertaken. This appendix outlines that regional modeling effort. The results of the regional modeling simulation are presented for the Basin in total and for 24-sites (10-fixed routine and 14-microscale) that measured toxic compounds during the period April 1, 1998 through March 31, 1999. This appendix also discusses the selection of air quality and meteorological models used for the simulation, the model input preparation, and the selection of the modeling domain. In addition, a characterization of model performance is provided to demonstrate the capacity of the simulation to recreate concentration of both toxic and criteria compounds measured in the Basin during the monitoring period. Finally, spatially resolved estimates of risk to the Basin population are provided.

3-Dimensional Regional Simulation Models Evaluated

The Urban Airshed Model (UAM) was used to simulate the regional dispersion of air toxic compounds based on their emission rates as discussed in Chapter 4 of the main document. The UAM has been the U.S. Environmental Protection Agency's (EPA) recommended model for ozone attainment demonstrations. There are several models currently available for ozone simulation. These models are undergoing evaluations as potential models for the next AQMP revision. While the EPA's version of the UAM may be considered dated, the model has been proven for ozone air quality analysis. Specifically, the dispersion algorithms are still appropriate to analyze the dispersion of inert species (or compounds). As such, the UAM is used to simulate the dispersion of the toxic compounds.

In addition to the EPA's version of UAM, a special version of UAM (called UAM-TOX) was applied to simulate the atmospheric reactions of volatile organic compounds (VOCs) and oxides of nitrogen (NO_x) to account for the formation and/or destruction of several toxic VOC compounds. Specifically, the UAM-TOX is used model VOC compounds such as 1,3 butadiene, (which reacts in the atmosphere) and carbonyls such as formaldehyde and acetaldehyde (which form in the atmosphere).

Modeling Domain

Figure V-1 shows the modeling domain used in the modeling analysis. The horizontal modeling domain covers 210 kms from west to east and 120 kms from south to north. The modeling domain is somewhat smaller than the domain used for the AQMP regional modeling simulations. However, each square shaped grid cell with side dimension of 2 km provides significantly better resolution than the 5 km resolution used for the regional modeling demonstration for the criteria pollutants.

The vertical dimensions of the modeling domain extended to 2000 m above the surface using a terrain following coordinates system terrain. Five vertical layers were used in the simulation to characterize horizontal and vertical transport and dispersion.

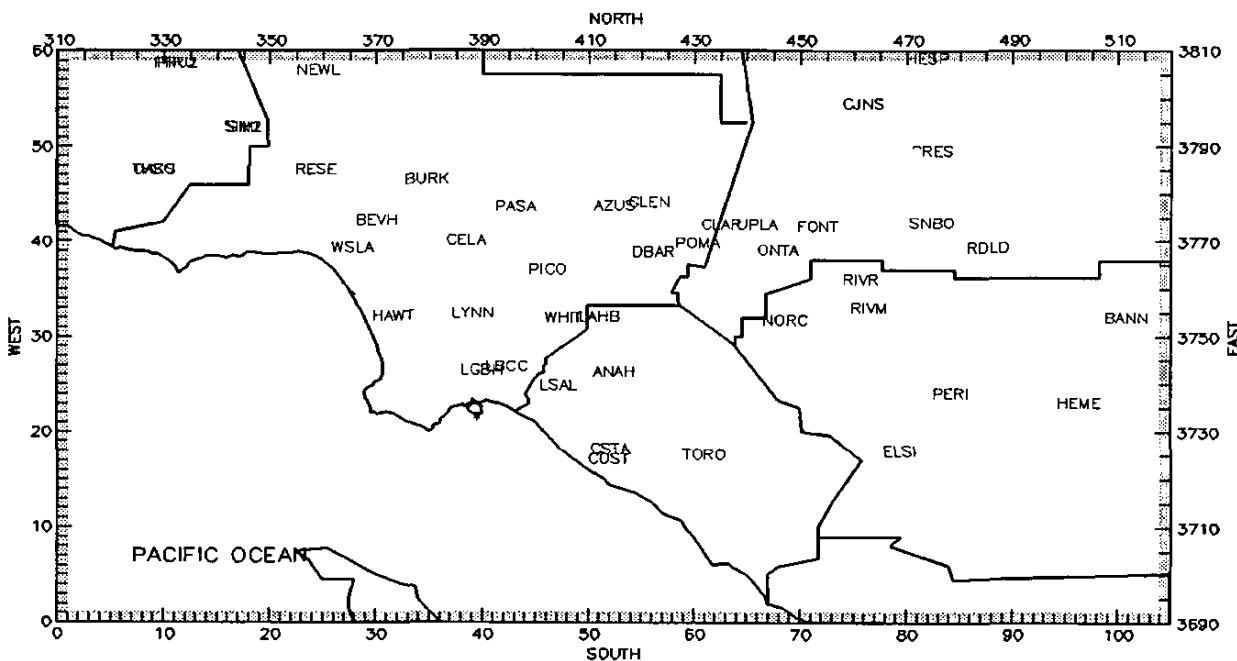


Figure V-1. UAM MATES II regional modeling domain.

Toxic Compounds Modeled

A total of 34 compounds are modeled as part of the regional model evaluation and 29 of the modeled compounds have measurements collected at the 10 MATES II sites. Table V-1 provides the locations of the MATES II sites and Table V-2 provides a list of the toxic compounds that were both modeled and measured. Table V-2 also provides the instrument's detection limit for compound measurement for reference. In some cases,

modeled concentrations for those toxic compounds having measurements at or near the detection limit fall below the range of instrument detection.

Table V-1. Locations of the MATES II Toxic Monitoring Network

Location	Type Site
Anaheim	District Monitoring Network
Burbank	District Monitoring Network
Compton	MATES II Special Study Site
Fontana	District Monitoring Network
Huntington Park	MATES II Special Study Site
Central LA	District Monitoring Network
Long Beach	District Monitoring Network
Pico Rivera	District Monitoring Network
Rubidoux	District Monitoring Network
Wilmington	MATES II Special Study Site

Meteorological Model Description

The CALMET meteorological model was used to generate hourly gridded three-dimensional meteorological fields. CALMET consists of a diagnostic wind field module and micrometeorological module for the boundary layer. The diagnostic wind field module uses a two step approach to develop hourly wind fields. In the first step, CALMET generates an initial-guess wind field using selected subsets of the observational data to characterize the mean hourly wind flow. This initial-guess is then adjusted for kinematic effect of terrain, slope flows, and terrain blocking effects to produce a Step1 wind field. The second step consists of an objective analysis procedure to introduce observational data into the Step 1 wind field to produce a final wind field. The micrometeorological module calculates boundary layer parameters such as surface heat flux, surface momentum flux, and the boundary layer height based on the energy budget method. Several additional parameters, including the friction velocity, convective velocity scale, stability class, Monin-Obukov length, are derived. The reader is referred to U.S. EPA et al. (1995) for a complete description of the CALMET meteorological model.

Preparation of Surface Meteorological Data Input

CALMET requires surface temperature, pressure, wind speed and direction, relative humidity, cloud cover and precipitation data. Hourly data, covering the MATES II field monitoring program period from approximately 140 surface monitoring stations were used to develop the surface meteorological fields. These data were obtained from a number of sources including the District monitoring network, the EPA Aerometric Information Retrieval System (AIRS) for surrounding districts, the Federal Aviation Administration (FAA) surface observation data, as well as the California Irrigation Management In-

formation System (CIMIS) data. Figure V-2 illustrates the density of the surface meteorological data used for the meteorological modeling.

Table V-2. Toxic Compounds Measured and Modeled at the 10 MATES-II Sites

Toxic Compound	Measurable Detection Limit ($\mu\text{g}/\text{m}^3$)	
	ARB	AQMD
Benzene	0.639	0.319
1,3Butadiene	0.088	0.221
p-Dichlorobenzene	1.202	0.601
Methylene Chloride	3.476	0.348
Chloroform	0.098	0.488
Perchloroethylene	0.068	0.678
Trichloroethylene	0.107	0.537
Carbon Tetrachloride	0.126	1.258
Ethylene Dibromide	--	0.768
Propylene Oxide	--	--
Ethylene Dichloride	--	0.405
Vinyl Chloride	--	0.511
Dioxane[1,4]	--	--
Ethylene Oxide	--	--
Formaldehyde	0.123	0.123
Acetaldehyde	0.180	0.180
Acetone	--	0.238
Methyl Ethyl Ketone	0.295	0.295
Styrene	0.426	0.426
Toluene	0.754	0.377
1,1Dichloroethane	--	0.405
Chloromethane	--	0.206
Diesel PM	--	--
Arsenic	0.003	0.004
Elemental Carbon	--	--
Organic Carbon	--	--
Chromium	0.002	0.002
Hexavalent Chromium	0.0002	0.0006
Cadmium	--	0.01
Lead (point sources)	0.003	0.001
Lead (area sources)	0.003	0.001
Nickel	0.002	0.001
Selenium	0.002	0.001

Off shore observational wind, temperature and sea surface data were obtained from the Data Zoo at Center for Coastal Studies (SCRIPPS Institute of Oceanography). The Data Zoo contained three-buoy sites along the coast in the modeling domain (not shown in Figure V-2). The buoy data was available for all of 1998. Daily data from April 1, 1998 through December 31, 1998 were directly ingested by CALMET. Monthly average values of the buoy data observed in 1988 for January through March were calculated and substituted for the offshore characterization for the first quarter of 1999.

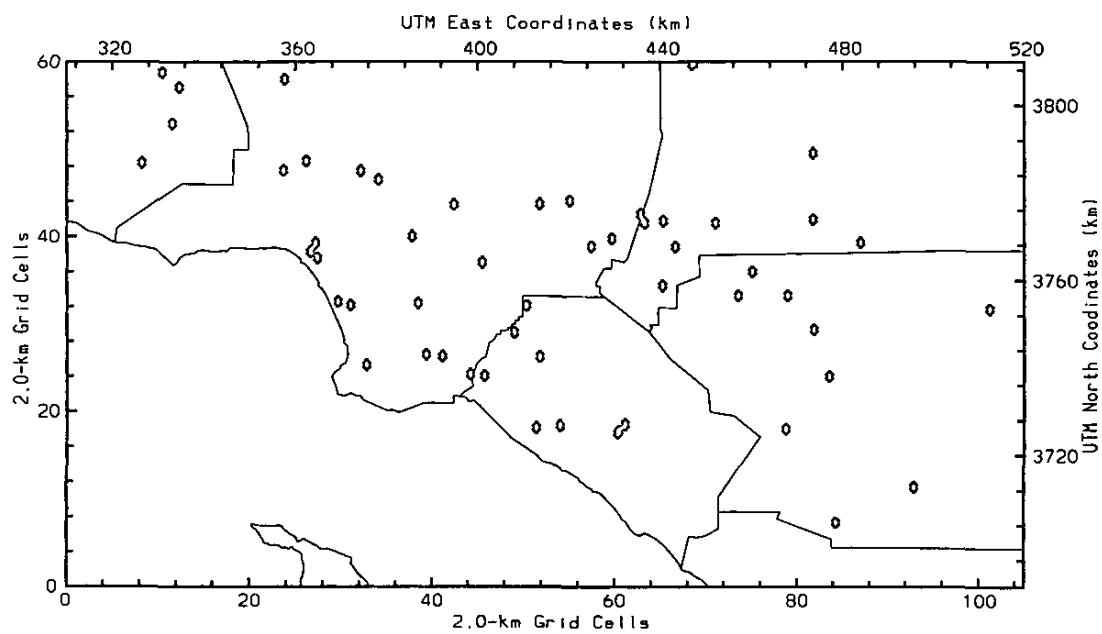


Figure V-2. Locations of surface meteorological monitoring sites.

The surface data was subjected to a series of quality assurance tests to screen the data and remove any invalid points. For the temperature data a range test was employed, where any observations over 125°F were discarded. For the wind data, the twenty-five highest wind speeds at each monitoring site were examined manually. Data was discarded if it was determined to be inconsistent or have an abnormally high speed.

CALMET ingests monitored data directly from the station readings. In the cases where hours in the data archives were missing or data was ruled to be invalid, a series of procedures were undertaken to estimate the missing data. If a missing data value was surrounded by valid data in the hours immediately preceding and following it, the value was estimated by linear interpolation in time. For all values other than wind speed and wind direction, remaining missing data values were filled in by spatial interpolation using inverse distance squared weighting. Relative humidity was interpolated using the following procedure. First of all, the relative humidity and temperature were used to calculate the absolute humidity. Then, the absolute humidity was spatially interpolated. Finally the temperature and absolute humidity were used to calculate the relative humidity.

Pressure, ceiling height, cloud cover and precipitation was measured at fewer stations than wind temperature and moisture. As a result, for hours when no data was available for one of these parameters, default values of one atmosphere for pressure, no cloud cover or precipitation and unlimited ceiling were substituted in the data field.

Since geographic features generate localized winds no attempt was made to spatially interpolate individual hours having missing values prior to running the meteorological processor. CALMET treated gaps in the wind data for periods of six hours or less by substituting observed winds from the preceding hour. If a gap existed of longer than six hours then the data from that wind station was automatically excluded from the analysis for the month in question.

Figures V-3a through V-3-d provide the July and January monthly averaged winds for 0600 PST and 1600 PST respectively, to illustrate the seasonal variability of the surface wind fields generated by CALMET for the MATES II monitoring period. While the averaged wind vector fields do not represent day-to-day variations in the winds they provide a means of judging whether the seasonal climatic features are characterized by the flow pattern. Figure V-3a depicts a moderate offshore flow regime for the early morning hours during winter. During summer (Figure V-3c), the early morning winds are more stagnant and disorganized. Figure V-3b presents the January afternoon sea breeze that is well organized but weaker than the summer sea breeze illustrated in Figure V-3d. These patterns are consistent with the climatological description of the morning and afternoon flow regimes described by DeMarrias et. al. (1965) in U.S. Weather Bureau Technical Report No. 54, long considered a benchmark analysis of the wind climatology of Southern California.

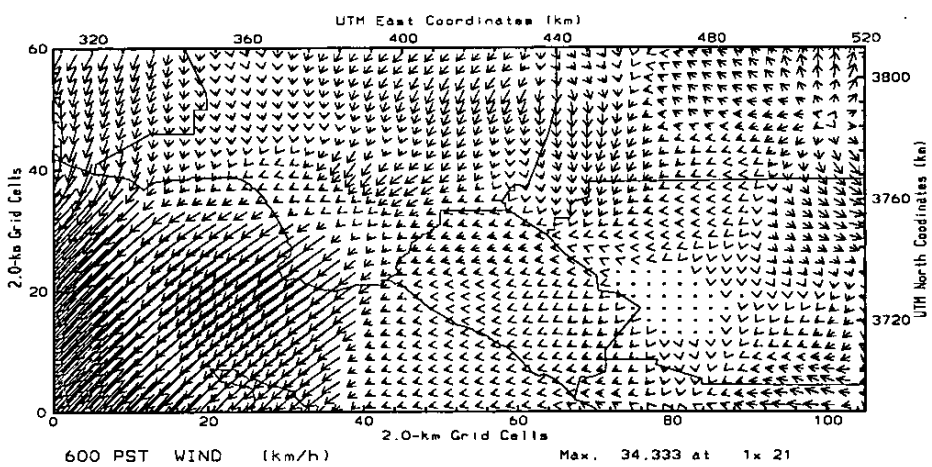


Figure V-3a. January 0600 PST average surface CALMET wind field.

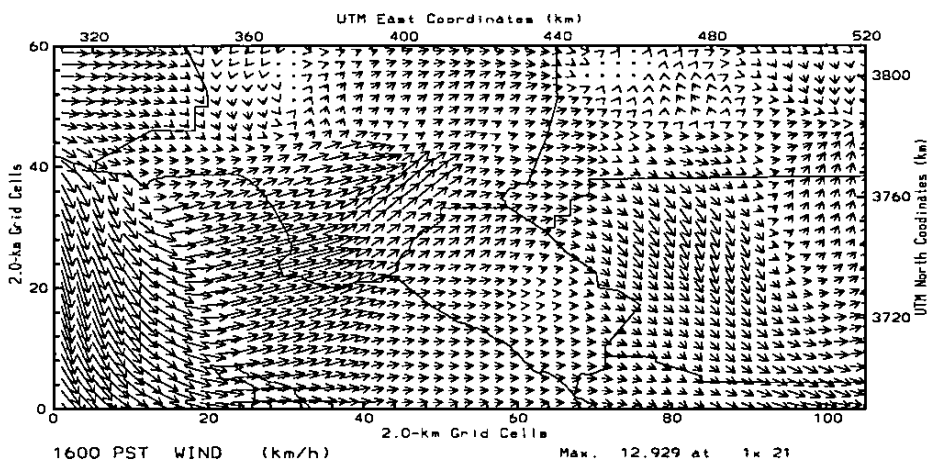


Figure V-3b. January 1600 PST average surface CALMET wind field.

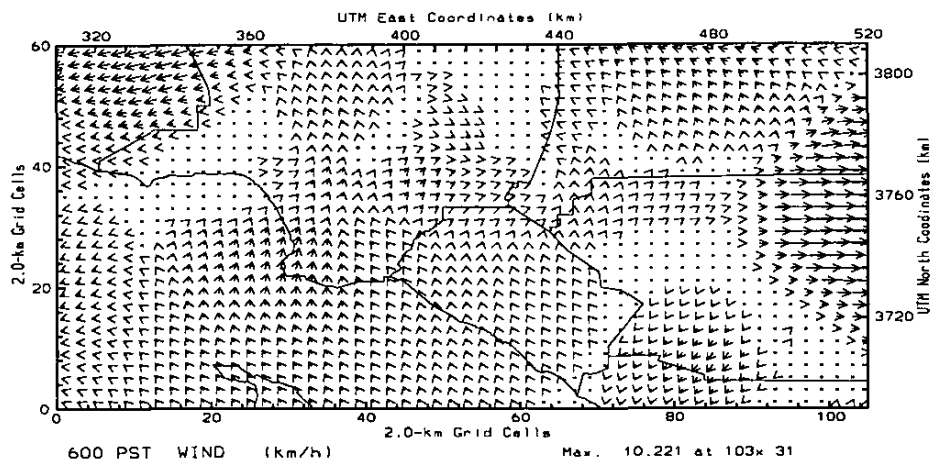


Figure V-3c. July 0600 PST average surface CALMET wind field.

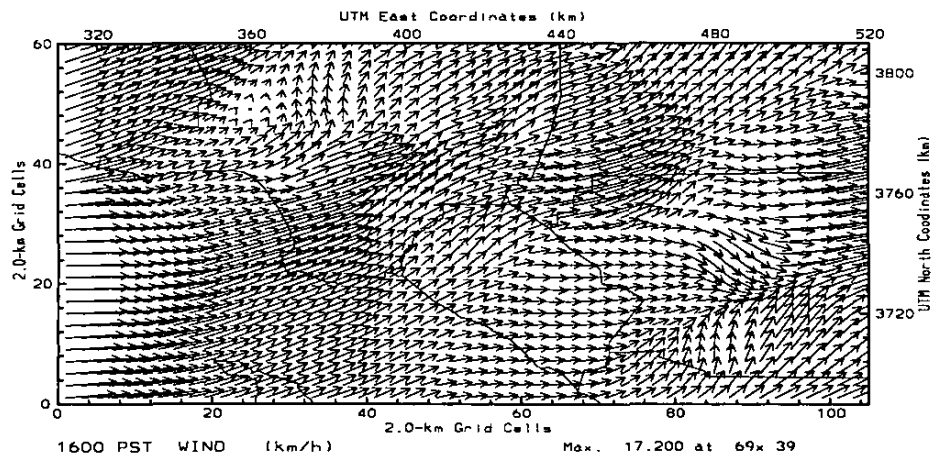


Figure V-3d. July 1600 PST average surface CALMET wind field.

Preparation of Upper Air Data Input

Upper air wind and temperature data monitored at 11 radar wind profiler (RWP) and radio acoustic sounding system (RASS) sites in or near the Basin comprised the backbone of the upper air data set. The continuous upper air profiling was augmented by surface meteorological at each monitoring location. The RWP/RASS sites included the District's PAMS Los Angeles Airport (LAX), Ontario Airport (ONT), Ventura County APCD's Simi Valley (SIM), and the San Diego APCD's Point Loma (PTL), and Valley Center (VLC). Supplemental sites operated by National Oceanic and Atmospheric Administration (NOAA) at Goleta (GLA), University of Southern California (USC), Santa Catalina (SCL) and San Clemente Island (SCE) and by the California Air Resources Board (CARB) at Riverside (RIV) and Tustin (TUS) completed the upper air network. Figure V-4 depicts the locations of the upper air monitoring stations.

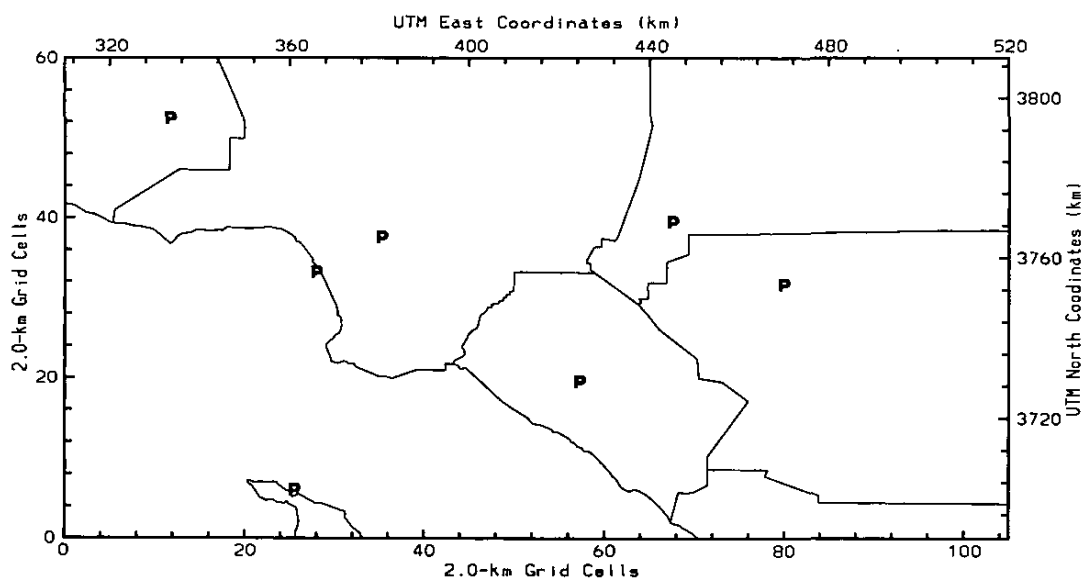


Figure V-4. Locations of upper air meteorological monitoring sites.

These RWP and RASS data were preprocessed for each station as follows. First, any observation that did not reach to above 1 km was discarded. In addition, any hour for which both temperature and wind data were not available was discarded.

The RWP winds from high and low resolution operating modes were merged directly to form a comprehensive vertical profile. The virtual temperature measured by RASS was converted to the dry bulb temperature using observed surface temperature and relative humidity. Typically, at heights above the marine layer where the atmosphere has less available moisture, little difference exists between the virtual and dry bulb temperature. As a consequence, no attempt was made to convert the virtual temperature to dry bulb temperatures at levels greater than the estimated mixing height. Since the temperatures were at different levels than the winds, the temperature data were interpolated to the levels at which there were wind data by linear interpolation.

The CALMET model requires a complete upper air data profile the surface to the top of the modeling domain. Periodically, surface observations for selected profiler sites were no available. In order to satisfy the CALMET completeness requirement, the observational data were extended as follows. Values of temperature, pressure and wind speed and direction at surface level were obtained from the surface data as described above. The only change was that missing values for the wind were obtained by spatial interpolation. This spatial interpolation of the wind may not be as accurate as one would have liked. However, it did allow the use of a sounding which otherwise would have to be discarded.

RWP/RASS data that extended pass 1 km, but not to the top of the modeling domain were extended as follows. The highest level of valid wind reading was continued to the top of the modeling domain. Above the highest level of valid temperature reading, the temperature was assumed to decrease according to the standard atmospheric lapse rate.

The pressure was calculated from the value of the surface pressure and the temperature profile using the hypsometric equation.

CALMET Model Simulation

The CALMET meteorological modeling region was overlaid upon the UAM modeling region with an equivalent 2 X 2 km grid resolution. The top of the meteorological modeling domain differed from that specified for the air quality simulation. The top of the modeling region was set to 2500 meters and a total of 12 vertical cells were used by CALMET to simulate the vertical wind structure. Table V-3 lists the vertical layer structure for the CALMET simulation.

CALMET offers various options and default values for simulating the meteorological fields depending on the characteristics and length of the episode evaluated. Two options were important for the development of the hourly meteorological fields: First, the surface wind observations were extrapolated to upper layers using similarity theory. This option enables the observational data that is set to the shallow first layer of the modeling domain (0-20m) to exert a greater level of influence on the layers immediately above the surface. This option also provides a measure of wind field consistency throughout the marine or mixed layer.

While fields of hourly mixing heights can be imported as an input to the CALMET simulation, the option exists to have CALMET directly calculate gridded fields of mixing based upon modeled estimations of mechanical and thermodynamic turbulence. This option was employed for the CALMET simulation and a minimum mixing height for the analysis was set to 100 m above ground level. The mixing heights derived from CALMET were temporally and spatially smoothed using 3-hour moving average and a five-point smoothing method.

Table V-3. CALMET Vertical Layers

Layer	Height (meters)
1	0-20
2	20-60
3	60-100
4	100-200
5	200-300
6	300-400
7	400-600
8	600-800
9	800-1000
10	1000-1500
11	1500-2000
12	2000-2500

Figures V-5a through V-5d provide examples of the CALMET simulated hour mixing height fields for each day during the 1-year modeling period at the coastal site of Wilmington, Central LA in the metropolitan area, Burbank in the San Fernando Valley and Rubidoux, in the inland empire. The mixing height field depicts a clear diurnal trend with minimum mixing at night and maximum mixing midday. The seasonal variation at all of the sites indicated a shallower mixed layer in the winter when radiation inversions are persistent and winds are weakest. Conversely, summer daytime mixing heights are typically 150 percent of those observed in the fall and winter. Spatially, the valley and Inland Empire sites depict higher values of mixing, reflecting the greater variation in the

daytime temperature structure. Figures V-6a and V-6b show the average January and July spatial variation in afternoon (1600 PST) mixing across the basin. In general, Basin mixing is lower in January however, the gradation of increasing mixing inland is simulated for each season.

UAM Simulations

Prior to initiating the UAM and UAM-TOX simulations, the 12-layer CALMET wind fields were interpolated and averaged to conform to the UAM 5-layer structure. A wind layer-matching scheme (UAMWND) developed by Douglas et al. (1990) was used for the interpolation. UAMWND weights surface layer wind influence to layers aloft on the basis of stability. For this application, the weighting factor was modified to enhance surface layer influence to the upper layers. This procedure ensured that the wind field in the lowest two layers of the UAM simulation domain retained the characteristics of the wind in the mixed layer. This modification resulted in about 65-70 percent influence of the surface (CALMET layer-1) winds at the mixing height. In addition, a five-point filter was applied to smooth the field and dampen the horizontal shear.

Table V-4 provides the initial boundary concentrations specified for the UAM simulations.

Model Performance Goals UAM and UAM-TOX

The output of the UAM and UAM-TOX models is 24-hour average concentrations for the one-year period modeled. For the current analysis, the 24-hour average concentrations are compared to the measurements (that are also 24-hour average values) individually. In addition, a comparison is made between the annual and seasonal average concentrations to determine how well the model performs for longer averaging periods. Traditionally, risk calculations are based on annual averaged concentrations. While variations may exist between model simulations and measurements on a daily basis, the longer-term averages tend to be more similar.

Model performance goals have not been established for simulating toxic compounds. However, based on prior ozone model evaluation experience, VOC model performance can vary by as much as one order of magnitude while ozone model performance can vary by as much as 50 percent. For the current model evaluation, the hourly ozone simulated during the one-year period is compared to measured ozone concentrations to provide a gauge on how well the model is simulating the toxic compounds. However, based on prior AQMP ozone modeling applications and recent information regarding mobile source emissions, it is anticipated that high measured ozone levels will be underestimated in the current analysis.

Table V-4 Boundary Concentrations used for the MATES II modeling.

<u>Compound</u>	<u>Boundary Concentration ($\mu\text{g}/\text{m}^3$)</u>
Benzene	0.640
13butadiene	0.008
p-Dichlorobenzene	0.008
Methylene chloride	0.139
Chloroform	0.074
PERC	0.237
TCE	0.065
Carbon Tetra.	0.777
Ethylene dibromide	0.008
MTBE	0.008
Propylene oxide	0.008
Ethylene Dichloride	0.102
Vinyl chloride	0.012
14Dioxane	0.008
Ethylene oxide	0.008
Formaldehyde	0.540
Acetaldehyde	0.008
Acetone	0.008
MEK	0.029
Styrene	0.008
Toluene	0.008
1,1dichloroethane	0.030
methyl chloride	1.229
Secondary	
Formaldehyde	1.800
Secondary	
Acetaldehyde	0.018
Diesel	0.450
Arsenic	4.1E-05
EC	0.450
OC	0.450
Chromium	4.1E-05
Cr+6	8.2E-14
Cadmium	8.2E-14
Pb	1.6E-13
Nickel	8.2E-14
Selenium	8.2E-14

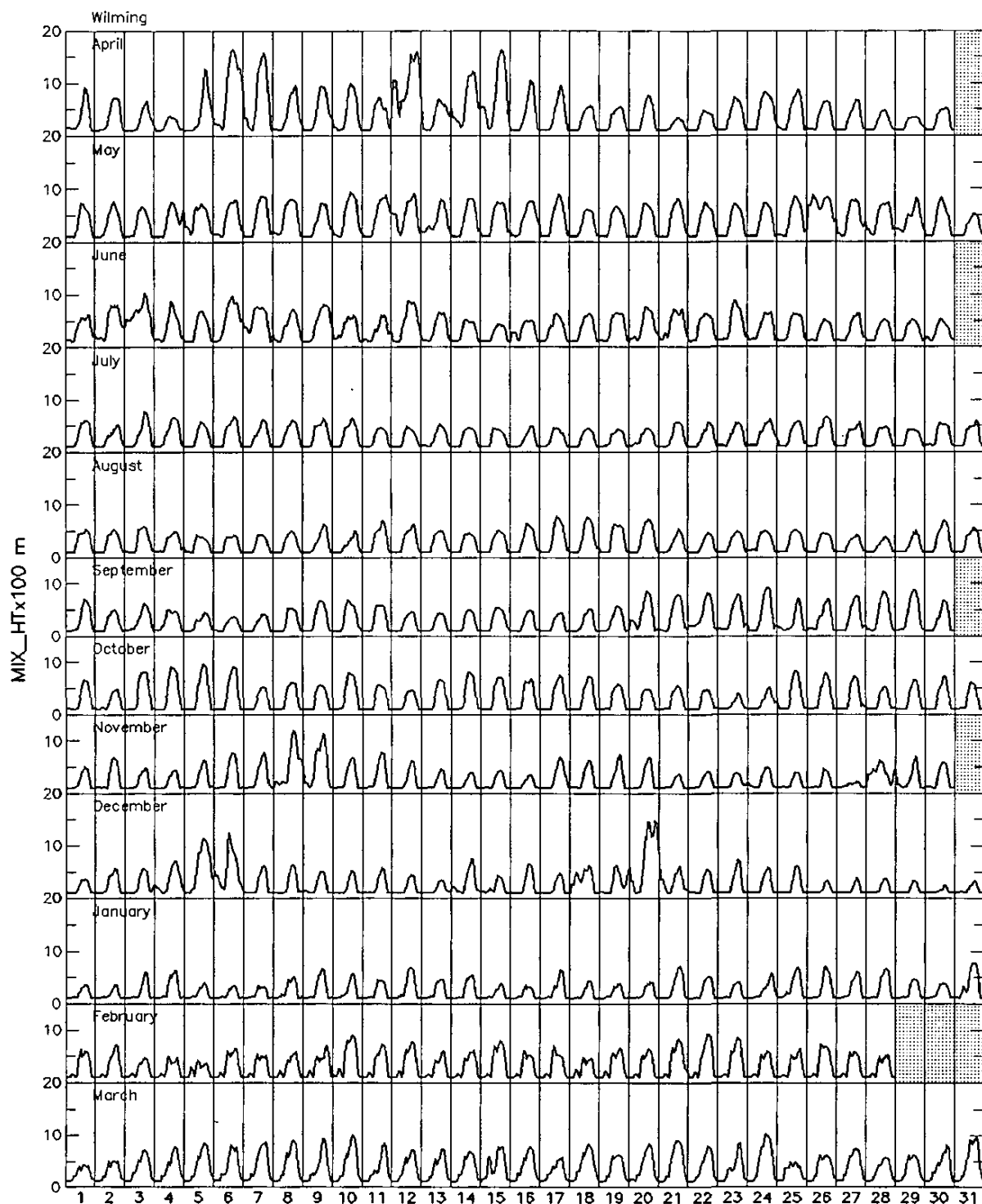


Figure V-5a. Diurnal variation of mixing at Wilmington (April 1998 - March 1999)

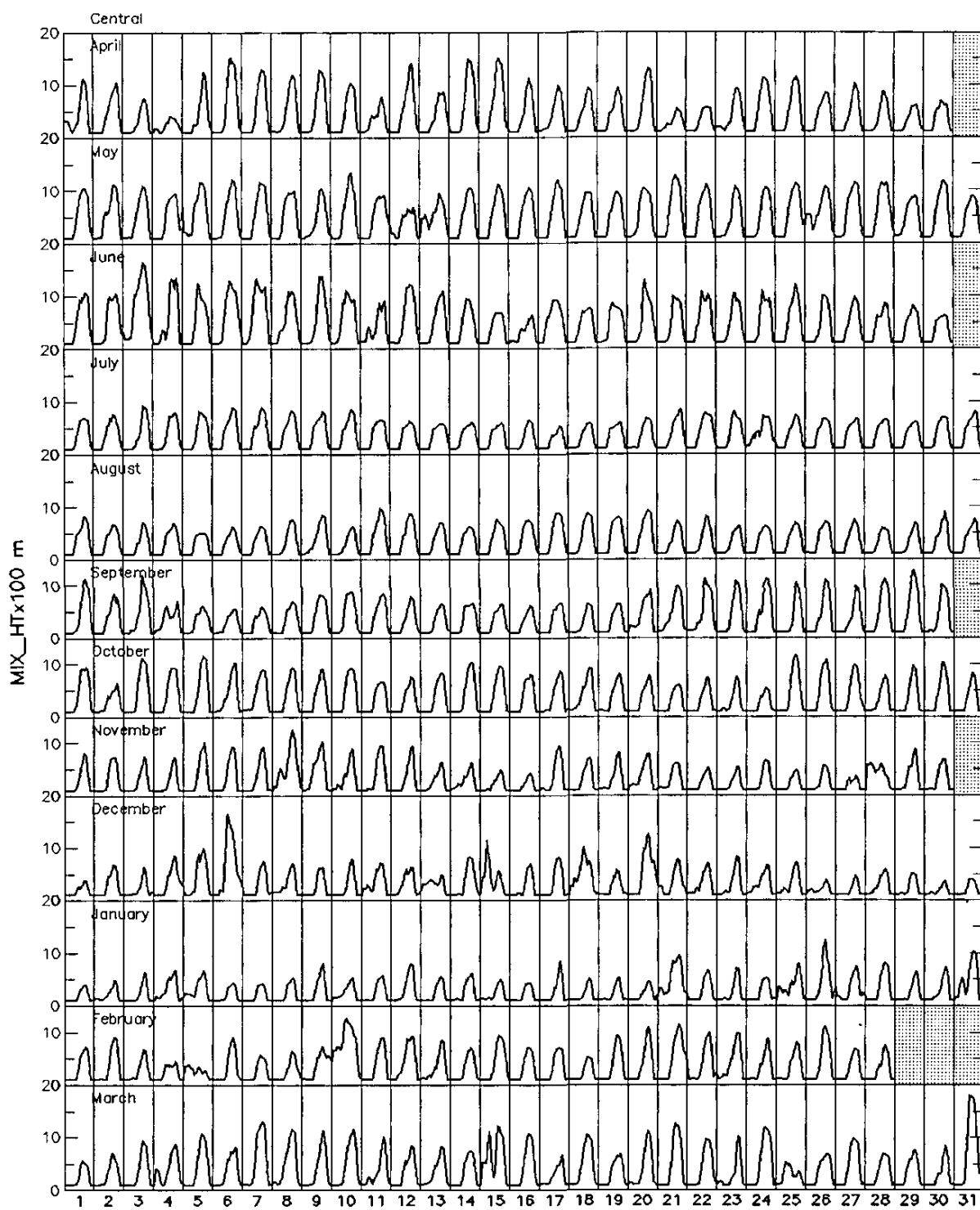


Figure V-5b. Diurnal variation of mixing at Central LA (April 1998 - March 1999)

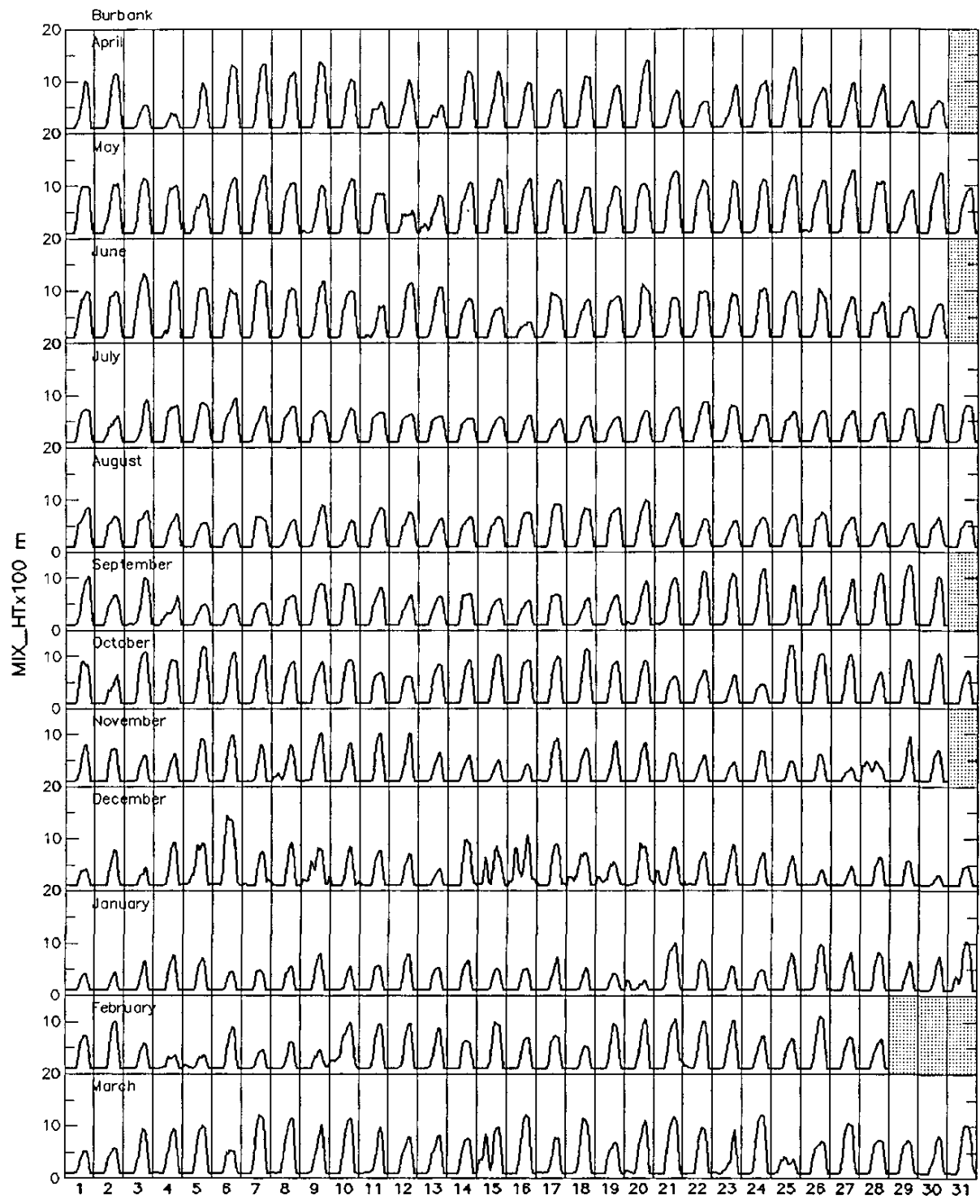


Figure V-5c. Diurnal variation of mixing at Burbank (April 1998 - March 1999)

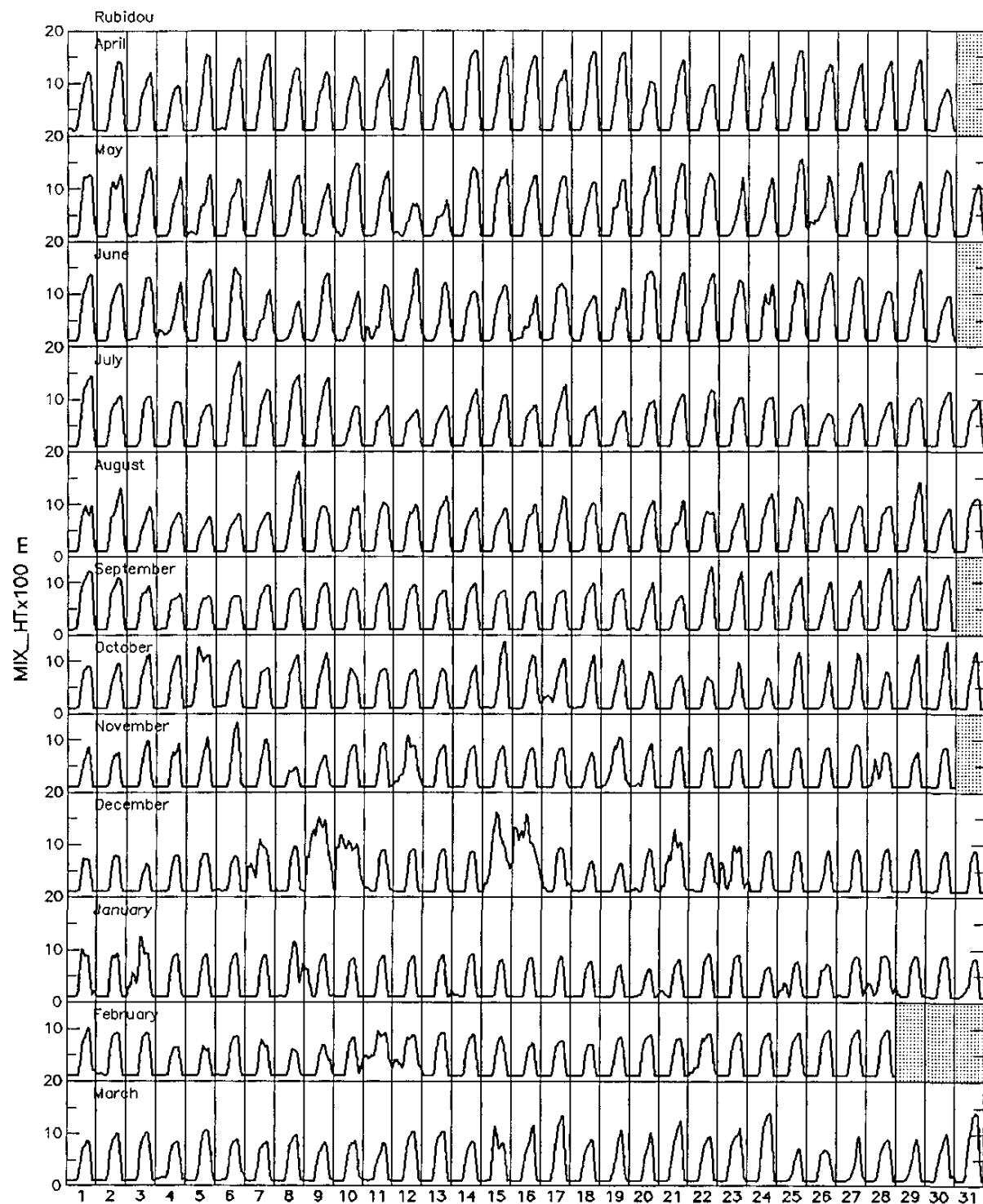


Figure V-5d. Diurnal variation of mixing at Wilmington (April 1998 - March 1999)

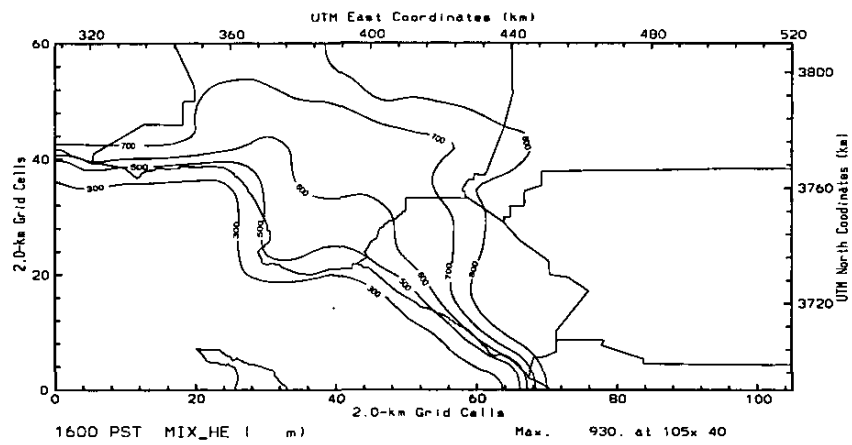


Figure V-6a. January 1999 average 1600 PST spatial variation of mixing in the Basin.

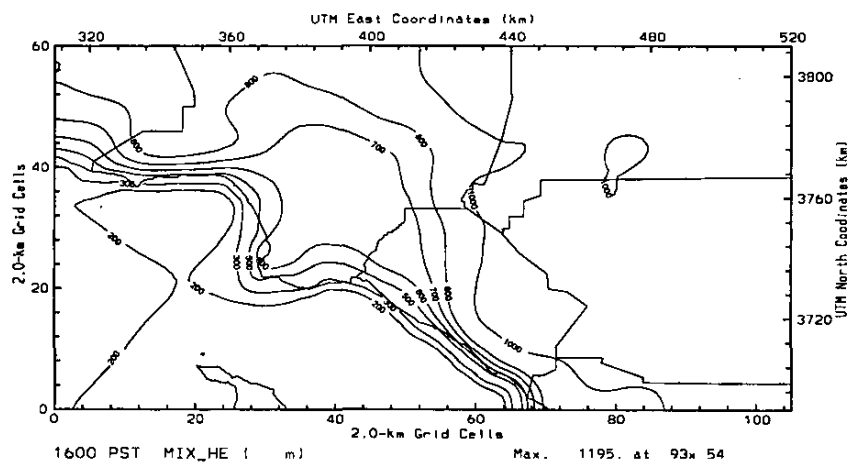


Figure V-6b. July 1998 average 1600 PST spatial variation of mixing in the Basin.

No attempt is made at this time to test the sensitivity of the model simulation by varying the emissions. As such, it is expected that mobile source risk contributions will be underestimated by the simulation models. However, when ARB releases the latest version of the on-road mobile source emissions factor model (EMFAC) and new off-road mobile source emissions, the model performance will be reevaluated.

Figures V-7a through V-7h illustrate the performance of the UAM-TOX simulation in its ability to recreate the daily diurnal trend of observed 1-hour average ozone for each day from April 1, 1998 through March 31, 1999. Seven stations including Hawthorne, Central LA, Azusa, Pomona, Upland, San Bernardino, Riverside and Crestline were selected to depict the ability to simulate ozone formation along the primary west-to-east transport through the Basin. As expected, the peak concentrations that were observed in the Basin in June through and August of 1998 were under predicted. However, the timing of ozone prediction, the relative spatial increase in ozone prediction from west-to-east and the magnitude of under prediction in the eastern portion of the basin provide a measure of confidence that the meteorological models and initial conditions input to the simulation were performing well.

Model Performance Evaluation

Tables V-5a through V-5ac provides summaries of the overall model performance for 29 compounds that were simulated. The overall model performance is compared to measurements collected at the ten MATES-II sites. The performance is provided on a monthly and annual basis for each compound and the monitoring sites having the highest measured and highest simulated are provided. Measures of simulation performance include estimates of systematic bias, gross error, and accuracy (where measurements were available). For this analysis which is focused on an annual average concentration simulation, systematic bias provides the general tendency of the model simulation. Bias estimates for those compounds measured at the detection limits reflect a significant degree of under-prediction however the differences between simulated and measured concentrations are negligible. On an annual basis model performance statistics are generally within 50 to 60 percent of measured annual concentrations.

Figures V-8a through V-8ac show the time-series plots of simulated and measured concentrations for those of the 29 compounds modeled at each of the ten MATES-II monitoring sites. While the time-series plots for compounds such as benzene, 1,3-butadiene, perchloroethylene, toluene, and elemental carbon depict a clear trend, many of the compounds were measured at or slightly above the detection limit. The time-series depiction of the modeled trend for these compounds does not show significant performance “above the noise of the modeling uncertainties.”

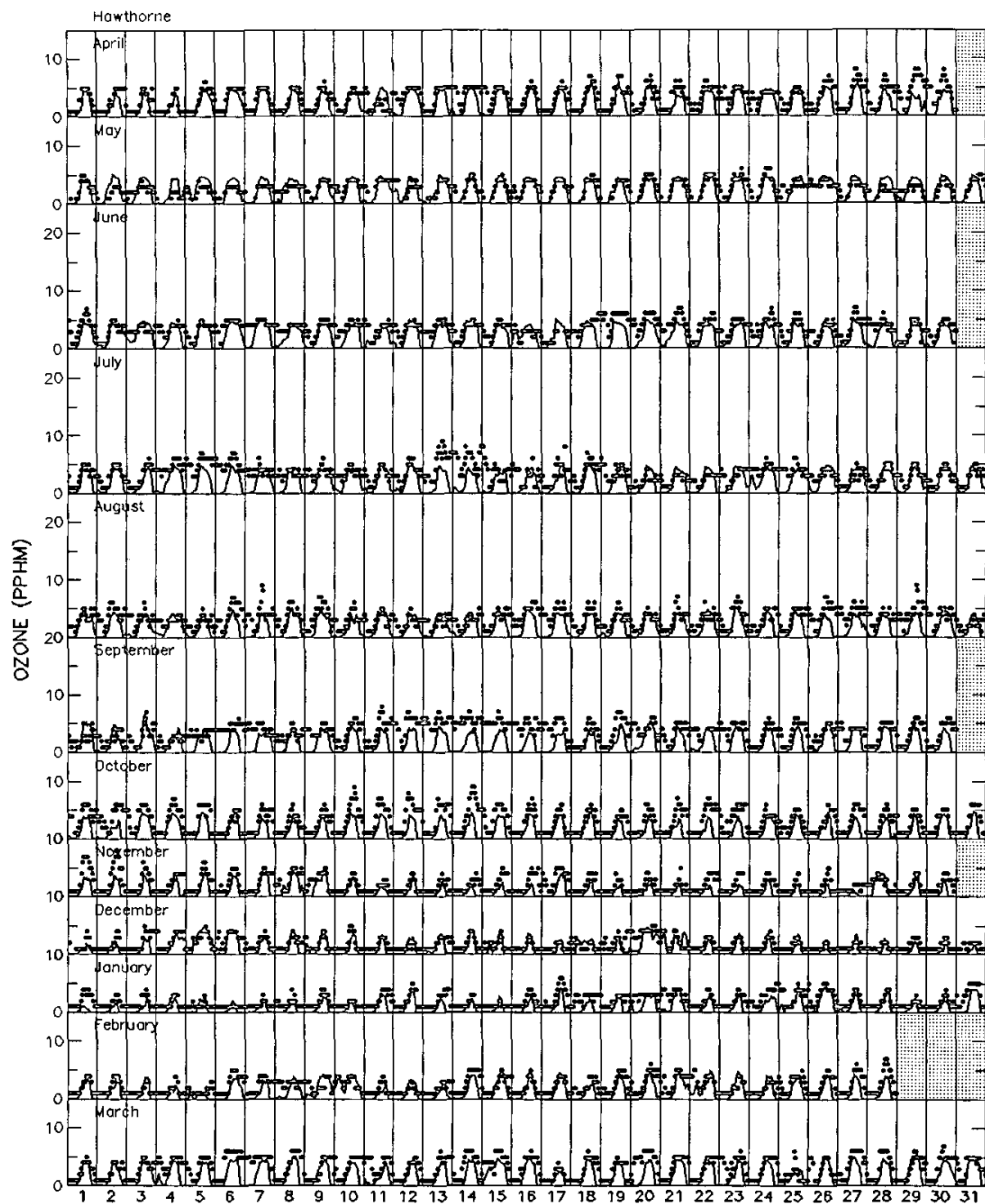


Figure V-7a. Comparison between UAM-TOX predicted (solid line) and measured (points) 1-hour average ozone concentrations (pphm) at Hawthorne (April 1, 1998 – March 31, 1999).

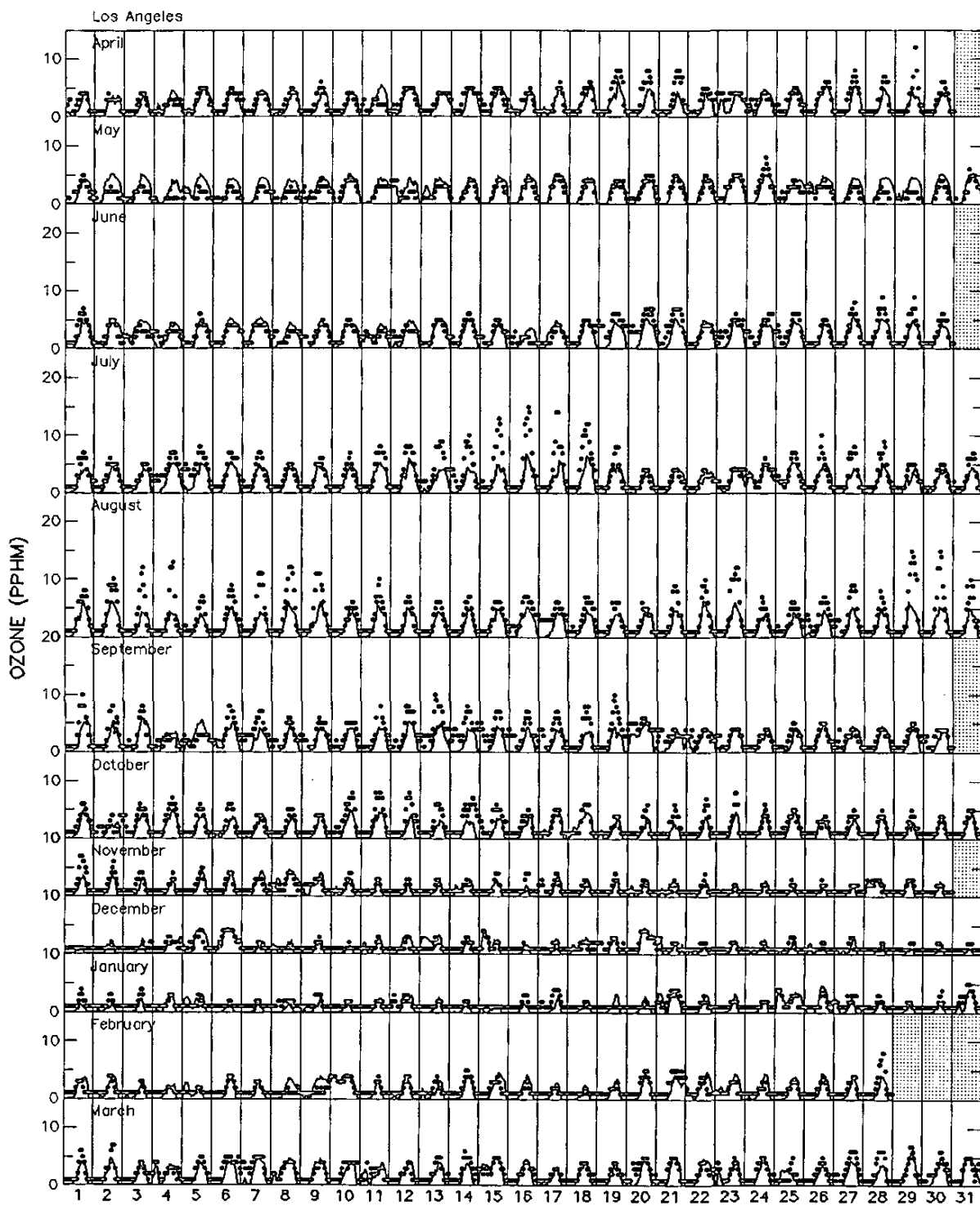


Figure V-7b. Comparison between UAM-TOX predicted (solid line) and measured (points) 1-hour average ozone concentrations (pphm) at Central LA (April 1, 1998 – March 31, 1999).

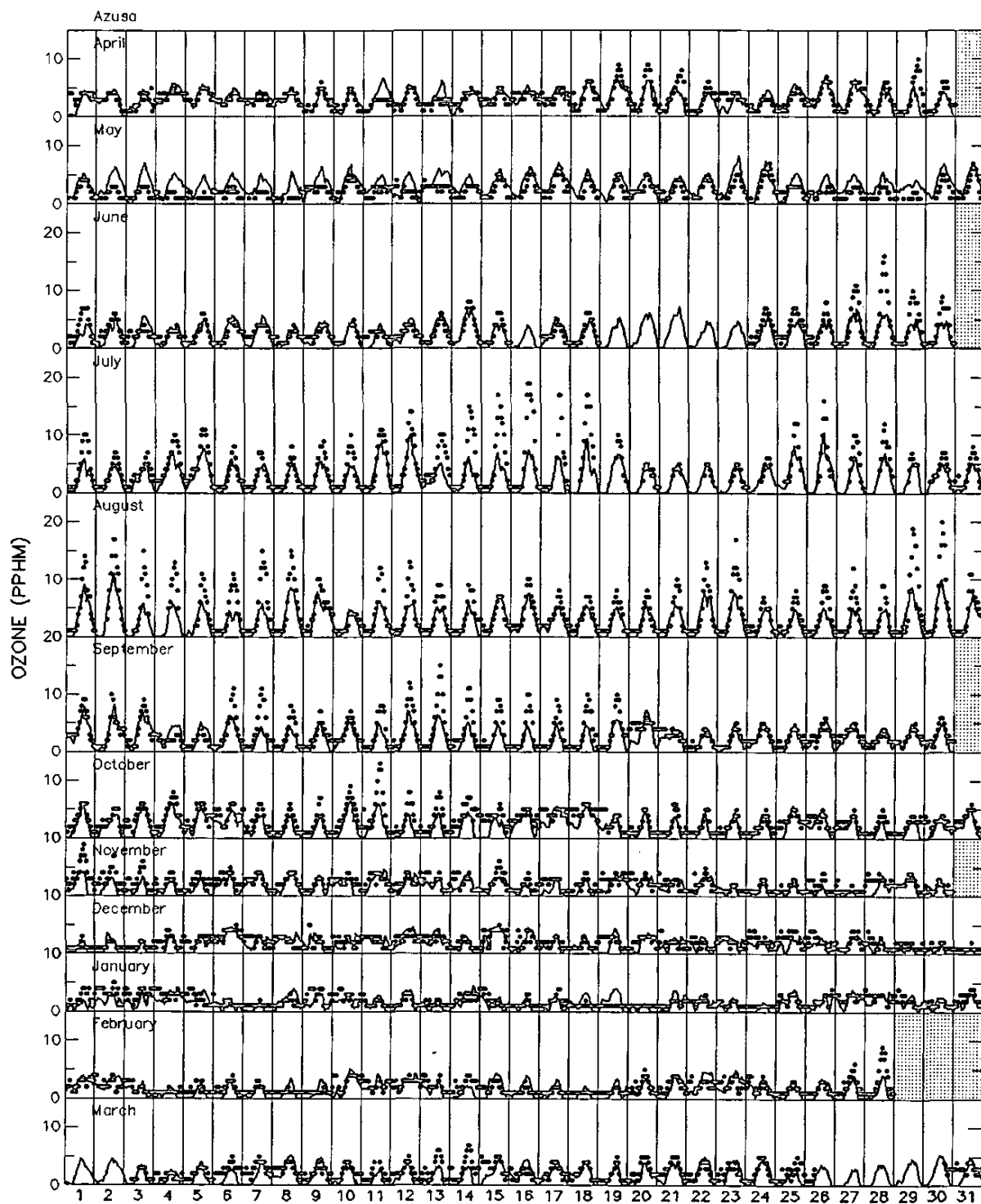


Figure V-7c. Comparison between UAM-TOX predicted (solid line) and measured (points) 1-hour average ozone concentrations (pphm) at Azusa (April 1, 1998 – March 31, 1999).



Figure V-7d. Comparison between UAM-TOX predicted (solid line) and measured (points) 1-hour average ozone concentrations (pphm) at Pomona (April 1, 1998 – March 31, 1999).

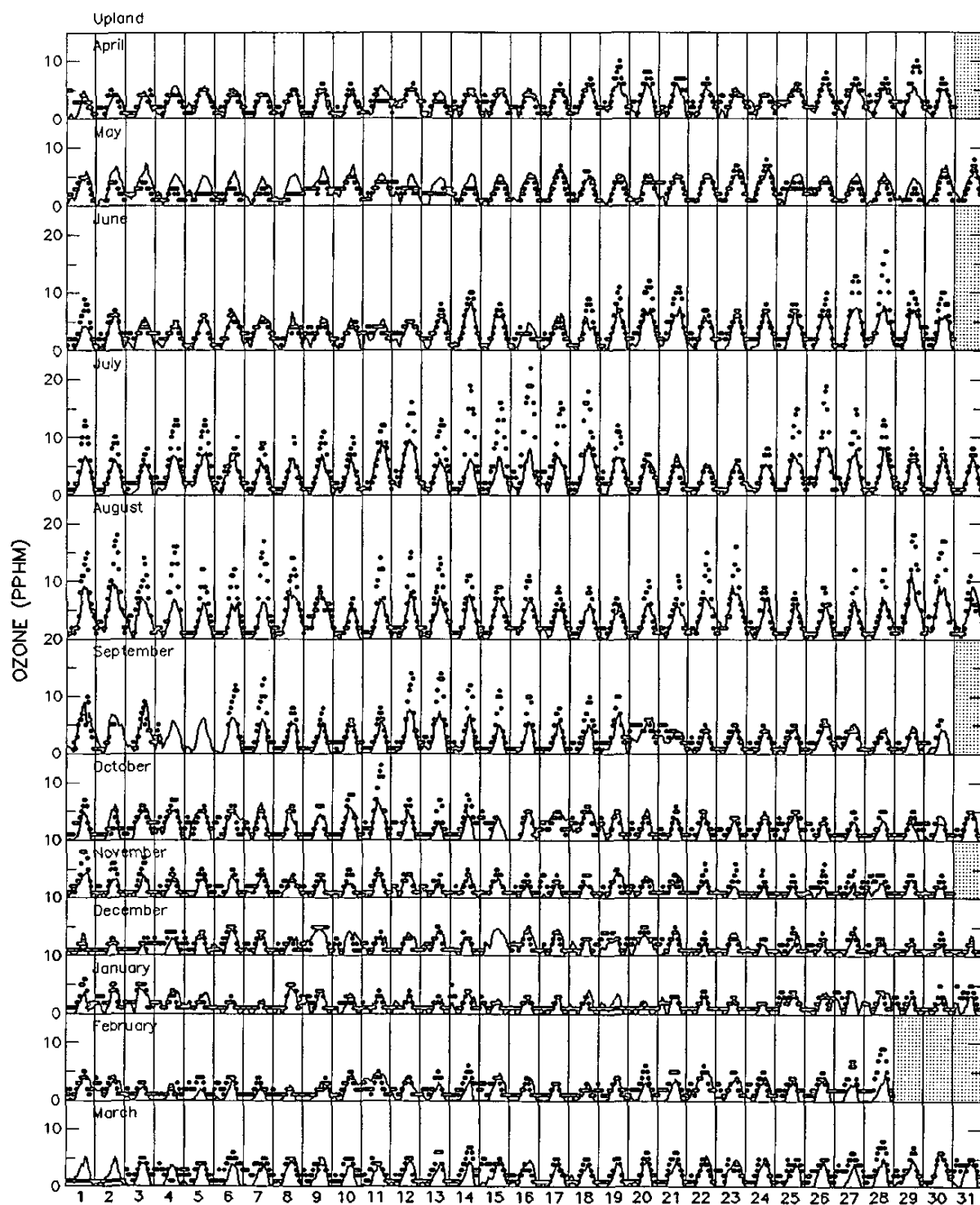


Figure V-7e. Comparison between UAM-TOX predicted (solid line) and measured (points) 1-hour average ozone concentrations (pphm) at Upland (April 1, 1998 – March 31, 1999).

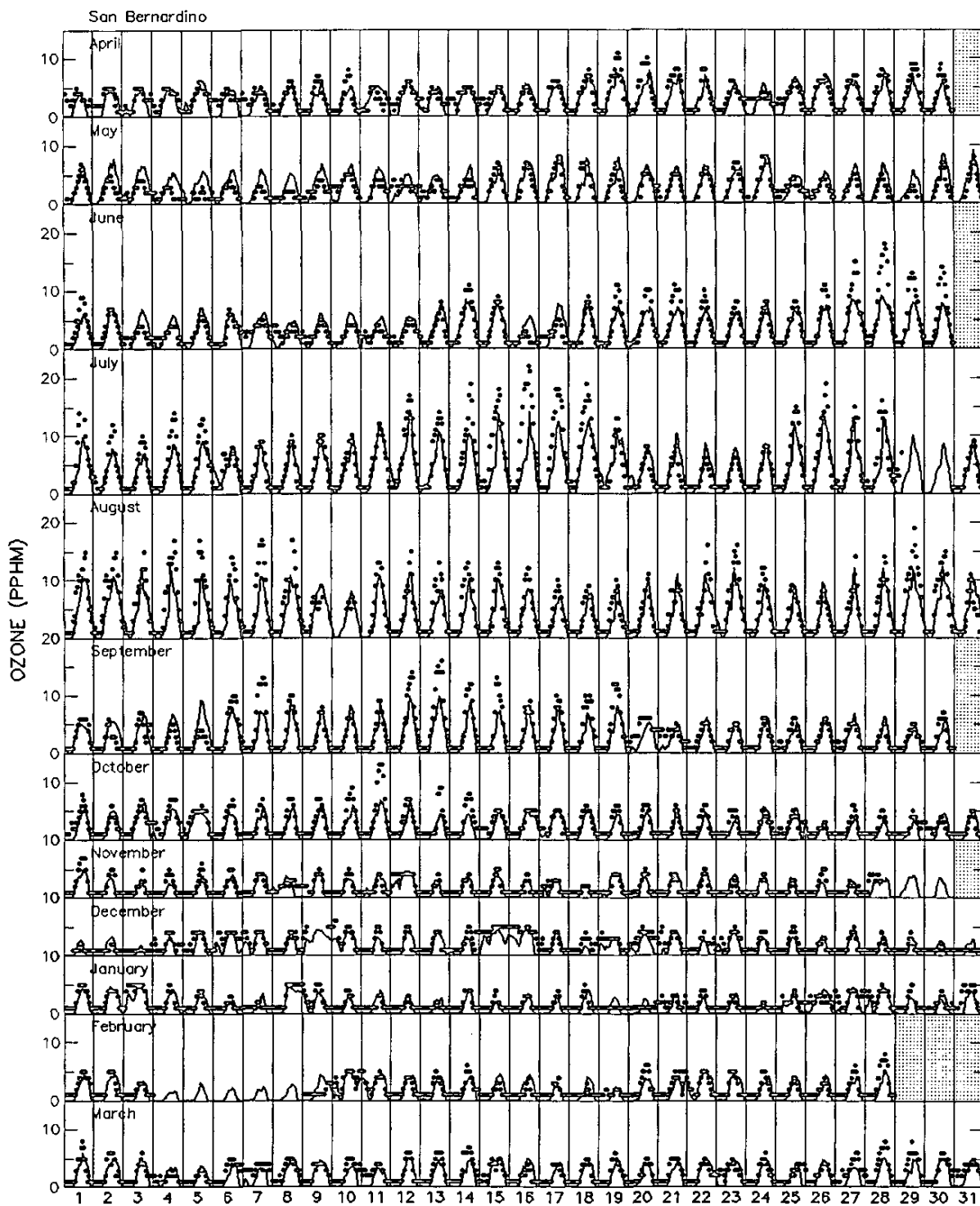


Figure V-7f. Comparison between UAM-TOX predicted (solid line) and measured (points) 1-hour average ozone concentrations (pphm) at San Bernardino (April 1, 1998 – March 31, 1999).

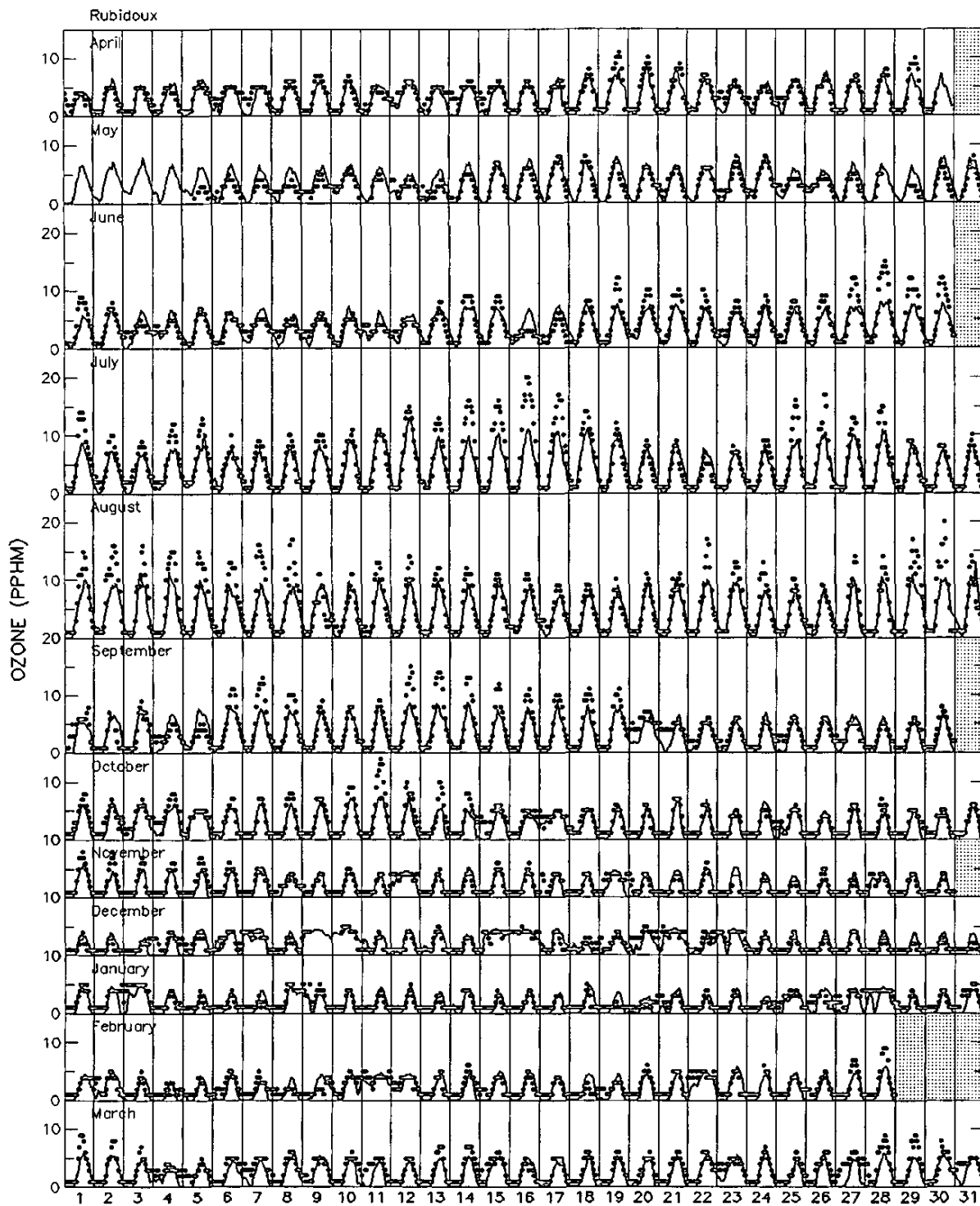


Figure V-7g. Comparison between UAM-TOX predicted (solid line) and measured (points) 1-hour average ozone concentrations (pphm) at Rubidoux (April 1, 1998 – March 31, 1999).

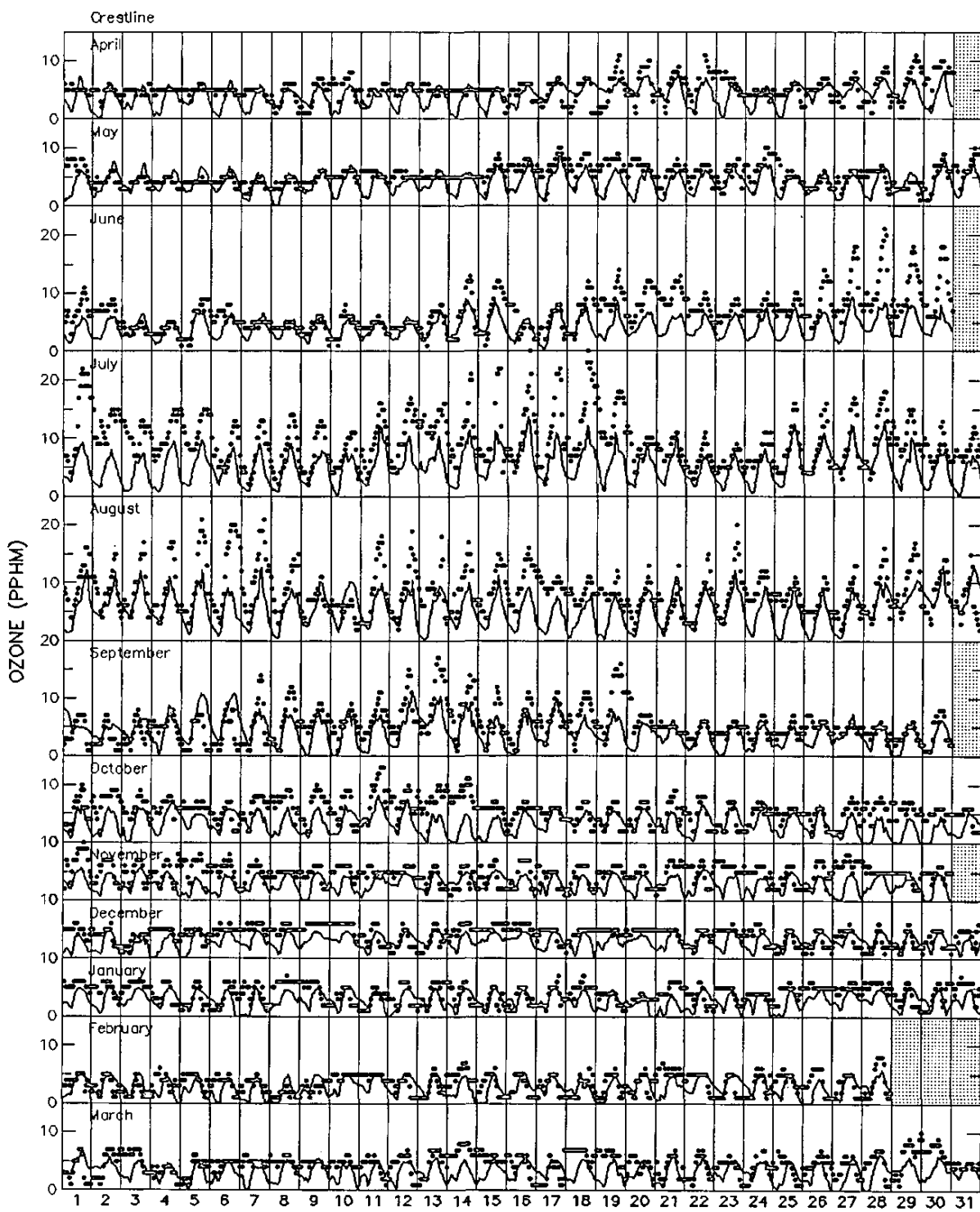


Figure V-7h. Comparison between UAM-TOX predicted (solid line) and measured (points) 1-hour average ozone concentrations (pphm) at Crestline (April 1, 1998 – March 31, 1999).

Figures V-9a through V-9ac show time-series plots of the residuals for the five compounds. As seen in the figures, day to day variations between model estimates and measured concentrations may be as large as 100 percent or more. Yet, the large variations between simulated and measured concentrations may reflect the subtle shifts in the timing of wind transport and its impact on the calculation of the 24-hour average.

Figures V-10a through V-10ac show scatterplots for the 29 compounds (merged for the 10 monitoring sites). The solid diagonal line represents the perfect fit line (i.e., when measured and predicted values are exactly the same and the dotted lines represent over- or underpredictions by 50 percent. As seen in the figures, the models tend to simulate measured concentrations within for lower concentrations with a slight tendency for overprediction. The higher concentrations for most of the compounds are generally underestimated.

For perchloroethylene, a compound found primarily from stationary and area source usage, the models tend to overpredict measured values. In particular, the models tend to overpredict at Anaheim (see Figure V-10). More in-depth review of the perchloroethylene emissions inventory shows that there are several facilities with reported perchloroethylene in the Anaheim area. At this time, it is not clear whether the Anaheim monitoring site is located such that it is predominantly upwind of these sources or if the model is accurately simulating these sources. One process for confirming the impact of these sources is to conduct a focused monitoring program in and around these sources to determine if higher concentrations do occur.

Table V-6 presents the simulated and measured annual average concentration for the 29 compounds measured at the 10 sites. The simulated annual averages were based on the 24-hour averages calculated for those days when 24-hour average measurements were taken. The comparison between concentration reflects a reasonable degree of agreement, particularly when the prediction and measurement were above the detection limits of the field analysis.

Table V-5a. Performance Statistics for Methyl Chloride ($\mu\text{g}/\text{m}^3$)

	Apr 98	May 98	Jun 98	Jul 98	Aug 98	Sep 98	Oct 98	Nov 98	Dec 98	Jan 99	Feb 99	Mar 99	All
Peak station measurement	1.55	1.86	1.45	1.45	2.48	5.16	1.65	2.07	1.45	1.65	1.65	1.65	5.16
Peak station	Long Be Pico Ri	Pontana Rubidou	Rubidou Compton	Wilming Rubidou	Anaheim Wilming	Compton Compton	Wilming Rubidou	Fontana Anaheim	Fontana Compton	Compton Compton	Fontana Compton	Fontana Wilming	
Peak day (Julian)	113	137	173	197	221	257	281	317	365	24	36	60	281
Accuracy (percent) :													
Paired peak prediction	-20.465	-33.800	-14.810	-14.394	-14.879	-50.161	-76.288	-25.424	-38.208	-13.910	-24.031	-25.363	-76.288
(Peak prediction)	1.23	1.23	1.23	1.24	1.23	1.24	1.22	1.23	1.28	1.24	1.25	1.23	1.22
Temporally-paired peak pred.	-19.948	-33.692	-14.325	-12.664	-14.187	-49.435	-75.707	-24.153	-38.160	-12.249	-24.031	-24.395	-75.707
(Peak prediction)	1.24	1.23	1.24	1.26	1.24	1.24	1.25	1.25	1.28	1.27	1.25	1.25	1.25
(Station at pred. peak)	Central	Central	Central	Hunting	Central	Hunting	Hunting	Hunting	Hunting	Central	Compton	Hunting	Hunting
Spatially-paired peak pred.	-20.207	-33.531	-14.464	-14.325	-14.325	-49.839	-76.036	-25.182	-38.208	-13.910	-24.031	-25.121	-75.688
(Peak prediction)	1.24	1.24	1.24	1.24	1.24	1.24	1.24	1.24	1.28	1.24	1.25	1.24	1.25
(Day of pred. peak)	107	149	167	209	215	245	293	329	365	24	36	78	365
Unpaired peak prediction	-19.561	-33.208	-13.287	-12.664	-13.356	-49.435	-75.688	-23.366	-38.160	-12.249	-24.031	-24.395	-75.262
(Peak prediction)	1.25	1.24	1.25	1.26	1.25	1.25	1.25	1.25	1.27	1.28	1.27	1.25	1.28
(Station at pred. peak)	Burbank	Burbank	Pico Ri	Central	Central	Hunting	Burbank	Hunting	Central	Compton	Hunting	Hunting	
(Day of pred. peak)	119	143	167	197	239	257	293	329	365	24	36	60	365
Average peak prediction	18.145	27.481	12.830	21.160	12.385	36.083	54.076	23.366	31.071	12.332	24.461	24.461	
Normalized systematic bias (%)	9.926	7.709	5.094	43.549	25.139	-5.333	29.376	-9.648	-1.331	2.349	-12.901	-16.935	6.537
Systematic bias ($\mu\text{g}/\text{m}^3$)	0.084	0.049	0.043	0.332	0.226	-0.124	-0.499	-0.179	-0.164	0.013	-0.192	-0.266	-0.067
Variance	0.040	0.063	0.023	0.035	0.027	0.088	0.888	0.050	0.150	0.019	0.012	0.020	0.123
Normalized gross error (%)	17.401	18.749	9.963	44.700	26.683	15.644	72.779	18.645	26.236	8.016	12.982	17.020	25.330
Gross error ($\mu\text{g}/\text{m}^3$)	0.195	0.225	0.113	0.349	0.248	0.224	0.625	0.256	0.330	0.095	0.193	0.267	0.273

Table V-5b. Performance Statistics for Vinyl Chloride ($\mu\text{g}/\text{m}^3$)

	Apr 98	May 98	Jun 98	Jul 98	Aug 98	Sep 98	Oct 98	Nov 98	Dec 98	Jan 99	Feb 99	Mar 99	All
Peak station measurement	0.26	0.26	0.26	0.26	0.26	0.26	0.26	0.26	0.26	0.26	0.26	0.26	0.26
Peak station	Fontana	Fontana	Rubidou										
Peak day (Julian)	113	149	173	209	233	269	299	329	365	365	48	72	72
Accuracy (percent) :													
Paired peak prediction (Peak prediction)	-95.313	-95.313	-95.313	-95.313	-95.313	-95.313	-95.313	-95.313	-95.313	-95.313	-95.313	-95.313	-95.313
Temporally-paired peak pred. (Peak prediction) (Station at pred. peak)	-95.313	-95.313	-94.922	-95.313	-94.922	-94.922	-94.922	-94.922	-94.922	-94.922	-94.531	-94.922	-94.922
Spatially-paired peak pred. (Peak prediction) (Day of pred. peak)	-95.313	-95.313	-95.313	-95.313	-95.313	-95.313	-95.313	-95.313	-95.313	-95.313	-95.313	-95.313	-95.313
Unpaired peak prediction (Peak prediction) (Station at pred. peak) (Day of pred. peak)	-95.313	-94.922	-94.922	-94.922	-94.922	-94.922	-94.922	-94.922	-94.922	-94.922	-94.531	-94.922	-94.531
Average peak prediction	95.313	95.039	95.039	95.000	95.000	95.039	95.039	95.039	95.039	95.039	94.766	95.039	95.029

Normalized systematic bias (%)	-95.313	-95.290	-95.282	-95.281	-95.234	-95.273	-95.241	-95.269	-95.284	-95.273	-95.269	-95.267	-95.271
Systematic bias ($\mu\text{g}/\text{m}^3$)	-0.244	-0.244	-0.244	-0.244	-0.244	-0.244	-0.244	-0.244	-0.244	-0.244	-0.244	-0.244	-0.244
Variance	0.000	0.000	0.000	0.000	0.000	0.000	0.000	0.000	0.000	0.000	0.000	0.000	0.000
Normalized gross error (%)	95.313	95.290	95.282	95.281	95.234	95.273	95.241	95.269	95.284	95.273	95.269	95.267	95.271
Gross error ($\mu\text{g}/\text{m}^3$)	0.244	0.244	0.244	0.244	0.244	0.244	0.244	0.244	0.244	0.244	0.244	0.244	0.244

Table V-5c. Performance Statistics for 1,3 Butadiene ($\mu\text{g}/\text{m}^3$)

	Apr 98	May 98	Jun 98	Jul 98	Aug 98	Sep 98	Oct 98	Nov 98	Dec 98	Jan 99	Feb 99	Mar 99	All
Peak station measurement	1.26	0.66	0.66	1.11	1.77	2.88	3.21	5.31	5.09	3.10	2.83	5.31	
Peak station	Central Pico	Ri	Huntington	Central Huntington	Huntington	Compton	Compton	Compton	Compton	Compton	Huntington	Compton	
Peak day (Julian)	119	137	173	197	233	269	281	329	359	6	42	60	359
Accuracy (percent) :													
Paired peak prediction	-63.125	-84.187	-76.807	-56.781	-81.582	-85.424	-83.136	-63.498	-80.976	-77.752	-75.912	-81.886	-80.976
(Peak prediction)	0.47	0.10	0.15	0.48	0.33	0.26	0.49	1.17	1.01	1.13	0.75	0.51	1.01
Temporally-paired peak pred.	-63.125	-72.289	-53.163	-56.781	-77.740	-82.147	-79.694	-55.393	-74.458	-68.298	-75.912	-75.777	-74.458
(Peak prediction)	0.47	0.18	0.31	0.48	0.39	0.32	0.58	1.43	1.36	1.61	0.75	0.69	1.36
(Station at pred. peak)	Central Anaheim	Anaheim	Central Anaheim	Anaheim	Anaheim	Anaheim	Anaheim	Anaheim	Anaheim	Anaheim	Anaheim	Anaheim	Anaheim
Spatially-paired peak pred.	-63.125	-74.096	-53.765	-56.781	-73.220	-75.650	-81.885	-63.498	-80.524	-77.752	-75.912	-81.886	-77.943
(Peak prediction)	0.47	0.17	0.31	0.48	0.47	0.43	0.52	1.17	1.03	1.13	0.75	0.51	1.17
(Day of pred. peak)	119	149	175	197	239	251	293	329	365	6	42	60	329
Unpaired peak prediction	-63.125	-65.964	-53.163	-56.781	-70.339	-70.508	-79.312	-55.393	-70.823	-68.298	-75.912	-68.362	-69.618
(Peak prediction)	0.47	0.23	0.31	0.48	0.52	0.52	0.60	1.43	1.55	1.61	0.75	0.90	1.61
(Station at pred. peak)	Central Anaheim	Anaheim	Central Central	Central	Central	Central	Anaheim	Anaheim	Anaheim	Anaheim	Compton	Anaheim	Anaheim
(Day of pred. peak)	119	149	173	197	215	251	293	329	365	6	42	72	6
Average peak prediction	62.862	63.647	48.878	56.644	61.734	36.907	79.061	62.137	65.040	66.299	70.755	68.879	61.904
Normalized systematic bias (%)	-22.204	-21.359	-27.670	-26.450	-41.771	-15.786	-45.146	-59.942	-24.986	-41.957	-59.039	1.032	-31.909
Systematic bias ($\mu\text{g}/\text{m}^3$)	-0.270	-0.112	-0.139	-0.120	-0.261	-0.149	-0.573	-0.885	-0.714	-0.753	-0.719	-0.348	-0.447
Variance	0.094	0.024	0.026	0.023	0.085	0.080	0.402	0.394	0.750	0.804	0.369	0.309	0.309
Normalized gross error (%)	71.754	57.087	54.809	37.590	52.881	49.903	55.415	61.568	71.123	52.398	59.726	74.918	58.378
Gross error ($\mu\text{g}/\text{m}^3$)	0.325	0.139	0.172	0.138	0.279	0.199	0.601	0.893	0.815	0.814	0.723	0.434	0.491

Table V-5d. Performance Statistics for Methylene Chloride ($\mu\text{g}/\text{m}^3$)

	Apr	May	Jun	Jul	Aug	Sep	Oct	Nov	Dec	Jan	Feb	Mar	ALL
Peak station measurement	15.99	20.16	8.34	3.48	4.52	7.30	17.38	45.18	8.34	11.12	17.03	4.52	45.18
Peak station	Long Be	Pico	Ri	Central	Burbank	Anaheim	Hunting	Burbank	Hunting	Central	Hunting	Central	Hunting
Peak day (Julian)	113	143	168	197	215	245	287	311	364	6	48	90	311
Accuracy (percent) :													
Paired peak prediction	-97.498	-97.182	-91.440	-32.135	-74.723	-96.232	-90.200	-97.295	-73.372	-75.733	-90.206	-79.593	-97.295
(Peak prediction)	0.40	0.57	0.71	2.36	1.14	0.28	1.70	1.22	2.22	2.70	1.67	0.92	1.22
Temporally-paired peak pred.	-91.756	-95.615	-91.440	-32.135	-57.371	-72.763	-90.200	-96.722	-73.372	-60.016	-86.970	-79.593	-96.722
(Peak prediction)	1.32	0.88	0.71	2.36	1.93	1.99	1.70	1.48	2.22	4.45	2.22	0.92	1.48
(Station at pred. peak)	Central	Burbank	Central	Central	Central	Central	Anaheim	Burbank	Burbank	Anaheim	Central	Anaheim	Burbank
Spatially-paired peak pred.	-95.697	-95.873	-83.887	-32.135	-73.882	-88.533	-84.918	-93.294	-55.401	-72.559	-90.206	-60.248	-91.771
(Peak prediction)	0.69	0.83	1.34	2.36	1.18	0.84	2.62	3.03	3.72	3.05	1.67	1.80	3.72
(Day of pred. peak)	107	149	155	197	233	264	281	329	335	18	48	60	365
Unpaired peak prediction	-90.105	-95.615	-76.957	-32.135	-56.707	-69.790	-84.918	-87.575	-25.081	-60.016	-85.825	-34.639	-86.170
(Peak prediction)	1.58	0.88	1.92	2.36	1.96	2.20	2.62	5.61	6.25	4.45	2.41	2.95	6.25
(Station at pred. peak)	Central	Burbank	Anaheim	Central	Central	Central	Anaheim	Anaheim	Anaheim	Central	Anaheim	Central	Anaheim
(Day of pred. peak)	99	143	161	197	239	251	281	329	359	6	36	78	359
Average peak prediction	86.096	90.866	73.894	33.732	58.424	30.765	74.699	76.088	36.630	47.251	78.119	48.026	61.216
Normalized systematic bias (%)	-32.741	6.542	-51.260	-34.580	-57.555	-41.054	-29.432	-56.673	13.126	-12.320	-39.207	-57.612	-33.138
Systematic bias (ug/m3)	-2.341	-1.844	-1.009	-0.681	-1.212	-0.859	-2.029	-3.420	-0.686	-1.343	-2.248	-1.351	-1.532
Variance	15.847	24.651	1.683	0.262	0.573	1.190	6.272	41.977	3.839	7.011	9.100	0.781	8.490
Normalized gross error (%)	71.672	90.938	56.048	44.857	58.528	48.844	76.344	63.941	80.415	60.731	72.813	62.468	64.835
Gross error (ug/m3)	2.497	2.014	1.049	0.727	1.229	0.920	2.120	3.541	1.420	1.935	2.557	1.444	1.746

Table V-5e. Performance Statistics for 1,1-Dichloroethane ($\mu\text{g}/\text{m}^3$)

	Apr 98	May 98	Jun 98	Jul 98	Aug 98	Sep 98	Oct 98	Nov 98	Dec 98	Jan 99	Feb 99	Mar 99	All
Peak station measurement	0.20	0.20	0.20	0.20	0.20	0.20	0.20	0.20	0.20	0.20	0.20	0.20	0.20
Peak station	Fontana	Fontana	Rubidou										
Peak day (Julian)	113	149	173	209	233	269	299	329	365	24	48	72	72
Accuracy (percent) :													
Paired peak prediction (Peak prediction)	-85.149	-85.149	-85.149	-85.149	-85.149	-85.149	-85.149	-85.149	-85.149	-85.149	-85.149	-85.149	-85.149
0.03	0.03	0.03	0.03	0.03	0.03	0.03	0.03	0.03	0.03	0.03	0.03	0.03	0.03
Temporally-paired peak pred. (Peak prediction) (Station at pred. peak)	-85.149	-85.149	-85.149	-85.149	-85.149	-85.149	-85.149	-85.149	-85.149	-85.149	-85.149	-85.149	-85.149
0.03	0.03	0.03	0.03	0.03	0.03	0.03	0.03	0.03	0.03	0.03	0.03	0.03	0.03
Spatially-paired peak pred. (Peak prediction) (Day of pred. peak)	-85.149	-85.149	-85.149	-85.149	-85.149	-85.149	-85.149	-85.149	-85.149	-85.149	-85.149	-85.149	-85.149
0.03	0.03	0.03	0.03	0.03	0.03	0.03	0.03	0.03	0.03	0.03	0.03	0.03	0.03
Unpaired peak Prediction (Peak prediction) (Station at pred. peak) (Day of pred. peak)	-85.149	-85.149	-85.149	-85.149	-85.149	-85.149	-85.149	-85.149	-85.149	-85.149	-85.149	-85.149	-85.149
0.03	0.03	0.03	0.03	0.03	0.03	0.03	0.03	0.03	0.03	0.03	0.03	0.03	0.03
Average peak prediction	85.149	85.149	85.149	85.149	85.149	85.149	85.149	85.149	85.149	85.149	85.149	85.149	85.149
Normalized systematic bias (%)	-85.149	-85.149	-85.149	-85.149	-85.149	-85.149	-85.149	-85.149	-85.149	-85.149	-85.149	-85.149	-85.149
Systematic bias ($\mu\text{g}/\text{m}^3$)	-0.172	-0.172	-0.172	-0.172	-0.172	-0.172	-0.172	-0.172	-0.172	-0.172	-0.172	-0.172	-0.172
Variance	0.000	9.999	0.000	0.000	0.000	0.000	0.000	0.000	0.000	0.000	0.000	0.000	0.000
Normalized gross error (%)	85.149	85.149	85.149	85.149	85.149	85.149	85.149	85.149	85.149	85.149	85.149	85.149	85.149
Gross error ($\mu\text{g}/\text{m}^3$)	0.172	0.172	0.172	0.172	0.172	0.172	0.172	0.172	0.172	0.172	0.172	0.172	0.172

Table V-5f. Performance Statistics for Chloroform ($\mu\text{g}/\text{m}^3$)

	Apr 98	May 98	Jun 98	Jul 98	Aug 98	Sep 98	Oct 98	Nov 98	Dec 98	Jan 99	Feb 99	Mar 99	All
Peak station measurement	0.73	0.98	1.07	0.83	0.98	0.34	0.98	1.47	0.49	1.17	0.29	0.49	1.47
Peak station	Long Be	Central	Long Be	Hunting	Hunting	Wilming	Hunting	Burbank	Fontana	Hunting	Burbank	Hunting	
Peak day (Julian)	113	125	179	182	233	251	281	317	347	18	54	60	317
Accuracy (percent) :													
Paired Peak prediction (Peak prediction)	-89.481	-92.426	-91.155	-91.084	-92.323	-78.363	-88.843	-94.881	-83.811	-93.686	-74.744	-83.607	-94.881
Temporally-paired Peak pred. (Peak prediction) (Station at pred. peak)	0.08	0.07	0.09	0.07	0.08	0.07	0.11	0.08	0.08	0.07	0.07	0.08	0.08
Spatially-paired peak pred. (Peak prediction) (Day of pred. peak)	-89.481	-92.221	-91.155	-91.084	-86.387	-62.865	-88.843	-93.515	-83.197	-91.809	-68.942	-81.762	-93.515
Unpaired peak prediction (Peak prediction) (Station at pred. peak) (Day of pred. peak)	-87.705	-92.323	-91.155	-90.723	-92.323	-77.778	-88.639	-94.812	-82.582	-93.430	-73.720	-83.402	-94.471
Average peak prediction	86.072	88.922	87.668	74.659	84.691	62.416	83.887	90.849	77.930	81.334	67.747	81.885	80.672
Normalized systematic bias (%)	-60.116	-53.870	-53.418	-49.759	-62.396	-53.501	-66.097	-67.037	-65.178	-66.925	-62.600	-22.937	-56.371
Systematic bias ($\mu\text{g}/\text{m}^3$)	-0.179	-0.158	-0.152	-0.146	-0.200	-0.138	-0.194	-0.234	-0.164	-0.207	-0.145	-0.081	-0.164
Variance	0.022	0.028	0.029	0.015	0.021	0.005	0.019	0.060	0.004	0.033	0.002	0.009	0.018
Normalized gross error (%)	64.754	62.190	60.220	64.692	69.113	63.247	66.097	67.037	65.178	66.925	62.600	56.921	64.121
Gross error ($\mu\text{g}/\text{m}^3$)	0.181	0.162	0.155	0.153	0.203	0.142	0.194	0.234	0.164	0.207	0.145	0.098	0.168

Table V-5g. Performance Statistics for Ethylene Dichloride ($\mu\text{g}/\text{m}^3$)

	Apr 98	May 98	Jun 98	Jul 98	Aug 98	Sep 98	Oct 98	Nov 98	Dec 98	Jan 99	Feb 99	Mar 99	All
Peak station measurement	5.26	6.07	0.20	0.20	0.20	0.20	0.81	0.20	0.20	0.20	0.20	0.20	6.07
Peak station	Long Be	Central Rubidou	Rubidou	Rubidou	Rubidou	Rubidou	Wilming	Rubidou	Rubidou	Rubidou	Rubidou	Rubidou	Central
Peak day (Julian)	113	125	173	209	233	269	281	329	365	24	48	72	125
Accuracy (percent) :													
Paired peak prediction (Peak prediction)	-98.062	-98.320	-49.505	-49.505	-49.010	-49.505	-87.268	-49.505	-49.505	-49.505	-49.505	-49.505	-98.320
	0.10	0.10	0.10	0.10	0.10	0.10	0.10	0.10	0.10	0.10	0.10	0.10	0.10
Temporally-paired peak pred. (Peak prediction) (Station at pred. peak)	-98.062	-98.287	-49.010	-48.515	-48.515	-43.069	-86.650	-45.545	-45.050	-49.010	-49.010	-43.069	-98.287
	0.10	0.10	0.10	0.10	0.10	0.10	0.12	0.11	0.11	0.11	0.10	0.12	0.10
Spatially-paired peak pred. (Peak prediction) (Day of pred. peak)	-98.043	-98.303	-49.010	-49.010	-49.010	-48.515	-87.268	-49.010	-49.010	-49.010	-49.010	-49.010	-98.270
	0.10	0.10	0.10	0.10	0.10	0.10	0.10	0.10	0.10	0.10	0.10	0.10	0.10
Unpaired peak prediction (Peak prediction) (Station at pred. peak) (Day of pred. peak)	-98.024	-98.287	-48.515	-46.535	-48.515	-43.069	-86.650	-42.574	-44.059	-44.059	-45.545	-43.069	-98.089
	0.10	0.10	0.10	0.11	0.11	0.10	0.12	0.11	0.12	0.11	0.11	0.12	0.12
Average Peak Prediction	88.221	93.363	48.861	47.723	48.861	44.802	59.460	44.554	44.951	45.545	46.436	44.752	54.794
Normalized systematic bias (%) Systematic bias ($\mu\text{g}/\text{m}^3$)	-58.199	-52.260	-49.429	-49.228	-49.356	-49.026	-50.636	-48.937	-48.992	-49.233	-49.257	-48.457	-49.850
Variance	-0.924	-0.445	-0.100	-0.099	-0.100	-0.099	-0.126	-0.099	-0.099	-0.099	-0.100	-0.098	-0.162
Normalized gross error (%) Gross error ($\mu\text{g}/\text{m}^3$)	3.419	2.026	0.000	0.000	0.000	0.000	0.017	0.000	0.000	0.000	0.000	0.000	0.272

Table V-5h. Performance Statistics for Benzene ($\mu\text{g}/\text{m}^3$)

	Apr 98	May 98	Jun 98	Jul 98	Aug 98	Sep 98	Oct 98	Nov 98	Dec 98	Jan 99	Feb 99	Mar 99	All
Peak station measurement	5.43	1.66	16.61	3.19	6.39	5.43	11.82	13.74	19.17	22.04	17.89	12.78	22.04
Peak station	Central Long Beach	Anaheim	Burbank	Huntington	Huntington	Wilmington	Huntington	Compton	Compton	Compton	Huntington	Compton	Compton
Peak day (Julian)	119	131	175	191	233	269	281	305	359	6	42	60	6
Accuracy (percent) :													
Paired peak prediction (Peak prediction)	-36.734 3.44	-4.997 1.58	-85.619 2.39	-20.689 2.53	-49.663 3.22	-54.299 2.48	-71.193 3.40	-70.175 4.10	-64.253 6.85	-60.940 8.61	-67.898 5.74	-66.669 5.74	-60.940 4.26
Temporally-paired peak pred. (Peak Prediction) (Station at pred. peak)	-33.254 3.63	12.583 1.87	-85.619 2.39	-2.191 3.13	-45.484 3.48	-48.021 2.82	-62.462 4.44	-68.152 4.38	-47.110 10.14	-48.691 11.31	-67.898 5.74	-55.157 5.73	-48.691 11.31
Spatially-paired peak pred. (Peak prediction) (Day of pred. peak)	-36.734 3.44	-4.997 1.58	-83.452 2.75	-14.523 2.73	-49.663 3.22	-42.239 3.14	-64.721 4.17	-48.009 7.14	-51.649 9.27	-60.940 8.61	-67.641 5.79	-66.669 5.79	-57.955 4.26
Unpaired peak prediction (Peak prediction) (Station at pred. peak) (Day of pred. peak)	-33.254 3.63	27.273 2.11	-80.821 3.19	26.792 4.05	-36.860 4.03	-21.856 4.24	-61.540 4.55	-25.566 10.23	-38.246 11.84	-48.691 11.31	-67.641 5.79	-48.560 6.57	-46.300 11.84
Average peak prediction	31.822	27.952	54.383	25.565	34.128	28.567	56.616	21.438	30.172	44.396	47.887	52.790	37.976
Normalized systematic bias (#) Systematic bias ($\mu\text{g}/\text{m}^3$)	72.998 0.124	195.871 0.762	56.542 0.113	70.332 0.638	12.074 -0.306	63.094 0.464	-3.803 -1.147	-17.891 -1.434	14.260 -0.574	27.016 -0.583	-15.289 -1.370	25.024 -0.626	33.521 -0.403
Variance	1.368	0.187	6.857	0.512	0.926	1.109	5.808	5.092	10.941	13.986	6.863	5.309	5.233
Normalized gross error (#) Gross error ($\mu\text{g}/\text{m}^3$)	98.323 0.969	196.255 0.768	69.067 1.109	77.502 0.832	40.417 0.720	76.712 0.933	40.163 1.871	33.928 2.017	58.847 2.411	65.701 2.721	37.390 1.916	62.584 1.716	65.209 1.581

Table V-5i. Performance Statistics for Carbon Tetrachloride ($\mu\text{g}/\text{m}^3$)

	Apr 98	May 98	Jun 98	Jul 98	Aug 98	Sep 98	Oct 98	Nov 98	Dec 98	Jan 99	Feb 99	Mar 99	ALL
Peak station measurement .	0.94	1.07	0.88	0.75	0.69	0.63	1.26	0.69	0.69	0.82	0.82	0.82	1.26
Peak station .	Fontana	Long Be	Fontana	Hunting	Compton	Rubidou	Wilming	Anaheim	Fontana	Hunting	Rubidou	Rubidou	Wilming
Peak day (Julian)	107	143	155	182	227	269	281	323	336	6	54	78	281
Accuracy (percent) :													
Paired peak prediction (Peak prediction)	-17.691	-27.103	-11.805	2.517	11.561	23.529	-33.943	12.283	-5.012	-5.012	-5.012	-33.943	
0.78	0.78	0.78	0.78	0.77	0.77	0.78	0.83	0.78	0.78	0.78	0.78	0.78	0.83
Temporally-paired peak pred. (Peak prediction) (Station at pred. peak)	-17.161	-27.103	-9.535	2.649	16.908	25.278	-33.943	23.988	22.832	1.345	-3.301	-3.423	-33.943
0.78	0.78	0.80	0.77	0.81	0.79	0.79	0.83	0.86	0.85	0.83	0.79	0.79	0.83
Spatially-paired peak pred. (Peak prediction) (Day of pred. peak)	-17.691	-26.729	-11.691	3.311	12.717	23.529	-33.545	12.861	12.283	-4.768	-5.012	-5.012	-28.855
0.78	0.78	0.78	0.78	0.78	0.78	0.78	0.84	0.78	0.78	0.78	0.78	0.78	0.89
Unpaired peak prediction (Peak prediction) (Station at pred. peak) (Day of pred. peak)	-15.996	-26.729	-8.400	11.126	27.746	33.068	-33.545	23.988	29.335	1.711	-2.078	-2.689	-28.855
0.79	0.78	0.81	0.84	0.88	0.84	0.84	0.84	0.86	0.89	0.83	0.80	0.80	0.89
Average peak prediction	10.827	23.699	6.992	16.926	18.179	31.240	20.973	22.414	17.789	4.021	3.704	3.423	15.016
Normalized systematic bias (%)	12.553	13.276	15.621	25.380	29.011	26.488	26.242	29.038	28.791	43.380	14.375	8.453	24.159
Systematic bias ($\mu\text{g}/\text{m}^3$)	0.071	0.076	0.098	0.156	0.170	0.161	0.152	0.175	0.168	0.131	0.088	0.051	0.132
Variance	0.012	0.013	0.006	0.001	0.003	0.001	0.009	0.002	0.004	0.014	0.007	0.007	0.006
Normalized gross error (%)	16.958	18.133	17.919	25.380	29.011	26.488	27.656	29.038	28.791	44.010	16.144	11.812	25.401
Gross error ($\mu\text{g}/\text{m}^3$)	0.110	0.122	0.117	0.156	0.170	0.161	0.170	0.175	0.168	0.136	0.102	0.079	0.143

Table V-5j. Performance Statistics for Trichloroethene ($\mu\text{g}/\text{m}^3$)

	Apr 98	May 98	Jun 98	Jul 98	Aug 98	Sep 98	Oct 98	Nov 98	Dec 98	Jan 99	Feb 99	Mar 99	ALL
Peak station measurement	1.67	2.15	6.99	2.15	2.69	1.61	4.30	2.69	2.69	5.37	2.96	2.85	6.99
Peak station	Central	Central	Central	Central	Central	Wilming	Central						
Peak day (Julian)	107	137	168	197	233	245	281	317	353	12	42	78	168
Accuracy (percent):													
Paired peak prediction (Peak prediction)	-84.034	-89.395	-97.695	-79.721	-86.230	-72.333	-96.767	-82.062	-84.592	-90.063	-88.227	-88.308	-97.695
	0.27	0.23	0.16	0.44	0.37	0.45	0.14	0.48	0.41	0.53	0.35	0.33	0.16
Temporally-paired peak pred. (Peak prediction)	-84.034	-89.395	-97.695	-79.721	-86.230	-72.333	-92.114	-81.727	-83.178	-90.063	-86.096	-86.973	-97.695
	0.27	0.23	0.16	0.44	0.37	0.45	0.34	0.49	0.45	0.53	0.41	0.37	0.16
(Station at pred. peak)	Central	Central	Central	Central	Central	Central	Burbank	Anaheim	Anaheim	Central	Burbank	Anaheim	Central
Spatially-paired peak pred. (Peak prediction)	-78.752	-89.395	-96.021	-79.721	-83.141	-67.556	-95.162	-72.721	-66.580	-82.229	-84.405	-81.320	-86.330
	0.35	0.23	0.28	0.44	0.45	0.52	0.21	0.73	0.90	0.95	0.46	0.53	0.95
(Day of pred. peak)	95	137	155	197	239	251	293	329	365	18	36	60	18
Unpaired peak prediction (Peak prediction)	-78.752	-88.372	-95.520	-79.721	-83.141	-67.556	-90.277	-69.371	-57.164	-81.076	-83.153	-81.320	-83.524
	0.35	0.25	0.31	0.44	0.45	0.52	0.42	0.82	1.15	1.02	0.50	0.53	1.15
(Station at pred. peak)	Central	Burbank	Burbank	Central	Central	Burbank	Burbank	Anaheim	Anaheim	Burbank	Central	Anaheim	Burbank
(Day of pred. peak)	95	143	167	197	239	251	275	329	365	6	36	60	365
Average peak prediction	76.522	80.241	87.603	72.530	77.757	62.027	82.632	66.359	59.482	77.396	80.303	79.805	75.222
Normalized systematic bias (%)	49.837	-17.385	64.389	-0.133	-5.777	-1.254	-17.774	5.615	106.280	65.492	12.342	45.261	26.736
Systematic bias ($\mu\text{g}/\text{m}^3$)	-0.158	-0.223	-0.224	-0.167	-0.199	-0.127	-0.415	-0.186	-0.081	-0.106	-0.135	-0.063	-0.171
Variance	0.146	0.181	1.422	0.197	0.191	0.076	0.843	0.288	0.258	0.776	0.278	0.163	0.389
Normalized gross error (%)	109.596	68.528	116.549	50.925	56.280	55.104	49.486	52.347	150.409	91.346	54.788	72.529	76.873
Gross error ($\mu\text{g}/\text{m}^3$)	0.253	0.259	0.323	0.206	0.240	0.171	0.456	0.298	0.317	0.329	0.249	0.153	0.273

Table V-5k. Performance Statistics for Toluene ($\mu\text{g}/\text{m}^3$)

	Apr 98	May 98	Jun 98	Jul 98	Aug 98	Sep 98	Oct 98	Nov 98	Dec 98	Jan 99	Feb 99	Mar 99	All
Peak station measurement	30.14	17.71	33.16	19.59	56.90	21.48	43.33	46.35	45.22	75.36	35.04	43.71	75.36
Peak station	Burbank	Pico	Ri	Anaheim	Central	Hunting	Hunting	Hunting	Compton	Compton	Burbank	Compton	Compton
Peak day (Julian)	119	143	175	197	233	269	281	305	359	6	42	60	6
Accuracy (percent) :													
Paired peak prediction (Peak prediction)	-50.438	-66.934	-66.884	15.872	-74.589	-51.942	-59.882	-65.180	-41.021	-58.508	-34.538	-55.654	-58.508
Temporally-paired peak pred. (Peak prediction)	14.94	5.86	10.98	22.70	14.46	10.32	17.38	16.14	26.67	31.27	22.94	19.38	31.27
Spatially-paired peak pred. (Peak prediction)	-41.776	-50.892	-66.884	15.872	-67.007	-20.090	-39.904	-48.896	14.793	-24.796	-34.538	-19.337	-24.796
Unpaired peak prediction (Peak prediction)	17.55	8.70	10.98	22.70	18.77	17.16	26.04	23.68	51.90	56.67	22.94	35.26	56.67
Average peak prediction	42.642	31.764	31.783	18.286	44.989	7.899	36.700	17.988	33.780	42.584	26.066	34.874	30.780
Normalized systematic bias (%)	-6.180	13.938	631.742	30.487	-2.883	69.955	15.387	-10.541	45.962	211.836	13.747	49.693	84.177
Systematic bias ($\mu\text{g}/\text{m}^3$)	-2.191	-0.938	0.639	-0.090	-3.282	1.357	-2.732	-5.055	1.699	2.713	-2.358	-0.901	-0.774
Variance	25.563	11.996	42.961	20.024	62.873	32.635	95.700	120.938	224.518	282.066	82.327	105.436	101.538
Normalized gross error (%)	42.546	57.613	668.465	59.810	46.099	91.628	58.562	44.355	92.419	242.351	65.983	87.142	124.682
Gross error ($\mu\text{g}/\text{m}^3$)	3.849	2.666	4.960	3.723	5.131	4.204	7.818	9.386	11.134	11.938	7.710	7.145	7.057

Table V-51. Performance Statistics for Ethylene Dinormide ($\mu\text{g}/\text{m}^3$)

	Apr 98	May 98	Jun 98	Jul 98	Aug 98	Sep 98	Oct 98	Nov 98	Dec 98	Jan 99	Feb 99	Mar 99	All
Peak station measurement	0.38	0.38	0.38	0.38	0.38	0.38	0.38	0.38	0.38	0.38	0.38	0.38	0.38
Peak station	Fontana	Fontana	Rubidou										
Peak day (Julian)	113	149	173	209	233	269	299	329	365	365	48	72	72
Accuracy (percent) :													
Paired peak prediction (Peak prediction)	-97.917	-97.917	-97.917	-97.656	-97.656	-97.656	-97.656	-97.656	-97.656	-97.917	-97.917	-97.917	-97.917
0.01	0.01	0.01	0.01	0.01	0.01	0.01	0.01	0.01	0.01	0.01	0.01	0.01	0.01
Temporally-paired peak pred. (Peak prediction) (Station at pred. peak)	-97.917	-97.917	-97.917	-97.656	-97.656	-97.656	-97.656	-97.656	-97.656	-97.917	-97.917	-97.917	-97.917
0.01	0.01	0.01	0.01	0.01	0.01	0.01	0.01	0.01	0.01	0.01	0.01	0.01	0.01
Spatially-paired peak pred. (Peak prediction) (Day of pred. peak)	-97.917	-97.917	-97.917	-97.656	-97.656	-97.656	-97.656	-97.656	-97.656	-97.917	-97.917	-97.917	-97.917
0.01	0.01	0.01	0.01	0.01	0.01	0.01	0.01	0.01	0.01	0.01	0.01	0.01	0.01
Unpaired peak prediction (Peak prediction) (Station at pred. peak) (Day of pred. peak)	-97.917	-97.917	-97.917	-97.656	-97.656	-97.656	-97.656	-97.656	-97.656	-97.917	-97.917	-97.917	-97.917
0.01	0.01	0.01	0.01	0.01	0.01	0.01	0.01	0.01	0.01	0.01	0.01	0.01	0.01
Average peak prediction	97.917	97.917	97.917	97.891	97.891	97.891	97.891	97.891	97.891	97.917	97.917	97.917	97.917
Normalized systematic bias (%)	-97.917	-97.917	-97.917	-97.896	-97.896	-97.899	-97.897	-97.897	-97.907	-97.917	-97.902	-97.917	-97.903
Systematic bias ($\mu\text{g}/\text{m}^3$)	-0.376	-0.376	-0.376	-0.376	-0.376	-0.376	-0.376	-0.376	-0.376	-0.376	-0.376	-0.376	-0.376
Variance	0.000	0.000	0.000	0.000	0.000	0.000	0.000	0.000	0.000	0.000	0.000	0.000	0.000
Normalized gross error (%)	97.917	97.917	97.917	97.896	97.891	97.899	97.881	97.897	97.907	97.917	97.902	97.917	97.903
Gross error ($\mu\text{g}/\text{m}^3$)	0.376	0.376	0.376	0.376	0.376	0.376	0.376	0.376	0.376	0.376	0.376	0.376	0.376

Table V-5m. Performance Statistics for Perchloroethylene ($\mu\text{g}/\text{m}^3$)

	Apr 98	May 98	Jun 98	Jul 98	Aug 98	Sep 98	Oct 98	Nov 98	Dec 98	Jan 99	Feb 99	Mar 99	All
Peak station measurement	4.55	2.71	2.51	4.07	13.57	2.71	10.18	17.64	12.21	12.89	5.02	8.82	17.64
Peak station Peak day (Julian)	Burbank 119	Central 125	Central 168	Central 197	Anaheim 233	Burbank 269	Anaheim 293	Burbank 317	Anaheim 364	Burbank 6	Huntington Beach 42	Anaheim 72	Anaheim 317
Accuracy (percent) :													
Paired peak prediction (Peak prediction)	-20.022 3.63	-66.347 0.91	-53.068 1.18	-34.103 2.68	-76.589 3.18	89.458 5.14	-63.646 3.70	-28.334 12.64	-43.694 6.88	-54.865 5.82	-13.050 4.36	31.765 11.62	-28.334 12.64
Temporally-paired Peak pred. (Peak prediction) (Station at pred. peak)	-20.022 3.63	-44.821 1.50	-53.068 1.18	-27.420 2.95	-55.300 6.06	89.458 5.14	-21.985 7.94	-28.334 12.64	-43.694 6.88	2.064 13.15	-13.050 4.36	31.765 11.62	-28.334 12.64
Spatially-paired peak pred. (Peak prediction) (Day of pred. peak)	-20.022 3.63	-56.027 1.19	-38.645 1.54	-34.103 2.68	-76.589 3.18	89.458 5.14	-58.241 4.25	-3.000 17.11	-53.624 11.53	-13.050 5.98	37.956 4.36	-3.000 12.16	-3.000 17.11
Unpaired peak prediction (Peak prediction) (Station at pred. peak) (Day of pred. peak)	-20.022 3.63	40.435 3.81	33.307 3.35	-27.420 2.95	-55.300 6.06	89.458 5.14	-6.654 9.50	-3.000 17.11	21.785 14.87	25.729 16.20	32.676 6.66	37.956 12.16	-3.000 17.11
Average peak prediction	20.022	32.376	31.355	30.052	65.944	55.510	32.447	12.149	13.665	66.007	24.826	42.713	35.589
Normalized systematic bias (%)	145.098	182.092	171.560	112.317	78.152	218.564	58.500	9.825	136.447	346.696	108.132	173.698	145.930
Systematic bias ($\mu\text{g}/\text{m}^3$)	0.218	0.437	0.490	0.241	-0.080	0.697	0.199	-0.575	1.096	1.772	0.473	0.777	0.519
Variance	1.1.231	0.598	0.923	0.557	4.215	0.914	4.981	6.582	11.081	15.155	2.765	5.638	5.037
Normalized gross error (%)	173.553	194.044	183.873	126.128	103.575	230.147	84.592	48.900	167.059	367.379	140.185	190.261	168.507
Gross error ($\mu\text{g}/\text{m}^3$)	0.901	0.669	0.751	0.639	0.998	0.899	1.503	1.595	2.239	2.783	1.249	1.264	1.374

Table V-5n. Performance Statistics for Styrene ($\mu\text{g}/\text{m}^3$)

	Apr 98	May 98	Jun 98	Jul 98	Aug 98	Sep 98	Oct 98	Nov 98	Dec 98	Jan 99	Feb 99	Mar 99	All
Peak station measurement	1.83	1.87	5.96	0.85	3.83	1.70	7.67	34.07	5.11	6.39	5.54	11.93	34.07
Peak station	Long Be Long	Be Central	Rubidou	Anaheim									
Peak day (Julian)	107	143	168	209	233	245	281	329	341	12	48	72	329
Accuracy (percent) :													
Paired peak prediction	-78.482	-97.652	-97.015	-51.995	-89.590	-46.538	-40.498	-73.968	-68.910	-58.444	-73.578	-76.690	-73.968
(Peak prediction)	0.39	0.04	0.18	0.41	0.40	0.91	4.56	8.87	1.59	2.65	1.46	2.78	8.87
Temporally-paired peak pred.	-78.482	-61.900	-97.015	1.291	-69.684	-46.538	-40.498	-73.968	-68.910	-58.444	-65.902	-76.690	-73.968
(Peak prediction)	0.39	0.71	0.18	0.86	1.16	0.91	4.56	8.87	1.59	2.65	1.89	2.78	8.87
(Station at pred. peak)	Long Be Pico	Pico Ri	Central	Anaheim	Hunting	Anaheim	Anaheim	Anaheim	Anaheim	Anaheim	Hunting	Anaheim	Anaheim
Spatially-paired peak pred.	-78.482	-97.118	-97.015	-51.995	-89.590	-46.538	-40.498	-73.968	33.790	68.837	-54.145	-75.725	-68.342
(Peak prediction)	0.39	0.05	0.18	0.41	0.40	0.91	4.56	8.87	6.84	10.79	2.54	2.89	10.79
(Day of pred. peak)	107	131	168	209	233	245	281	329	359	30	54	60	30
Unpaired peak prediction	-65.975	-50.907	-66.544	4.812	-69.684	-37.265	-40.498	-73.968	53.356	68.837	-54.145	-75.725	-68.342
(Peak prediction)	0.62	0.92	2.00	0.89	1.16	1.07	4.56	8.87	7.84	10.79	2.54	2.89	10.79
(Station at pred. peak)	Fontana	Fontana	Pico Ri	Hunting	Hunting	Pico Ri	Anaheim	Anaheim	Hunting	Anaheim	Anaheim	Anaheim	Anaheim
(Day of pred. peak)	113	149	155	182	233	251	281	329	365	30	54	60	30
Average peak prediction	72.493	61.601	65.527	26.819	61.795	67.477	59.313	79.233	41.496	58.139	53.263	72.921	60.006
Normalized systematic bias (%)	-57.826	-24.006	17.152	-9.742	-56.974	-12.086	-44.102	-61.253	28.970	-26.846	8.054	-57.326	-22.234
Systematic bias ($\mu\text{g}/\text{m}^3$)	-0.443	-0.184	-0.154	-0.142	-0.451	-0.203	-1.164	-3.242	-0.131	-0.444	-0.838	-1.284	-0.704
Variance	0.158	0.200	1.348	0.089	0.547	0.186	1.522	39.733	2.980	0.908	2.048	4.416	4.697
Normalized gross error (%)	60.688	77.202	97.802	67.367	60.612	66.922	66.227	66.279	116.587	43.806	95.049	57.492	74.350
Gross error ($\mu\text{g}/\text{m}^3$)	0.450	0.317	0.505	0.270	0.482	0.326	1.282	3.287	0.962	0.579	1.123	1.285	0.900

Table V-50. Performance Statistics for P-Dichlorobenzene ($\mu\text{g}/\text{m}^3$)

	Apr 98	May 98	Jun 98	Jul 98	Aug 98	Sep 98	Oct 98	Nov 98	Dec 98	Jan 99	Feb 99	Mar 99	All
Peak station measurement	1.92	1.80	6.61	3.01	4.81	1.80	3.61	4.21	3.01	1.20	0.60	2.40	6.61
Peak station	Pico Ri	Central	Hunting										
Peak day (Julian)	119	137	173	197	233	245	281	305	353	24	48	60	173
Accuracy (percent) :													
Paired peak prediction	-90.644	-93.126	-98.594	-90.452	-93.950	-83.093	-90.299	-85.792	-86.361	-56.775	-16.306	-78.337	-98.594
(Peak prediction)	0.18	0.12	0.09	0.29	0.29	0.31	0.35	0.60	0.41	0.52	0.50	0.52	0.09
Temporally-Paired peak pred.	-86.227	-92.627	-97.672	-90.452	-93.950	-83.093	-90.299	-85.792	-86.361	-47.049	-16.306	-78.337	-97.672
(Peak prediction)	0.26	0.13	0.15	0.29	0.29	0.31	0.35	0.60	0.41	0.64	0.50	0.52	0.15
(Station at pred. peak)	Burbank	Pico Ri	Anaheim	Hunting	Hunting	Hunting	Hunting	Hunting	Hunting	Central	Hunting	Hunting	Anaheim
Spatially-paired peak pred.	-90.644	-92.572	-97.626	-90.452	-92.827	-83.093	-87.140	-82.300	-61.577	-22.860	-0.998	-78.337	-82.537
(Peak prediction)	0.18	0.13	0.16	0.29	0.34	0.31	0.46	0.75	1.15	0.93	0.60	0.52	1.15
(Day of pred. peak)	119	143	175	197	221	245	293	329	365	18	36	60	365
Unpaired peak prediction	-86.227	-90.687	-95.237	-90.452	-92.827	-83.093	-87.140	-82.300	-61.577	-22.860	6.656	-78.337	-82.537
(Peak prediction)	0.26	0.17	0.31	0.29	0.34	0.31	0.46	0.75	1.15	0.93	0.64	0.52	1.15
(Station at pred. peak)	Burbank	Fontana	Pico Ri	Hunting	Hunting	Hunting	Hunting	Hunting	Hunting	Compton	Hunting	Hunting	
(Day of pred. peak)	119	143	167	197	221	245	293	329	365	18	36	60	365
Average peak prediction	83.881	90.865	92.915	91.001	91.473	70.695	81.342	64.921	120.579	73.568	18.611	59.385	78.270
Normalized systematic bias (%)	-72.642	-82.266	-87.930	-84.346	-88.268	-55.641	-63.187	-54.035	-3.521	4.324	4.378	-40.363	-52.340
Systematic bias ($\mu\text{g}/\text{m}^3$)	-0.582	-0.668	-1.711	-1.187	-1.832	-0.320	-0.851	-0.701	-0.230	-0.051	0.003	-0.333	-0.682
Variance	0.188	0.207	2.714	0.458	1.189	0.104	0.767	0.641	0.623	0.084	0.025	0.242	0.527
Normalized gross error (%)	72.642	82.266	87.930	84.346	88.268	55.641	63.187	54.379	71.774	38.467	38.590	43.763	65.497
Gross error ($\mu\text{g}/\text{m}^3$)	0.582	0.668	1.711	1.187	1.832	0.320	0.851	0.702	0.456	0.179	0.126	0.344	0.723

Table V-5p. Performance Statistics for Formaldehyde ($\mu\text{g}/\text{m}^3$)

	Apr 98	May 98	Jun 98	Jul 98	Aug 98	Sep 98	Oct 98	Nov 98	Dec 98	Jan 99	Feb 99	Mar 99	ALL
Peak station measurement	9.95	3.81	8.84	16.70	12.28	14.00	13.40	10.56	11.55	14.74	8.84	12.28	16.70
Peak station	Central Burbank	Fontana	Burbank	Rubidoux	Huntington	Huntington	Compton	Central Burbank	Burbank	Burbank	Burbank	Burbank	Burbank
Peak day (Julian)	119	143	179	197	215	245	293	325	359	6	48	60	197
Accuracy (percent) :													
Paired peak prediction (Peak prediction)	-35.917	-4.255	-60.455	-58.564	-60.585	-67.624	-44.642	-42.653	-20.728	-36.735	-21.769	-53.371	-58.564
	6.38	3.64	3.50	6.92	4.84	4.53	7.42	6.06	9.15	9.32	6.92	5.73	6.92
Temporally-paired peak pred. (Peak prediction) (Station at pred. peak)	-32.157	-4.255	-41.943	-50.081	-35.230	-33.169	-28.455	-42.653	18.346	5.028	-12.507	-33.423	-50.081
	6.75	3.64	5.13	8.34	7.95	9.36	9.59	6.06	13.66	15.48	7.74	8.18	8.34
Spatially-paired peak pred. (Peak Prediction) (Day of pred. peak)	-35.917	-0.026	-60.455	-58.564	-60.528	-67.624	-44.642	-0.114	2.919	-12.682	-18.444	-52.198	-21.643
	6.38	3.81	3.50	6.92	4.85	4.53	7.42	10.55	11.88	12.87	7.21	5.87	13.09
Unpaired peak prediction (Peak prediction) (Station at pred. peak) (Day of pred. peak)	-32.157	10.165	-32.432	-50.081	-22.130	-33.169	-28.455	31.339	30.931	5.028	3.053	-24.483	-7.328
	6.75	4.19	5.97	8.34	9.56	9.36	9.59	13.87	15.12	15.48	9.11	9.27	15.48
Average peak prediction	31.309	9.152	21.017	50.929	32.878	29.916	40.646	33.324	34.175	10.813	7.428	36.404	28.166
Normalized systematic bias (%)	566.604	91.874	41.268	30.428	116.773	202.238	22.639	97.974	304.5641227.803	617.713	551.559	326.687	
Systematic bias ($\mu\text{g}/\text{m}^3$)	0.830	1.266	0.222	-0.917	-1.921	0.130	-0.428	2.328	2.091	2.333	0.997	1.187	0.706
Variance	5.250	0.921	4.964	8.144	10.210	9.701	9.981	10.653	14.749	17.368	9.334	9.724	9.839
Normalized gross error (%)	581.187	94.510	65.201	71.030	175.673	225.813	51.086	106.925	321.1891244.992	641.858	570.355	350.718	
Gross error ($\mu\text{g}/\text{m}^3$)	2.022	1.361	1.778	2.332	3.132	2.428	2.405	3.014	3.364	3.840	2.631	2.850	2.716

Table V-5q. Performance Statistics for Acetaldehydes ($\mu\text{g}/\text{m}^3$)

	Apr 98	May 98	Jun 98	Jul 98	Aug 98	Sep 98	Oct 98	Nov 98	Dec 98	Jan 99	Feb 99	Mar 99	ALL
Peak station measurement	6.49	2.88	4.86	10.99	18.56	15.31	7.75	8.65	9.01	10.81	5.59	8.29	18.56
Peak station	Central	Central	Fontana	Burbank	Pico Ri	Fontana	Hunting	Central	Compton	Burbank	Burbank	Burbank	Pico Ri
Peak day (Julian)	119	137	179	197	221	245	281	326	359	6	48	60	221
Accuracy (percent) :													
Paired peak prediction (Peak prediction)	-17.253	32.466	-26.871	-42.120	-76.186	-76.211	-25.829	-30.574	-24.944	-30.916	4.584	-31.930	-76.186
5.37	3.82	3.56	6.36	4.42	3.64	5.75	6.00	6.76	7.47	5.84	5.64	4.42	
Temporally-paired Peak pred. (Peak prediction) (Station at pred. peak)	-3.639	41.970	5.263	-42.120	-70.710	-52.031	-13.050	-30.574	7.549	-8.002	13.894	-16.484	-70.710
6.25	4.09	5.12	6.36	5.43	7.35	6.74	6.00	9.69	9.94	6.36	6.92	5.43	
Spatially-paired Peak pred. (Peak prediction) (Day of pred. peak)	-17.253	52.099	-16.961	-42.120	-70.026	-62.727	-10.740	-6.094	7.693	-30.916	4.584	-31.930	-55.044
5.37	4.39	4.04	6.36	5.56	5.71	6.91	8.12	9.70	7.47	5.84	5.64	8.34	
Unpaired peak prediction (Peak prediction) (Station at pred. peak) (Day of pred. peak)	-3.639	55.741	22.245	-42.120	-60.643	-52.031	-4.892	8.684	23.512	-8.002	39.552	-12.622	-40.041
6.25	4.49	5.95	6.36	7.30	7.35	7.37	9.40	11.13	9.94	7.79	7.24	11.13	
Average peak prediction	3.364	59.894	20.145	42.120	52.930	36.042	5.573	9.673	37.720	16.062	28.358	20.790	27.722
Normalized systematic bias (%)	151.060	218.913	167.301	222.931	363.444	367.241	103.492	135.909	371.954	847.743	770.314	485.724	367.148
Systematic bias ($\mu\text{g}/\text{m}^3$)	1.948	2.577	1.816	1.388	0.048	1.533	1.769	2.438	2.850	2.999	2.578	2.450	2.053
Variance	2.052	0.329	2.591	3.902	13.798	10.552	3.595	4.019	7.000	7.674	3.240	3.391	5.479
Normalized gross error (%)	155.758	218.913	174.428	230.959	389.352	379.698	109.780	140.164	376.757	855.209	770.943	490.128	374.619
Gross error ($\mu\text{g}/\text{m}^3$)	2.220	2.577	2.137	1.960	2.554	2.908	2.205	2.742	3.184	3.587	2.607	2.753	2.671

Table V-5r. Performance Statistics for Acetone ($\mu\text{g}/\text{m}^3$)

	Apr 98	May 98	Jun 98	Jul 98	Aug 98	Sep 98	Oct 98	Nov 98	Dec 98	Jan 99	Feb 99	Mar 99	ALL
Peak station measurement	4.82	5.06	3.33	7.63	8.79	7.84	20.19	23.68	20.43	16.39	10.93	13.54	23.68
Peak station	Burbank	Central	Rubidoux	Rubidoux	Fontana	Rubidoux	Burbank	Rubidoux	Hunting	Rubidoux	Fontana	Fontana	Burbank
Peak day (Julian)	113	137	173	209	233	245	281	317	341	12	48	60	317
Accuracy (percent) :													
Paired peak prediction (Peak prediction)	-58.689	-78.340	-26.518	-72.603	-74.718	-84.169	-87.772	-80.290	-80.014	-84.722	-70.248	-89.350	-80.290
	1.99	1.10	2.44	2.09	2.22	1.24	2.47	4.67	4.08	2.50	3.25	1.44	4.67
Temporally-paired peak pred. (Peak prediction) (Station at pred. peak)	-43.198	-78.340	-26.518	-55.357	-55.615	-48.297	-79.644	-72.482	-79.463	-62.396	-61.617	-72.482	
	2.74	1.10	2.44	3.40	3.90	4.05	4.11	6.52	4.17	3.37	4.11	5.20	6.52
Spatially-paired peak pred. (Peak prediction) (Day of pred. peak)	-31.916	-70.059	-1.954	-60.826	-36.466	-58.490	-82.725	-64.966	-56.239	-68.591	-70.248	-65.192	-61.073
	3.28	1.51	3.26	2.99	5.58	3.25	3.49	8.30	8.94	5.15	3.25	4.71	9.22
Unpaired peak prediction (Peak prediction) (Station at pred. peak) (Day of pred. peak)	-27.706	7.115	4.600	-38.072	-36.466	-13.981	-74.033	-59.621	-41.289	-47.474	-49.099	-57.688	-49.356
	3.49	5.42	3.48	4.72	5.58	6.74	5.24	9.56	11.99	8.61	5.56	5.73	11.99
Average peak prediction	28.127	57.455	7.403	60.481	40.977	15.219	74.828	62.294	37.679	15.665	51.069	61.962	42.991
Normalized systematic bias (%)	17.832	4.673	-24.415	11.134	-33.462	29.253	-52.847	-34.028	109.761	140.173	64.128	-32.272	18.620
Systematic bias ($\mu\text{g}/\text{m}^3$)	-0.409	-0.660	-0.614	-0.253	-1.742	-0.337	-6.302	-5.600	-2.310	-0.110	-0.500	-4.237	-2.119
Variance	1.338	2.608	0.487	2.744	4.854	3.810	35.077	40.075	58.860	24.227	11.282	17.188	19.040
Normalized gross error (%)	55.095	65.767	36.969	45.868	50.764	66.087	53.840	53.372	185.525	181.757	103.460	71.782	84.006
Gross error ($\mu\text{g}/\text{m}^3$)	0.852	1.246	0.827	1.108	2.095	1.331	6.328	6.262	5.983	3.711	2.514	4.685	3.376

Table V-5s. Performance Statistics for Methyl Ethyl Ketone ($\mu\text{g}/\text{m}^3$)

	Apr 98	May 98	Jun 98	Jul 98	Aug 98	Sep 98	Oct 98	Nov 98	Dec 98	Jan 99	Feb 99	Mar 99	All
Peak station measurement	2.21	0.86	1.00	1.80	2.95	1.47	3.51	6.46	3.77	3.83	4.42	3.24	6.46
Peak station Peak day (Julian)	Burbank 119	Burbank 143	Fontana 155	Rubidoux 209	Compton 233	Anaheim 257	Burbank 293	Burbank 317	Pico Ri 341	Burbank 6	Burbank 54	Burbank 60	Burbank 317
Accuracy (percent) :													
Paired peak prediction (Peak prediction)	1.627	59.532	-33.500	-30.573	-44.083	17.300	-29.980	-52.121	-54.637	6.079	-78.092	-78.113	-52.121
2.25	1.36	0.67	1.25	1.65	1.73	2.46	3.09	1.71	4.07	0.97	0.71	3.09	
Temporally-paired peak pred. (Peak prediction)	17.541	59.532	72.084	14.452	6.273	73.270	0.684	-21.400	-19.687	49.335	-69.749	24.044	-21.400
2.60	1.36	1.73	2.06	3.13	2.55	3.53	5.08	3.03	5.72	1.34	4.02	5.08	
(Station at pred. peak)	Central	Burbank	Central	Central	Central	Central	Anaheim	Anaheim	Central	Anaheim	Anaheim	Anaheim	Anaheim
Spatially-paired peak pred. (Peak prediction)	1.627	59.532	9.771	-30.573	-44.083	36.431	-20.348	-14.230	6.704	19.958	-30.884	-48.428	-2.075
2.25	1.36	1.10	1.25	1.65	2.01	2.80	5.54	4.03	4.60	3.06	1.67	6.32	
(Day of pred. peak)	119	143	167	209	233	245	281	329	365	24	36	78	335
Unpaired peak prediction (Peak prediction)	17.541	59.532	111.765	98.221	6.273	114.586	0.684	14.122	105.670	65.771	-26.611	38.625	20.192
2.60	1.36	2.12	3.57	3.13	3.16	3.53	7.37	7.76	6.35	3.25	4.50	7.76	
(Station at pred. peak)	Central	Burbank	Pico Ri	Central	Central	Central	Anaheim	Anaheim	Anaheim	Central	Compton	Anaheim	Anaheim
(Day of pred. peak)	119	143	167	197	233	251	293	329	365	24	36	72	365
Average peak prediction	15.949	59.532	205.616	258.528	53.801	131.809	5.797	14.176	123.094	61.190	28.320	25.935	81.979
Normalized systematic bias (%)	140.681	219.716	308.751	436.402	187.482	358.484	221.192	104.650	378.065	417.500	193.008	218.764	273.339
Systematic bias ($\mu\text{g}/\text{m}^3$)	0.529	0.455	0.537	0.954	0.439	0.902	0.790	0.222	1.269	1.246	-0.027	0.437	0.693
Variance	0.429	0.098	0.416	0.599	0.383	0.365	1.016	2.775	5.185	3.948	1.779	1.249	1.866
Normalized gross error (%)	143.436	219.716	319.199	438.511	198.185	360.322	232.962	133.342	404.407	439.393	243.582	238.096	291.547
Gross error ($\mu\text{g}/\text{m}^3$)	0.555	0.455	0.622	0.992	0.623	0.925	1.104	1.212	1.783	1.762	1.043	0.872	1.114

Table V-5t. Performance Statistics for Organic Carbon ($\mu\text{g}/\text{m}^3$)

	Apr 98	May 98	Jun 98	Jul 98	Aug 98	Sep 98	Oct 98	Nov 98	Dec 98	Jan 99	Feb 99	Mar 99	All
Peak station measurement	9.79	4.88	9.33	15.16	12.42	12.39	12.81	21.10	19.70	26.13	11.13	11.69	26.13
Peak station	Fontana	Central	Fontana	Fontana	Rubidou	Rubidou	Fontana	Fontana	Hunting	Hunting	Hunting	Hunting	
Peak day (Julian)	119	137	179	197	215	245	293	311	336	6	42	60	6
Accuracy (percent) :													
Paired peak prediction	-56.241	-36.885	-6.131	-53.173	-52.053	-59.540	-26.386	-70.066	-46.761	-57.313	-42.920	-49.760	-57.313
(Peak prediction)	4.28	3.08	8.76	7.10	5.95	5.01	9.43	6.32	10.49	11.15	6.35	5.87	11.15
Temporally-paired peak pred.	-36.742	3.012	-6.131	-42.982	-44.887	-50.880	-26.386	-55.066	-21.660	-21.370	-42.354	-0.222	-21.370
(Peak prediction)	6.19	5.03	8.76	8.64	6.84	6.09	9.43	9.48	15.43	20.55	6.42	11.66	20.55
(Station at pred. peak)	Central	Rubidou	Fontana	Central	Central	Central	Rubidou	Rubidou	Anaheim	Anaheim	Burbank	Anaheim	Anaheim
Spatially-paired peak pred.	-48.938	-26.721	-6.131	-48.780	-44.235	0.783	-26.386	-60.749	-46.761	-57.313	-40.099	-49.427	-49.977
(Peak prediction)	5.00	3.58	8.76	7.76	6.93	12.49	9.43	8.28	10.49	11.15	6.67	5.91	13.07
(Day of pred. peak)	101	143	179	191	218	248	293	329	336	6	48	84	365
Unpaired peak prediction	-36.742	88.934	-6.131	-42.982	-40.089	0.783	-1.429	-13.479	-6.660	-21.370	0.764	-0.222	-21.370
(Peak prediction)	6.19	9.22	8.76	8.64	7.44	12.49	12.63	18.26	18.39	20.55	11.22	11.66	20.55
(Station at pred. peak)	Central	Fontana	Central	Fontana	Central	Rubidou	Fontana	Anaheim	Anaheim	Anaheim	Rubidou	Anaheim	Anaheim
(Day of pred. peak)	119	149	179	197	227	248	275	329	365	6	48	60	6
Average peak prediction	25.354	32.794	6.878	26.069	27.250	15.240	17.465	14.623	7.789	14.758	10.938	16.449	17.905
Normalized systematic bias (%)	4.133	16.282	23.210	-23.986	-31.833	7.394	7.391	-5.881	5.472	34.740	9.912	14.933	4.218
Systematic bias ($\mu\text{g}/\text{m}^3$)	-0.183	0.522	0.389	-1.955	-2.547	-0.246	-0.155	-1.306	-0.783	1.103	-0.244	0.254	-0.503
Variance	2.666	2.605	2.937	4.785	3.880	6.828	7.697	18.394	21.512	26.054	10.422	7.230	9.870
Normalized gross error (%)	26.906	32.259	43.195	30.821	33.170	40.270	34.630	33.163	49.983	54.478	52.820	43.223	40.169
Gross error ($\mu\text{g}/\text{m}^3$)	1.128	1.021	1.409	2.220	2.613	1.983	2.390	3.150	3.765	3.738	2.683	2.034	2.447

Table V-5u. Performance Statistics for Elemental Carbon ($\mu\text{g}/\text{m}^3$)

	Apr 98	May 98	Jun 98	Jul 98	Aug 98	Sep 98	Oct 98	Nov 98	Dec 98	Jan 99	Feb 99	Mar 99	ALL
Peak station measurement	4.63	1.72	4.14	8.29	6.34	5.94	10.15	9.02	13.40	10.57	6.89	6.01	13.40
Peak station	Central Fontana	Fontana	Rubidoux	Huntington	Rubidoux	Pico Ri	Huntington	Fontana	Huntington	Huntington	Huntington	Huntington	Fontana
Peak day (Julian)	119	149	173	197	233	245	281	329	336	6	42	60	336
Accuracy (percent) :													
Paired peak prediction (Peak prediction)	-7.862	89.186	-46.014	-65.127	-41.215	-55.152	-62.059	-20.987	-58.970	-29.565	-33.962	-38.336	-58.970
Temporally-paired peak pred. (Peak prediction) (Station at pred. peak)	4.27	3.25	2.23	2.89	3.73	2.66	3.85	7.13	5.50	7.45	4.55	3.71	5.50
Spatially-paired peak pred. (Peak prediction) (Day of pred. peak)	-7.862	89.186	-22.440	-31.556	-32.145	-26.818	-44.985	17.905	-32.321	11.050	-33.962	0.982	-32.321
Unpaired peak prediction (Peak prediction) (Station at pred. peak) (Day of pred. peak)	4.27	3.25	3.21	5.67	4.30	4.35	5.58	10.64	9.07	11.74	4.55	6.07	9.07
Average peak prediction	7.862	89.186	-34.493	-62.388	-41.215	-46.364	-57.507	-20.987	-58.970	-29.565	-30.044	-35.092	-47.373
Normalized systematic bias (%)	60.829	95.497	35.442	-9.150	-0.929	47.454	9.377	-6.572	21.667	40.725	22.457	53.163	27.902
Systematic bias ($\mu\text{g}/\text{m}^3$)	0.705	0.887	0.212	-0.564	-0.501	0.458	-0.473	-0.745	-0.318	0.500	0.170	0.665	0.029
Variance	0.449	0.206	1.146	1.266	1.140	1.692	4.917	4.302	7.704	8.283	2.474	1.487	3.065
Normalized Gross error (%)	64.818	95.497	56.038	22.895	31.613	60.597	41.766	34.535	60.089	66.609	48.766	63.148	52.423
Gross error (ng/m^3)	0.839	0.887	0.888	0.846	0.878	1.029	1.726	1.699	2.147	2.158	1.254	1.104	1.323

Table V-5v. Performance Statistics for Hexavalent Chromium ($\eta\text{g/m}^3$)

	Apr	May	Jun	Jul	Aug	Sep	Oct	Nov	Dec	Jan	Feb	Mar	Mar	All
Peak station measurement	0.60	0.20	0.30	0.44	0.71	0.58	0.80	0.72	0.92	0.70	1.10	0.46	1.10	
Peak station	Burbank	Rubidou	Burbank	Fontana	Wilming	Rubidou	Rubidou	Hunting	Hunting	Anheim	Compton	Burbank	Compton	
Peak day (Julian)	95	149	167	197	221	257	293	317	341	30	42	84	42	
Accuracy (percent) :														
Paired peak prediction (Peak prediction)	-66.333	-70.500	-52.333	-40.227	-75.634	-90.000	-82.125	-26.528	-51.951	-77.286	-72.182	-44.783	-72.182	
0.20	0.06	0.14	0.26	0.17	0.06	0.14	0.14	0.53	0.39	0.16	0.31	0.25	0.31	
Temporally-paired peak pred. (Peak prediction)	-52.500	13.000	-26.000	-12.273	-63.099	24.310	18.625	61.667	5.122	71.857	-56.273	0.217	-56.273	
0.28	0.23	0.22	0.39	0.26	0.72	0.95	1.16	0.86	1.20	0.48	0.46	0.46	0.48	
(Station at pred. peak)	Long Be	Fontana	Pico	Ri	Central	Pico	Ri	Wilming	Wilming	Burbank	Wilming	Hunting	Wilming	
Spatially-paired peak pred. (Peak prediction)	-55.167	-70.500	-52.333	-40.227	27.042	-81.897	-82.125	-13.056	42.439	-65.429	-68.091	-23.261	-50.727	
0.27	0.06	0.14	0.26	0.90	0.10	0.14	0.14	0.63	1.17	0.24	0.35	0.35	0.54	
(Day of pred. peak)	107	149	167	197	233	264	293	329	365	24	36	78	365	
Unpaired peak Prediction (Peak prediction)	-4.500	13.000	-26.000	18.409	27.042	24.310	26.625	61.667	108.415	85.000	-48.636	4.130	55.364	
0.57	0.23	0.22	0.52	0.90	0.72	1.01	1.16	1.71	1.29	0.56	0.48	1.71	0.058	
(Station at pred. peak)	Long Be	Fontana	Pico	Ri	Compton	Wilming	Wilming	Wilming	Wilming	Wilming	Hunting	Wilming		
(Day of pred. peak)	107	149	167	209	233	257	275	317	365	6	36	60	365	
Average peak prediction	13.467	15.200	30.100	42.848	16.405	35.819	34.579	46.939	108.087	106.161	39.145	10.826	41.631	
Normalized systematic bias (%)	105.556	-19.119	-12.522	2.189	72.796	41.662	111.498	125.663	204.341	173.570	24.633	58.632	82.152	
Systematic bias (ug/m3)	0.078	-0.048	-0.034	-0.013	0.041	0.017	0.086	0.140	0.166	0.134	-0.041	0.058	0.058	
Variance	0.041	0.007	0.005	0.012	0.030	0.034	0.057	0.073	0.145	0.111	0.068	0.014	0.054	
Normalized gross error (%)	126.944	50.548	46.417	51.120	99.869	95.054	135.448	146.749	247.269	203.801	84.200	81.066	121.102	
Gross error (ug/m3)	0.155	0.081	0.068	0.087	0.117	0.129	0.183	0.201	0.280	0.264	0.186	0.099	0.161	

Table V-5w. Performance Statistics for Arsenic ($\mu\text{g}/\text{m}^3$)

	Apr 98	May 98	Jun 98	Jul 98	Aug 98	Sep 98	Oct 98	Nov 98	Dec 98	Jan 99	Feb 99	Mar 99	ALI
Peak station measurement	3.00	1.50	4.00	1.50	1.50	4.00	3.00	1.50	5.00	1.50	4.00	5.00	
Peak station	Fontana	Rubidoux	Rubidoux	Rubidoux	Rubidoux	Fontana	Hunting	Rubidoux	Fontana	Rubidoux	Compton	Fontana	
Peak day (Julian)	119	150	179	197	233	263	275	311	365	30	54	90	30
Accuracy (percent) :													
Paired peak prediction	-68.033	-38.267	-80.700	-11.000	-17.800	-44.800	-6.575	83.567	4.267	-70.300	-25.657	-88.625	-70.300
(Peak prediction)	0.96	0.93	0.77	1.34	1.23	0.83	3.74	5.51	1.56	1.49	1.12	0.46	1.49
Temporally-paired peak pred.	-35.200	-38.267	-71.375	77.533	276.600	-21.067	72.350	83.567	1617.400	-27.400	74.067	36.000	-27.400
(Peak prediction)	1.94	0.93	1.14	2.66	5.65	1.18	6.89	5.51	25.76	3.63	2.61	5.44	3.63
(Station at pred. peak)	Central	Rubidoux	Central	Central	Hunting	Central	Hunting	Hunting	Hunting	Compton	Compton	Hunting	Compton
Spatially-paired peak pred.	-51.400	-38.267	-76.100	-3.800	-15.933	-16.600	-6.575	209.867	19.800	-32.380	-25.667	-52.525	-25.260
(Peak prediction)	1.46	0.93	0.96	1.44	1.26	1.25	3.74	9.30	1.80	3.38	1.12	1.90	3.74
(Day of pred. peak)	113	150	161	191	215	259	275	305	336	24	54	84	275
Unpaired peak prediction	-35.200	69.467	25.800	82.533	276.600	220.800	107.200	209.867	1617.400	82.860	141.800	99.175	415.220
(Peak prediction)	1.94	2.54	5.03	2.74	5.65	4.81	8.29	9.30	25.76	9.14	3.63	7.97	25.76
(Station at pred. peak)	Central	Fontana	Hunting	Fontana	Hunting	Hunting	Hunting	Hunting	Hunting	Hunting	Hunting	Hunting	Hunting
(Day of pred. peak)	119	149	173	203	233	269	281	305	365	18	42	78	365
Average peak prediction	29.847	26.720	32.320	72.927	123.313	102.447	145.207	166.007	753.513	77.916	83.747	56.990	139.761
Normalized systematic bias (%)	-33.905	-47.239	-26.854	-19.391	-23.184	-19.845	40.535	73.224	74.917	63.737	-9.310	0.170	13.231
Systematic bias ($\mu\text{g}/\text{m}^3$)	-0.555	-0.709	-0.510	-0.291	-0.348	-0.298	0.604	1.130	1.124	0.933	-0.140	-0.044	0.184
Variance	0.212	0.263	1.162	0.337	0.735	0.648	2.500	3.607	15.009	3.578	0.805	2.396	3.091
Normalized gross error (%)	36.595	54.551	49.592	36.539	44.270	43.115	57.305	88.354	108.093	77.886	49.362	57.188	61.166
Gross error ($\mu\text{g}/\text{m}^3$)	0.595	0.818	0.851	0.548	0.664	0.647	0.863	1.357	1.621	1.310	0.740	0.904	0.949

Table V-5x. Performance Statistics for Chromium ($\mu\text{g}/\text{m}^3$)

	Apr 98	May 98	Jun 98	Jul 98	Aug 98	Sep 98	Oct 98	Nov 98	Dec 98	Jan 99	Feb 99	Mar 99	All
Peak station measurement	19.00	14.47	9.00	20.00	21.47	10.00	18.51	37.00	29.75	38.00	37.00	16.00	38.00
Peak station	Fontana	Fontana	Huntington	Fontana	Huntington	Burbank	Huntington	Huntington	Huntington	Huntington	Pico	Ri	Hunting
Peak day (Julian)	119	149	179	191	233	251	293	323	341	6	54	78	6
Accuracy (percent) :													
Paired peak prediction (Peak prediction)	-61.837	-11.645	-42.322	-31.640	-23.391	31.730	8.239	-30.914	-40.084	-9.839	-69.573	-14.644	-9.839
7.25	12.78	5.19	13.67	16.45	13.17	20.03	25.56	17.83	34.26	11.26	13.66	34.26	
Temporally-paired peak pred. (Peak prediction) (Station at pred. peak)	-12.421	-11.645	59.100	-31.640	-15.198	58.590	39.060	-10.105	-12.978	55.029	-50.589	68.950	55.029
16.64	12.78	14.32	13.67	18.21	15.90	25.74	33.26	25.89	58.91	18.28	27.03	58.91	
Spatially-paired peak pred. (Peak prediction) (Day of pred. peak)	-50.221	-11.645	-13.989	-27.885	-23.391	61.690	8.239	-17.457	53.906	-9.839	-55.119	3.575	20.492
9.46	12.78	7.74	14.42	16.45	16.17	20.03	30.54	45.79	34.26	16.61	16.57	45.79	
Unpaired peak prediction (Peak prediction) (Station at pred. peak) (Day of pred. peak)	-12.421	-11.645	72.744	14.260	-15.198	123.540	39.060	34.243	73.852	55.029	-34.751	68.950	55.029
16.64	12.78	15.55	22.85	18.21	22.35	25.74	49.67	51.72	58.91	24.14	27.03	58.91	
Average peak prediction	17.570	149.729	140.002	66.125	32.944	92.615	94.629	100.669	321.650	70.718	49.035	52.235	99.231
Normalized systematic bias (%)	418.007	419.410	373.023	444.271	313.542	663.914	665.6561488.32211129.9501028.273	290.603	586.935	702.673			
Systematic bias ($\mu\text{g}/\text{m}^3$)	4.996	4.923	5.626	5.320	4.615	8.312	11.094	17.308	15.476	17.530	2.612	7.228	9.557
Variance	32.141	7.482	14.503	31.245	26.931	27.366	35.276	132.777	152.833	122.265	91.400	52.748	63.980
Normalized gross error (%)	427.829	420.635	376.032	450.457	321.375	668.095	665.8571491.1881131.5871029.455	312.100	595.844	707.774			
Gross error ($\mu\text{g}/\text{m}^3$)	6.518	5.100	5.889	6.103	5.522	8.508	11.112	17.986	15.963	17.825	6.820	8.089	10.289

Table V-5y. Performance Statistics Lead - Point Source ($\mu\text{g}/\text{m}^3$)

	Apr 98	May 98	Jun 98	Jul 98	Aug 98	Sep 98	Oct 98	Nov 98	Dec 98	Jan 99	Feb 99	Mar 99	ALL
Peak station measurement	29.00	14.00	23.00	46.00	50.00	35.00	45.00	56.00	53.00	63.00	51.00	40.00	63.00
Peak station	Central Burbank	Huntington	Fontana	Pico Ri	Burbank	Hunting	Hunting	Hunting	Hunting	Rubidoux	Compton	Hunting	
Peak day (Julian)	119	143	179	191	215	251	299	323	359	6	54	90	6
Accuracy (percent):													
Paired peak prediction (Peak prediction)	-79.541 5.93	-98.586 0.20	-98.096 0.44	-91.385 3.96	-97.310 1.35	-99.726 0.10	-90.453 4.30	-88.911 6.21	-93.457 3.47	-88.900 6.99	-98.953 0.53	-98.955 0.42	-88.900 6.99
Temporally-paired peak pred. (Peak prediction) (Station at pred. peak)	-79.541 5.93	-93.250 0.94	-89.161 2.49	-81.026 8.73	-94.564 2.72	-83.060 5.93	-78.591 9.63	-60.155 22.31	-80.732 10.21	-78.041 13.83	-86.402 6.93	-82.823 6.87	-78.041 13.83
Spatially-paired peak pred. (Peak prediction) (Day of pred. peak)	-79.421 5.97	-97.686 0.32	-88.470 1.73	-89.891 2.65	-64.264 4.65	-98.857 17.87	-85.989 0.40	-87.970 6.30	-80.960 6.74	-88.900 10.09	-98.953 6.99	-94.945 0.53	-83.983 2.02
Unpaired peak prediction (Peak prediction) (Station at pred. peak) (Day of pred. peak)	-70.969 8.42	-65.257 4.86	-59.783 9.25	-61.846 17.55	-64.264 17.87	-58.440 14.55	-42.347 25.94	-39.564 33.84	-57.453 22.55	-44.192 35.16	-75.431 12.53	-25.575 29.77	-44.192 35.16
Average peak prediction	79.478	68.500	56.405	59.061	70.694	62.482	33.864	39.134	39.807	39.345	71.135	34.966	54.700
Normalized systematic bias (%) Systematic bias ($\mu\text{g}/\text{m}^3$)	-86.237 -13.955	-53.050 -6.740	-81.391 -7.864	-86.929 -17.647	-91.473 -19.054	-84.635 -9.340	-76.496 -14.596	-81.795 -20.091	-83.350 -19.704	-75.503 -21.730	-91.229 -21.730	-82.387 -24.777	-82.639 -12.220
Variance	55.513	38.522	32.664	117.070	157.745	78.229	62.079	193.822	140.751	282.259	230.658	64.269	121.532
Normalized gross error (%) Gross error ($\mu\text{g}/\text{m}^3$)	86.237 13.955	100.783 7.695	81.391 7.864	86.929 17.647	91.473 19.054	84.635 9.340	77.369 14.727	82.032 20.144	83.350 19.704	76.307 21.963	91.229 24.777	82.387 12.220	84.134 16.304

Table V-5z. Performance Statistics for Lead – Total ($\mu\text{g}/\text{m}^3$)

	Apr 98	May 98	Jun 98	Jul 98	Aug 98	Sep 98	Oct 98	Nov 98	Dec 98	Jan 99	Feb 99	Mar 99	All
Peak station measurement	29.00	14.00	23.00	46.00	50.00	35.00	45.00	56.00	53.00	63.00	51.00	40.00	63.00
Peak station	Central Burbank	Burbank	Fontana	Pico R.	Burbank	Hunting	Hunting	Hunting	Hunting	Rubidou	Compton	Hunting	
Peak day (Julian)	119	143	179	191	215	251	299	323	359	6	54	90	6
Accuracy (percent) :													
Paired peak prediction	118.783	201.721	-16.643	5.274	-28.690	31.960	6.718	44.961	23.592	83.235	-15.608	-58.257	83.235
(Peak prediction)	63.45	42.24	19.17	48.43	35.65	46.19	48.02	81.18	65.50	115.44	43.04	16.70	115.44
Temporally-paired peak pred.	118.783	201.721	138.513	5.502	9.666	75.617	48.018	105.093	23.592	261.432	41.300	-26.347	261.432
(Peak prediction)	63.45	42.24	54.86	48.53	54.83	61.47	66.61	114.85	65.50	227.70	72.06	29.46	227.70
(Station at pred. peak)	Central Burbank	Anaheim	Central	Anaheim	Anaheim	Central	Compton	Hunting	Anaheim	Anaheim	Central	Anaheim	
Spatially-paired peak pred.	118.783	201.721	5.357	10.050	29.120	57.057	45.049	70.423	149.408	83.235	-15.608	88.018	109.819
(Peak prediction)	63.45	42.24	24.23	50.62	64.56	54.97	65.27	95.44	132.19	115.44	43.04	75.21	132.19
(Day of pred. peak)	119	143	175	209	233	245	293	329	365	6	54	60	365
Unpaired peak prediction	118.783	201.721	160.557	114.128	44.376	146.260	119.902	233.605	241.019	261.432	73.141	164.636	261.432
(Peak prediction)	63.45	42.24	59.93	98.50	72.19	86.19	98.96	186.82	180.74	227.70	88.30	105.85	227.70
(Station at pred. peak)	Central Burbank	Anaheim	Central	Anaheim	Anaheim	Anaheim	Anaheim	Anaheim	Anaheim	Anaheim	Compton	Anaheim	Anaheim
(Day of pred. peak)	119	143	173	197	233	257	281	329	365	6	48	78	6
Average peak prediction	120.092	201.721	182.289	152.726	50.669	117.583	178.914	279.113	403.465	248.054	120.821	187.911	186.433
Normalized systematic bias (%)	211.435	426.314	420.092	187.248	122.831	318.769	252.053	214.607	258.220	337.360	69.914	209.934	240.390
Systematic bias ($\mu\text{g}/\text{m}^3$)	21.814	20.983	21.422	15.902	13.503	20.995	38.298	38.703	42.950	66.544	14.557	19.124	28.923
Variance	149.338	70.852	161.545	163.714	210.521	205.361	268.604	536.6151099.9751997.182	195.408	475.767	505.626		
Normalized gross error (%)	211.451	426.314	421.942	187.511	131.114	318.769	252.053	214.607	258.220	337.360	77.148	214.549	242.760
Gross error ($\mu\text{g}/\text{m}^3$)	21.818	20.983	21.847	15.999	16.821	20.995	38.298	38.703	42.950	66.544	15.674	20.829	29.674

Table V-5aa. Performance Statistics for Nickel ($\mu\text{g}/\text{m}^3$)

	Apr 98	May 98	Jun 98	Jul 98	Aug 98	Sep 98	Oct 98	Nov 98	Dec 98	Jan 99	Feb 99	Mar 99	Apr 99
Peak station measurement	38.00	18.44	19.61	27.16	18.00	24.28	30.17	24.92	153.25	25.69	19.00	19.56	153.25
Peak station	Central	Fontana	Central	Hunting	Hunting	Wilming	Compton	Burbank	Pico Ri	Wilming	Hunting	Wilming	Pico Ri
Peak day (Julian)	119	149	161	197	239	245	293	329	341	12	54	60	341
Accuracy (percent) :													
Paired peak prediction (Peak prediction)	-81.863	-69.094	-84.722	-72.066	-64.450	-67.306	-63.427	-26.264	-95.507	-28.167	-79.589	-36.846	-95.507
Temporally-paired peak pred. (Peak prediction) (Station at pred. peak)	6.89	5.70	3.00	7.59	6.40	7.94	11.03	18.38	6.89	18.45	3.88	12.35	6.89
Spatially-paired peak pred. (Peak prediction) (Day of pred. peak)	-62.292	-69.094	-79.730	-67.629	-13.017	-65.548	-59.088	-11.007	-90.786	-28.167	-31.163	-21.682	-90.786
Unpaired peak Prediction (Peak prediction) (Station at pred. peak) (Day of pred. peak)	14.33	5.70	3.97	8.79	15.66	8.36	12.34	22.18	14.12	18.45	13.08	15.32	14.12
Average peak prediction	57.783	24.164	35.619	55.600	18.534	27.122	49.289	20.152	55.388	34.428	31.781	31.788	36.824
Normalized systematic bias (%)	70.482	12.255	21.613	-41.051	-27.451	-23.825	18.346	34.756	167.892	158.052	2.435	60.895	42.272
Systematic bias ($\mu\text{g}/\text{m}^3$)	-2.479	-1.804	-1.578	-5.699	-3.167	-3.346	-1.332	0.748	0.386	4.599	-0.292	0.663	-0.971
Variance	67.029	15.129	31.244	32.200	19.345	33.908	57.217	38.665	595.227	54.978	26.394	10.354	95.490
Normalized gross error (%)	123.582	79.595	71.646	46.107	39.863	47.717	57.197	61.727	198.029	176.712	43.393	85.934	88.593
Gross error ($\mu\text{g}/\text{m}^3$)	5.165	3.255	3.977	5.974	4.179	4.924	5.603	4.933	10.464	7.157	3.484	2.761	5.405

Table V-5ab. Performance Statistics for Selenium ($\mu\text{g}/\text{m}^3$)

	Apr 98	May 98	Jun 98	Jul 98	Aug 98	Sep 98	Oct 98	Nov 98	Dec 98	Jan 99	Feb 99	Mar 99	Apr 99
Peak station measurement	3.97	5.41	3.58	19.99	9.02	6.00	20.69	16.27	7.44	8.00	4.00	4.12	20.69
Peak station	Pico Ri	Fontana	Fontana	Hunting	Hunting	Pico Ri	Hunting	Hunting	Hunting	Long Be	Compton	Hunting	
Peak day (Julian)	119	149	161	197	233	251	293	329	341	6	54	72	293
Accuracy (percent) :													
Paired peak prediction (Peak prediction)	-84.383	-53.623	-72.849	-90.520	15.344	-71.200	-60.875	-23.596	0.954	66.500	-80.850	-61.286	-60.875
	0.62	2.51	0.97	1.89	10.40	1.73	8.10	12.43	7.51	13.32	0.77	1.60	8.10
Temporally-paired peak pred. (Peak prediction) (Station at pred. peak)	-81.562	-53.623	-22.039	-90.520	15.344	-71.200	-60.875	-23.596	0.954	66.500	1.575	-61.286	-60.875
	0.73	2.51	2.79	1.89	10.40	1.73	8.10	12.43	7.51	13.32	4.06	1.60	8.10
Spatially-paired peak pred. (Peak prediction) (Day of pred. peak)	-80.655	-53.623	-41.648	-90.520	15.344	-49.267	-23.765	5.280	513.212	94.813	-77.100	-61.286	120.507
	0.77	2.51	2.09	1.89	10.40	3.04	15.77	17.13	45.62	15.59	0.92	1.60	45.62
Unpaired peak prediction (Peak prediction) (Station at pred. peak) (Day of pred. peak)	-47.582	-53.623	162.095	-80.030	15.344	45.850	-23.765	5.280	513.212	94.813	49.300	264.563	120.507
	2.08	2.51	9.38	3.99	10.40	8.75	15.77	17.13	45.62	15.59	5.97	15.02	45.62
Average peak prediction	46.309	56.139	92.231	77.522	44.560	54.390	48.023	37.753	220.415	56.753	41.326	142.180	76.631
Normalized systematic bias (%)	-41.222	-58.945	24.292	-46.246	-62.616	1.496	109.312	19.196	219.225	86.550	-4.023	57.432	38.829
Systematic bias ($\mu\text{g}/\text{m}^3$)	-0.857	-0.901	-0.531	-2.095	-1.483	-0.784	-0.247	-0.558	0.795	1.066	-0.092	0.290	-0.377
Variance	0.963	0.948	4.939	11.818	1.902	3.556	20.592	14.503	54.200	8.776	2.335	8.389	13.022
Normalized gross error (%)	69.013	63.997	145.648	77.365	66.745	105.604	193.041	86.270	291.170	110.107	77.865	140.101	129.231
Gross error ($\mu\text{g}/\text{m}^3$)	0.998	0.926	1.536	2.376	1.600	1.333	2.640	2.334	2.659	1.327	1.075	1.372	1.790

Table V-5ac. Performance Statistics for Cadmium ($\mu\text{g}/\text{m}^3$)

	Apr 98	May 98	Jun 98	Jul 98	Aug 98	Sep 98	Oct 98	Nov 98	Dec 98	Jan 99	Feb 99	Mar 99	ALL
Peak station measurement	5.00	5.00	5.00	5.00	5.00	5.00	5.00	5.00	5.00	5.00	5.00	5.00	192.74
Peak station Peak day (Julian)	113	150	161	197	233	259	299	317	365	365	48	84	317
Accuracy (percent) :													
Paired peak prediction (Peak prediction)	-71.460	-79.360	-79.580	-68.360	-72.900	-70.820	-58.580	-98.903	-63.420	-43.360	-77.260	-94.710	-98.903
	1.43	1.03	1.02	1.58	1.36	1.46	2.07	2.11	1.83	2.83	1.14	1.09	2.11
Temporally-paired peak pred. (Peak prediction) (Station at pred. peak)	-71.460	-79.360	-55.520	32.700	-63.560	-25.720	-12.860	-98.216	52.920	54.860	-11.700	-70.473	-98.216
	1.43	1.03	2.22	6.64	1.82	3.71	4.36	3.44	7.65	7.74	4.41	6.06	3.44
Spatially-paired peak pred. (Peak prediction) (Day of pred. peak)	-24.800	-79.360	-79.580	-65.660	-71.880	-70.820	-55.740	-98.433	-61.140	-43.360	-77.260	-92.828	-97.933
	3.76	1.03	1.02	1.72	1.41	1.46	2.21	3.02	1.94	2.83	1.14	1.47	3.98
Unpaired peak prediction (Peak prediction) (Station at pred. peak) (Day of pred. peak)	10.080	-16.140	-42.720	32.700	-23.500	1.940	41.840	-97.226	52.920	54.860	-11.700	-70.473	-95.983
	5.50	4.19	2.86	6.64	3.83	5.10	7.09	5.35	7.65	7.74	4.41	6.06	7.74
Average peak prediction	15.782	37.902	45.658	36.212	28.324	25.080	25.538	97.347	49.660	54.860	11.700	70.321	41.810
Normalized systematic bias (%) Systematic bias ($\mu\text{g}/\text{m}^3$)	-72.500	-77.349	-79.092	-65.979	-70.793	-66.346	-57.354	-49.710	-55.474	-42.455	-53.465	-63.339	-61.505
Variance	0.954	1.139	0.313	2.116	0.497	0.997	0.5491281.210	2.690	3.939	2.270	15.353	161.160	
Normalized gross error (%) Gross error ($\mu\text{g}/\text{m}^3$)	72.500	77.349	79.092	68.704	70.793	66.484	57.354	50.206	59.352	54.199	53.465	65.563	63.502

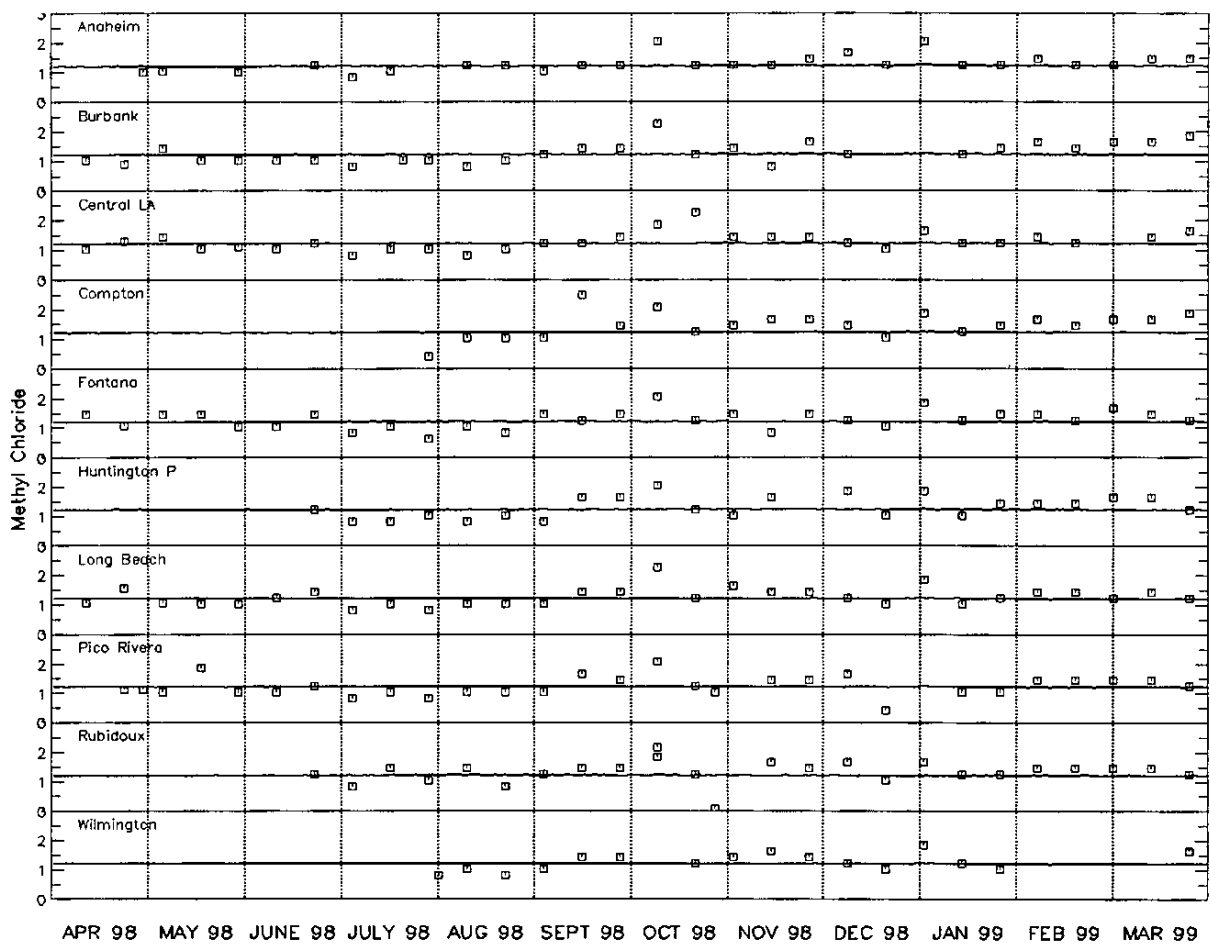


Figure V-8a. Time-series of simulated methyl chloride (solid line) versus measurements (squares and stars).

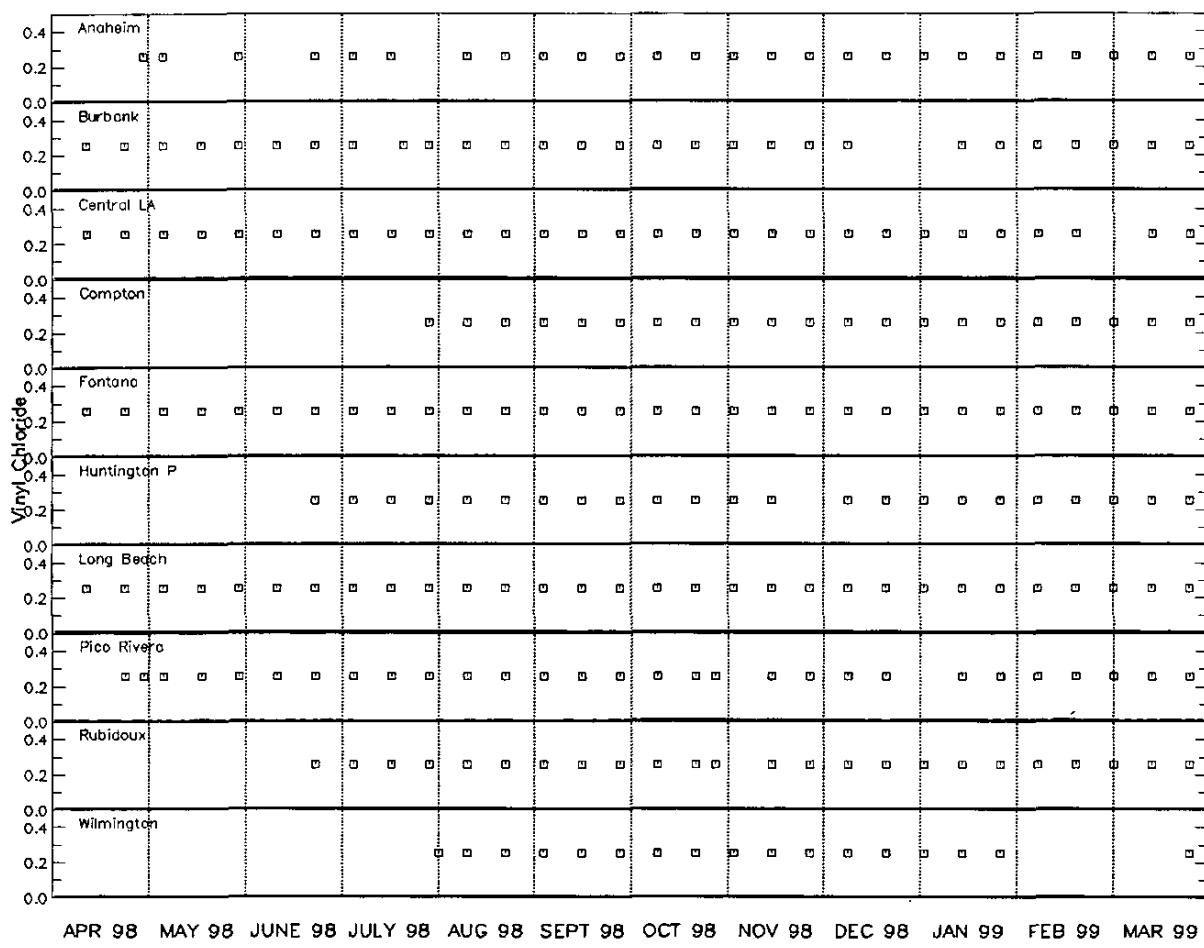


Figure V-8b. Time-series of simulated vinyl chloride (solid line) verses measurements (squares).

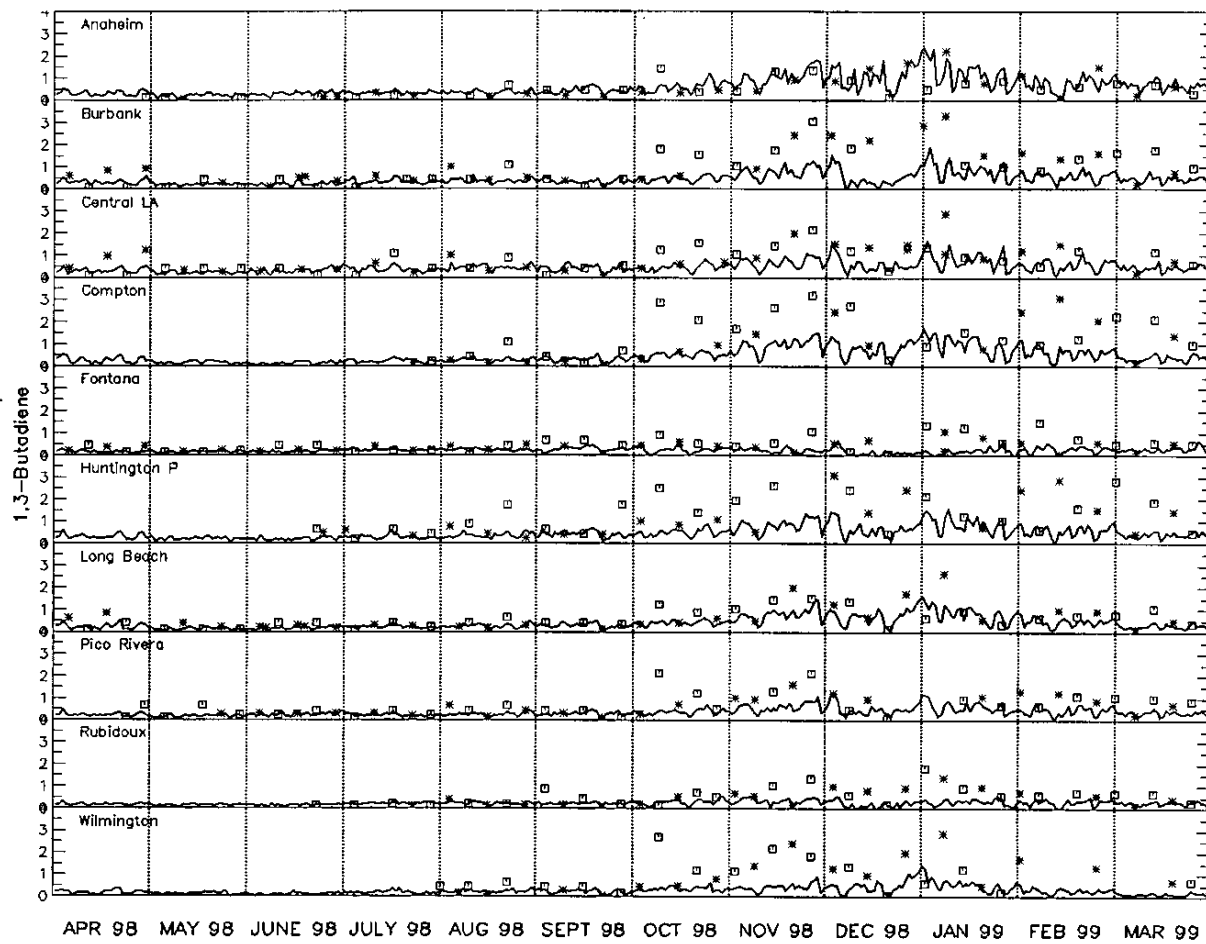


Figure V-8c. Time-series of simulated 1,3 butadiene (solid line) versus measurements (squares and stars).

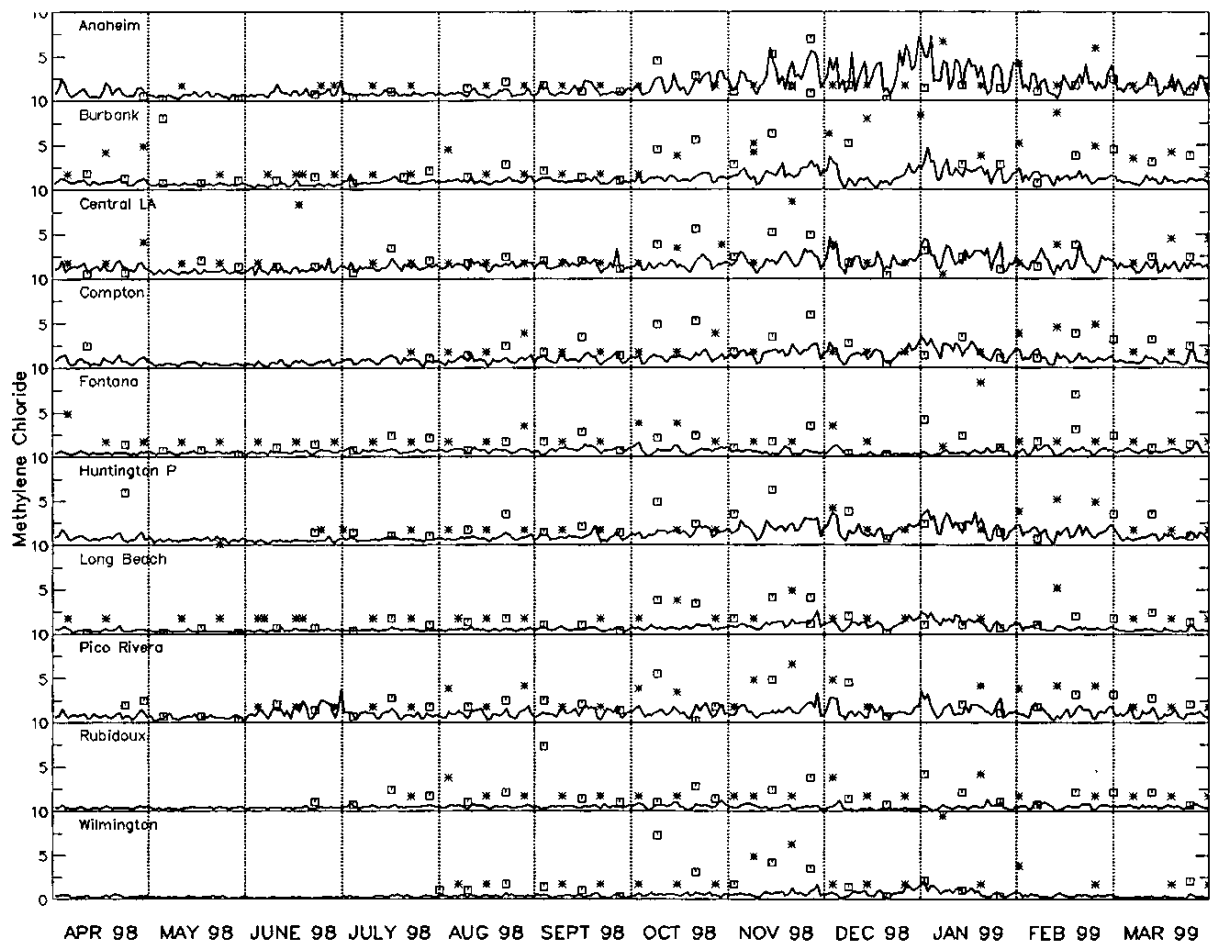


Figure V-8d. Time-series of simulated methylene chloride (solid line) versus measurements (squares and stars).

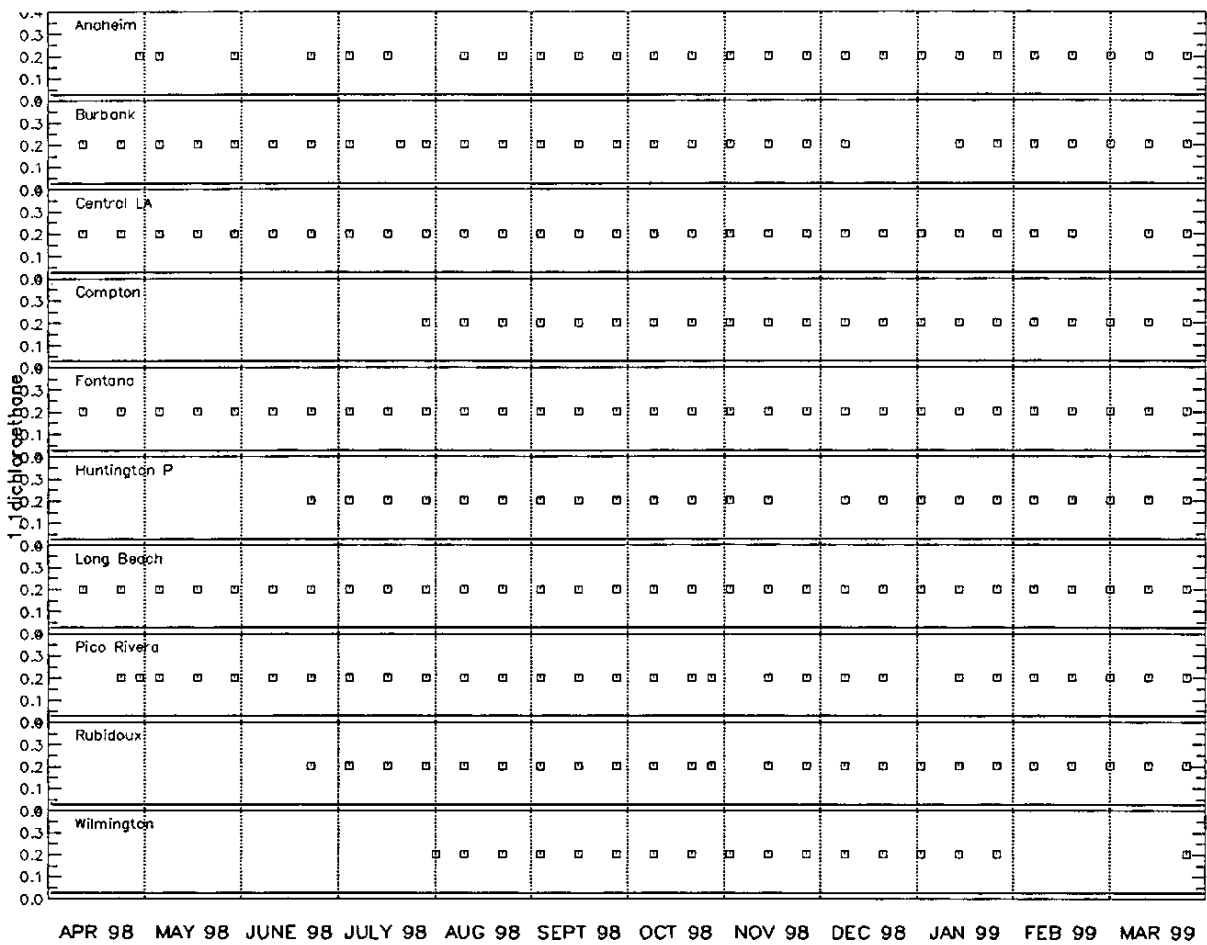


Figure V-8e. Time-series of simulated 1,2 dichloroethane (solid line) versus measurements (squares and stars).

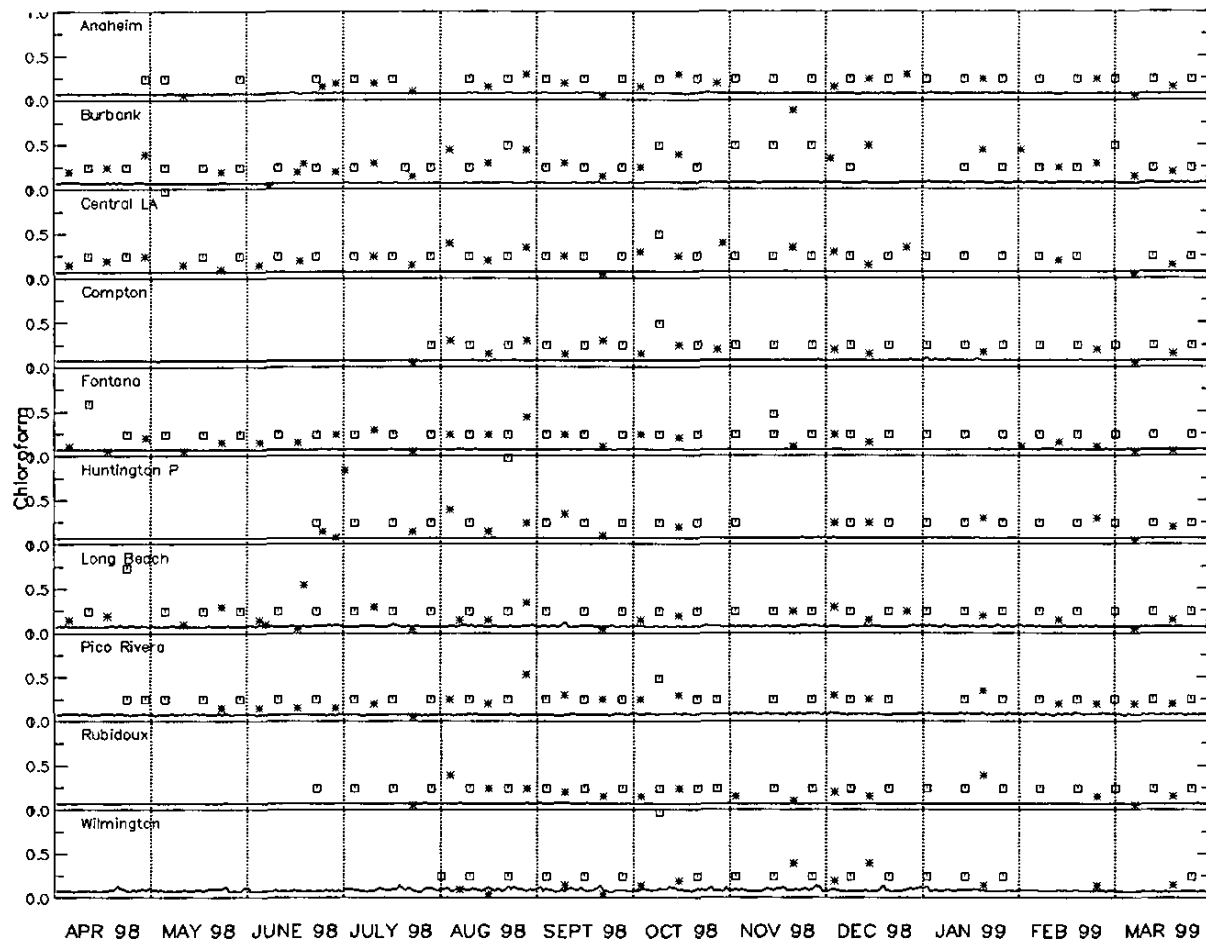


Figure V-8f. Time-series of simulated chloroform (solid line) versus measurements (squares and stars).

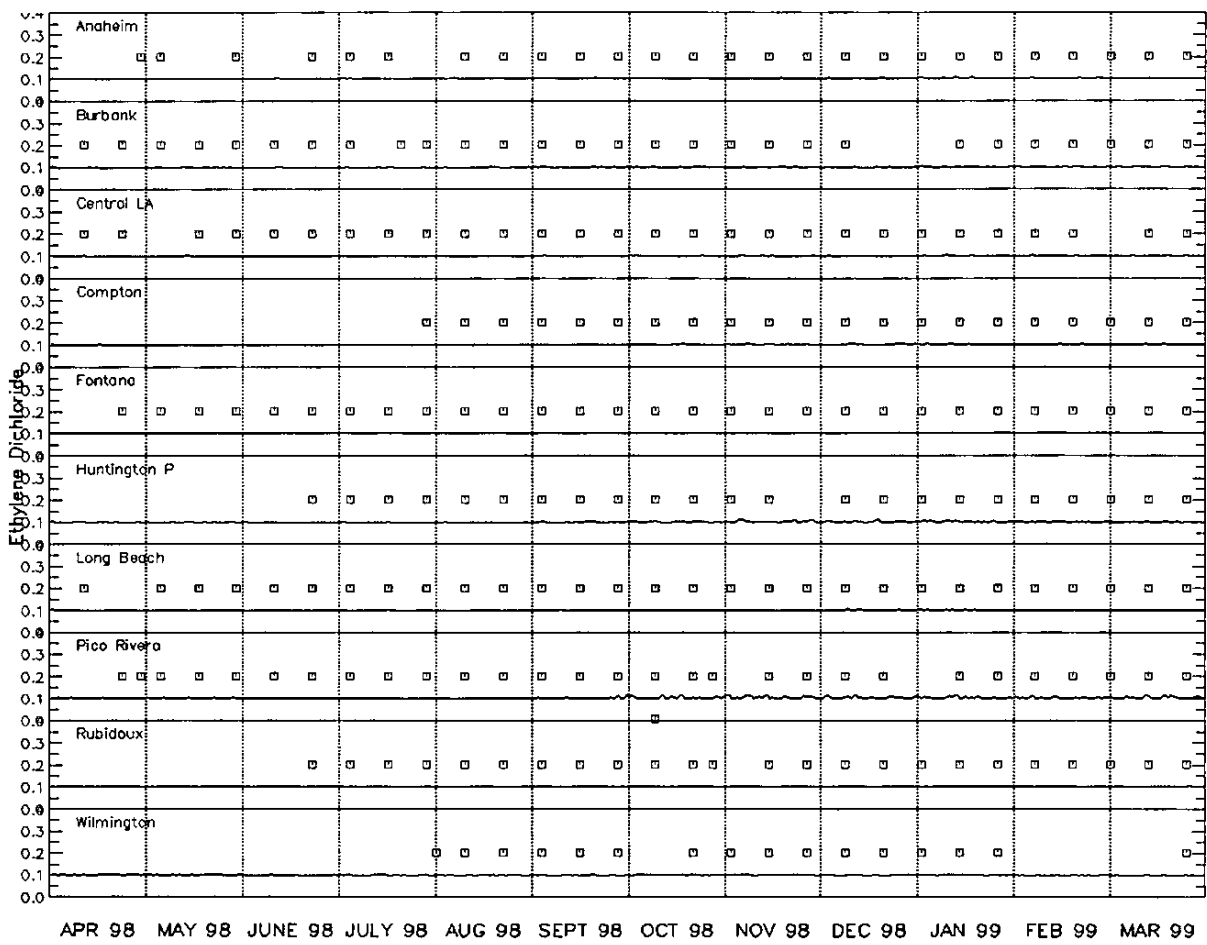


Figure V-8g. Time-series of simulated ethylene dichloride (solid line) verses measurements (squares and stars).

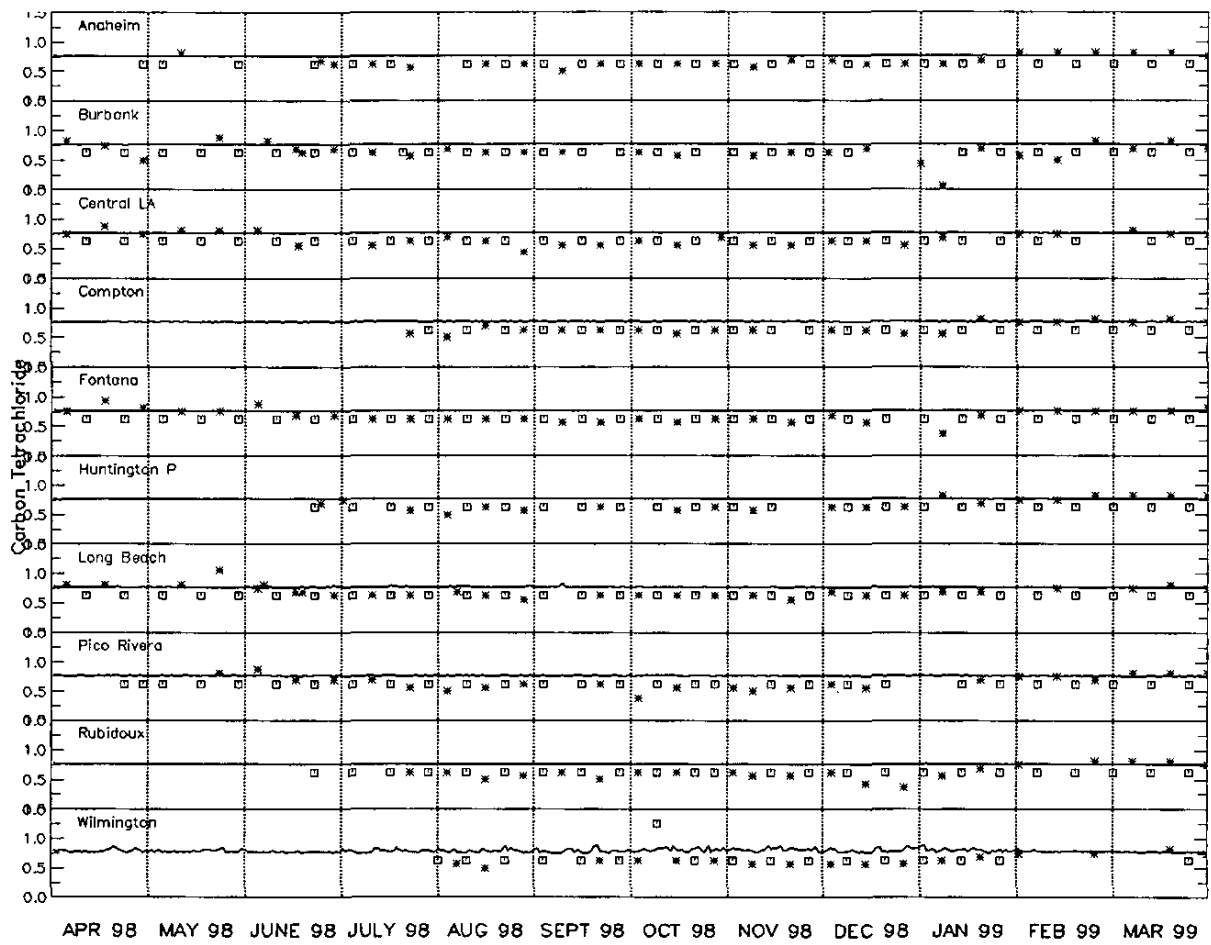


Figure V-8h. Time-series of simulated carbon tetrachloride (solid line) versus measurements (squares and stars).

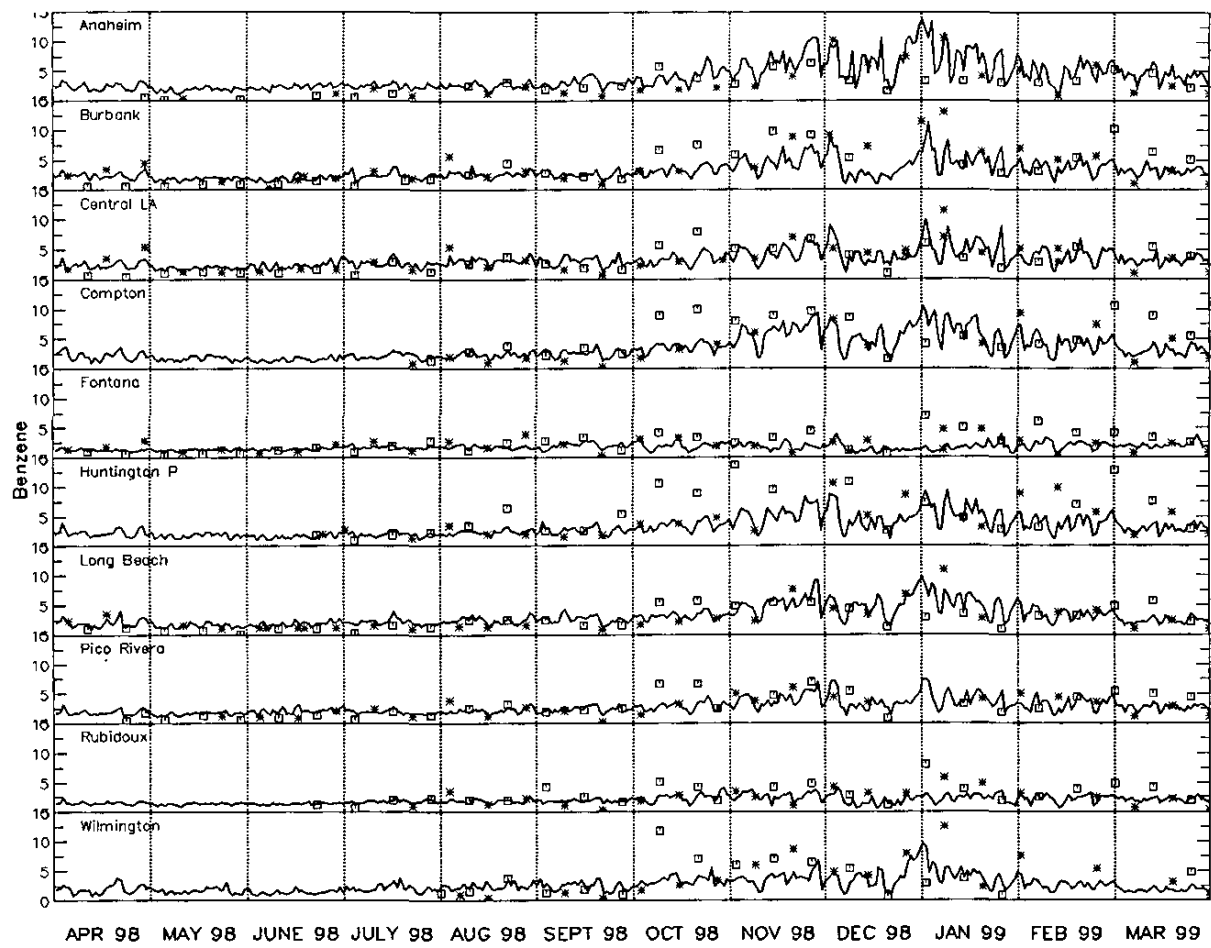


Figure V-8i. Time-series of simulated benzene (solid line) versus measurements (squares and stars).

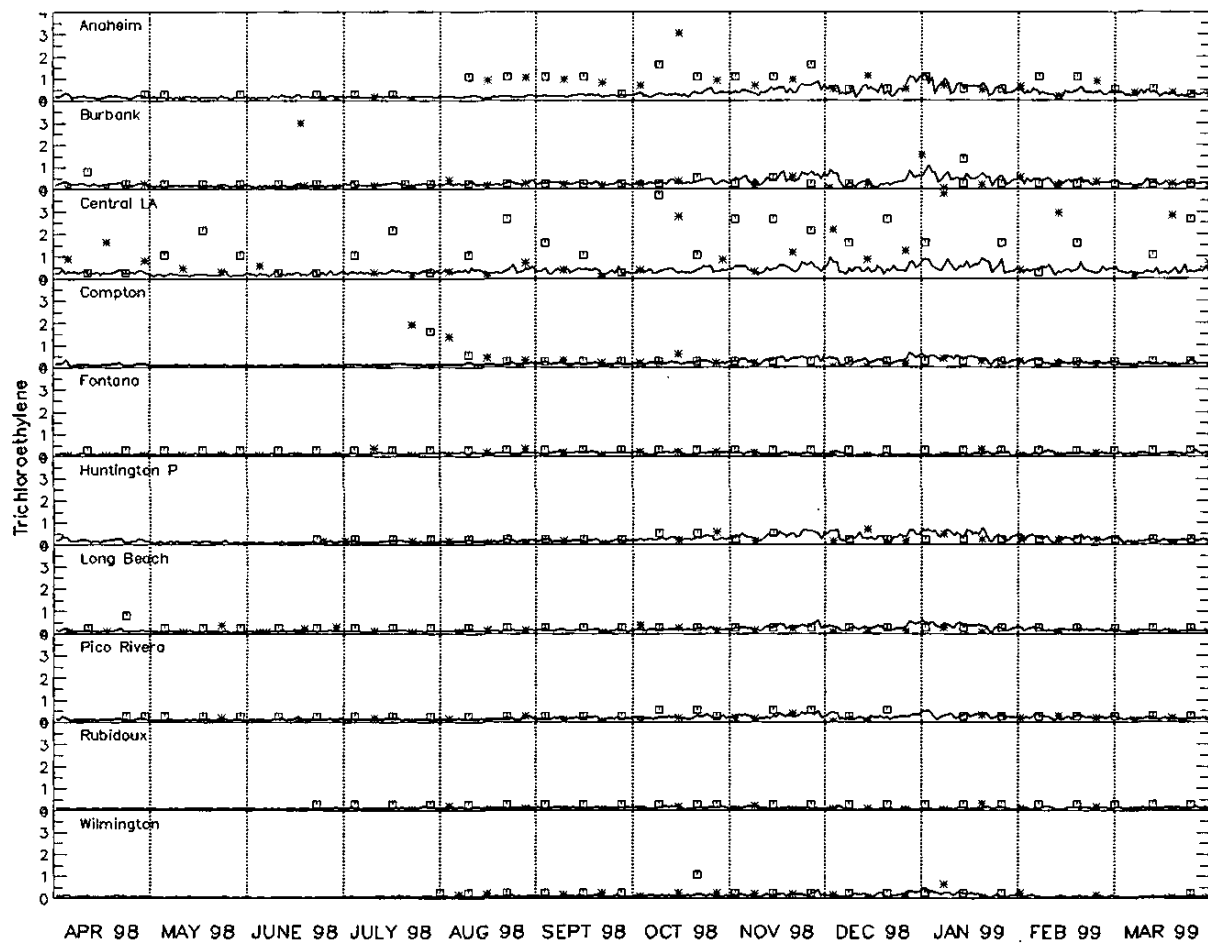


Figure V-8j. Time-series of simulated trichloroethene (solid line) versus measurements (squares and stars).

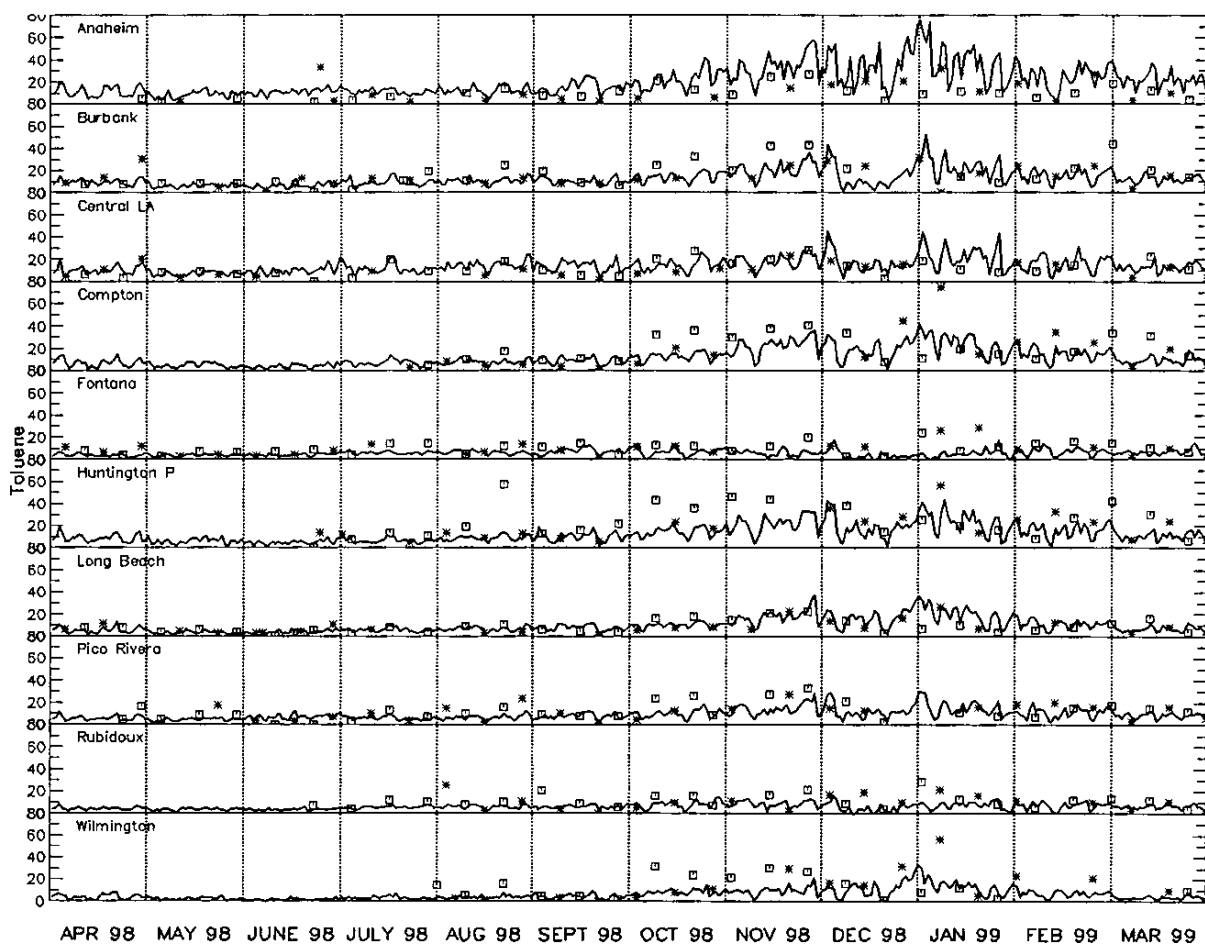


Figure V-8k. Time-series of simulated toluene (solid line) versus measurements (squares and stars).

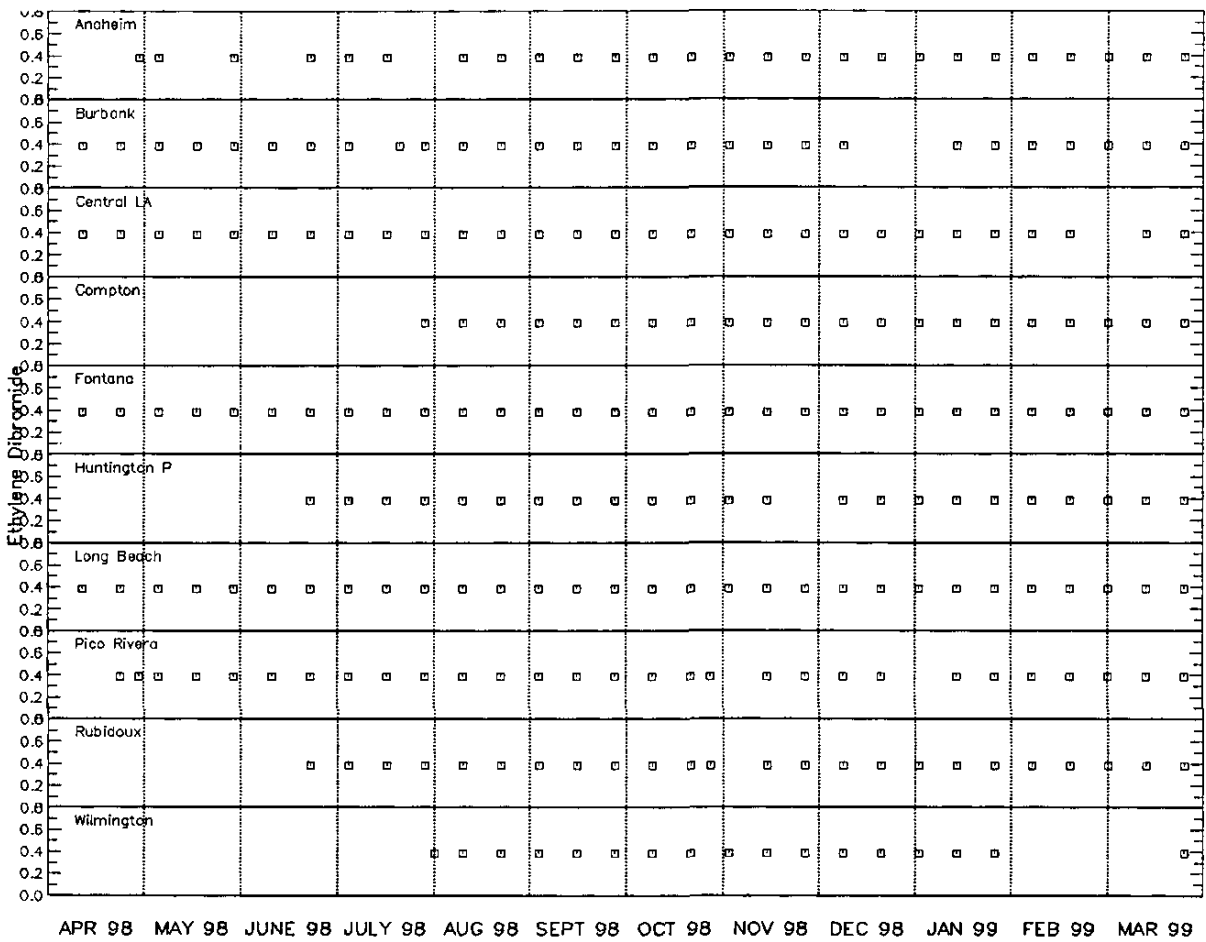


Figure V-81. Time-series of simulated ethylene dibromide (solid line) verses measurements (squares and stars).

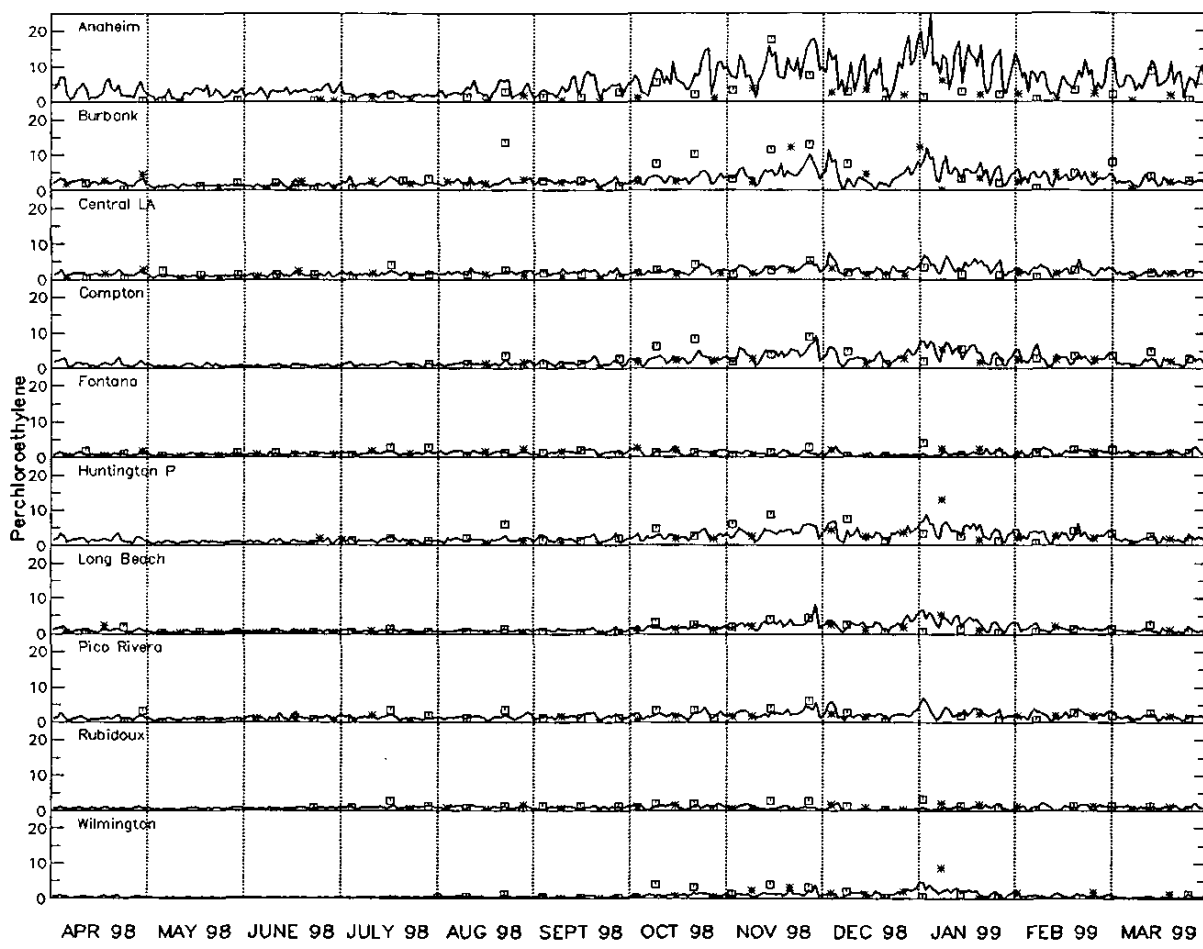


Figure V-8m. Time-series of simulated perchloroethylene (solid line) versus measurements (squares and stars).

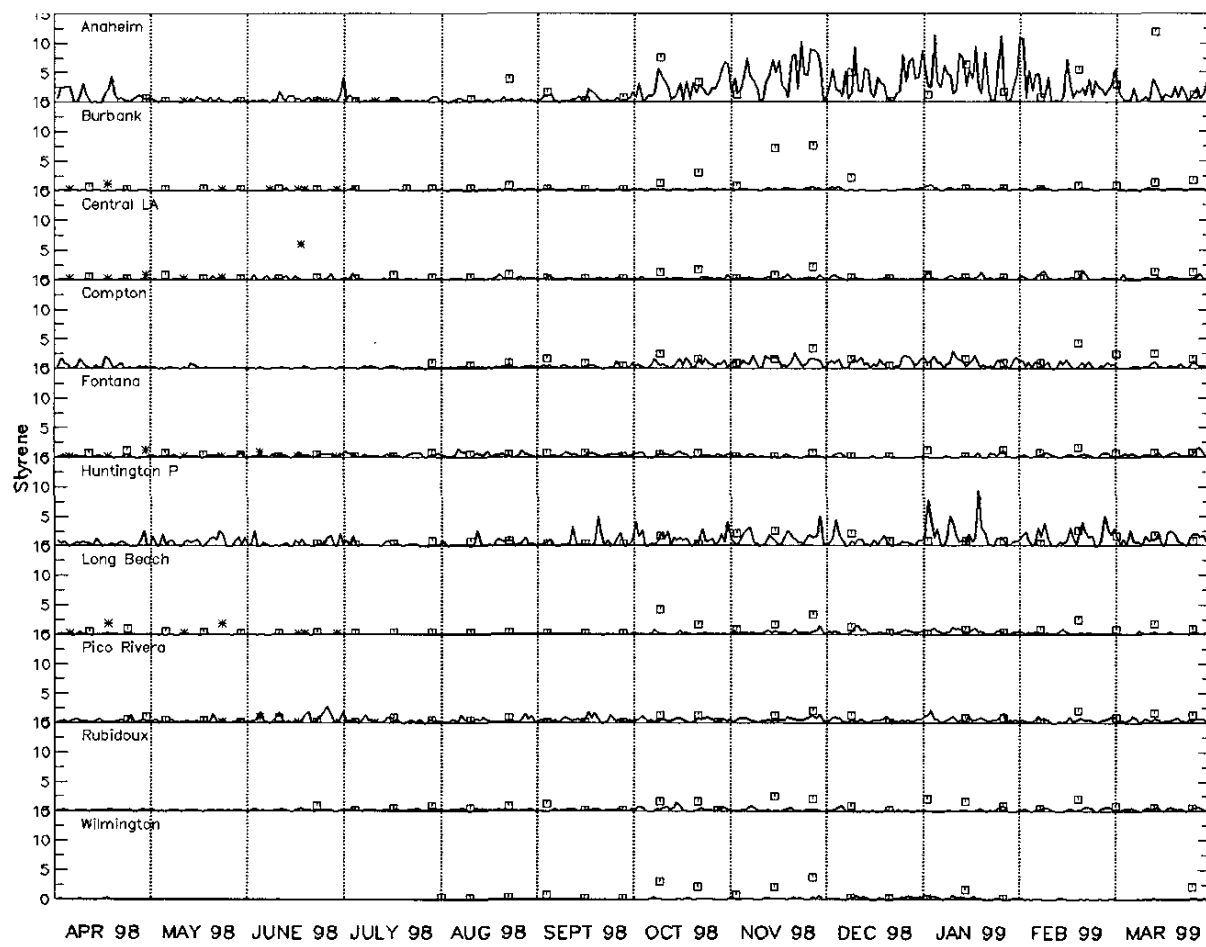


Figure V-8n. Time-series of simulated styrene (solid line) versus measurements (squares and stars).

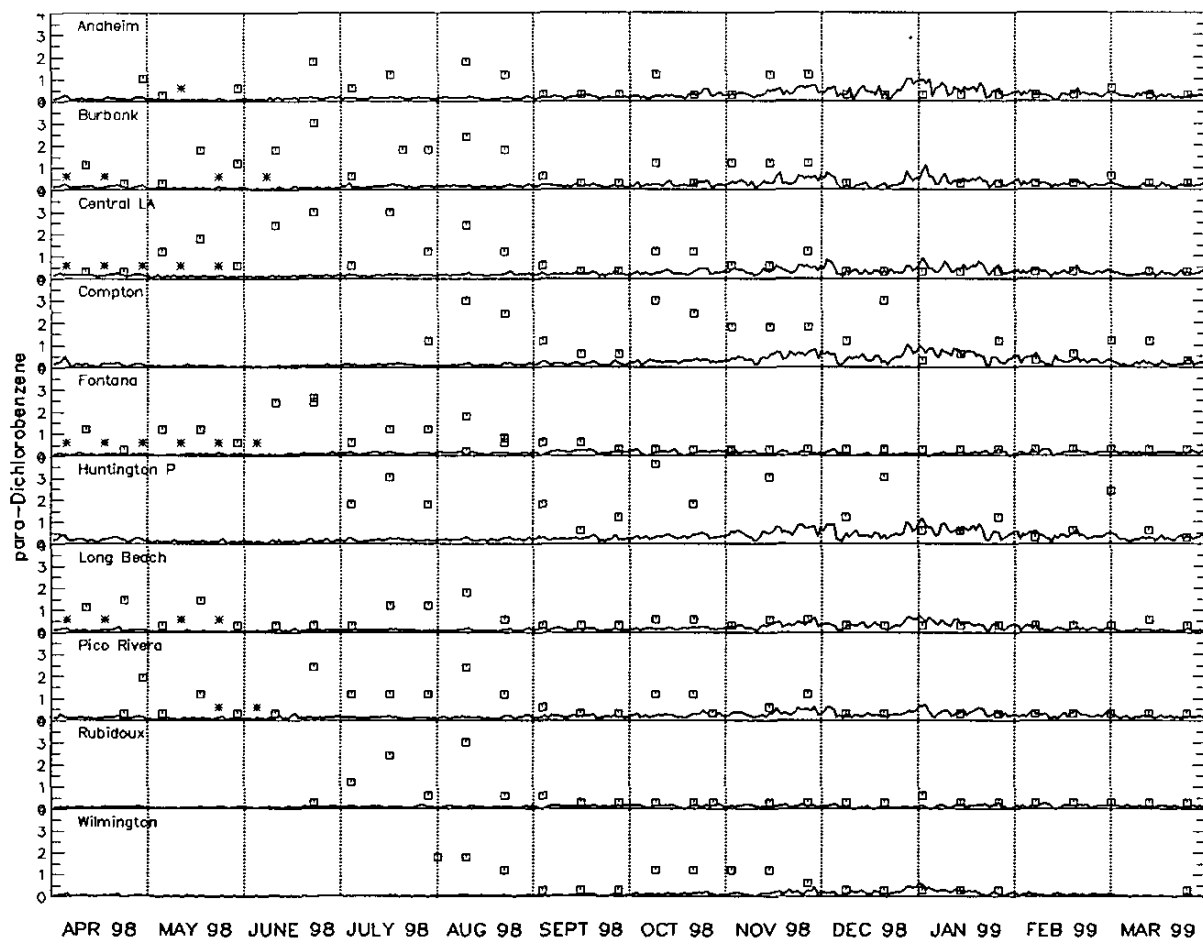


Figure V-8o. Time-series of simulated p-dichlorobenzene (solid line) versus measurements (squares and stars).

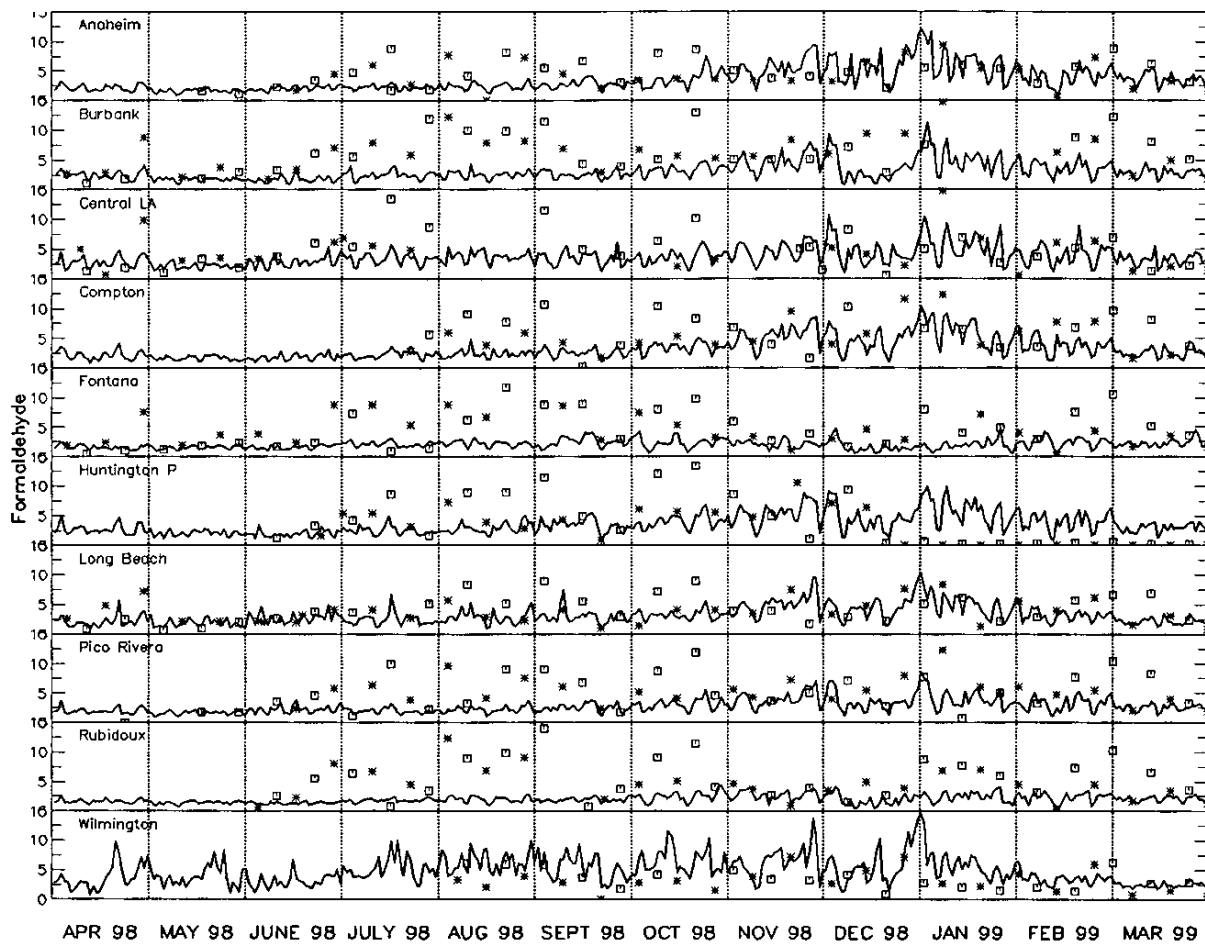


Figure V-8p. Time-series of simulated formaldehyde (solid line) versus measurements (squares and stars).

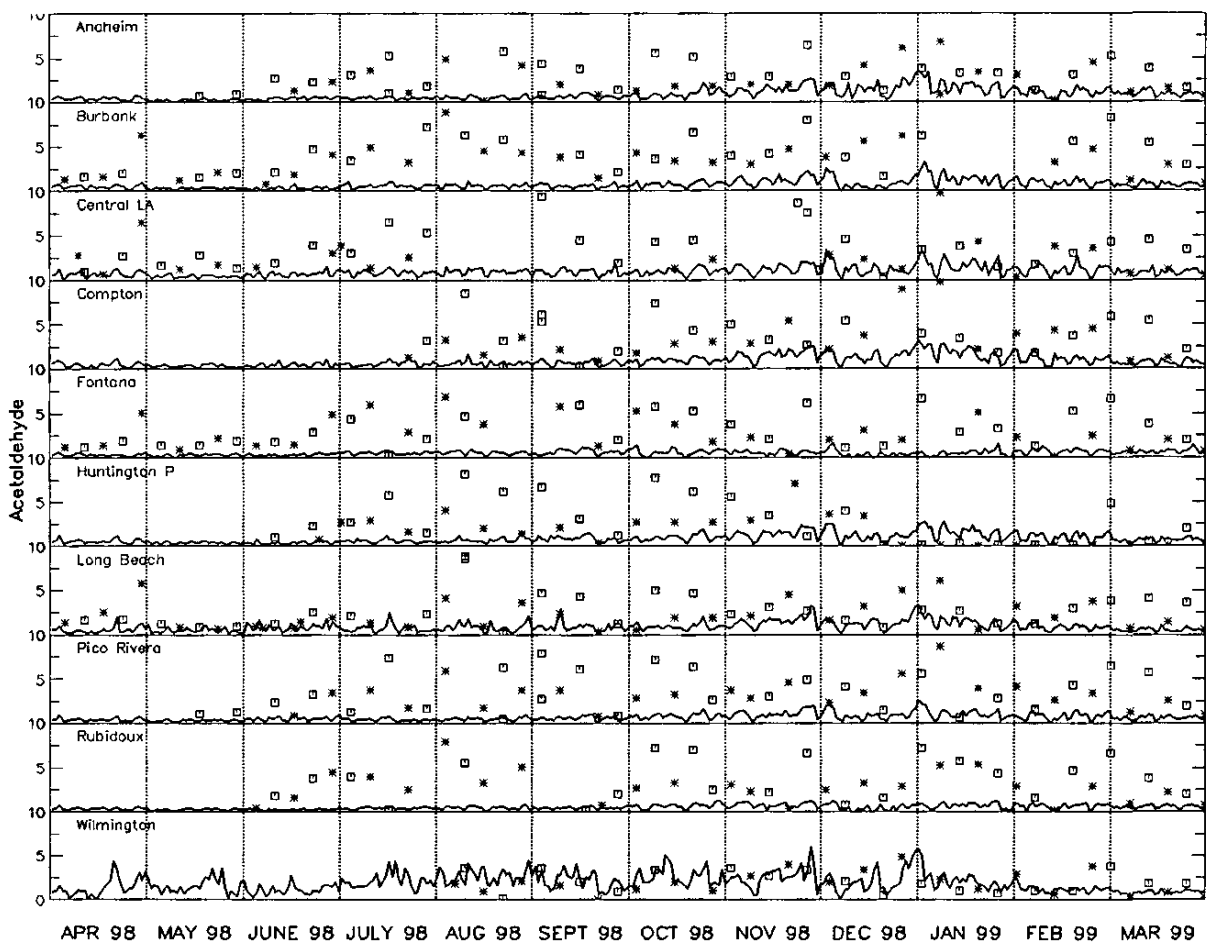


Figure V-8q. Time-series of simulated acetaldehyde (solid line) versus measurements (squares and stars).

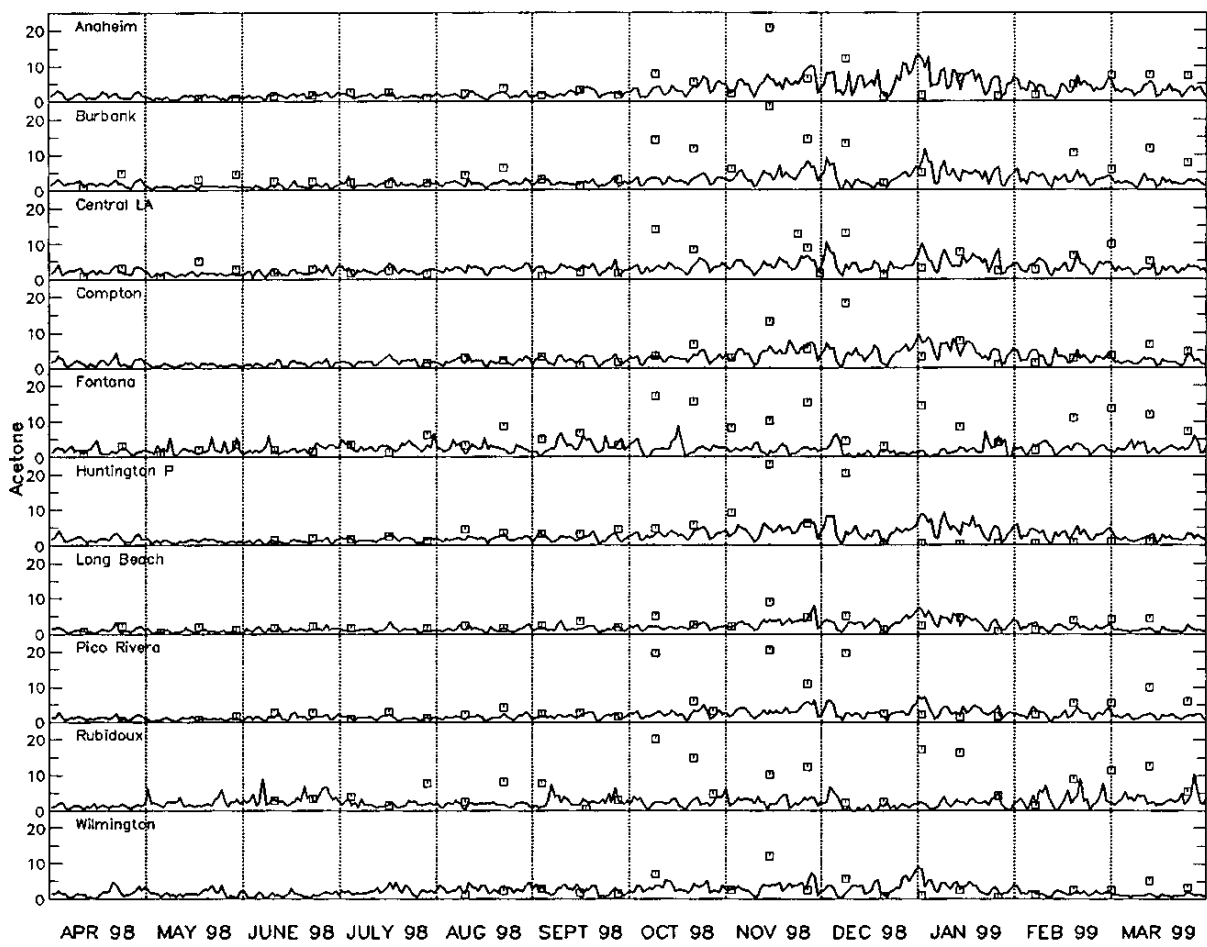


Figure V-8r. Time-series of simulated acetone (solid line) versus measurements (squares and stars).

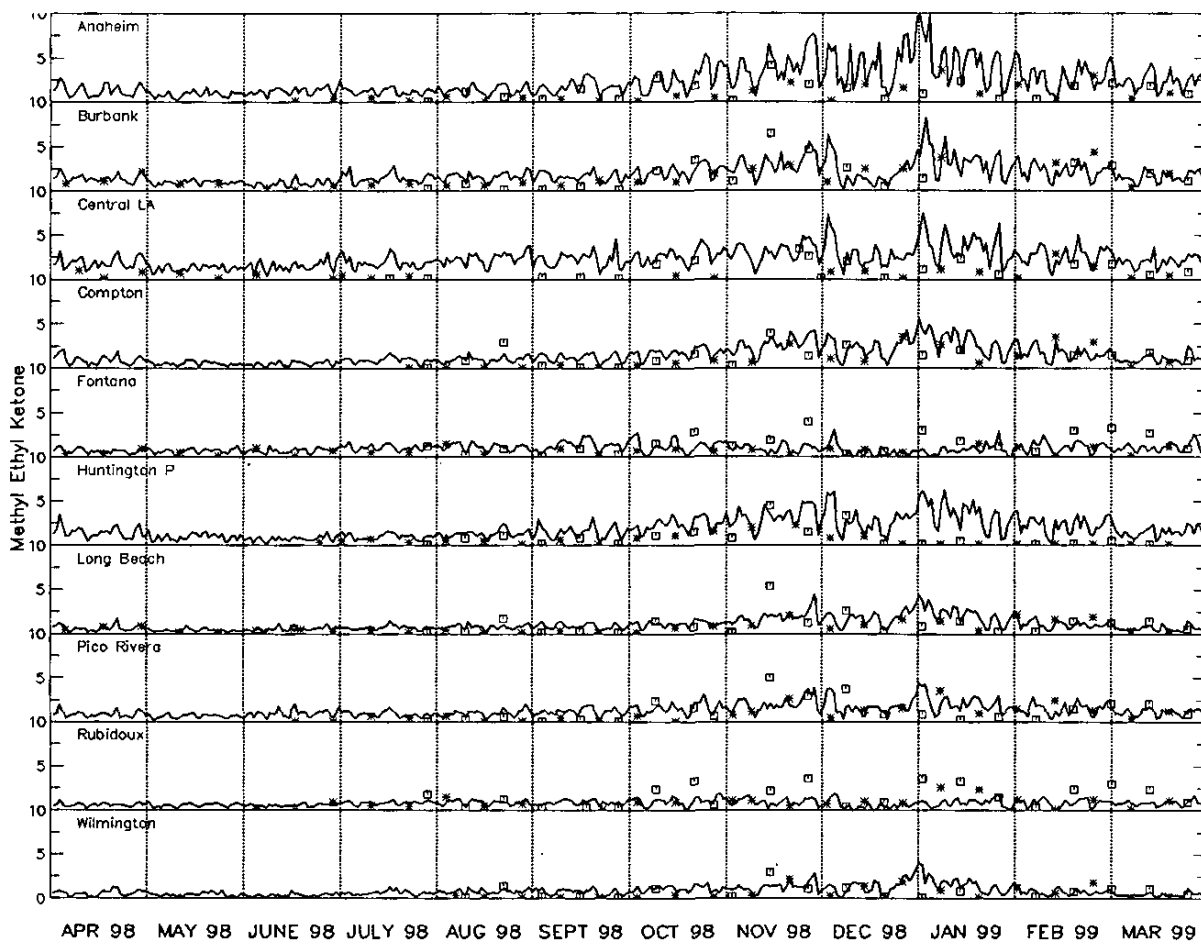


Figure V-8s. Time-series of simulated methyl ethyl ketone (solid line) versus measurements (squares and stars).

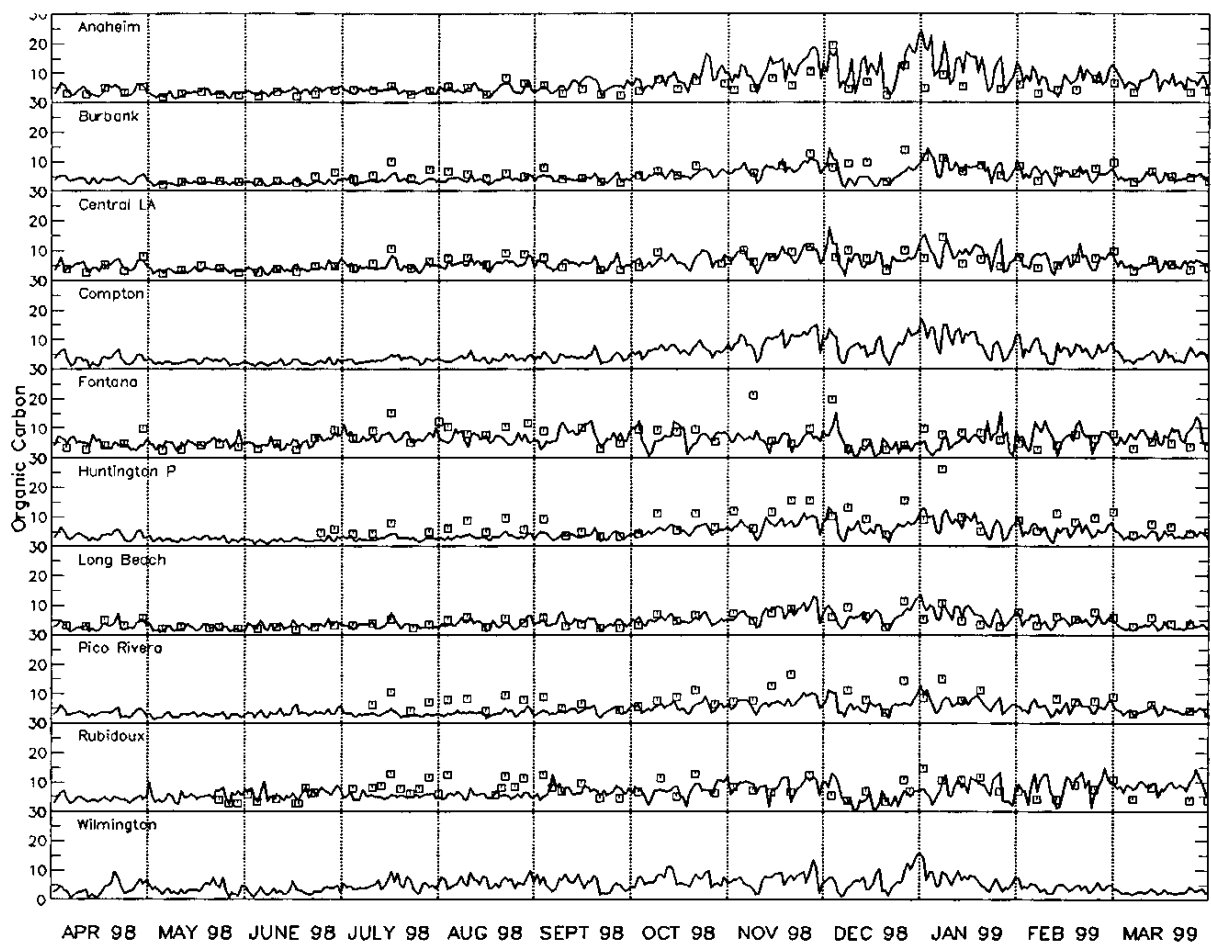


Figure V-8t. Time-series of simulated organic carbon (solid line) versus measurements (squares and stars).

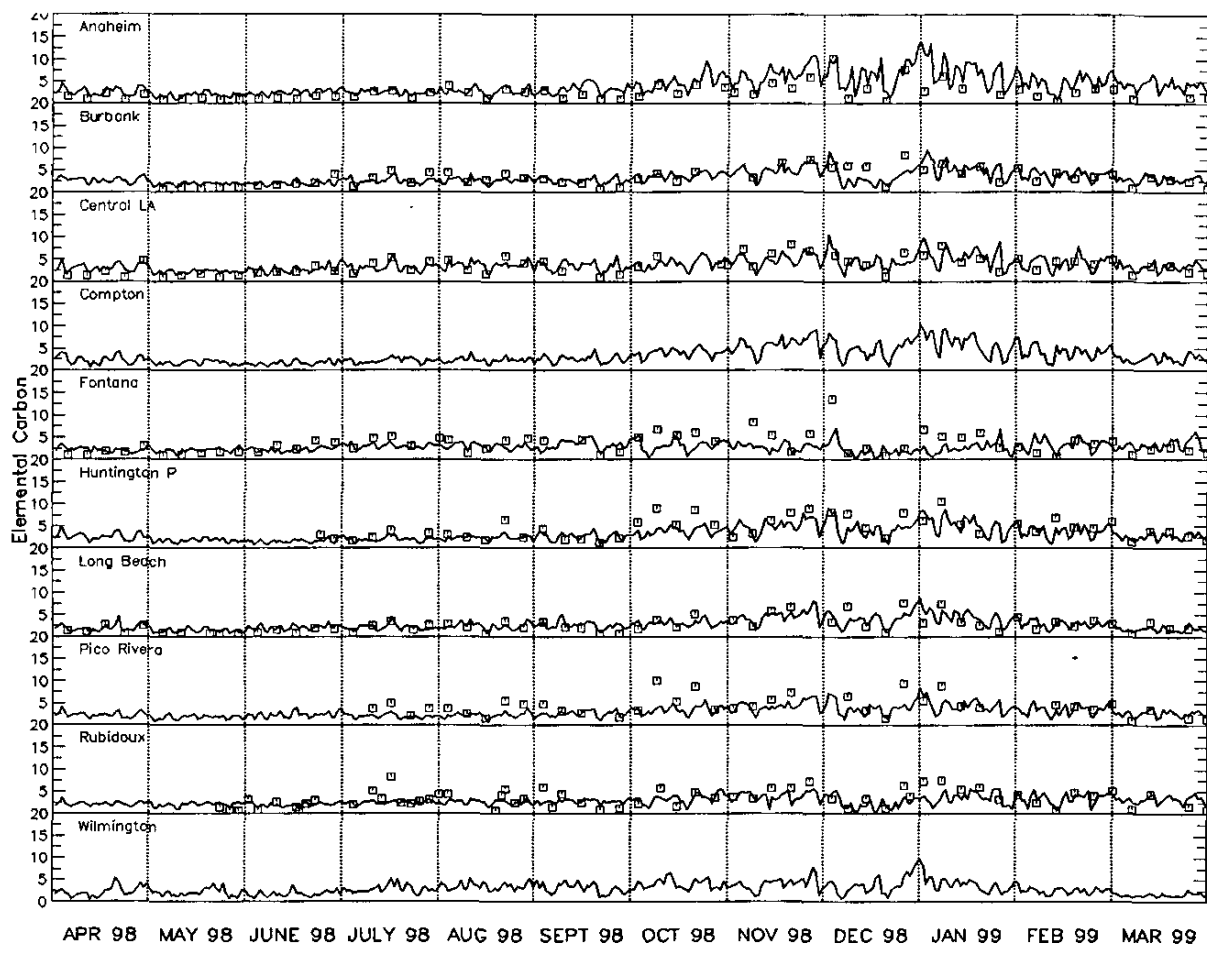


Figure V-8u. Time-series of simulated elemental carbon (solid line) versus measurements (squares and stars).

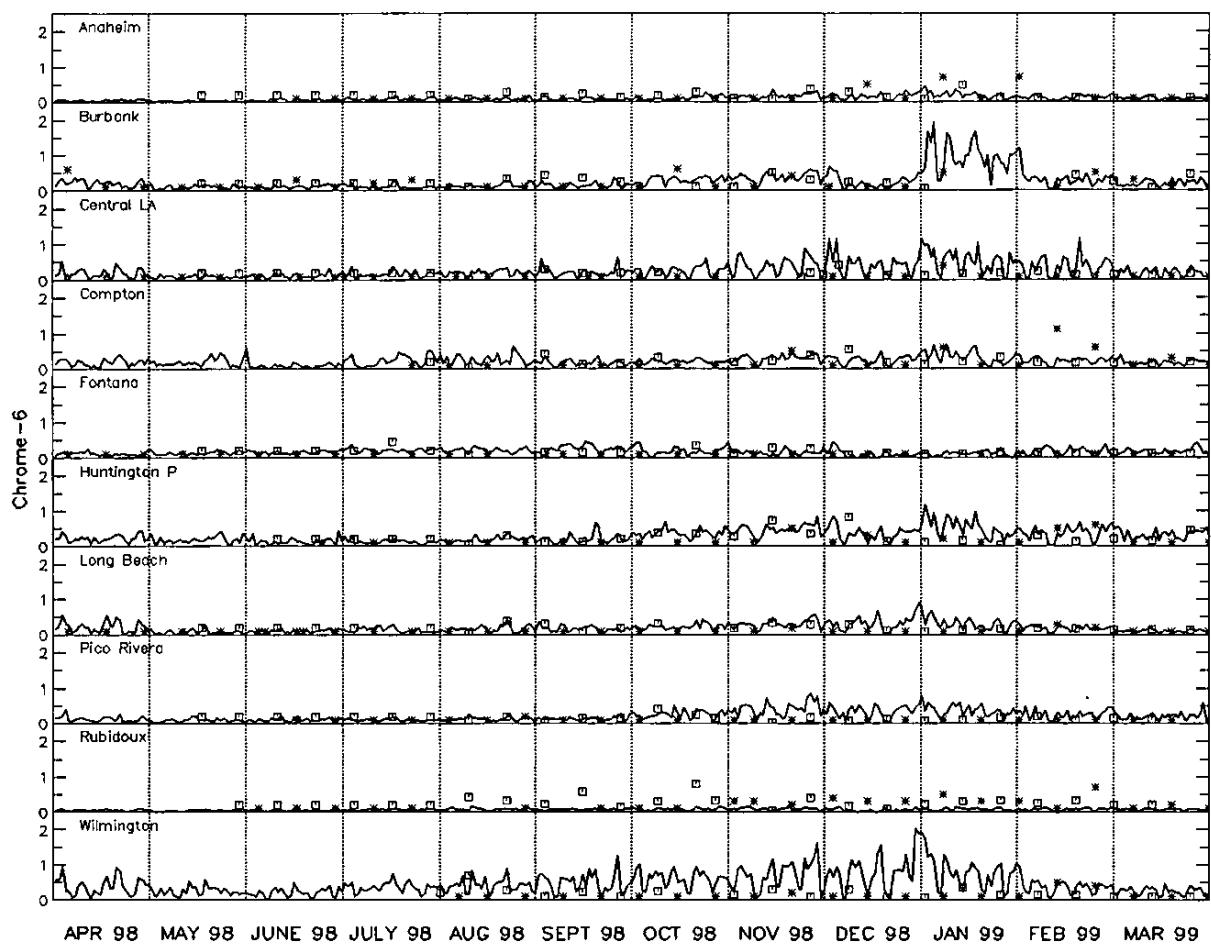


Figure V-8v. Time-series of simulated hexavalent chromium (solid line) versus measurements (squares and stars).

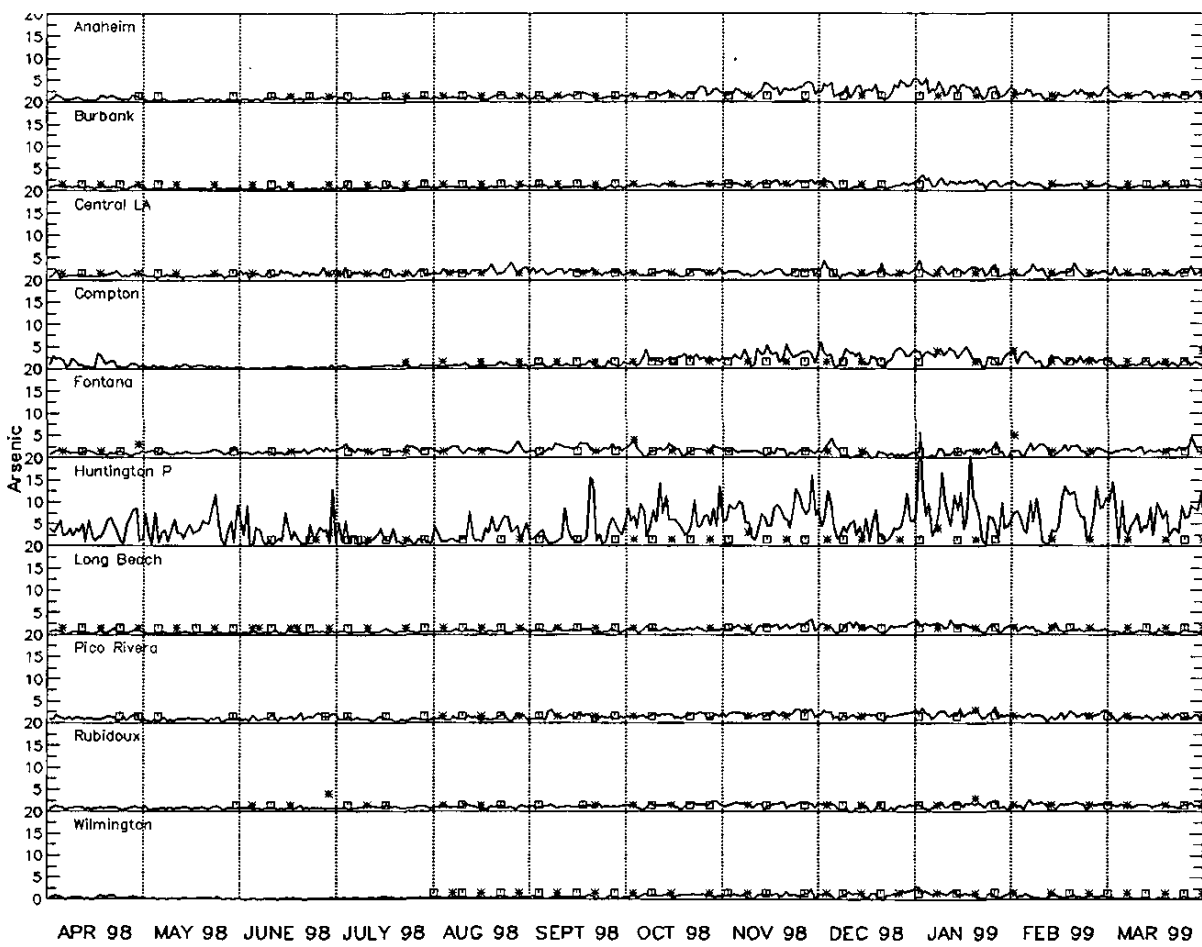


Figure V-8w. Time-series of simulated arsenic (solid line) versus measurements (squares and stars).

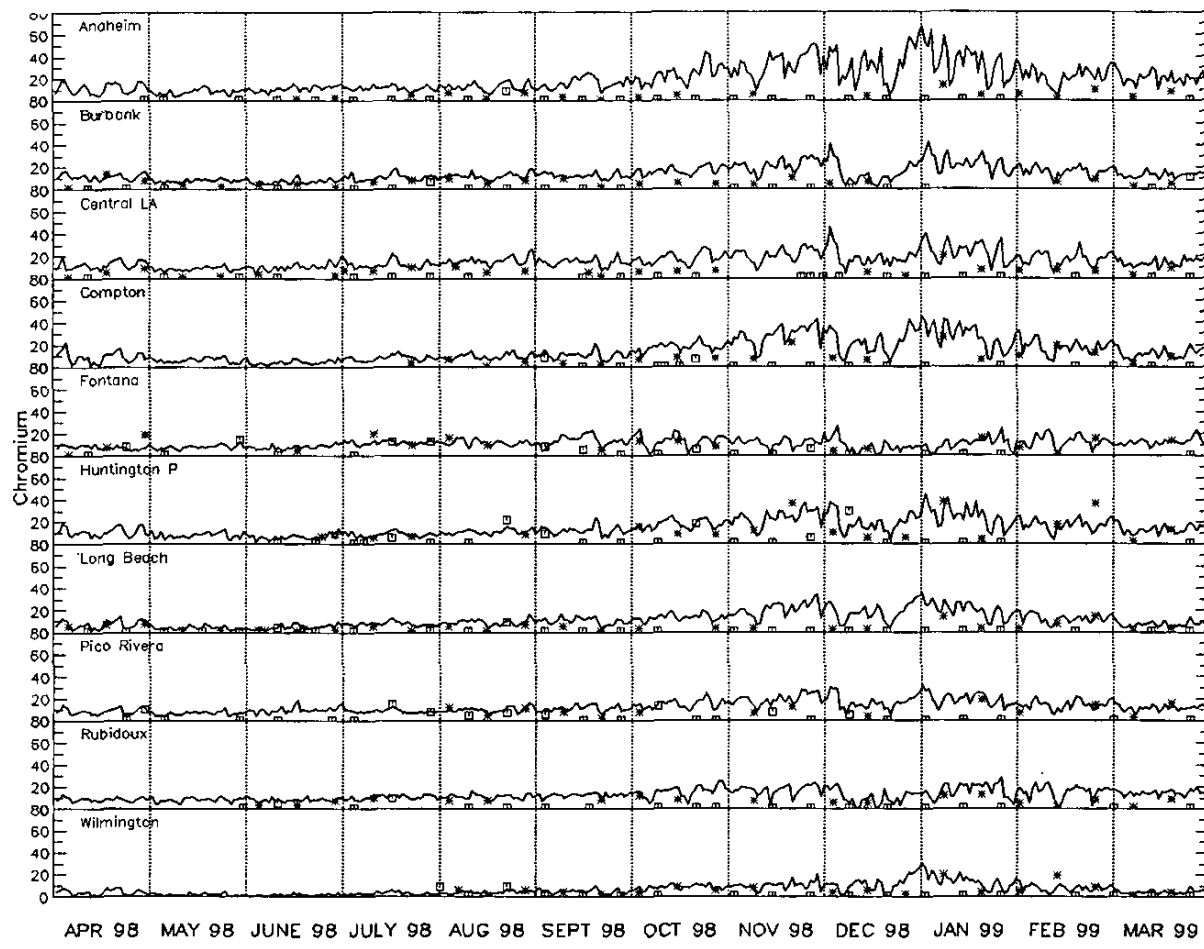


Figure V-8x. Time-series of simulated chromium (solid line) versus measurements (squares and stars).

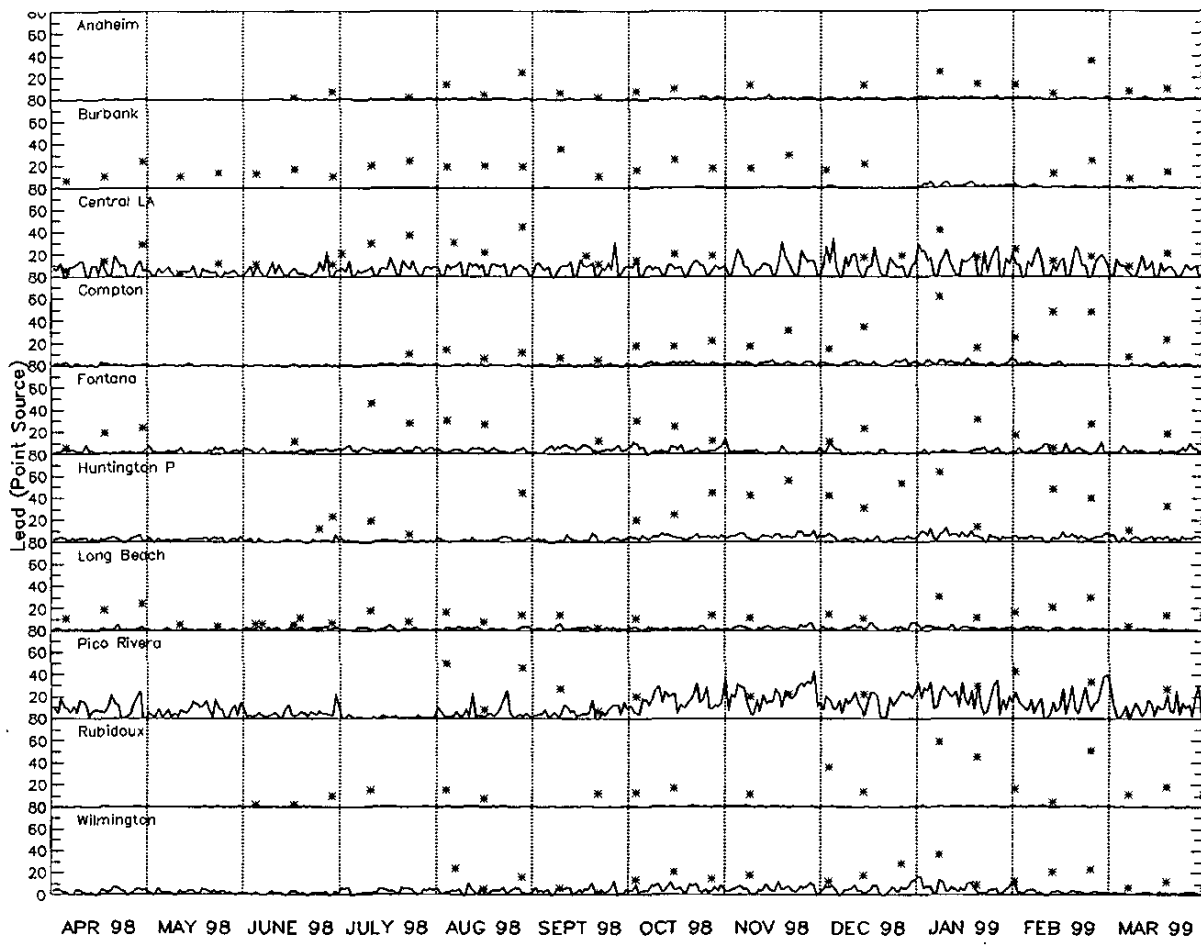


Figure V-8y. Time-series of simulated point source lead (solid line) versus measurements (squares and stars).

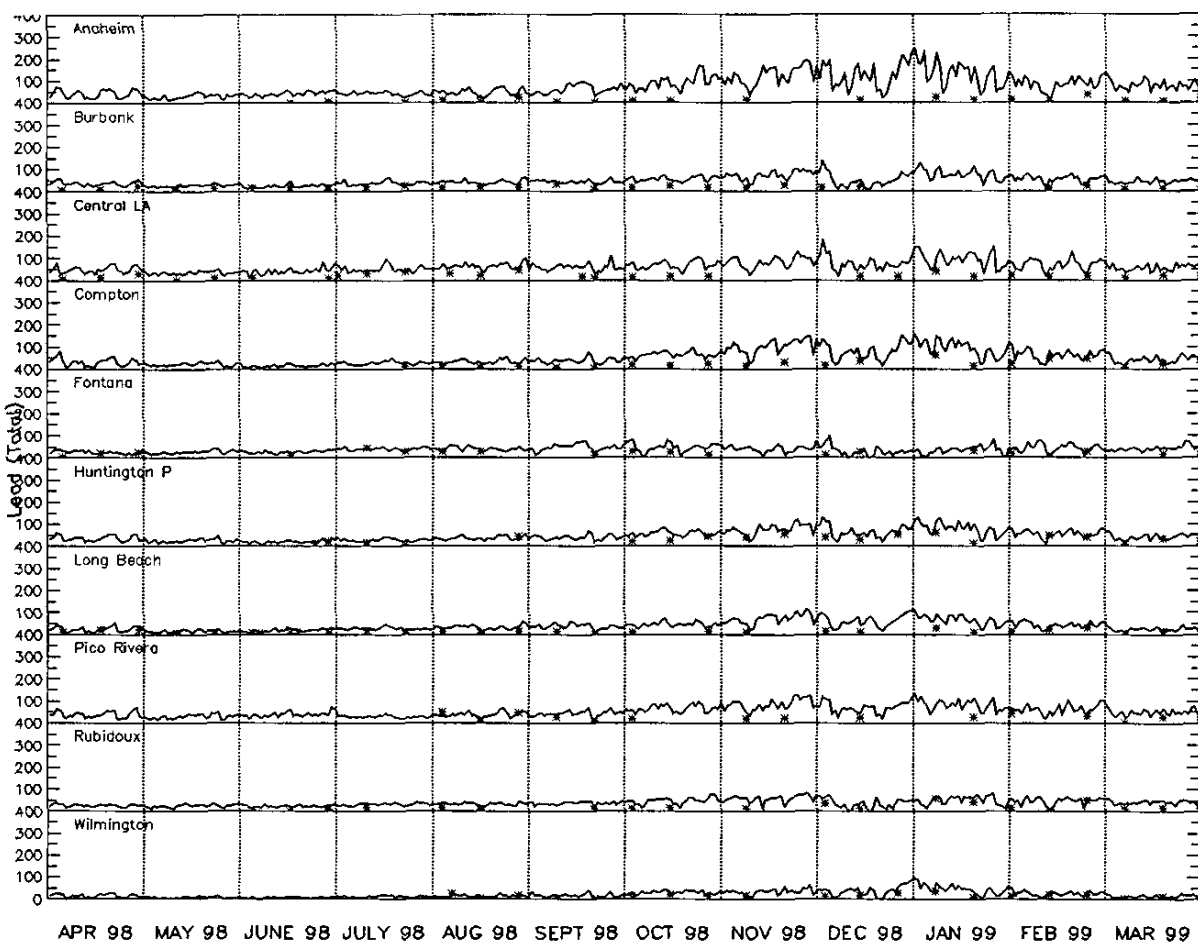


Figure V-8z. Time-series of simulated total lead (solid line) versus measurements (squares and stars).

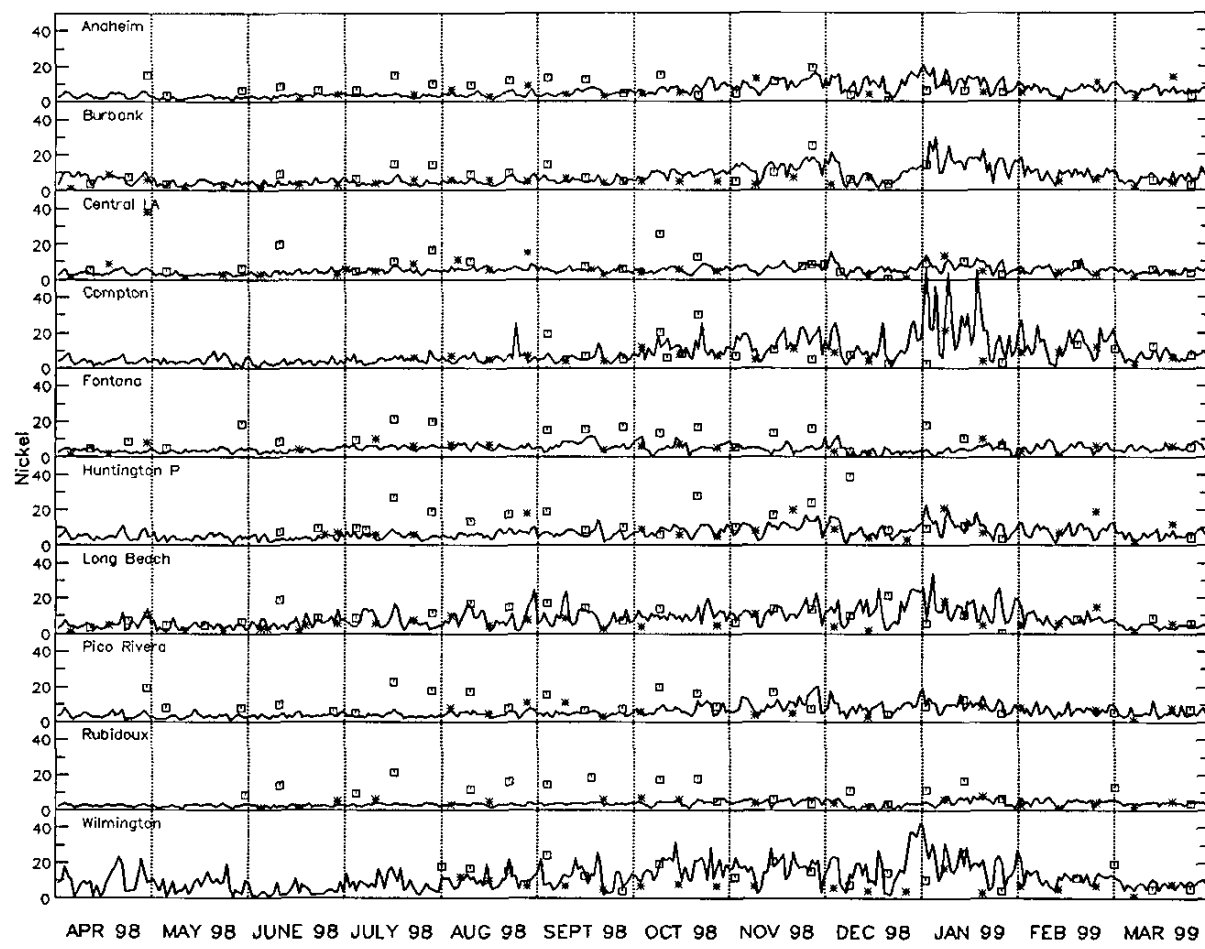


Figure V-8aa. Time-series of simulated nickel (solid line) versus measurements (squares and stars).

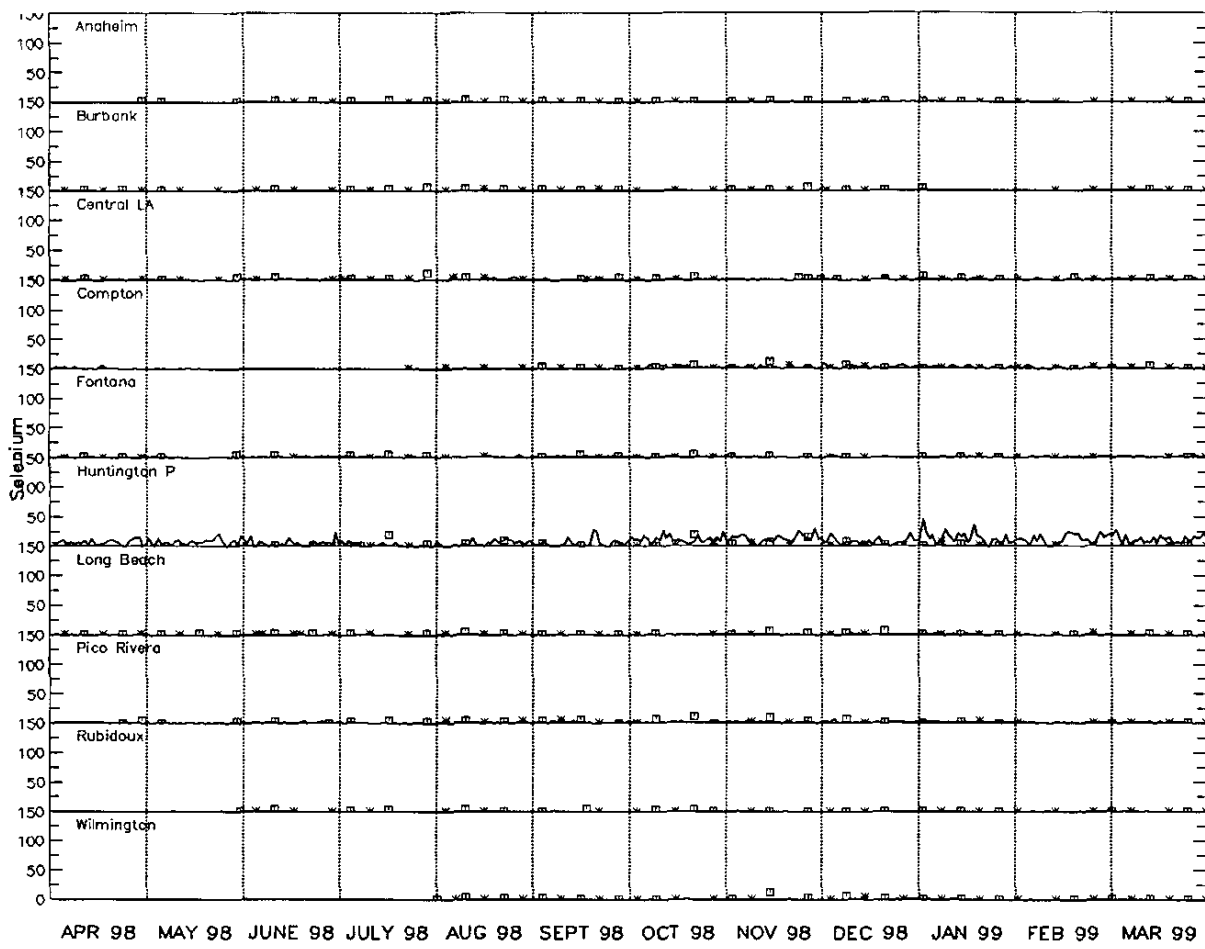


Figure V-8ab. Time-series of simulated selenium (solid line) versus measurements (squares and stars).

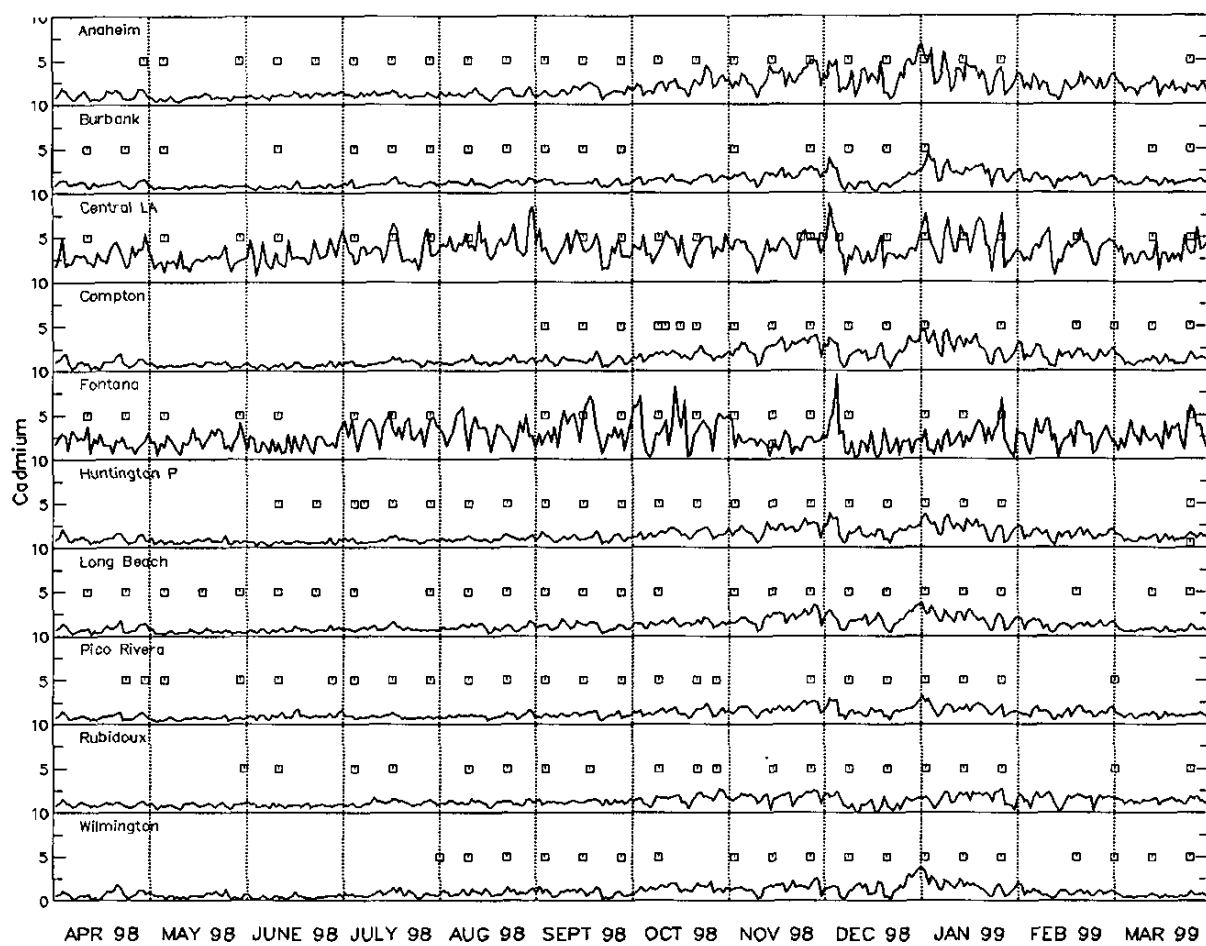


Figure V-8ac. Time-series of simulated cadmium (solid line) versus measurements (squares and stars).

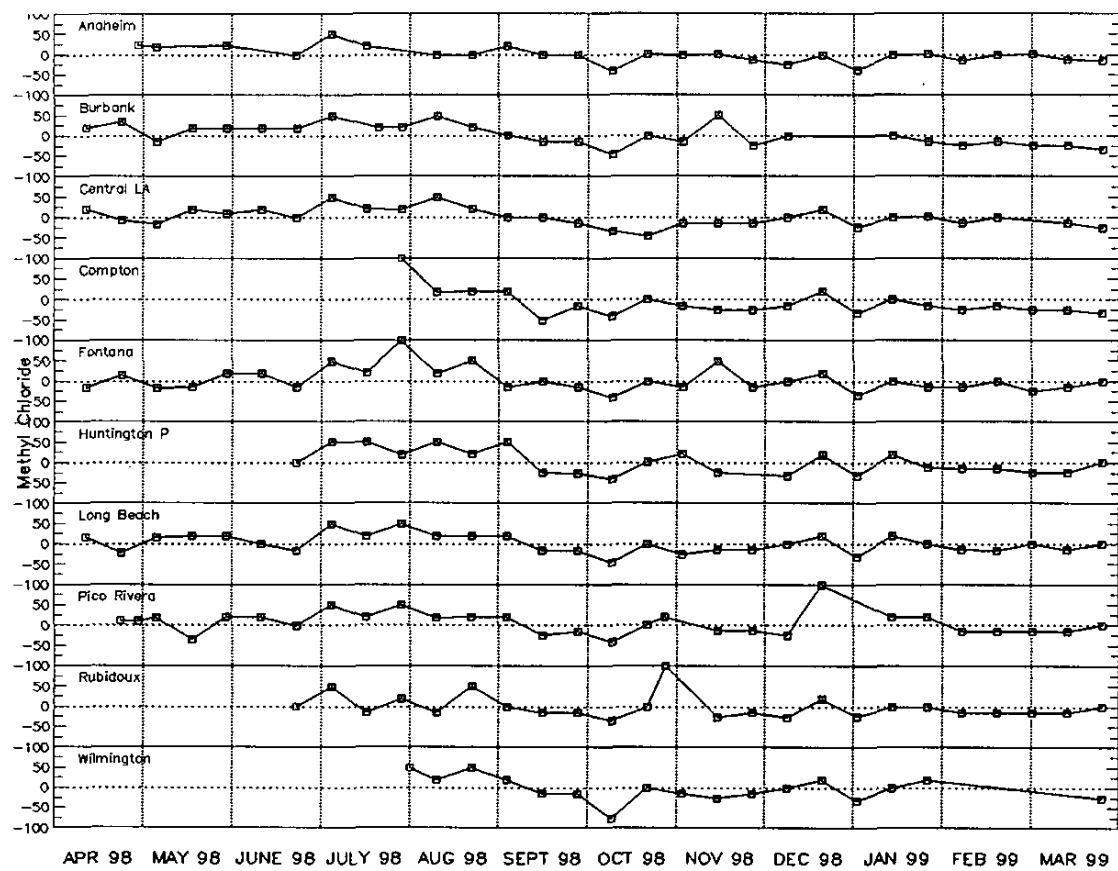


Figure V-9a. Time-series plot of the residuals between simulated and measured concentrations of methyl chloride.

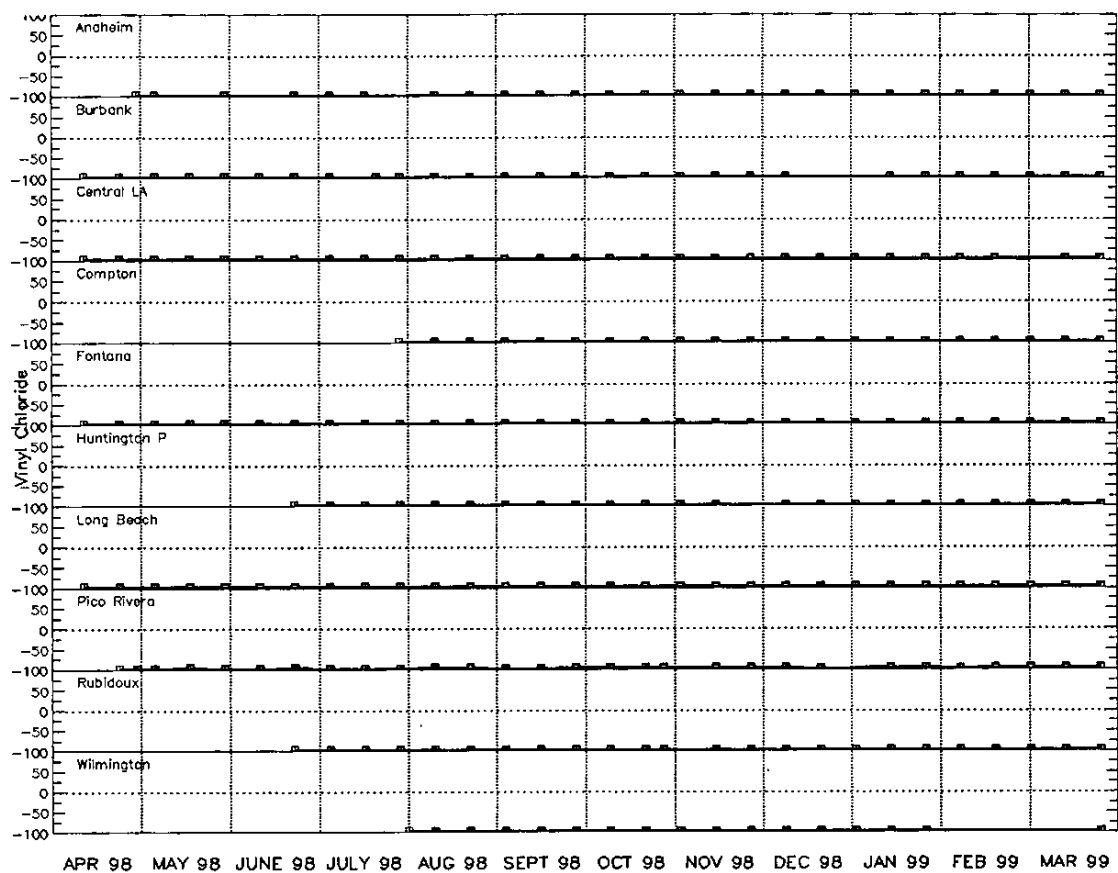


Figure V-9b. Time-series plot of the residuals between simulated and measured concentrations of vinyl chloride.

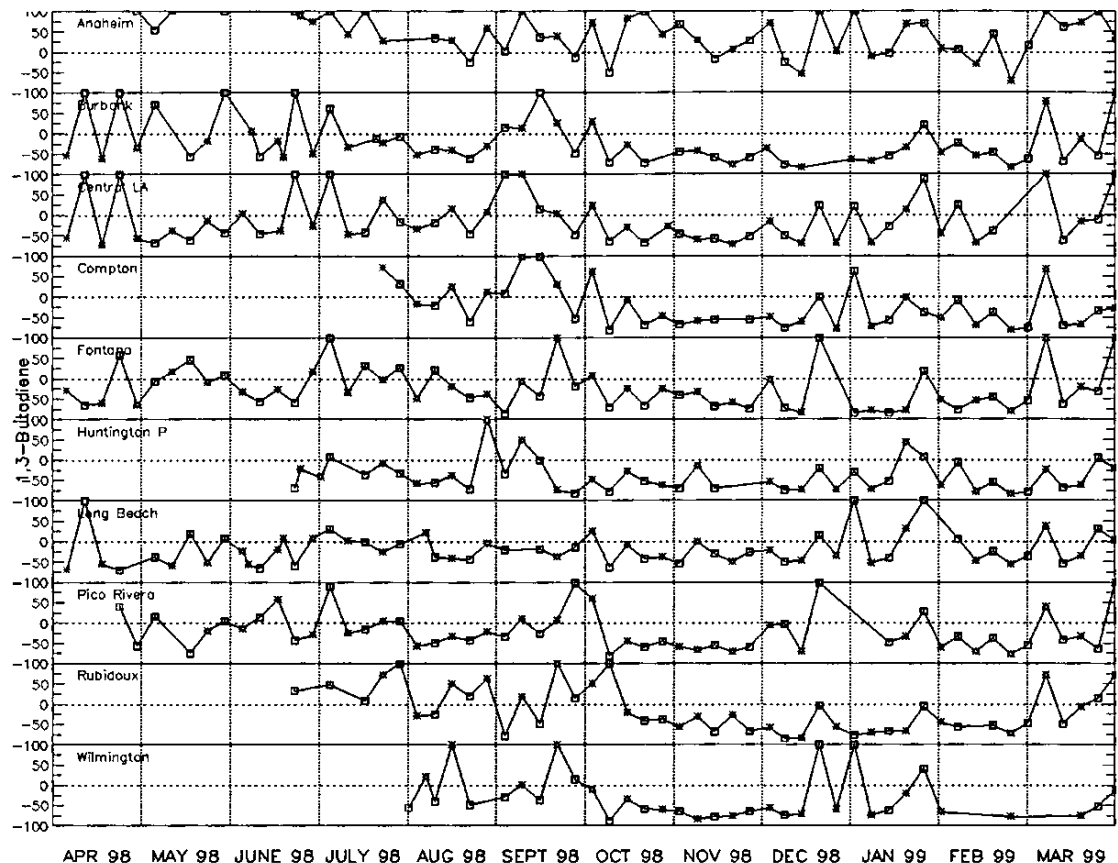


Figure V-9c. Time-series plot of the residuals between simulated and measured concentrations of 1,3-butadiene.

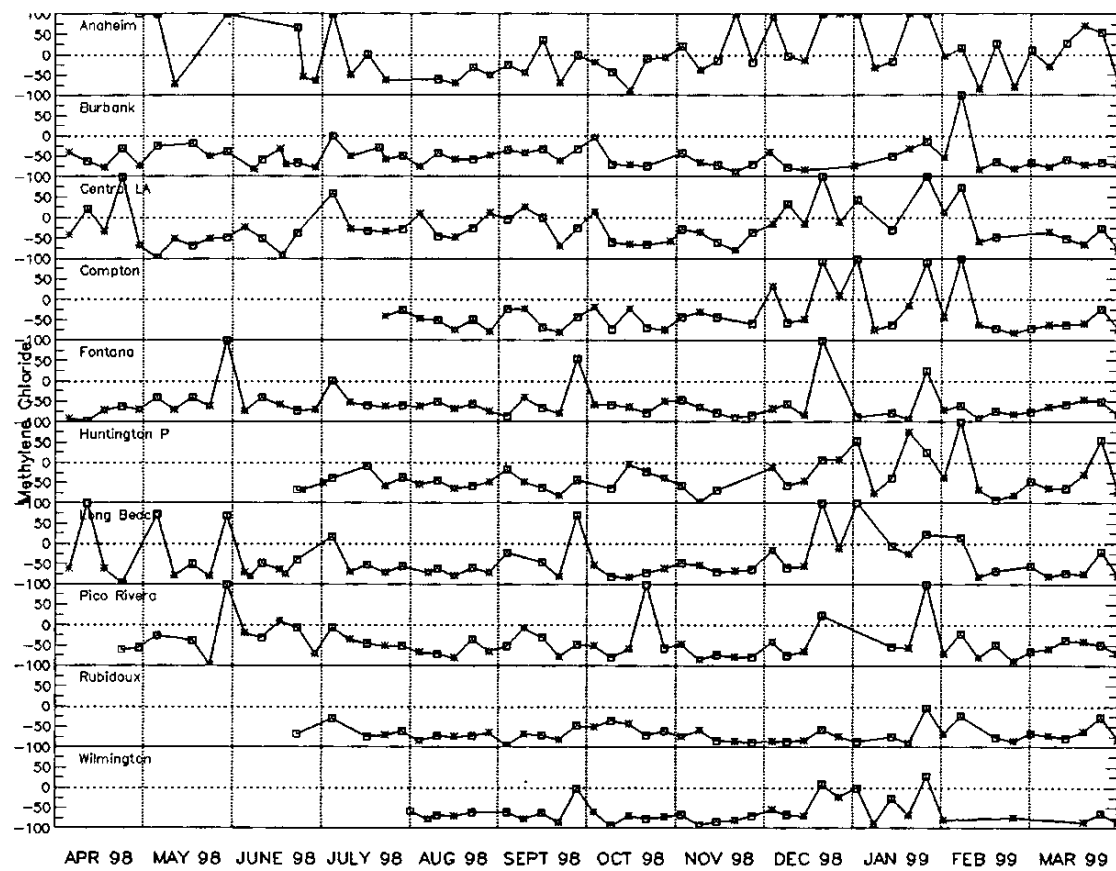


Figure V-9d. Time-series plot of the residuals between simulated and measured concentrations of methylene chloride.

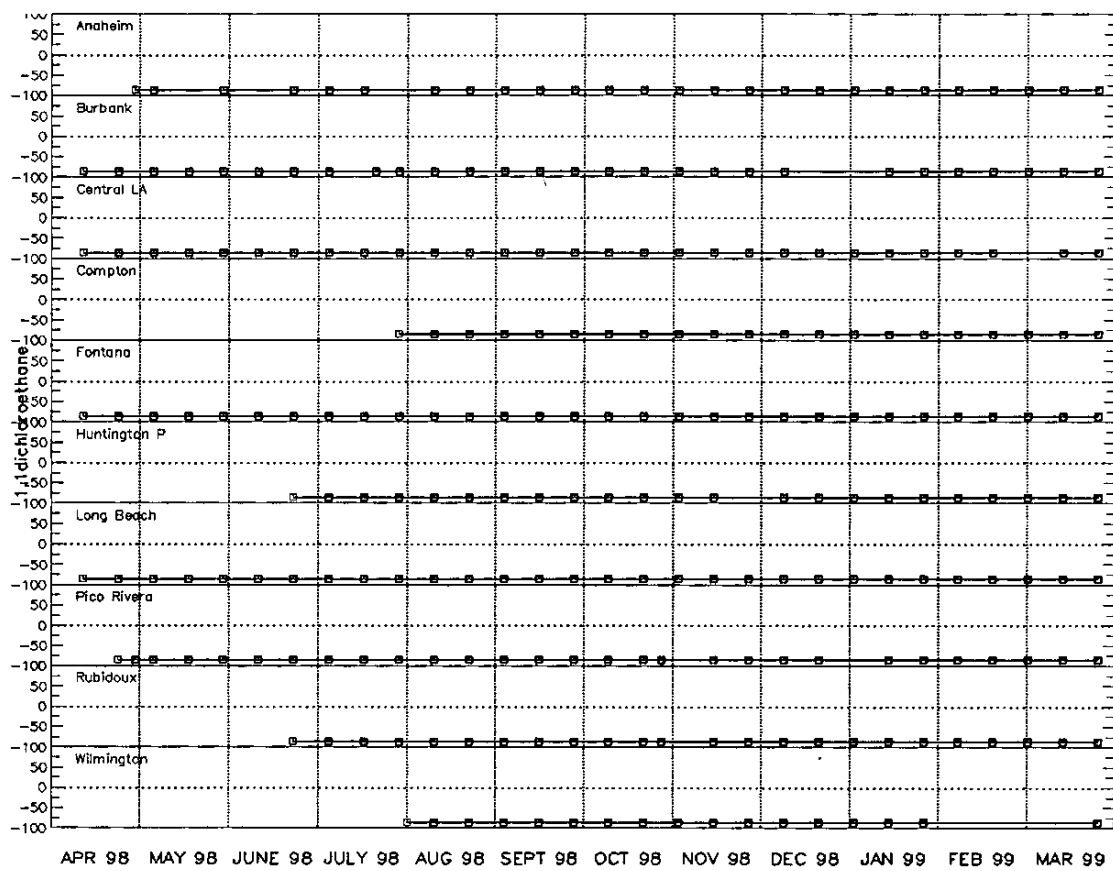


Figure V-9e. Time-series plot of the residuals between simulated and measured concentrations of 1,1 dichloroethane.

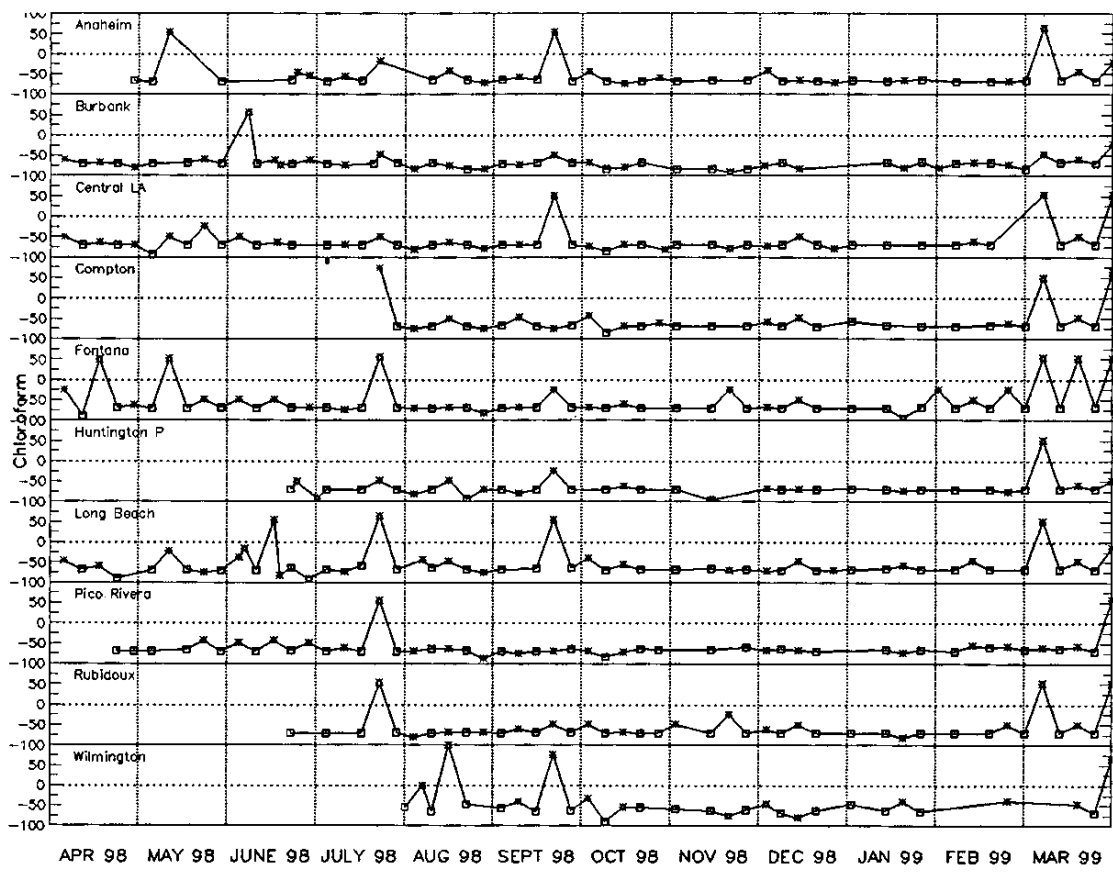


Figure V-9f. Time-series plot of the residuals between simulated and measured concentrations of chloroform.

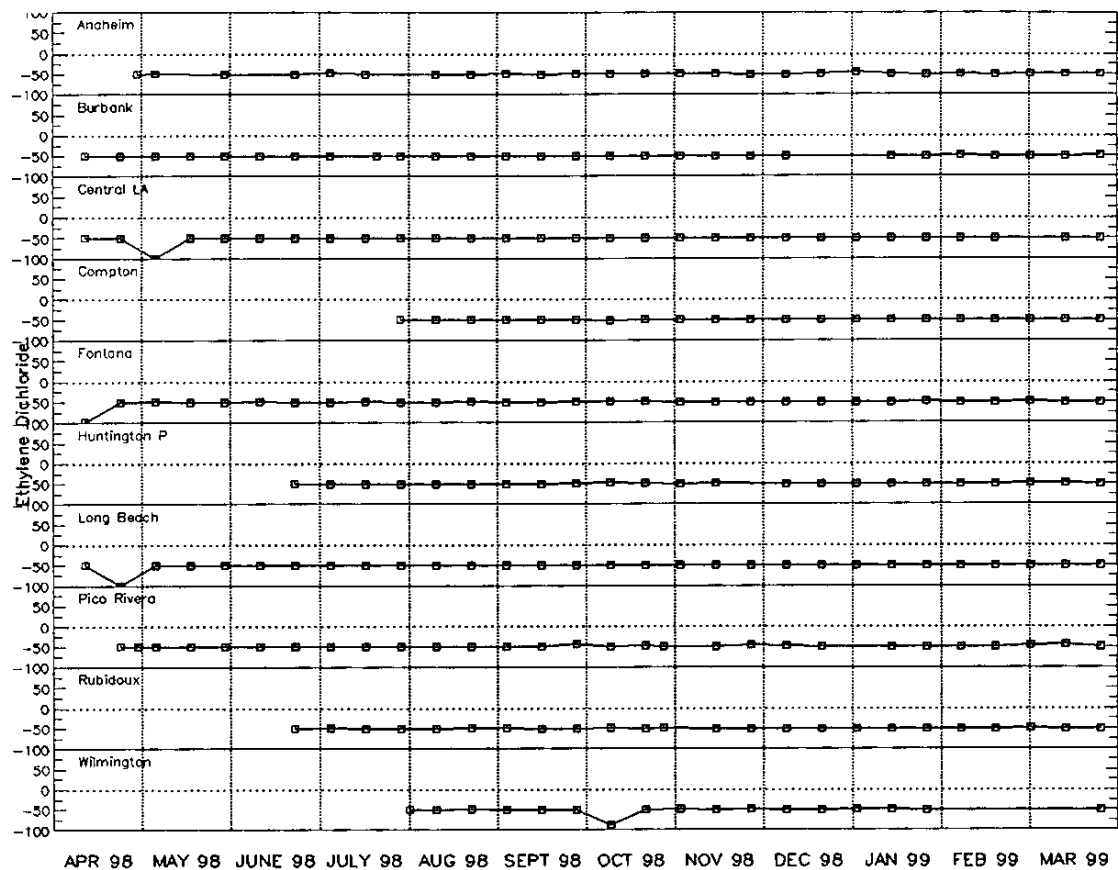


Figure V-9g. Time-series plot of the residuals between simulated and measured concentrations of ethylene dichloride.

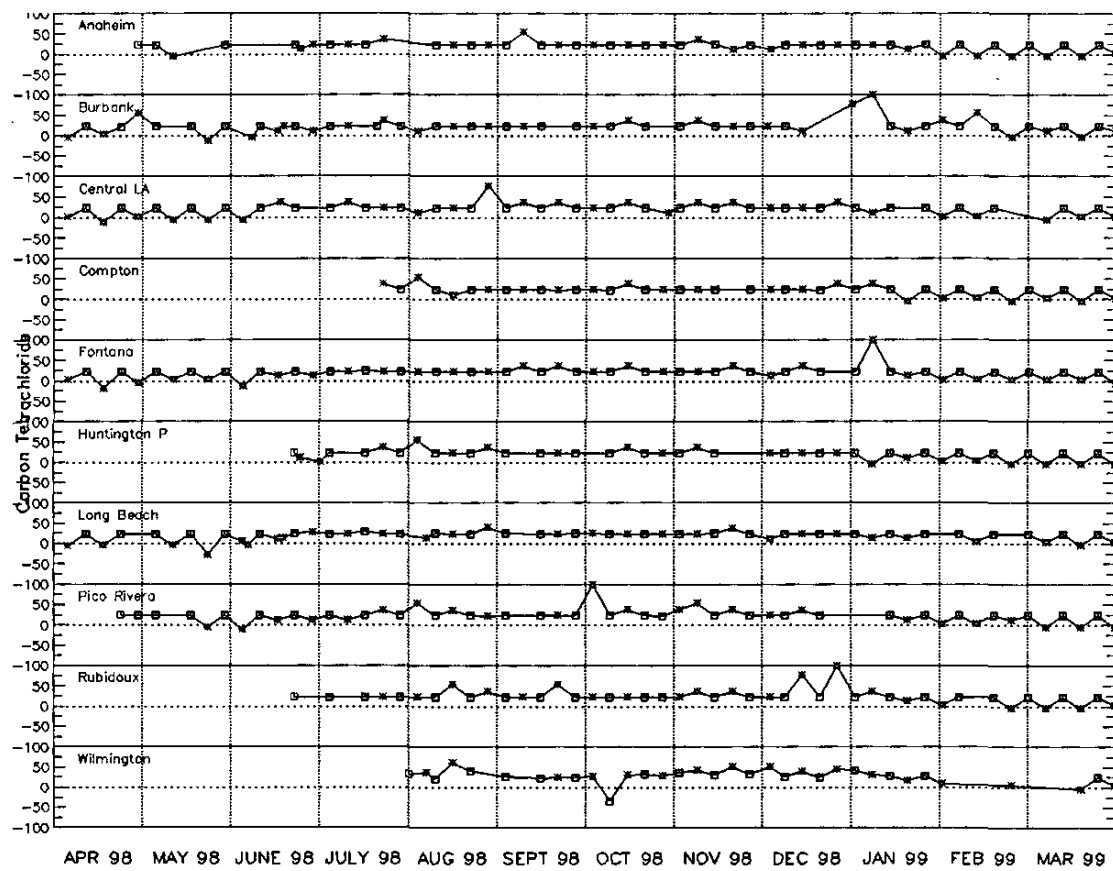


Figure V-9h. Time-series plot of the residuals between simulated and measured concentrations of carbon tetrachloride.

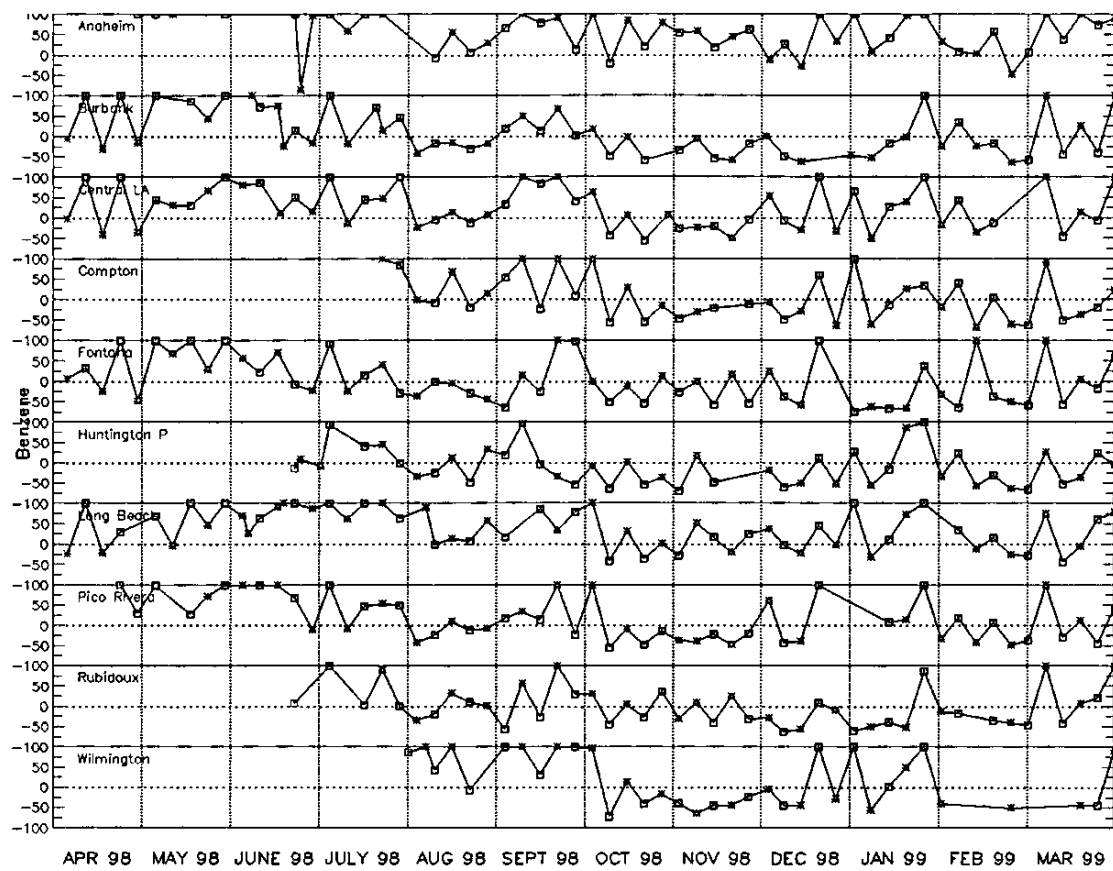


Figure V-9i. Time-series plot of the residuals between simulated and measured concentrations benzene.

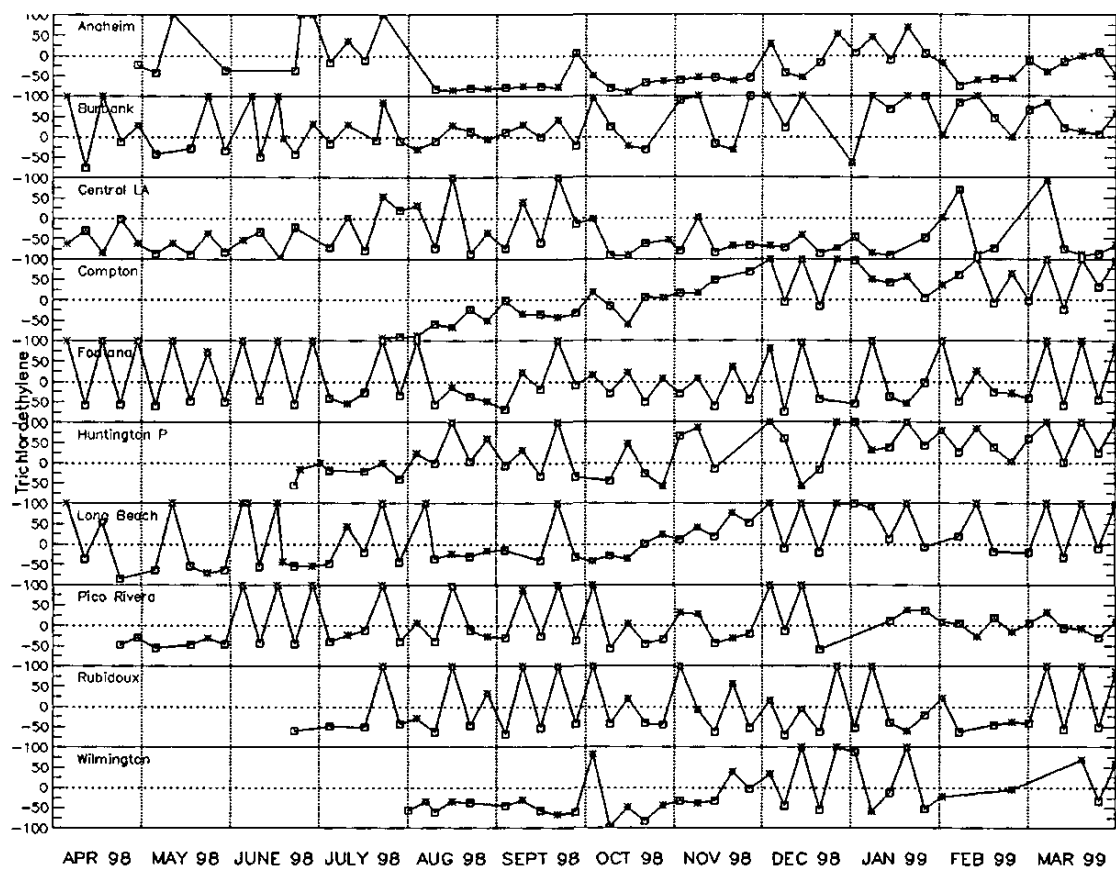


Figure V-9j. Time-series plot of the residuals between simulated and measured concentrations of trichloroethylene.

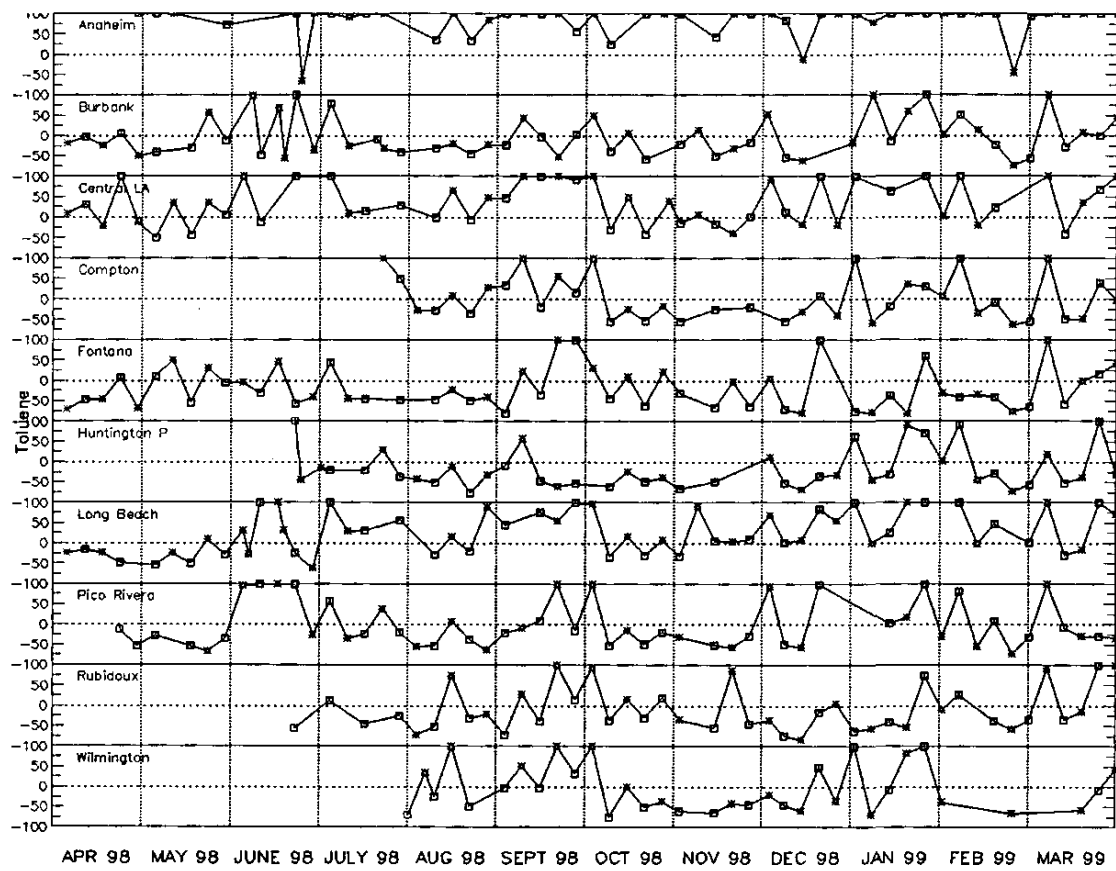


Figure V-9k. Time-series plot of the residuals between simulated and measured concentrations toluene.

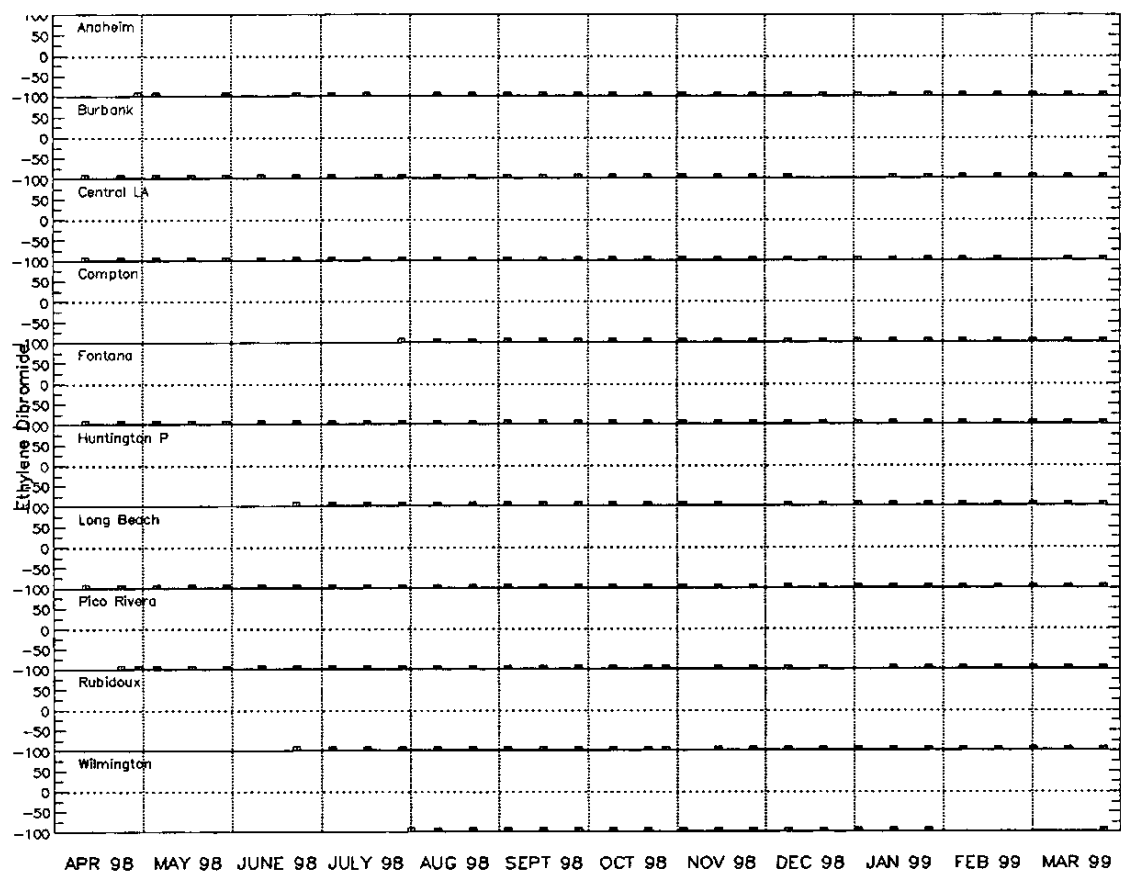


Figure V-91. Time-series plot of the residuals between simulated and measured concentrations ethylene dibromide.

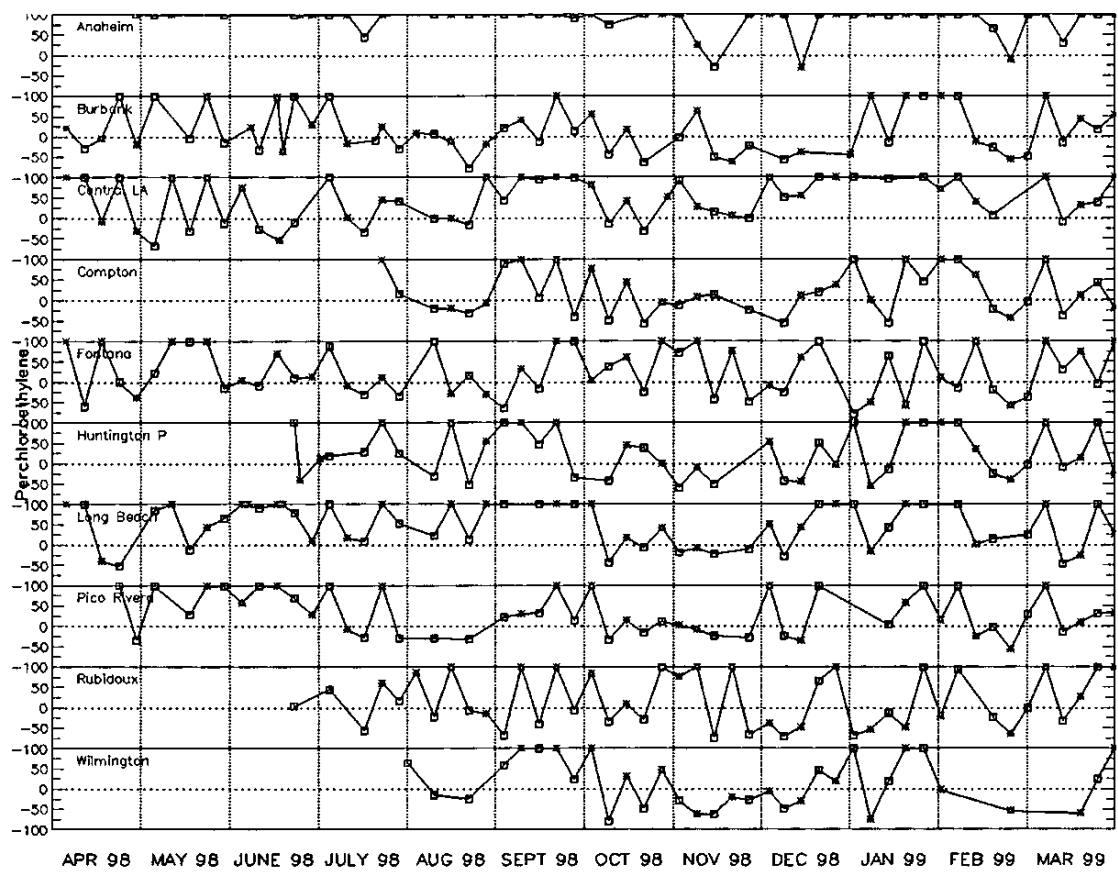


Figure V-9m. Time-series plot of the residuals between simulated and measured concentrations perchloroethylene.

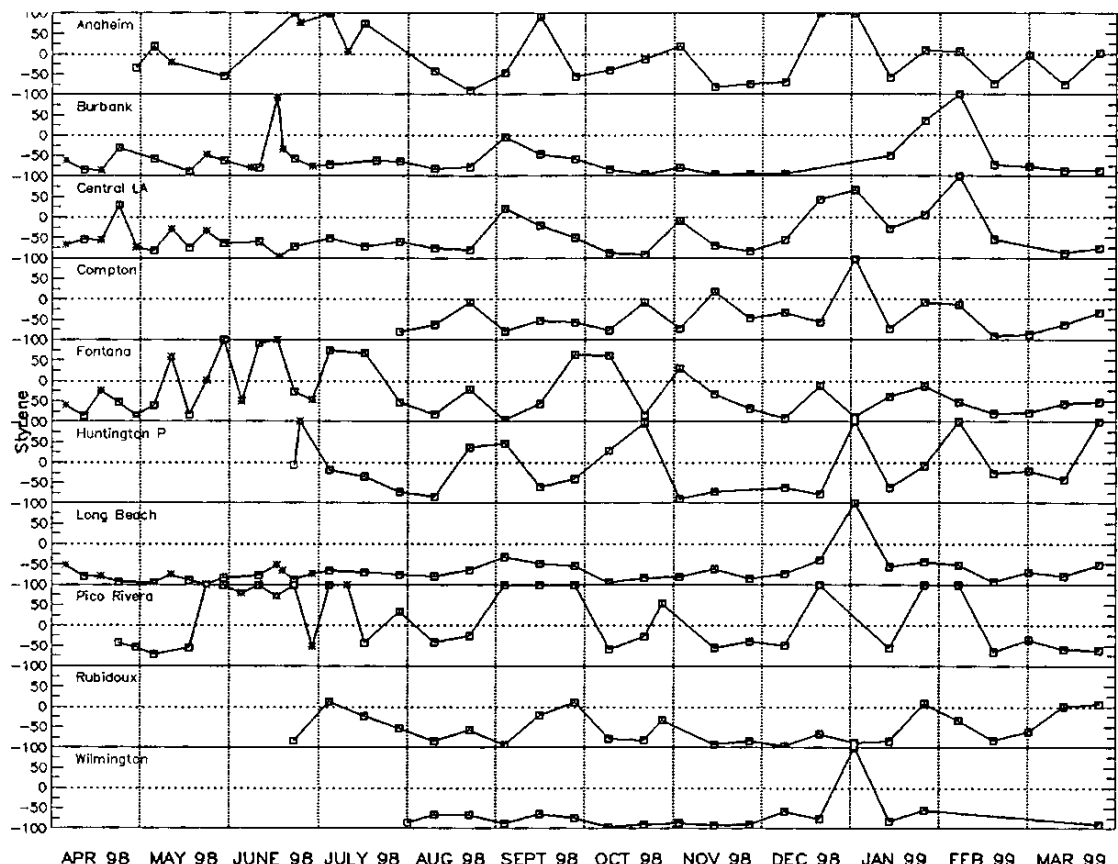


Figure V-9n. Time-series plot of the residuals between simulated and measured concentrations styrene

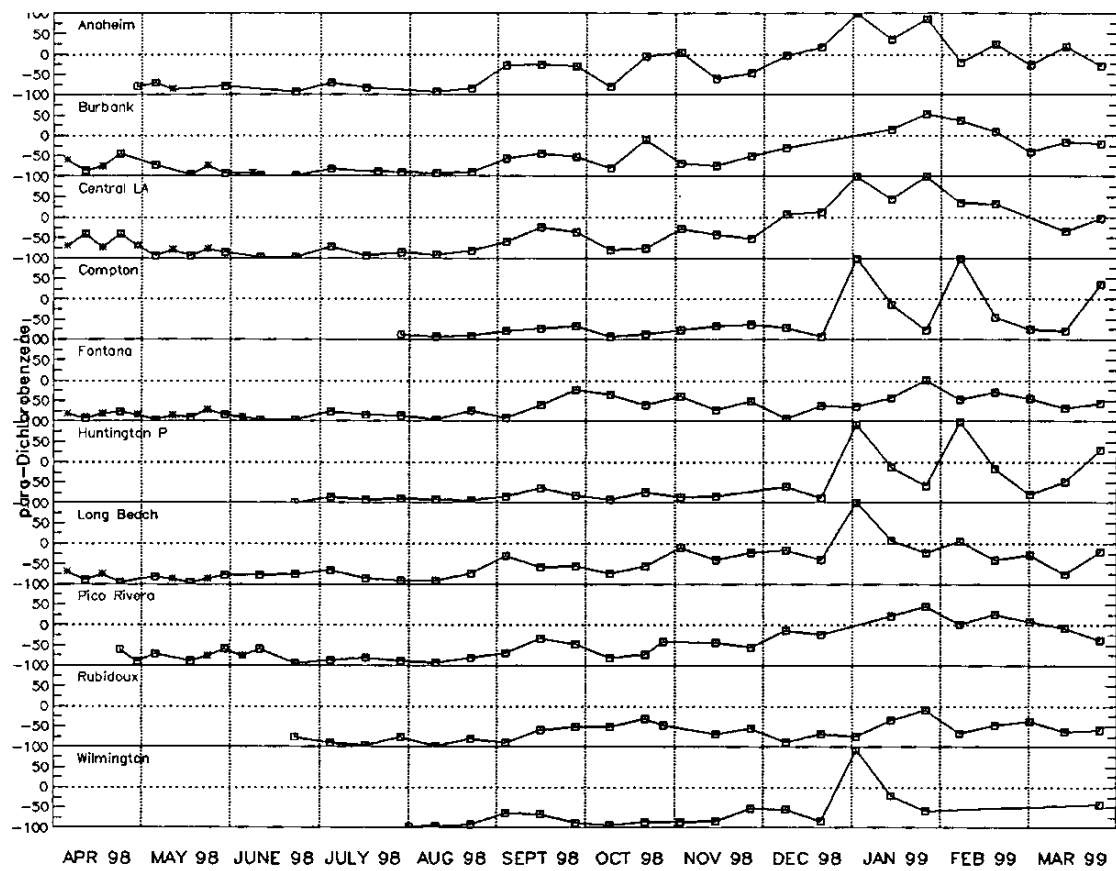


Figure V-9o. Time-series plot of the residuals between simulated and measured concentrations p-dichlorobenzene.

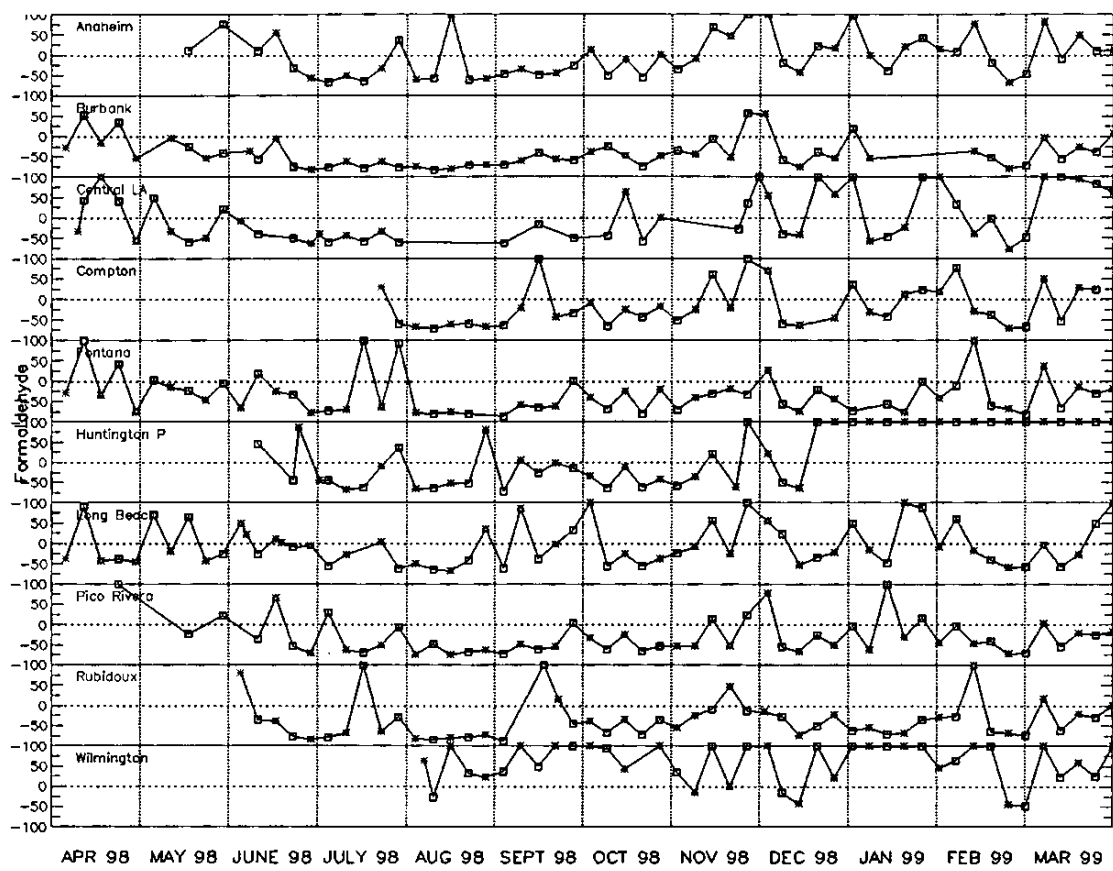


Figure V-9p. Time-series plot of the residuals between simulated and measured concentrations for formaldehyde.

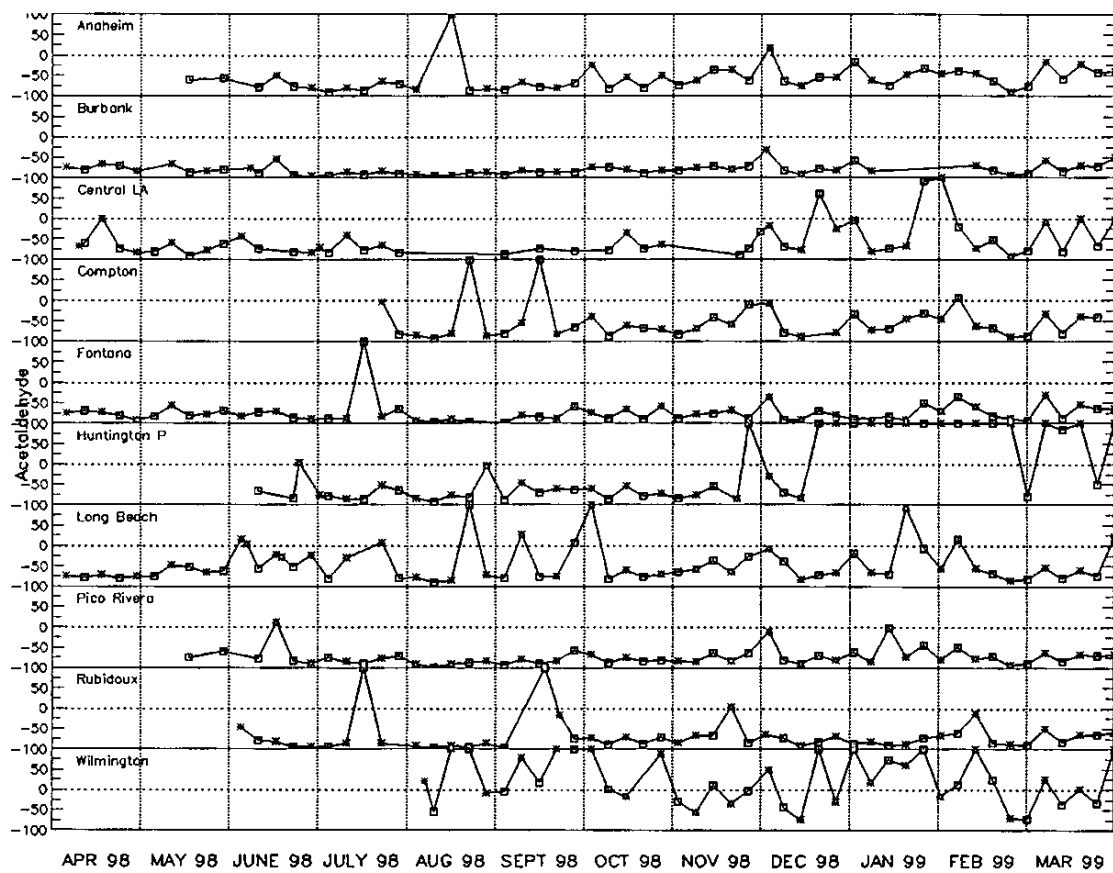


Figure V-9q. Time-series plot of the residuals between simulated and measured concentrations acetaldehyde.

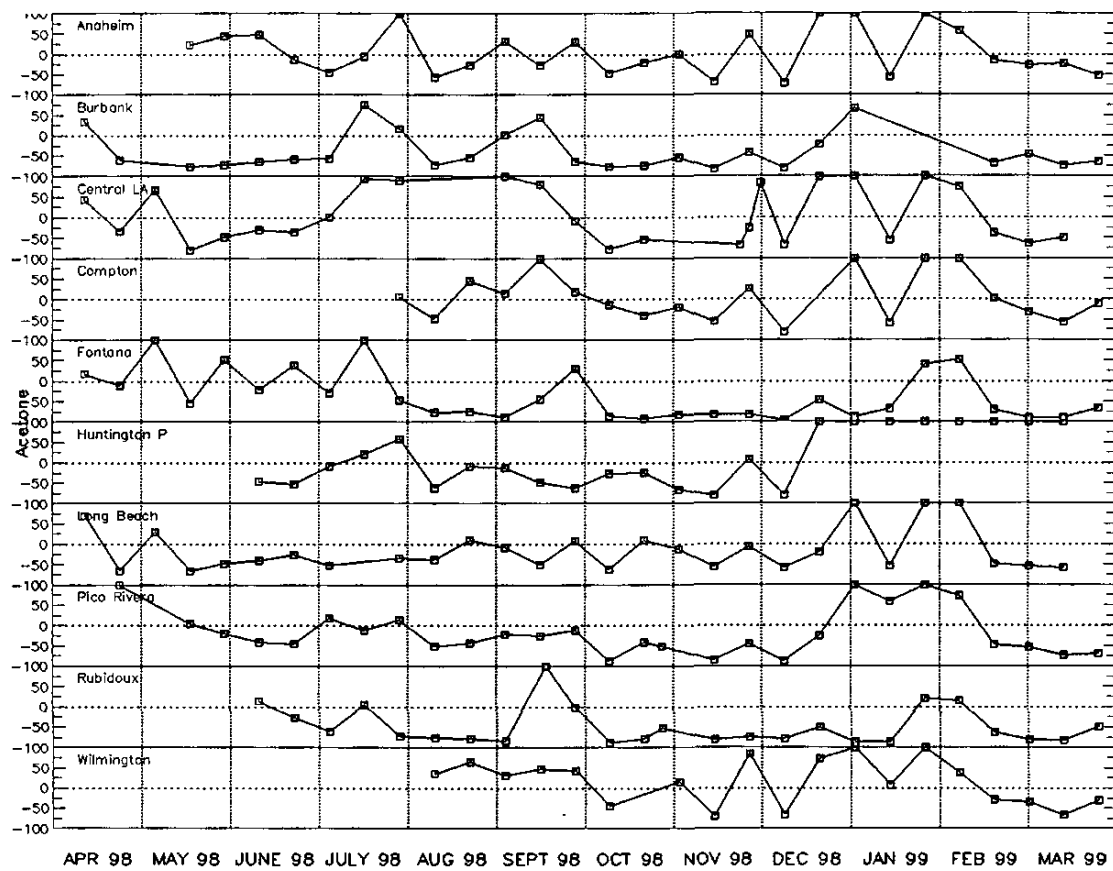


Figure V-9r. Time-series plot of the residuals between simulated and measured concentrations acetone.

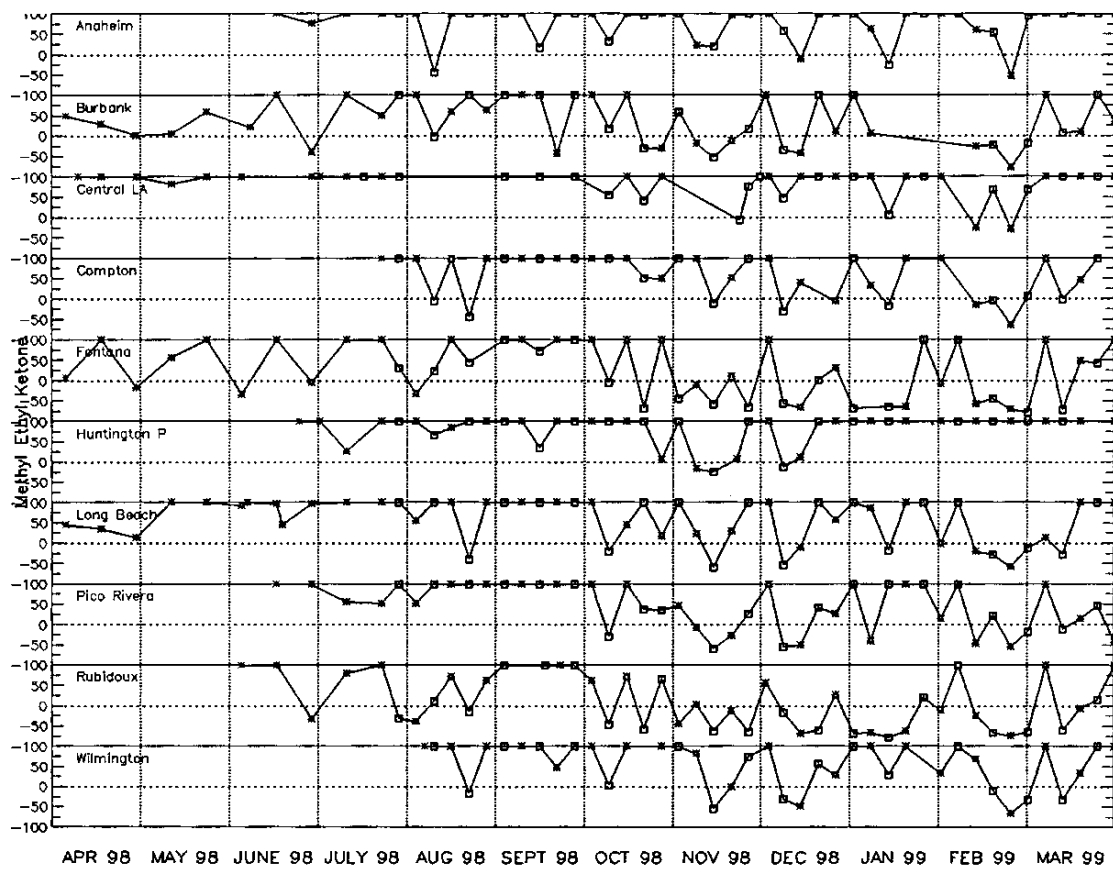


Figure V-9s. Time-series plot of the residuals between simulated and measured concentrations methyl ethyl ketone.

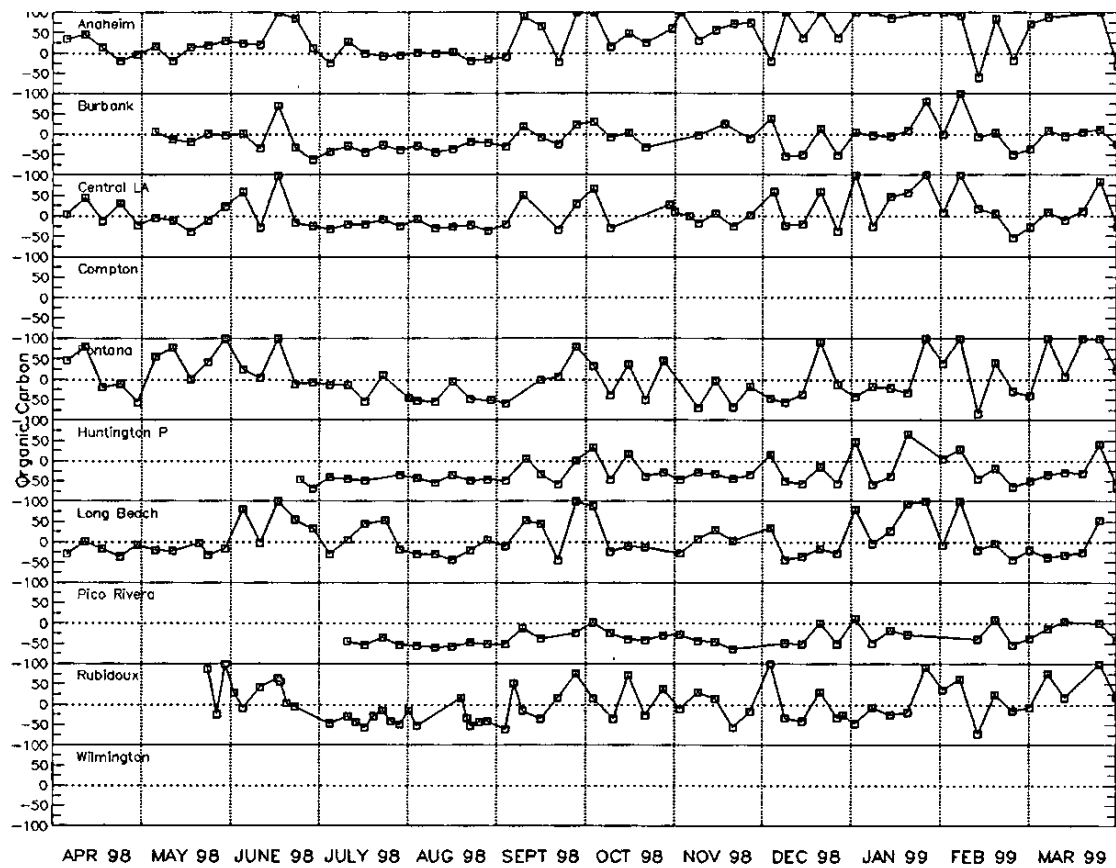


Figure V-9t. Time-series plot of the residuals between simulated and measured concentrations organic carbon.

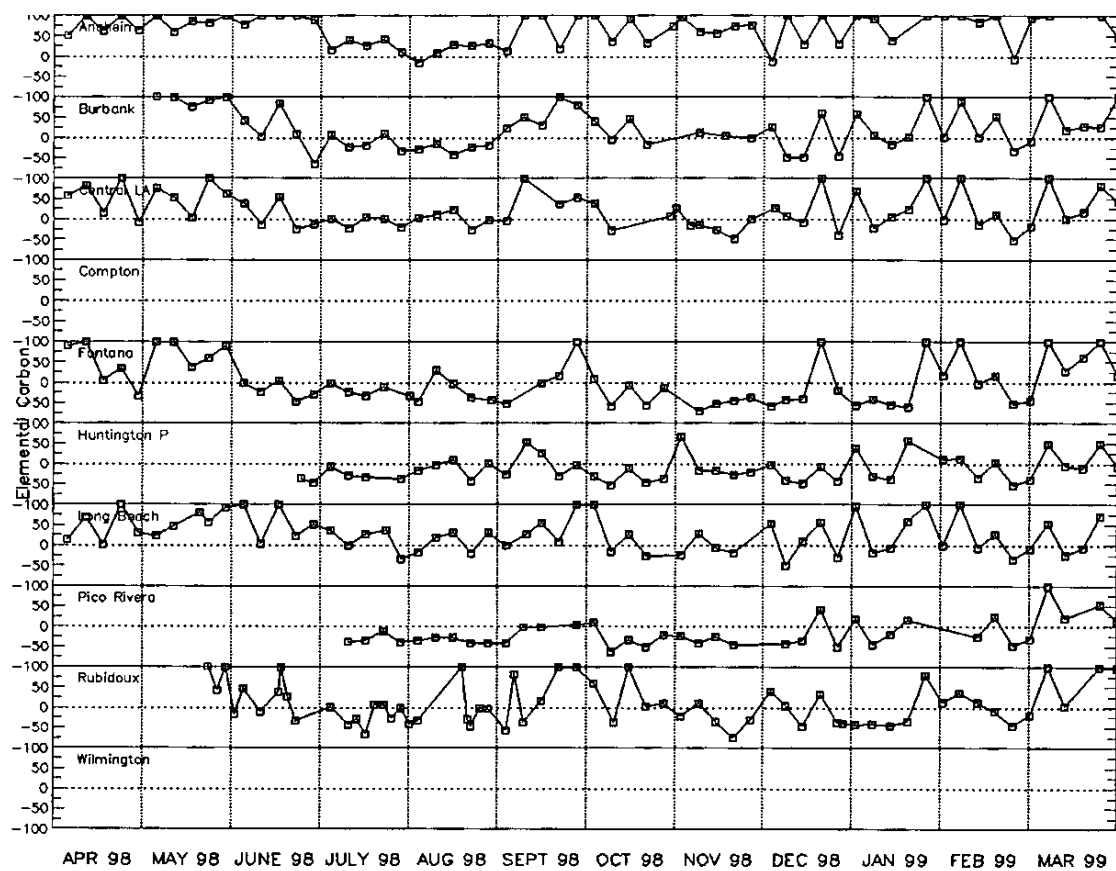


Figure V-9u. Time-series plot of the residuals between simulated and measured concentrations elemental carbon.

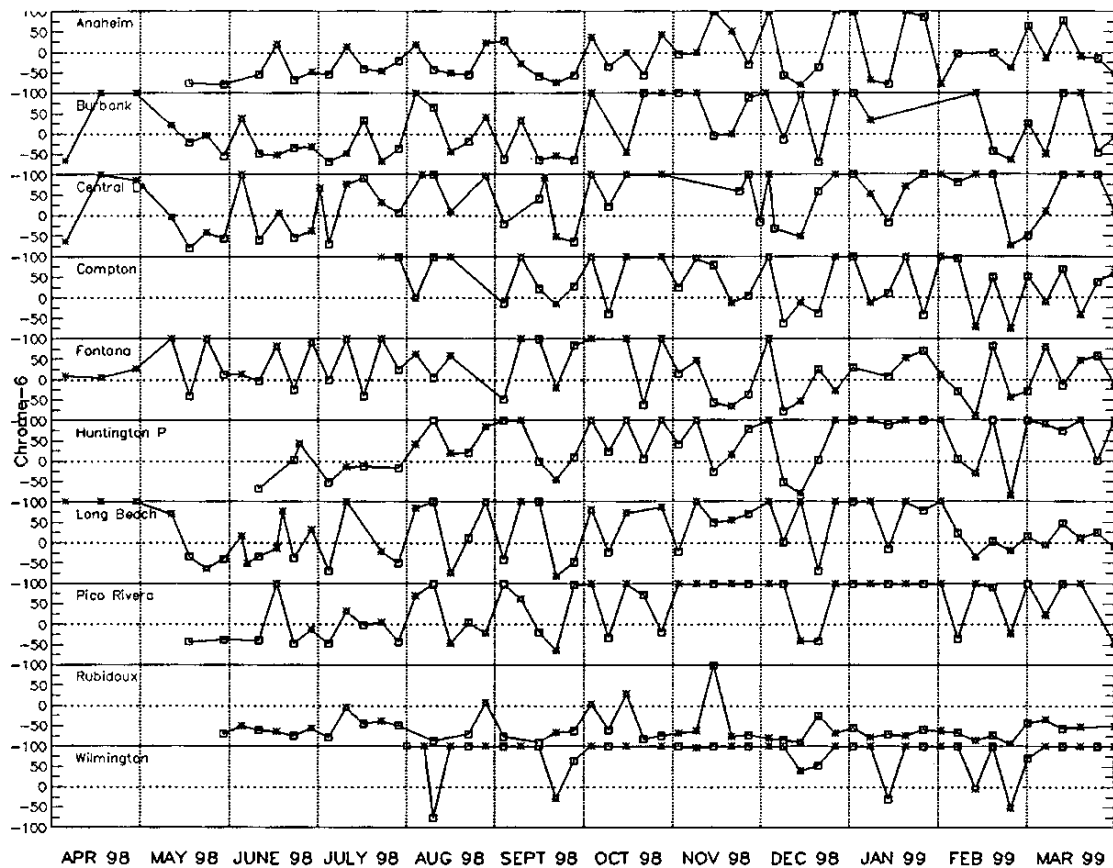


Figure V-9v. Time-series plot of the residuals between simulated and measured concentrations hexavalent chromium.

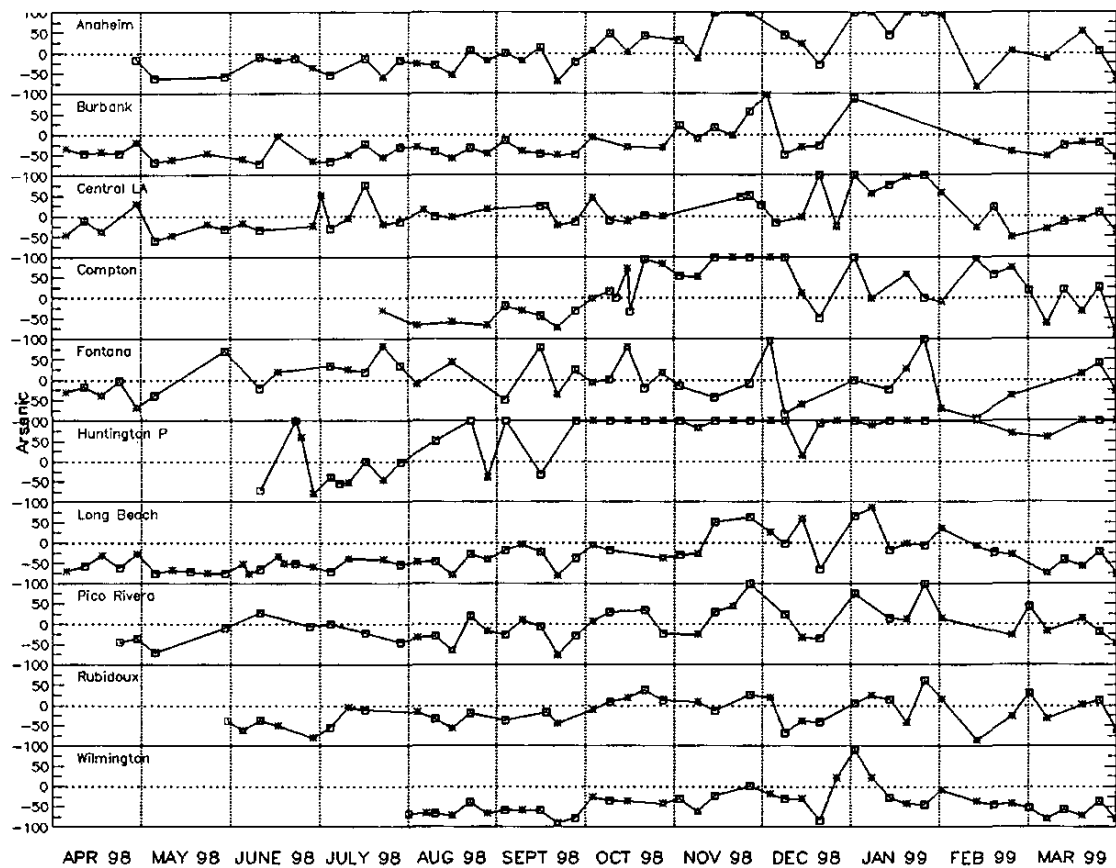


Figure V-9w. Time-series plot of the residuals between simulated and measured concentrations arsenic.

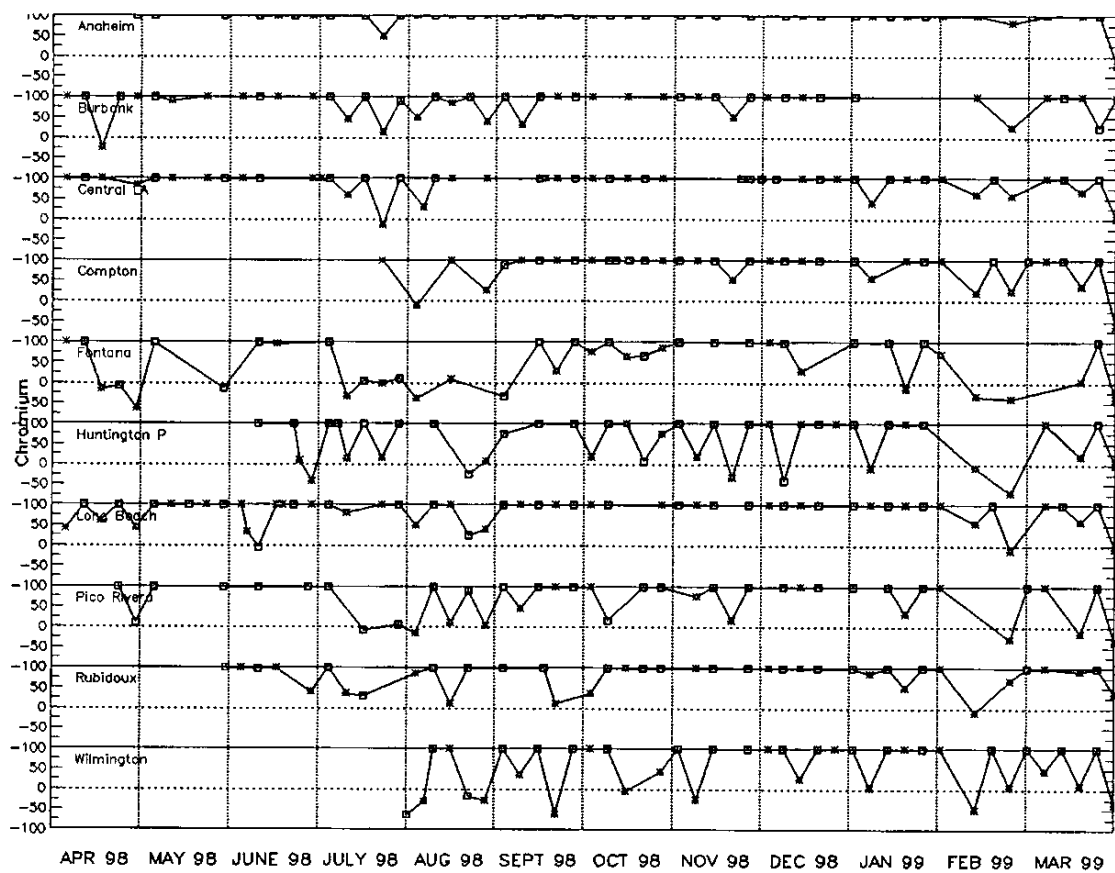


Figure V-9x. Time-series plot of the residuals between simulated and measured concentrations chromium.

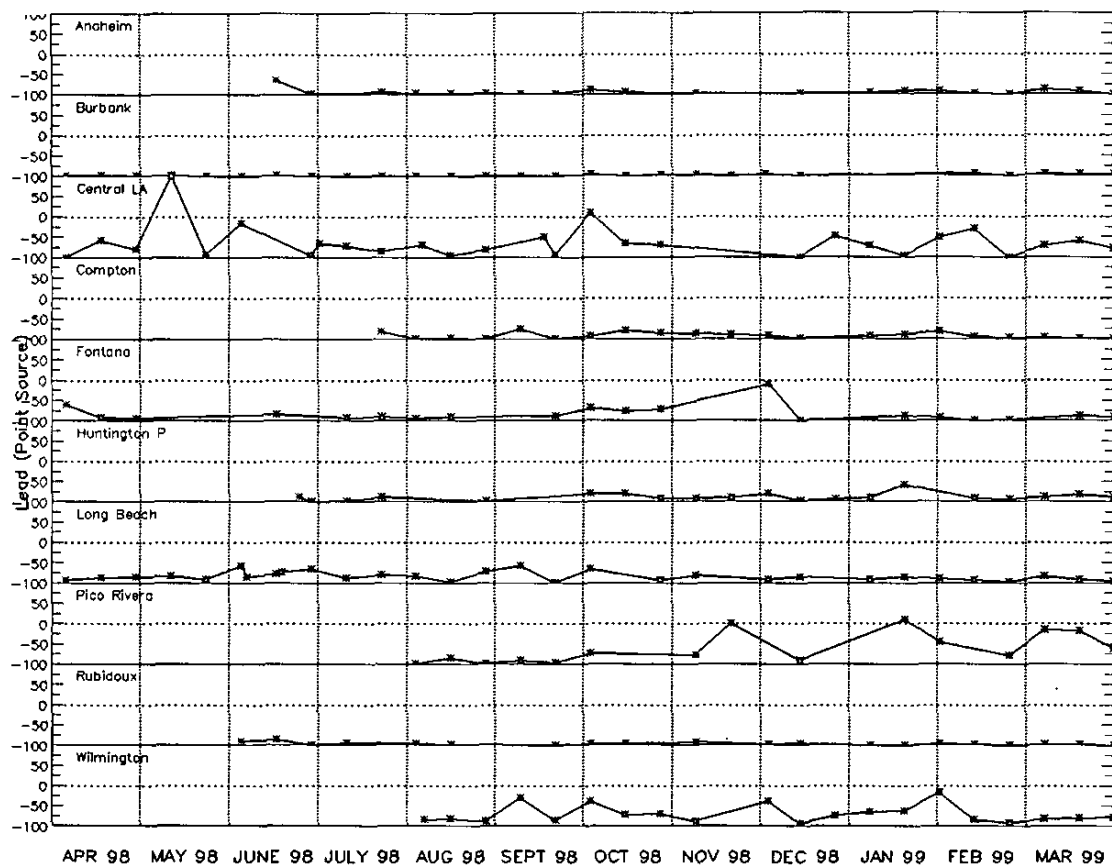


Figure V-9y. Time-series plot of the residuals between simulated and measured concentrations point source lead.

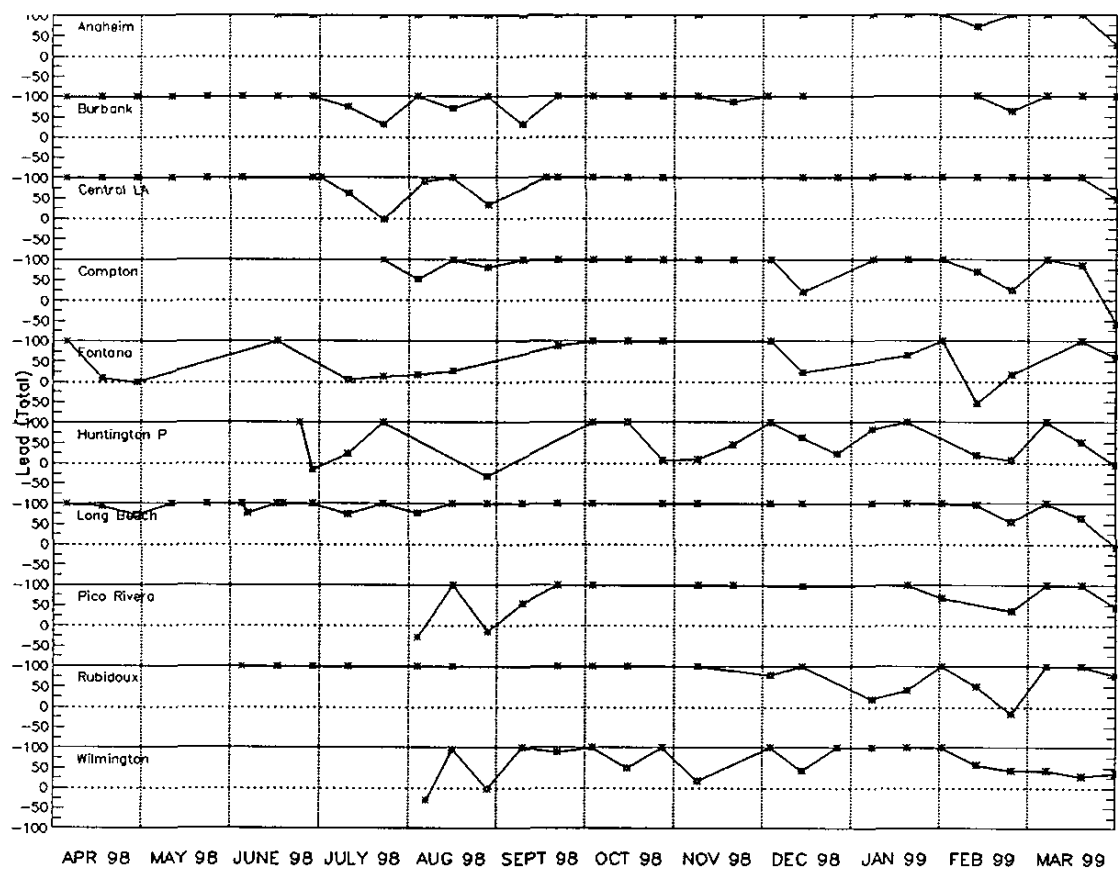


Figure V-9z. Time-series plot of the residuals between simulated and measured concentrations total lead.

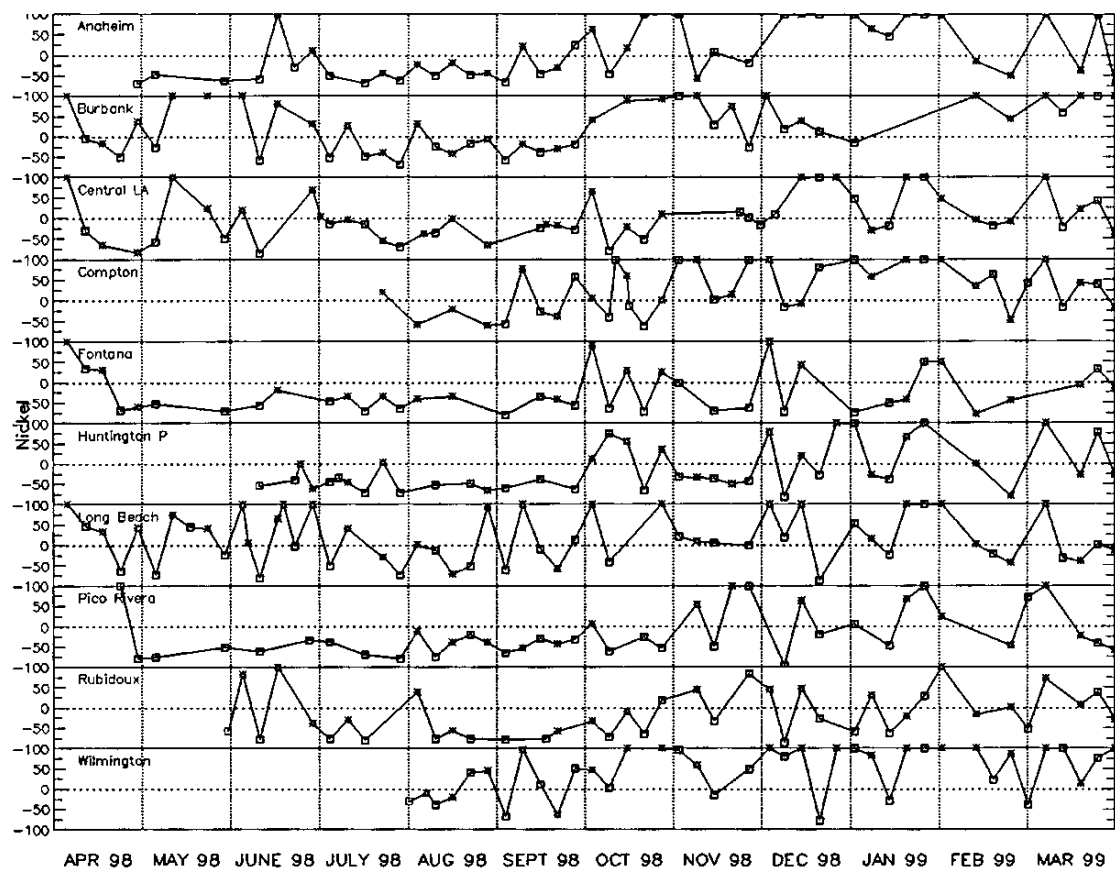


Figure V-9aa. Time-series plot of the residuals between simulated and measured concentrations nickel.

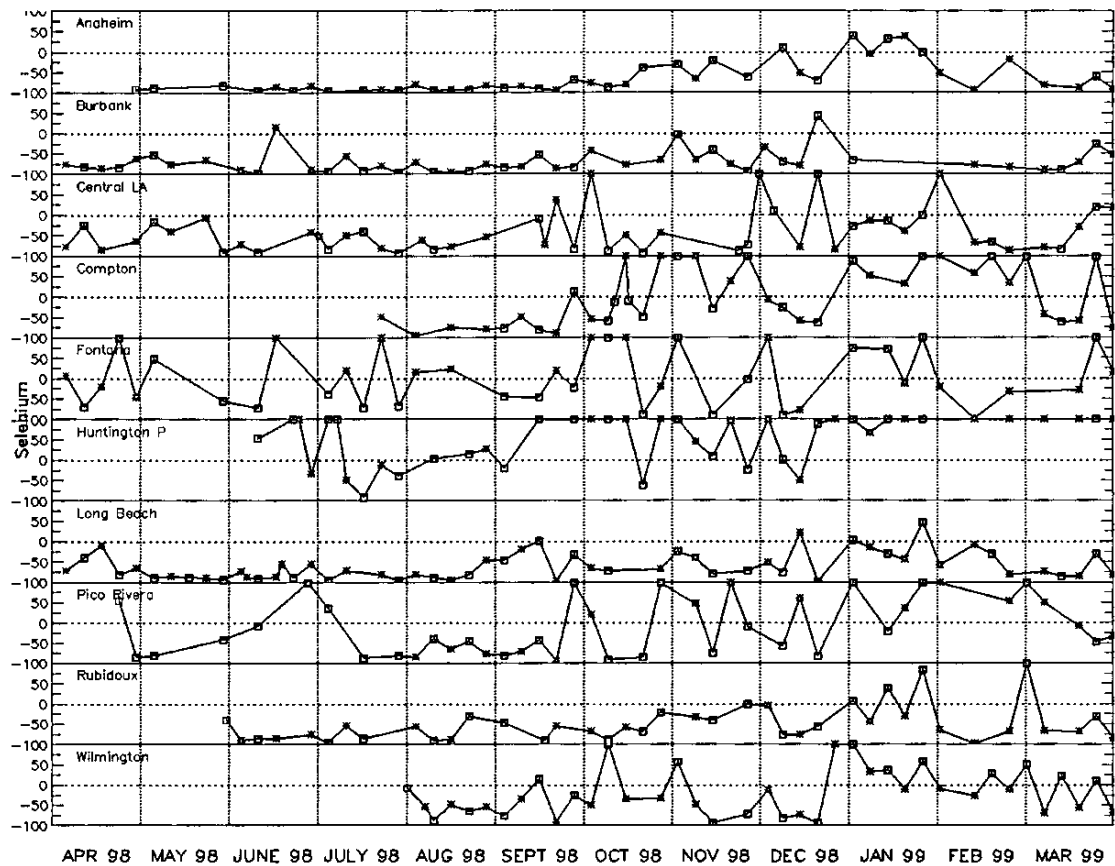


Figure V-9ab. Time-series plot of the residuals between simulated and measured concentrations of selenium.

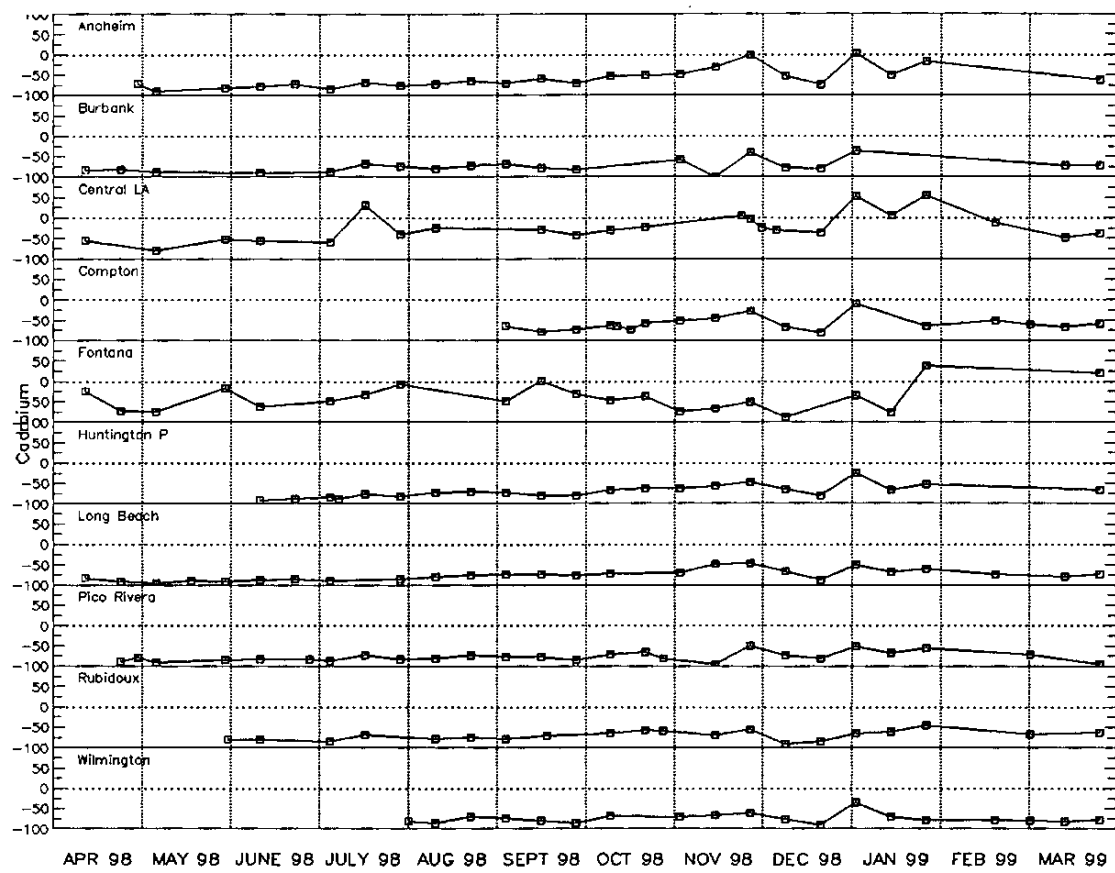
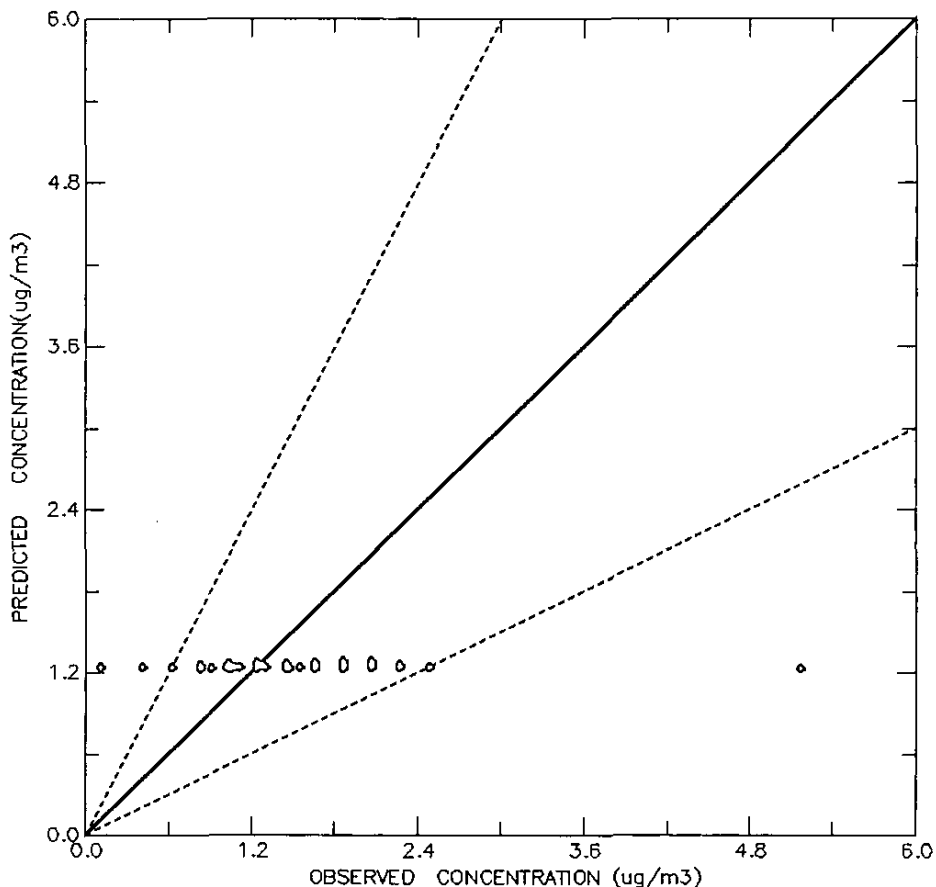


Figure V-9ac. Time-series plot of the residuals between simulated and measured concentrations of cadmium.

Chloromethane
DATA POINTS 247



Vinyl Chloride
DATA POINTS 247

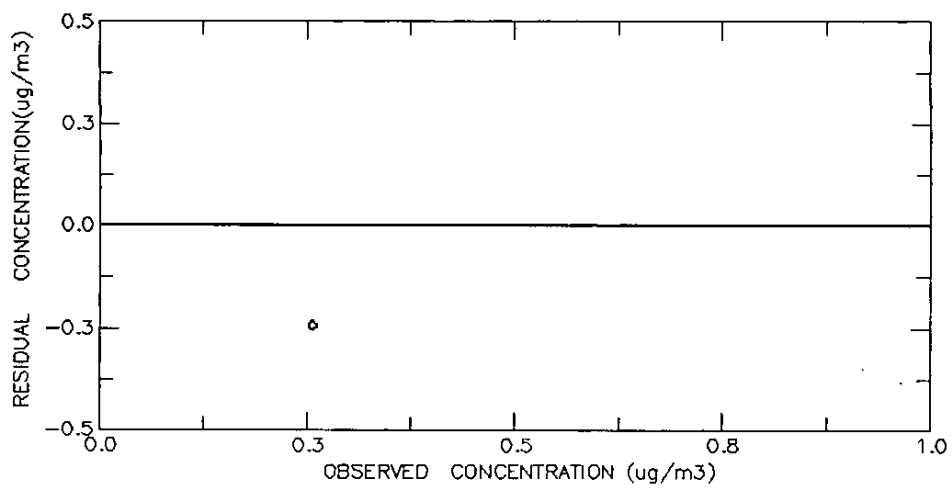
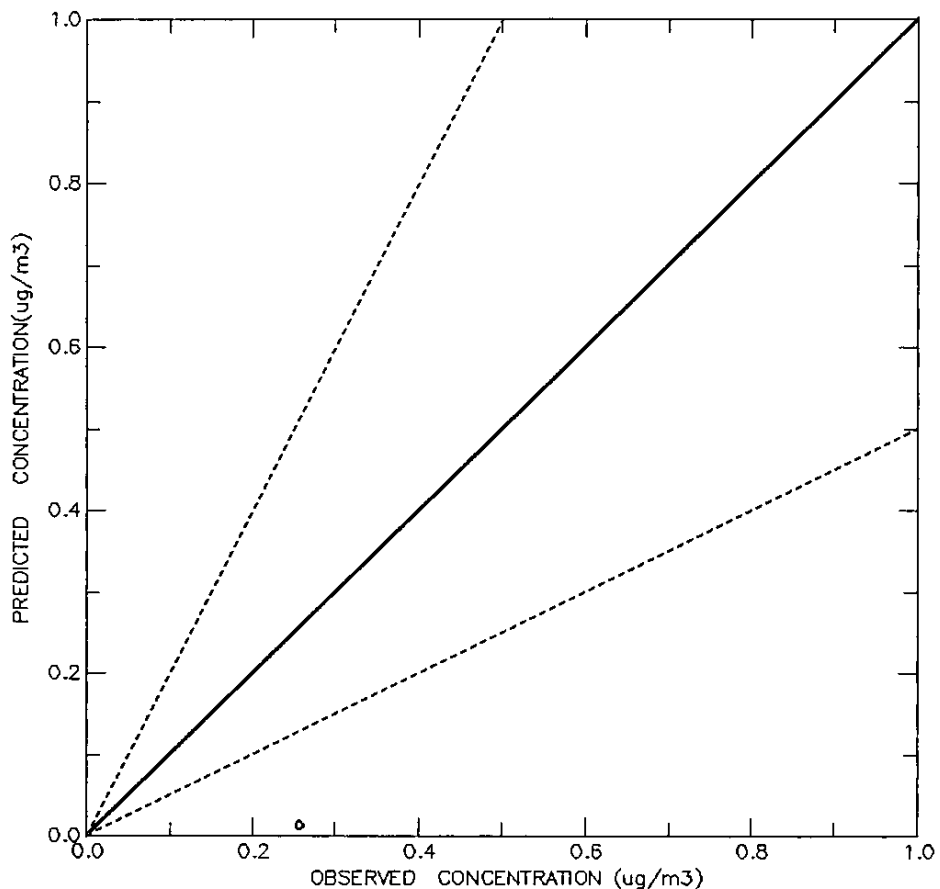


Figure V-10b. Scatter and residual plots of simulated and measured concentrations of vinyl chloride.

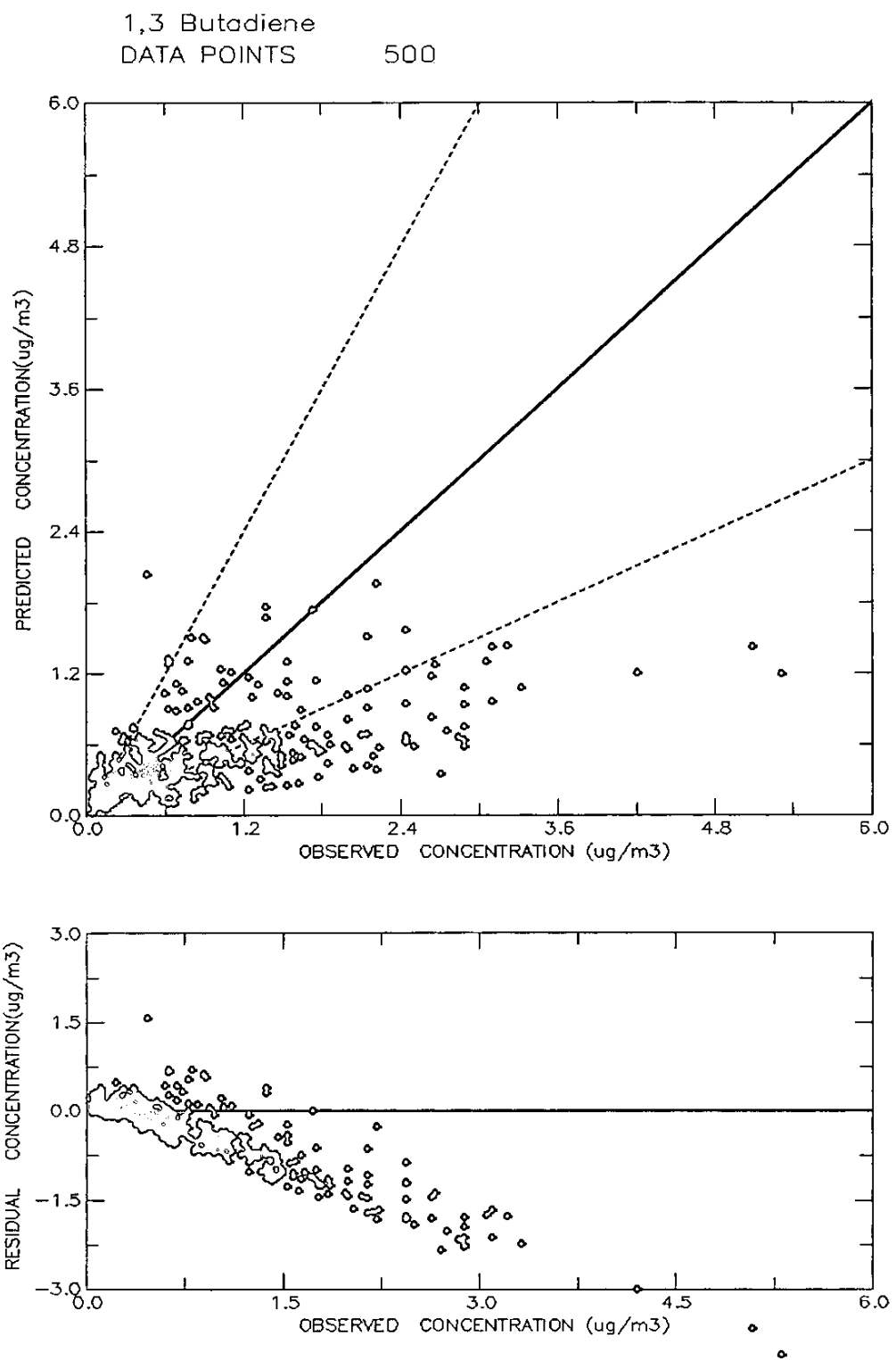


Figure V-10c. Scatter and residual plots of simulated and measured concentrations of 1,3 butadiene.

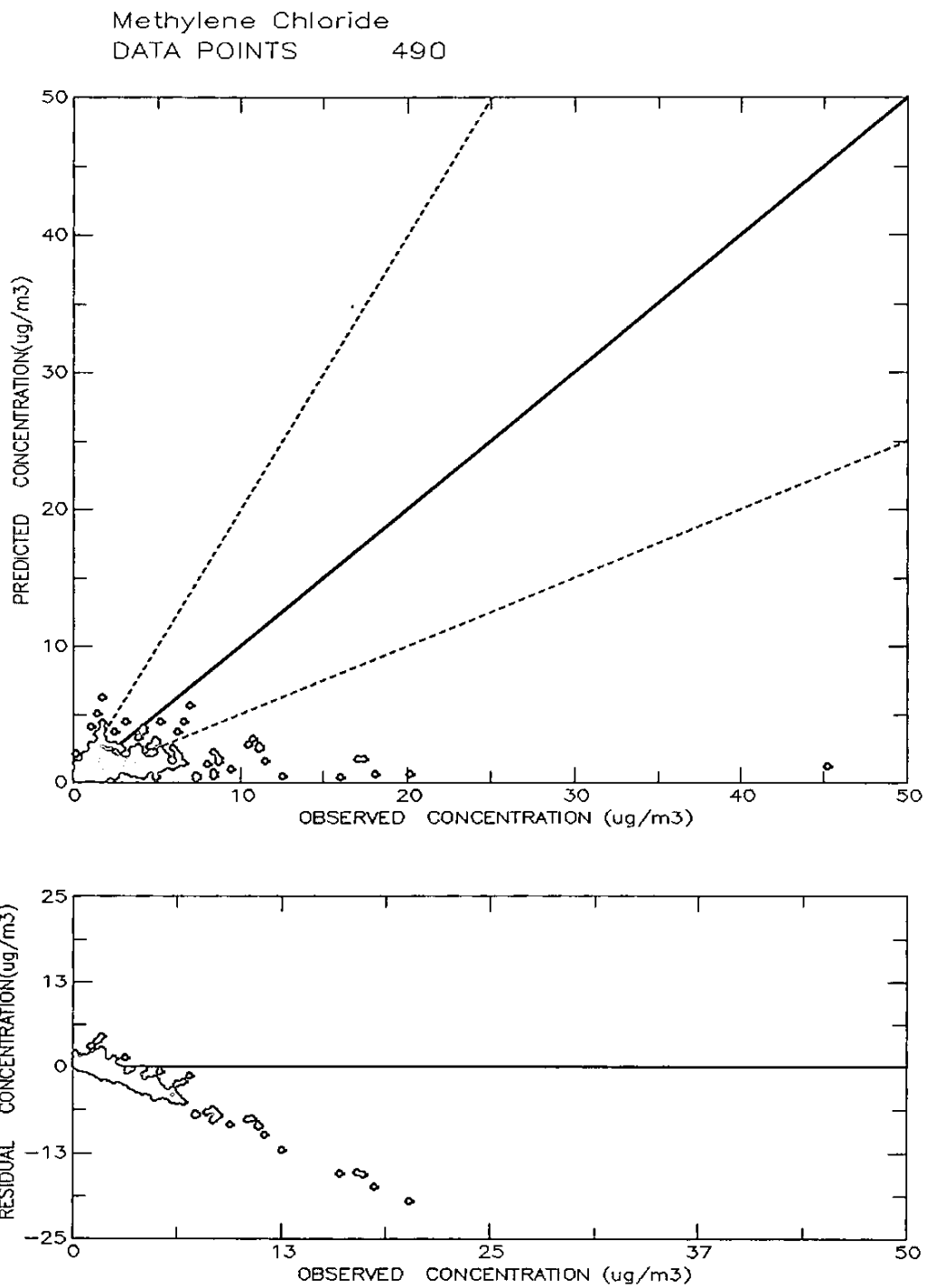


Figure V-10d. Scatter and residual plots of simulated and measured concentrations of methylene chloride.

1,1 Dichloroethane
DATA POINTS 247

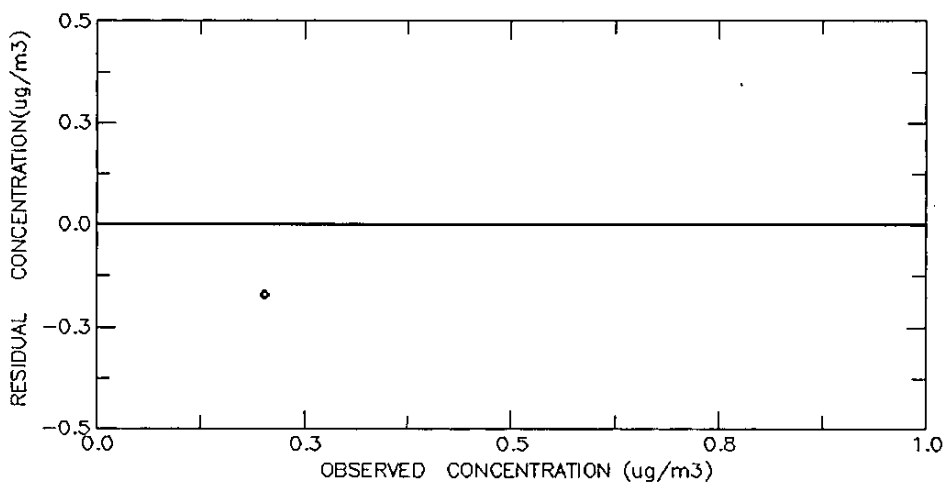
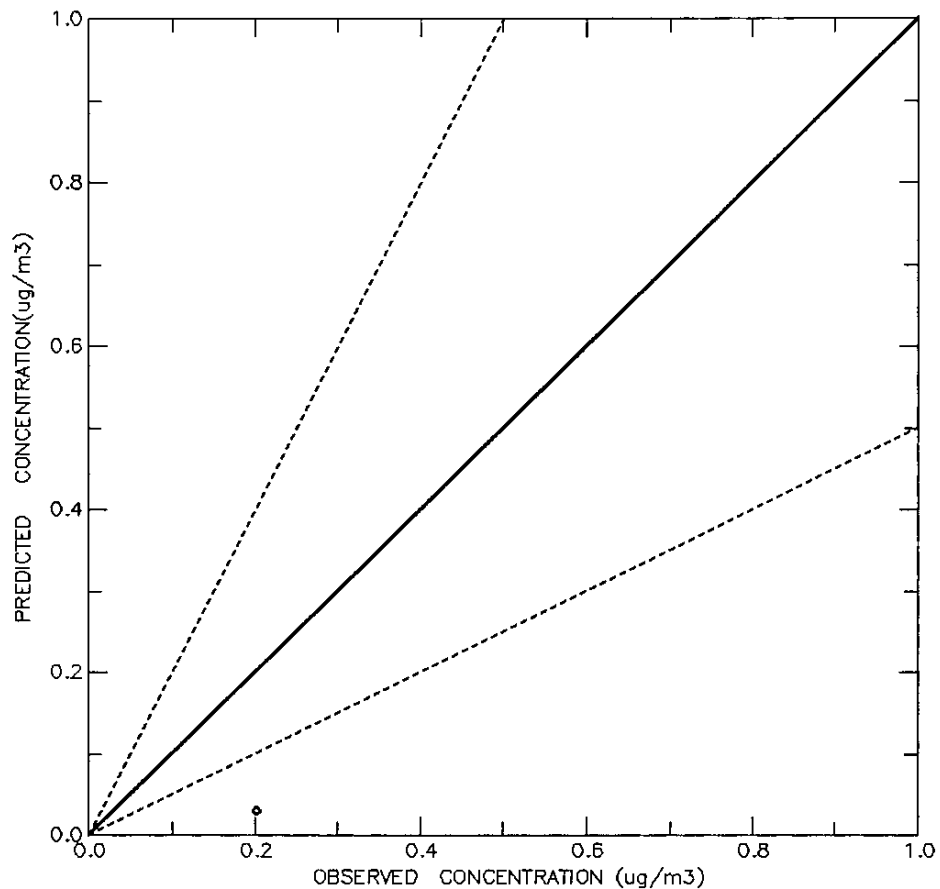


Figure V-10e. Scatter and residual plots of simulated and measured concentrations of 1,1 dichloroethane.

Chloroform
DATA POINTS 454

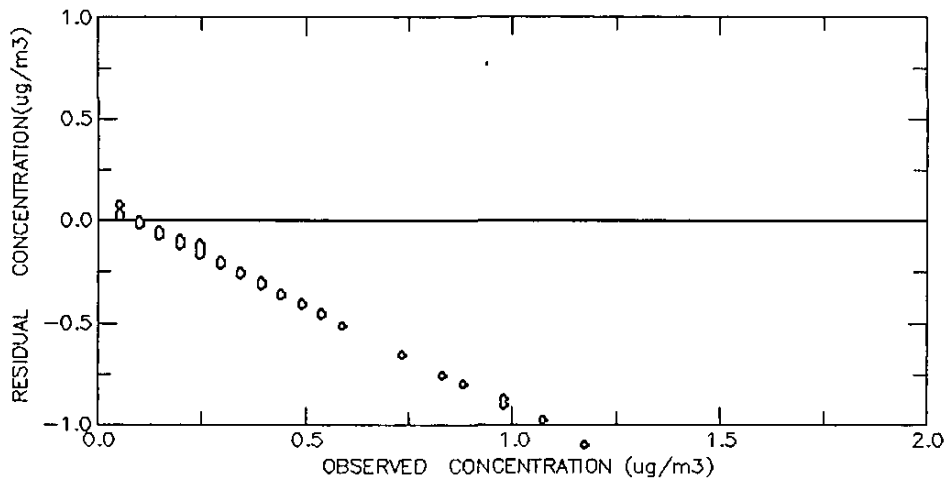
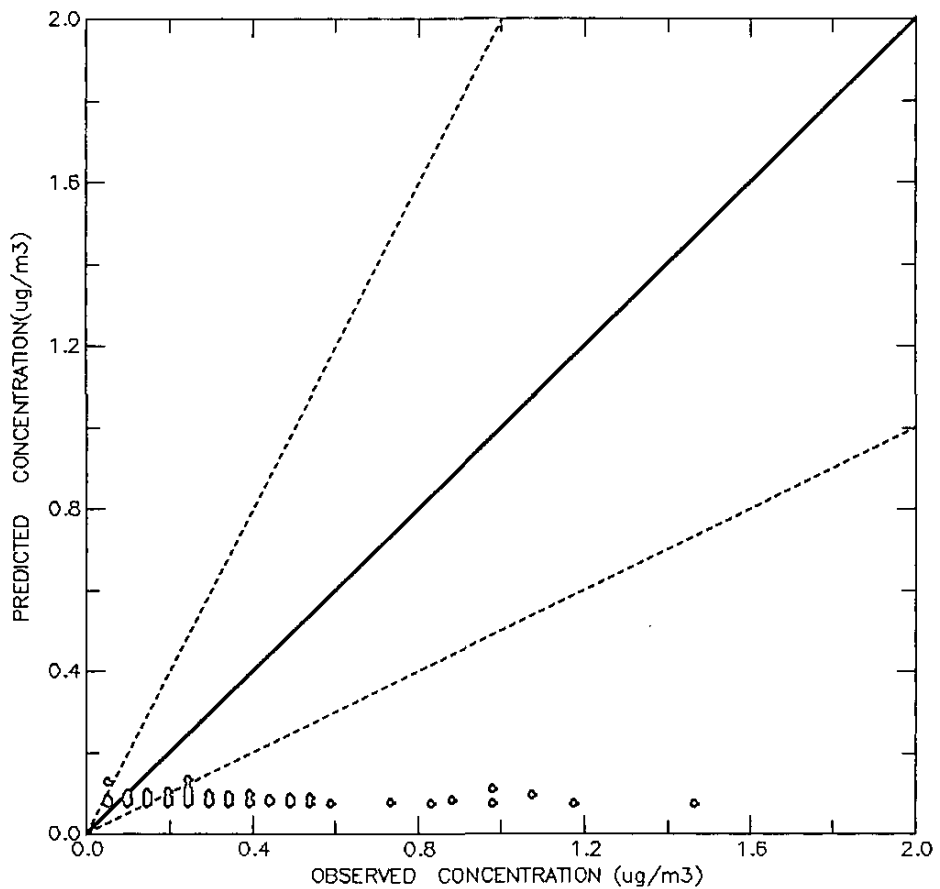


Figure V-10f. Scatter and residual plots of simulated and measured concentrations of chloroform.

Ethylene Dichloride
DATA POINTS 247

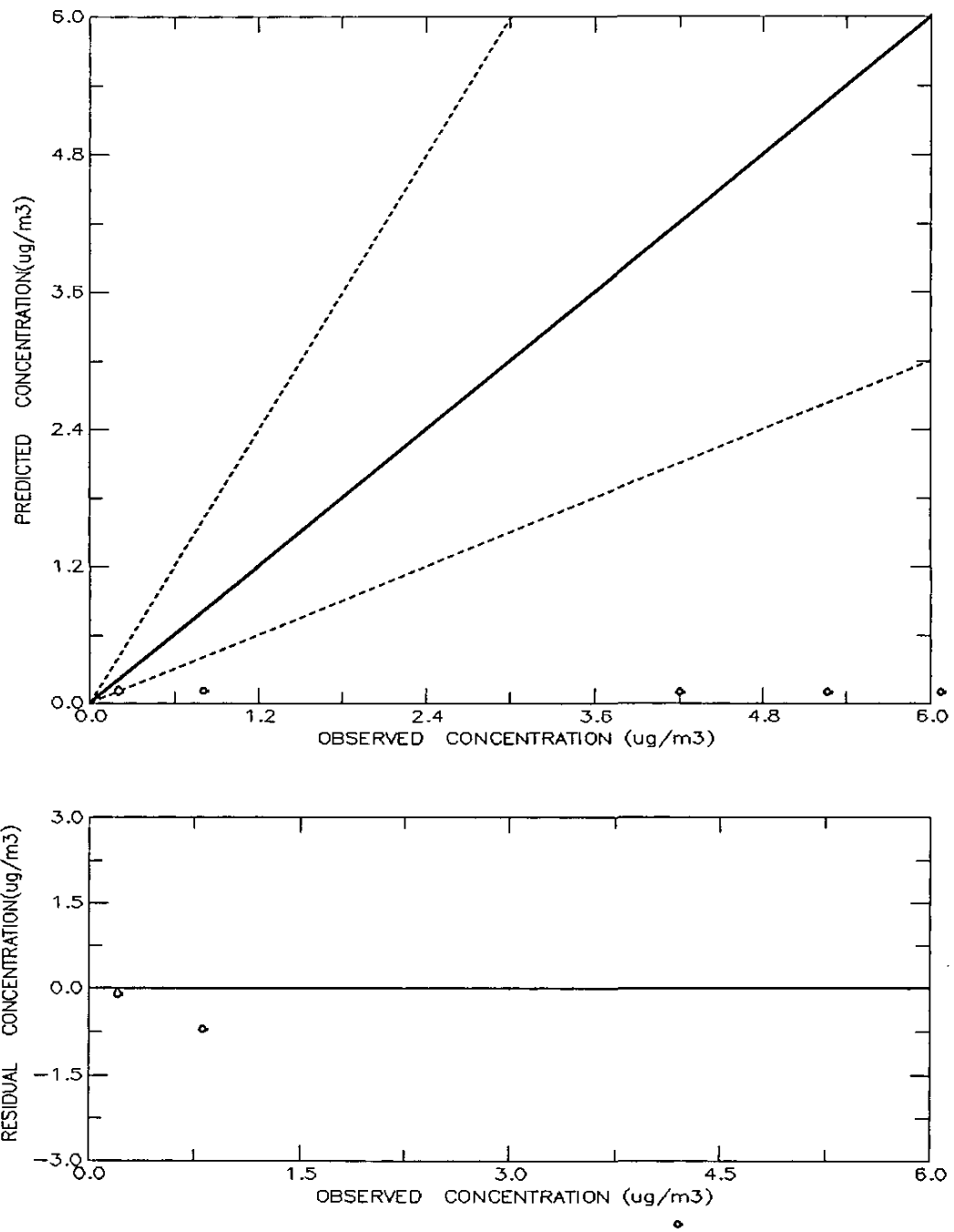


Figure V-10g. Scatter and residual plots of simulated and measured concentrations of ethylene dichloride.

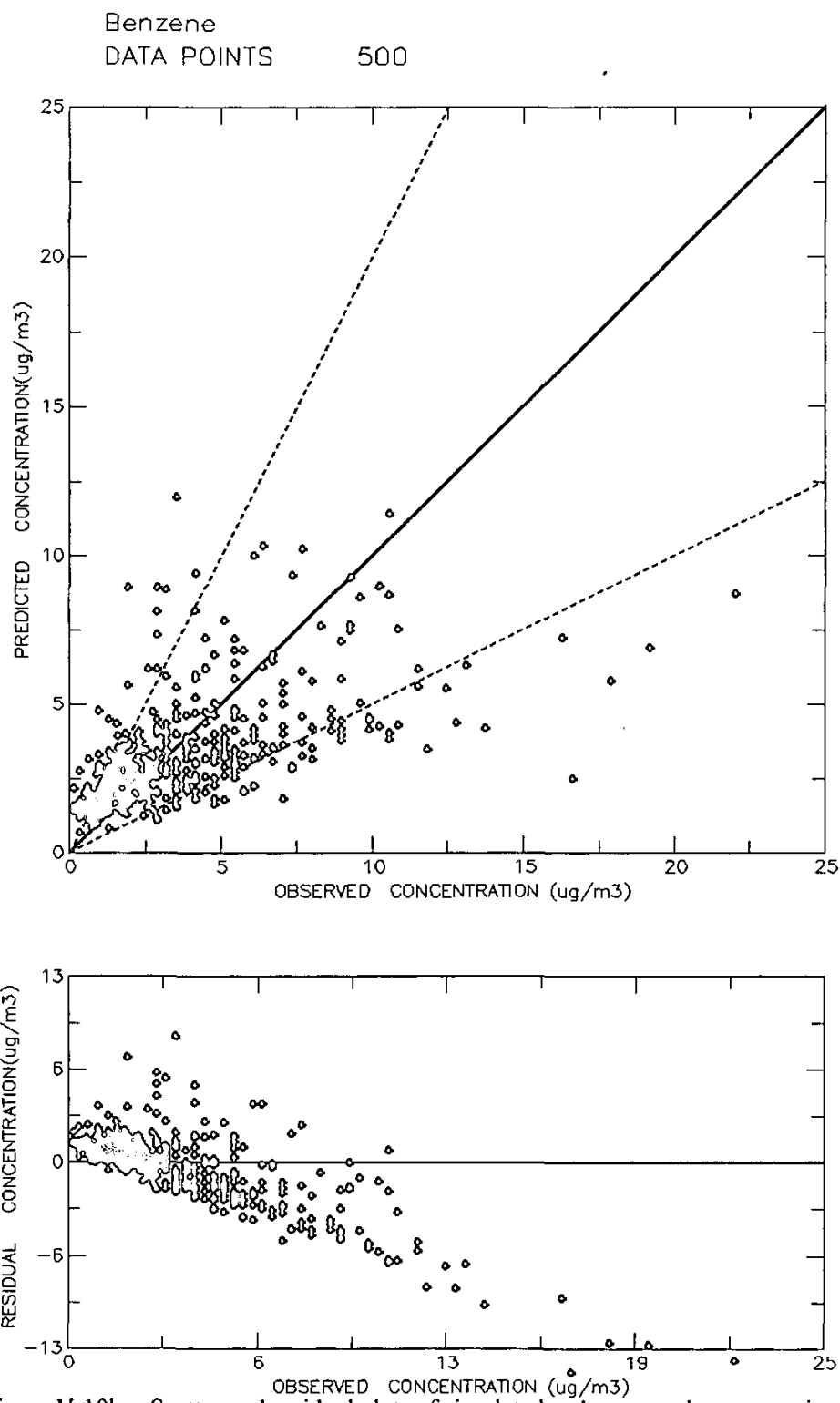


Figure V-10h. Scatter and residual plots of simulated and measured concentrations of benzene.

Carbon Tetrachloride
DATA POINTS 492

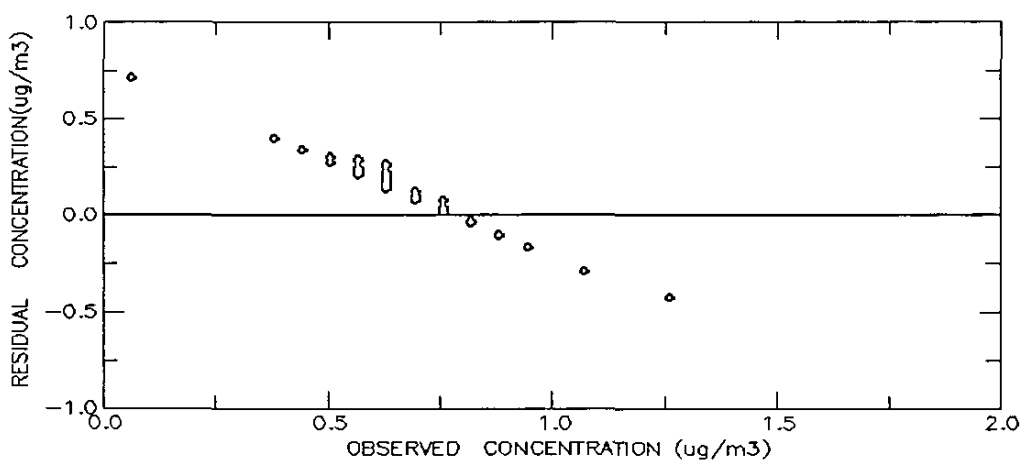
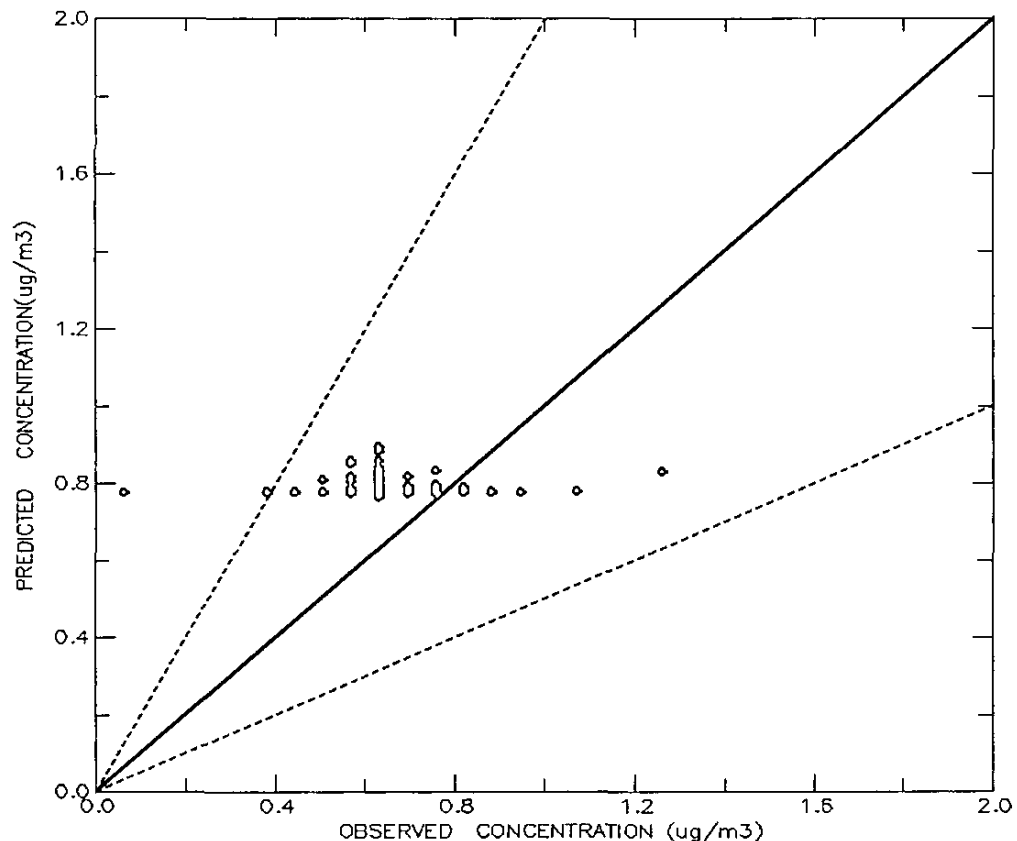


Figure V-10i. Scatter and residual plots of simulated and measured concentrations of carbon tetrachloride.

Trichloroethene
DATA POINTS . 496

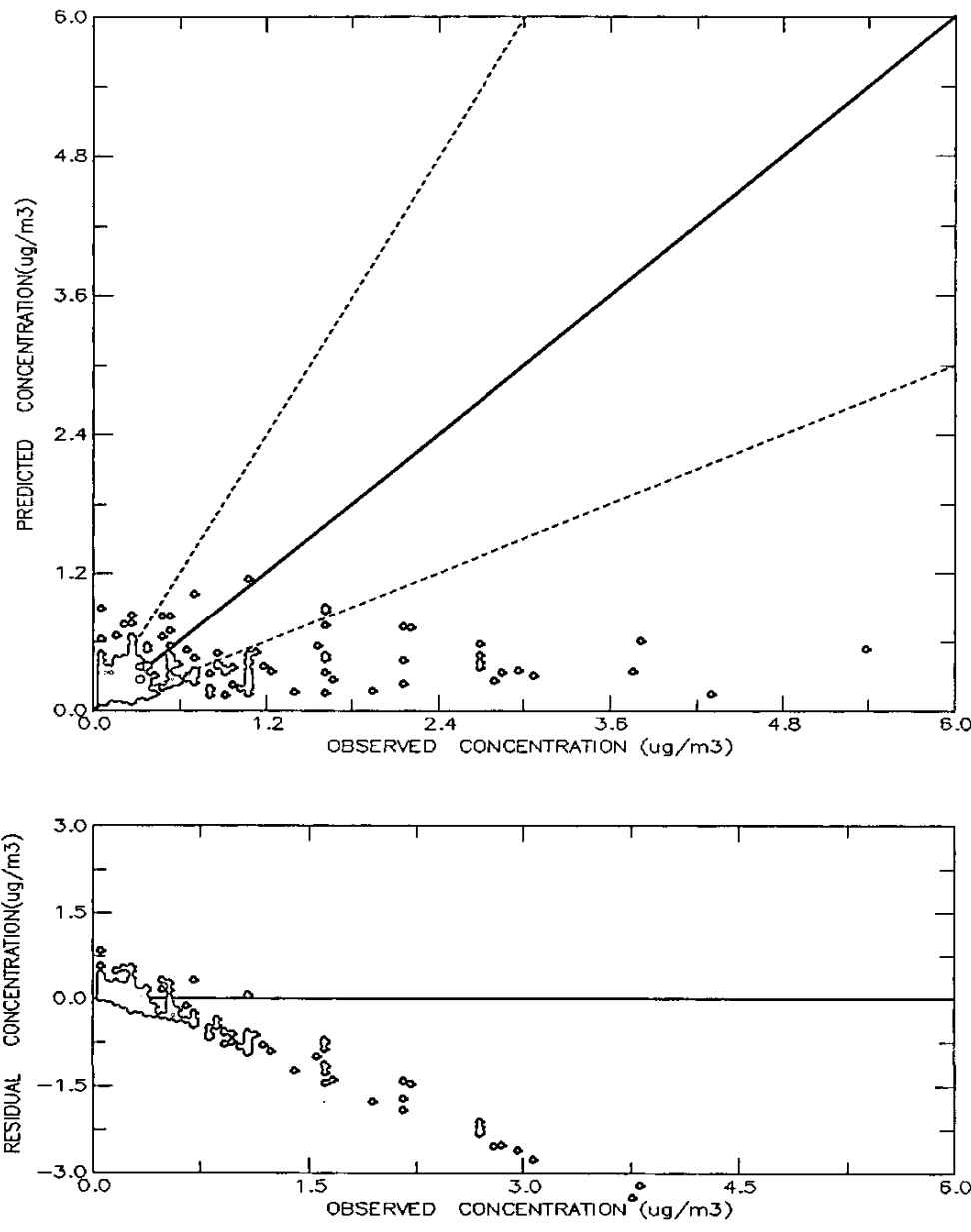


Figure V-10j. Scatter and residual plots of simulated and measured concentrations of trichloroethene.

Toluene
DATA POINTS 477

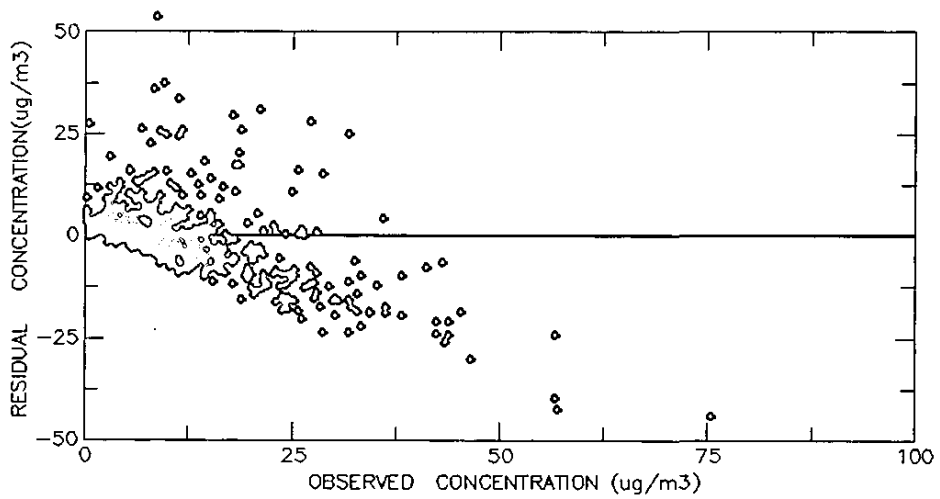
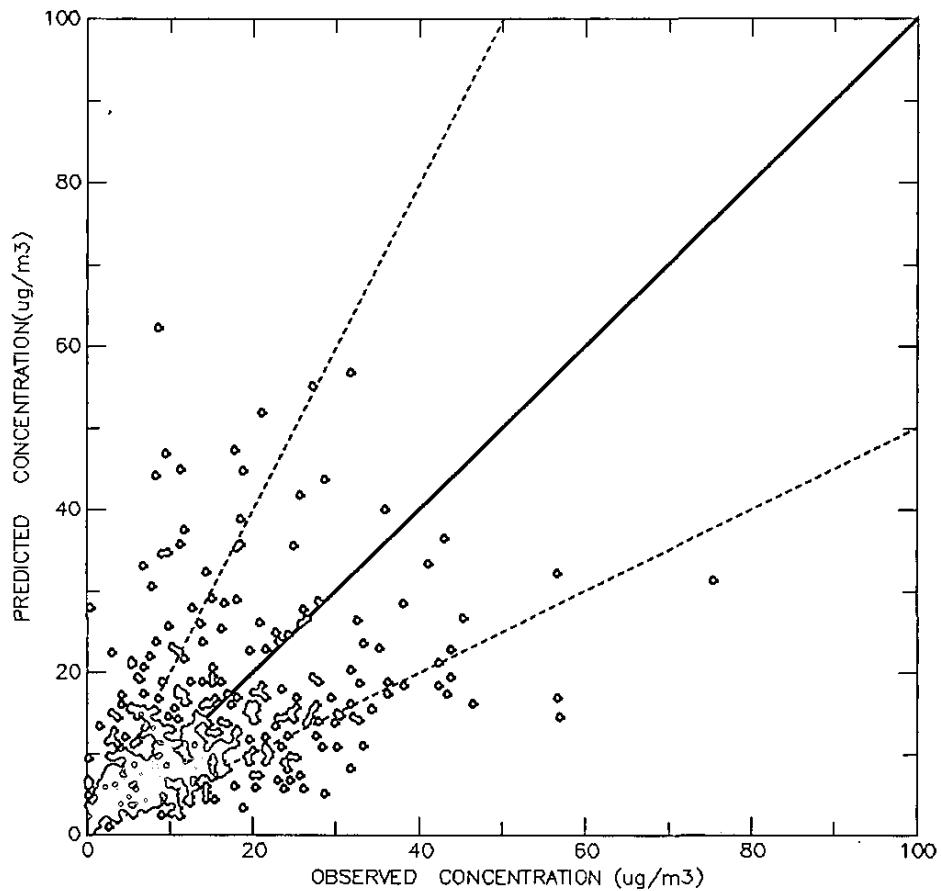


Figure V-10k. Scatter and residual plots of simulated and measured concentrations of toluene.

Ethylene Dibromide
DATA POINTS 247

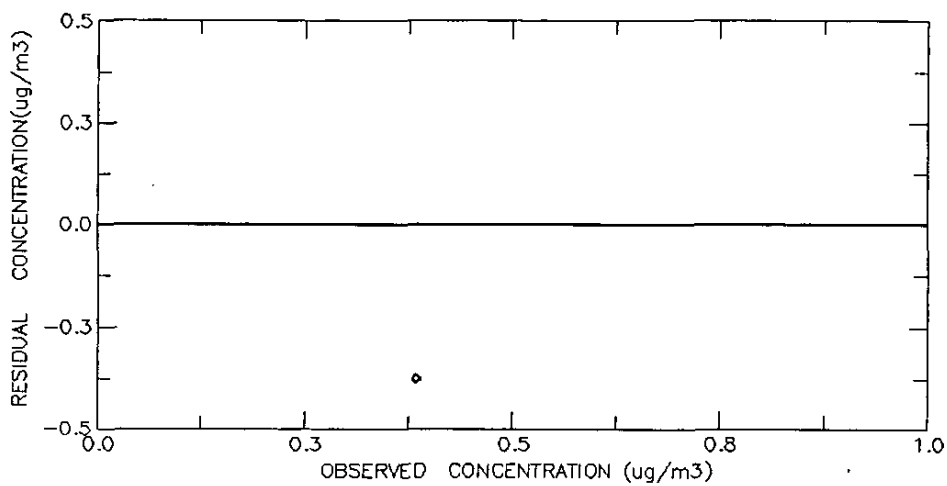
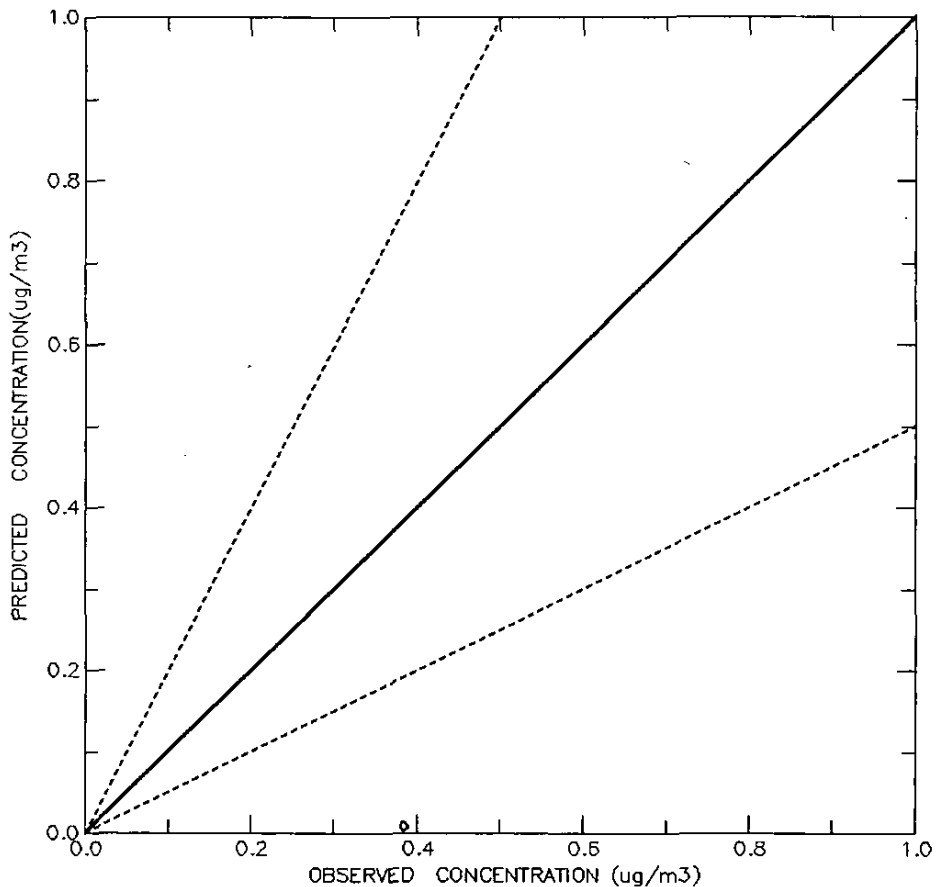


Figure V-10l. Scatter and residual plots of simulated and measured concentrations of ethylene dibromide.

Perchloroethylene
DATA POINTS 479

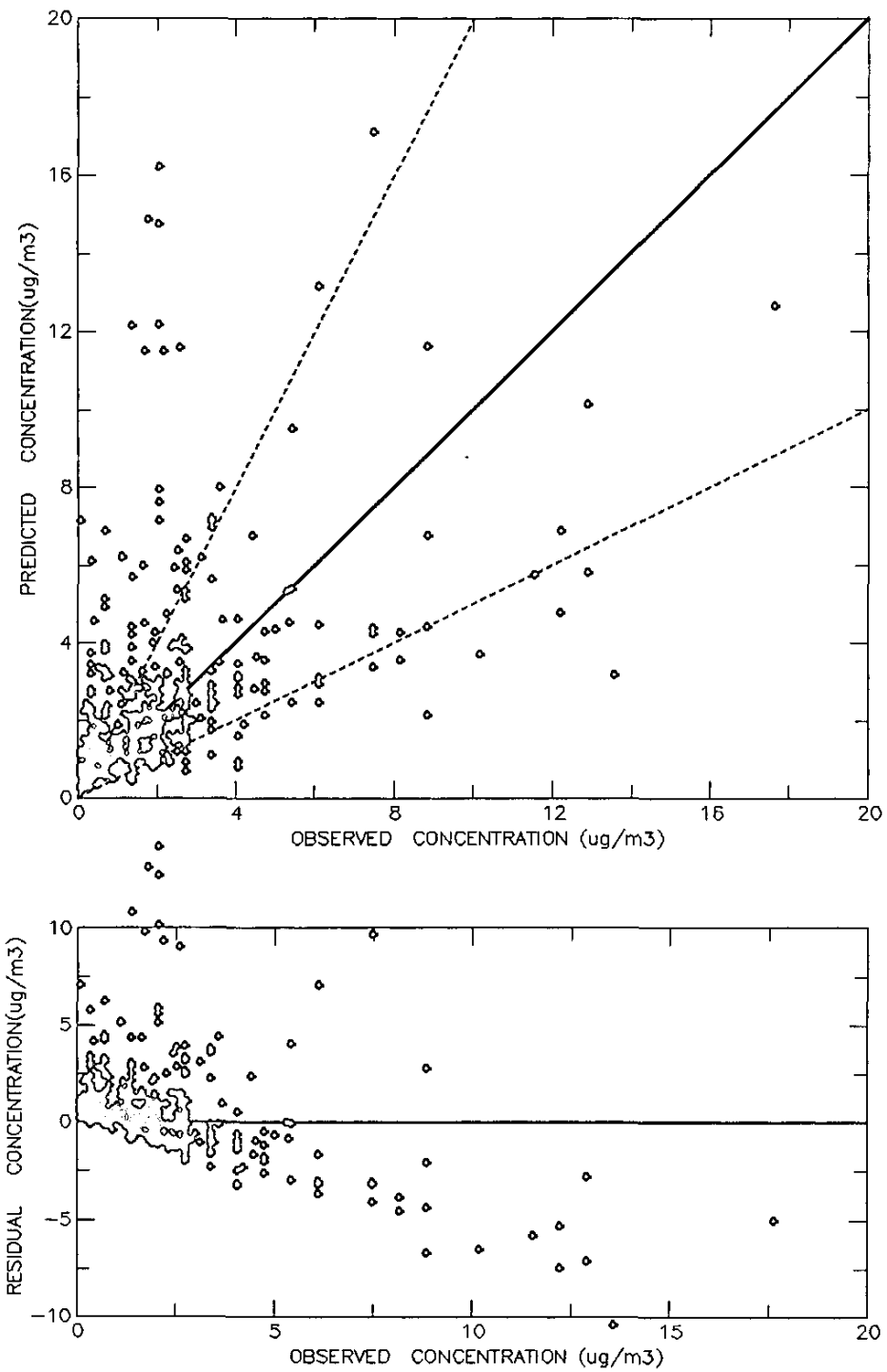


Figure V-10m. Scatter and residual plots of simulated and measured concentrations of perchloroethylene.

Styrene
DATA POINTS 284

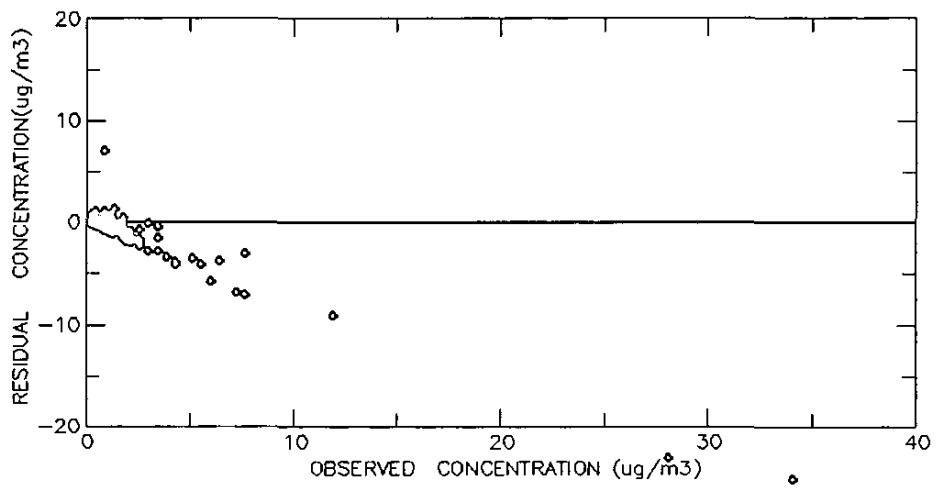
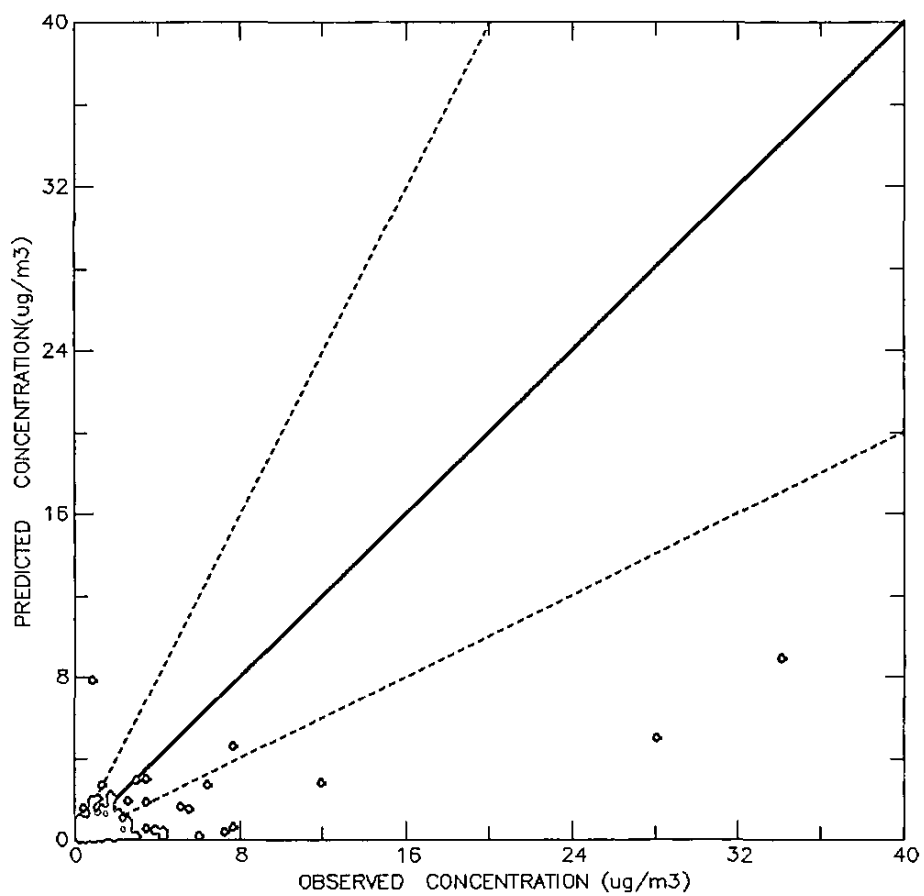


Figure V-10n. Scatter and residual plots of simulated and measured concentrations of styrene .

P-Dichlorobenzene
DATA POINTS 269

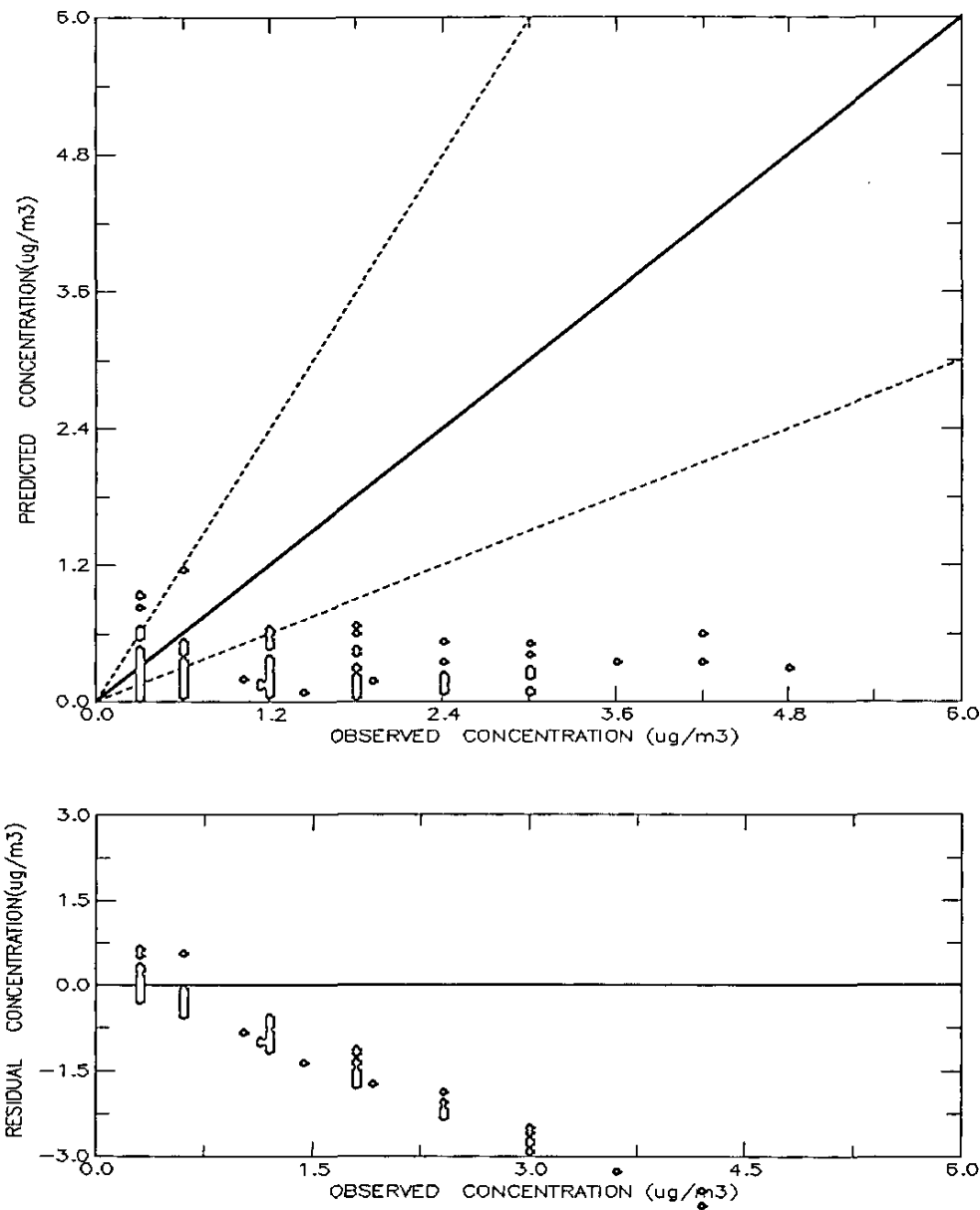


Figure V-10o. Scatter and residual plots of simulated and measured concentrations of p-dichlorobenzene.

Formaldehyde
DATA POINTS 501

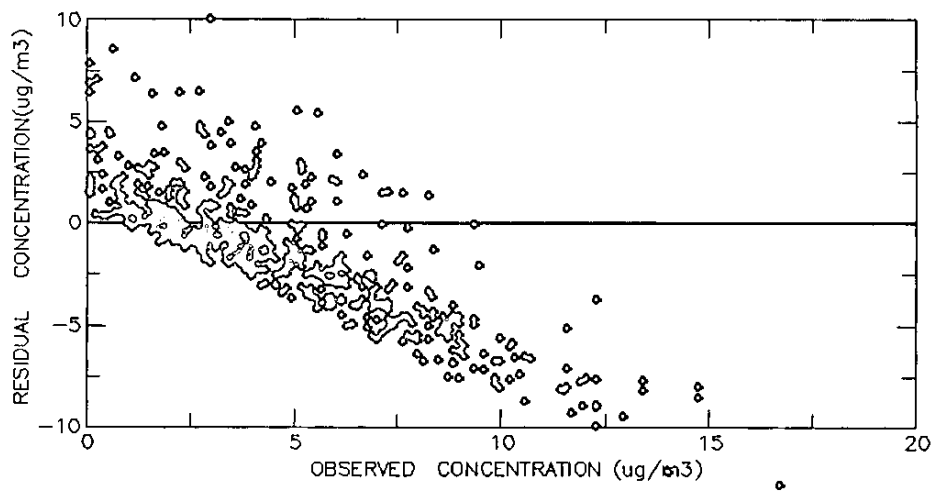
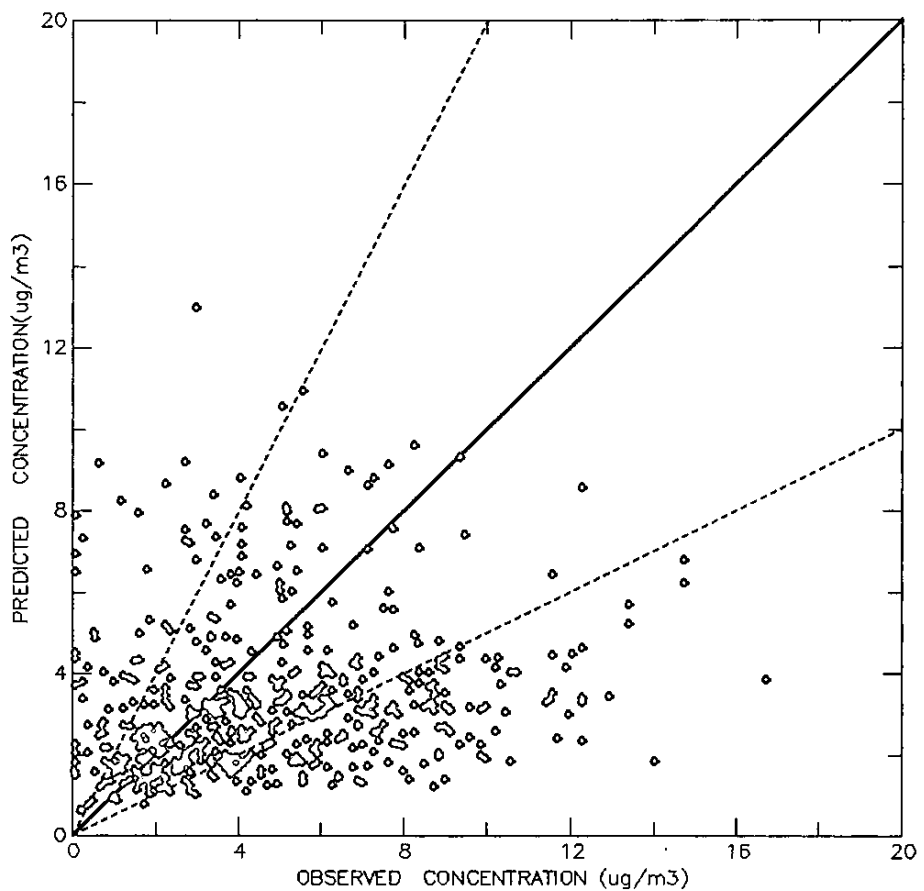


Figure V-10p. Scatter and residual plots of simulated and measured concentrations of formaldehyde.

Acetaldehydes
DATA POINTS 498

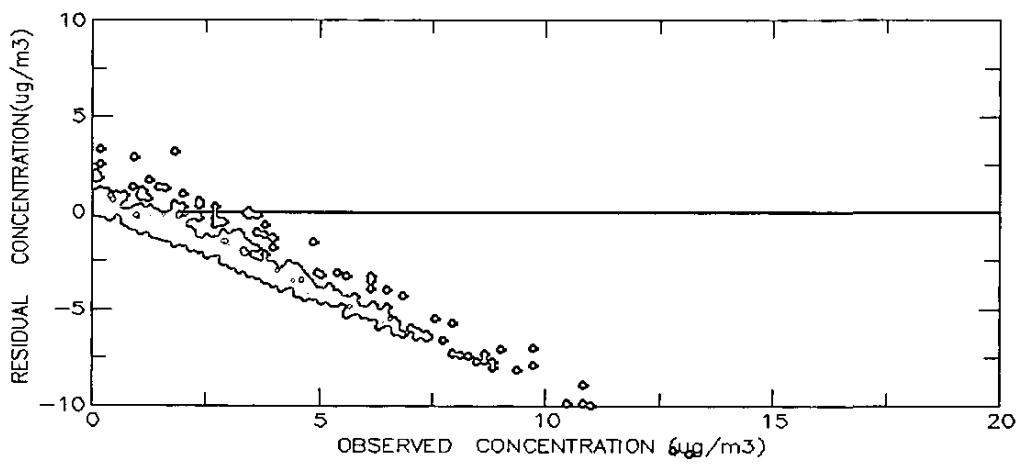
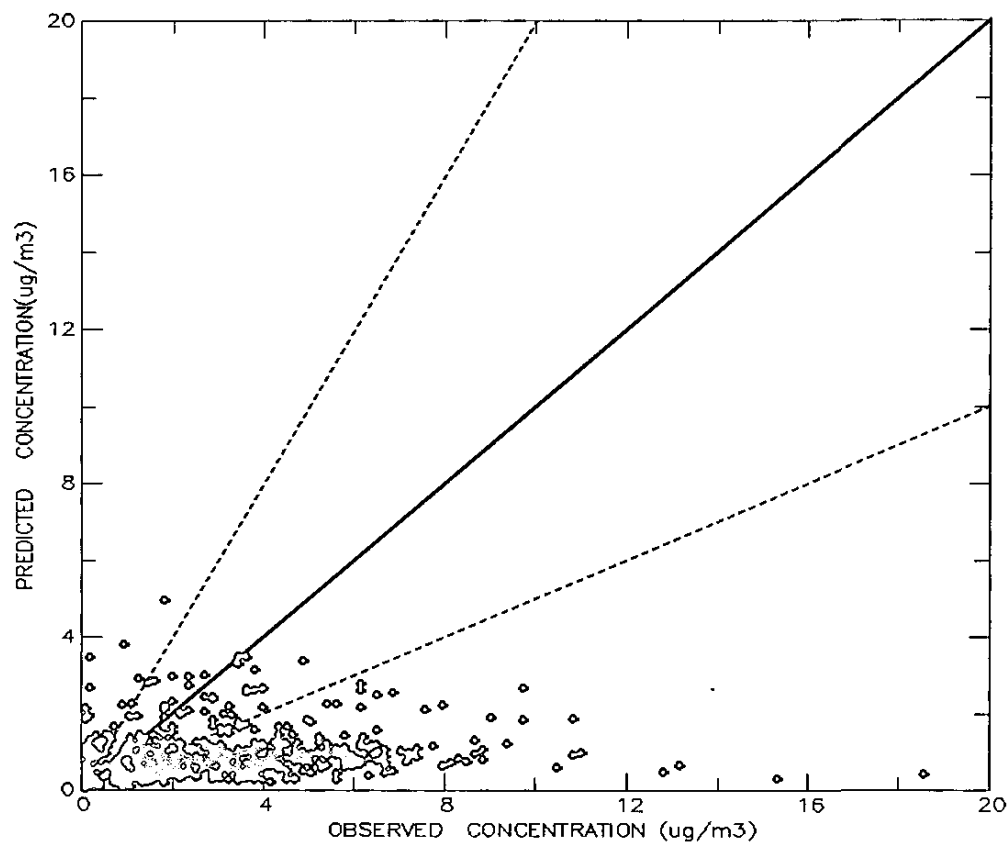


Figure V-10q. Scatter and residual plots of simulated and measured concentrations of acetaldehyde.

Acetone
DATA POINTS 247

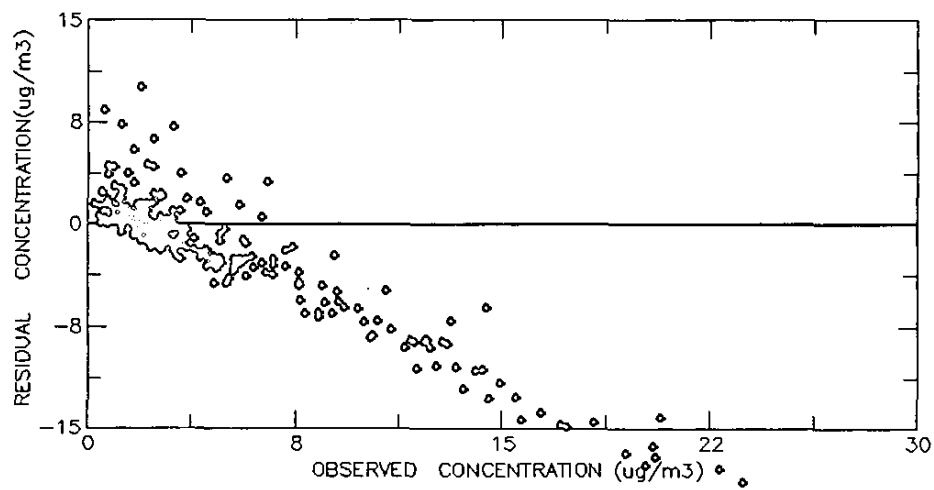
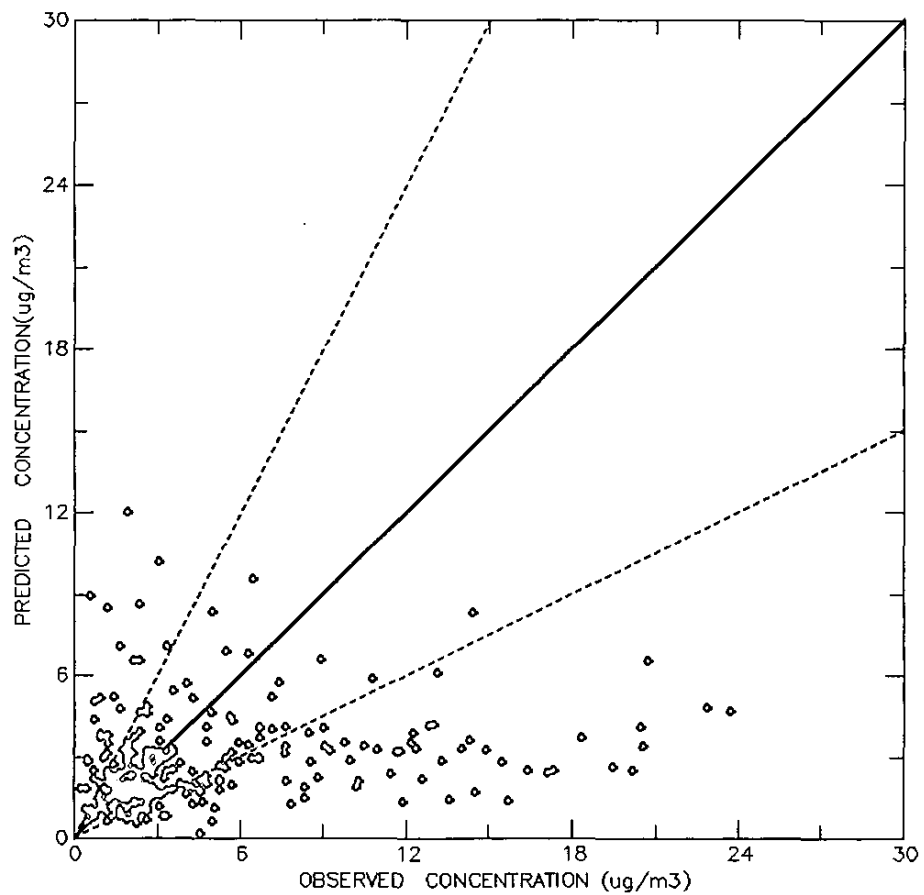


Figure V-10r. Scatter and residual plots of simulated and measured concentrations of acetone.

Methyl Ethyl Ketone
DATA POINTS 442

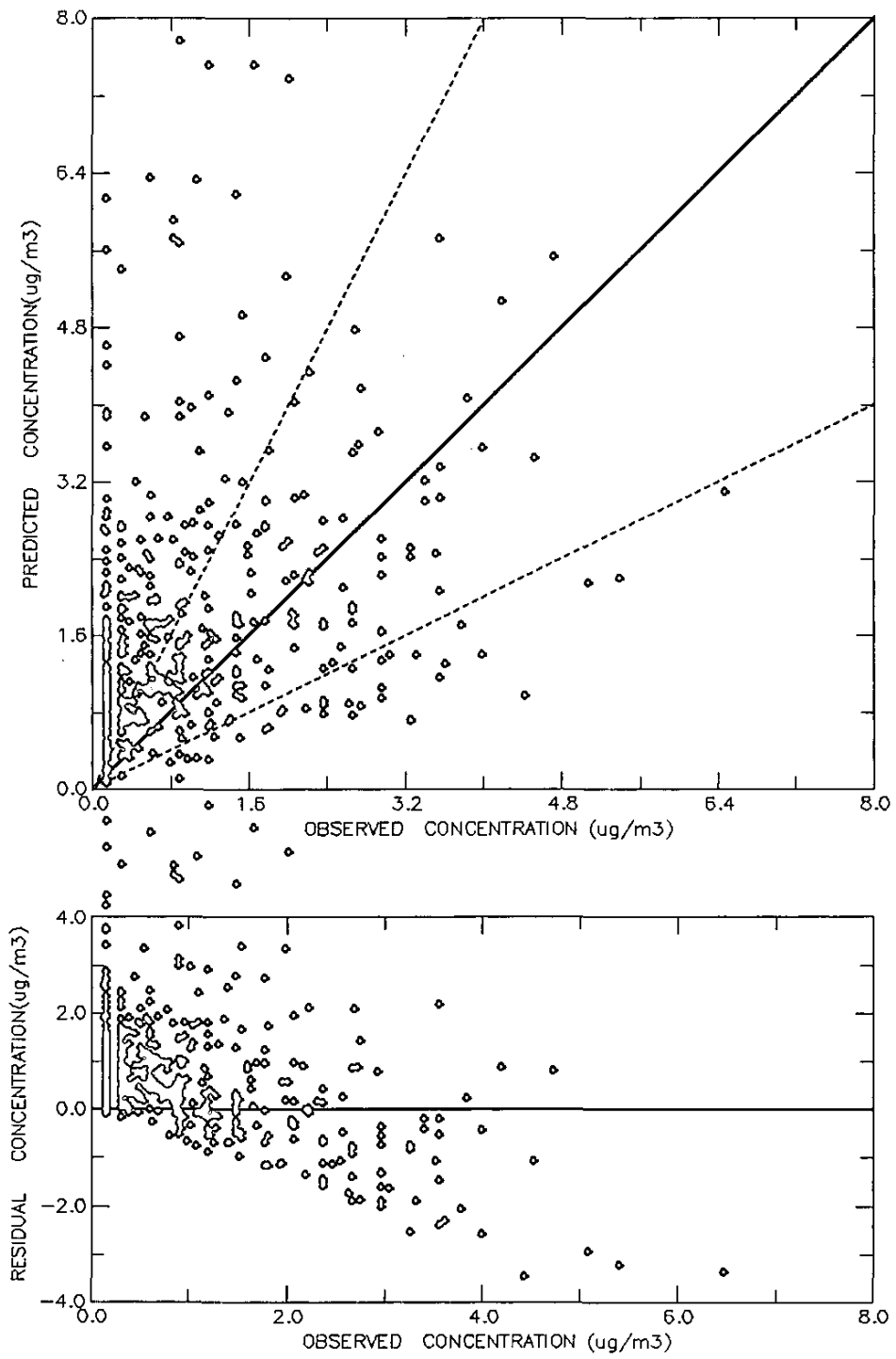


Figure V-10s. Scatter and residual plots of simulated and measured concentrations of methyl ethyl ketone.

Organic Carbon
DATA POINTS 433

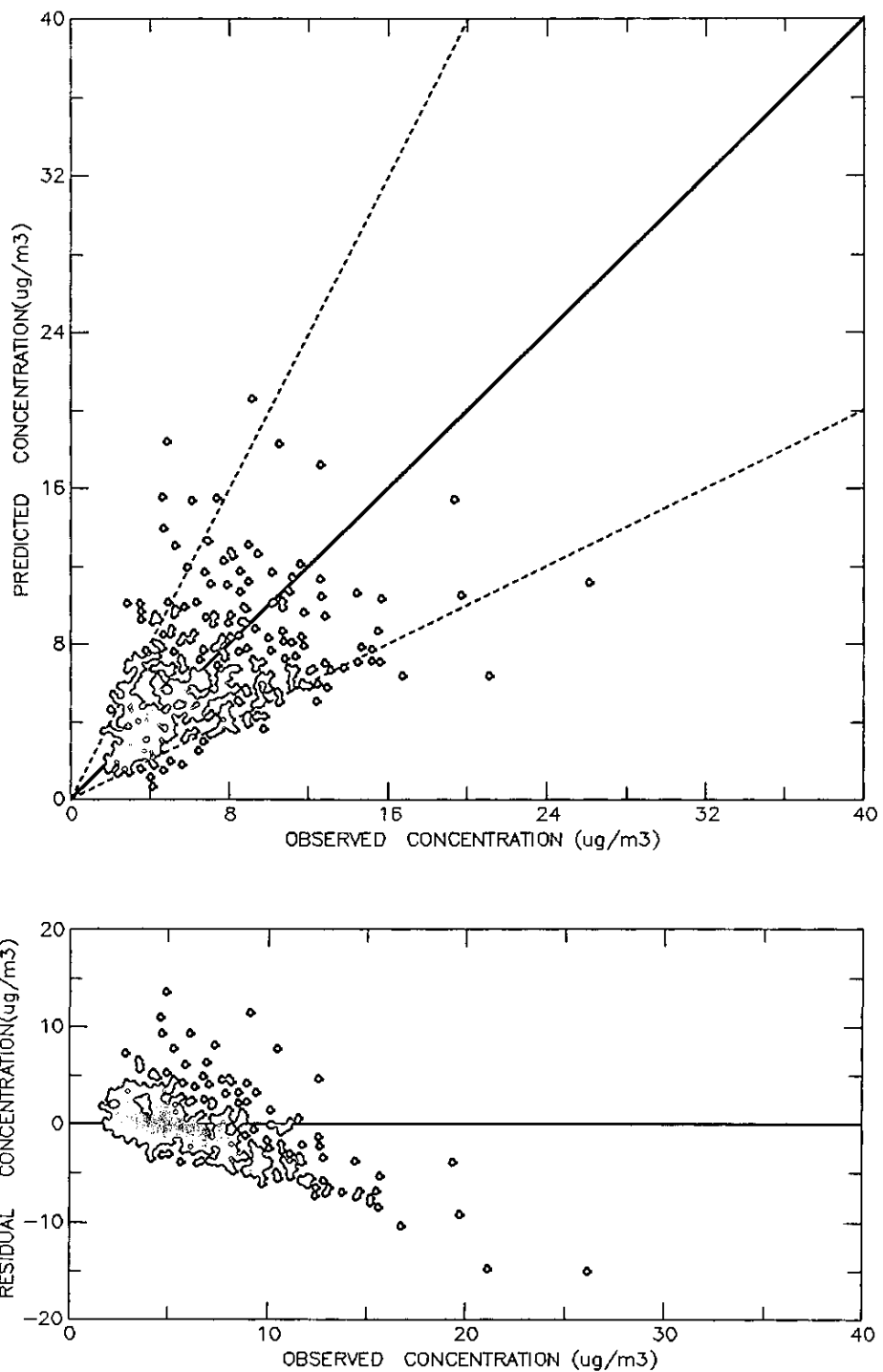


Figure V-10t. Scatter and residual plots of simulated and measured concentrations of organic carbon.

Elemental Carbon
DATA POINTS 433

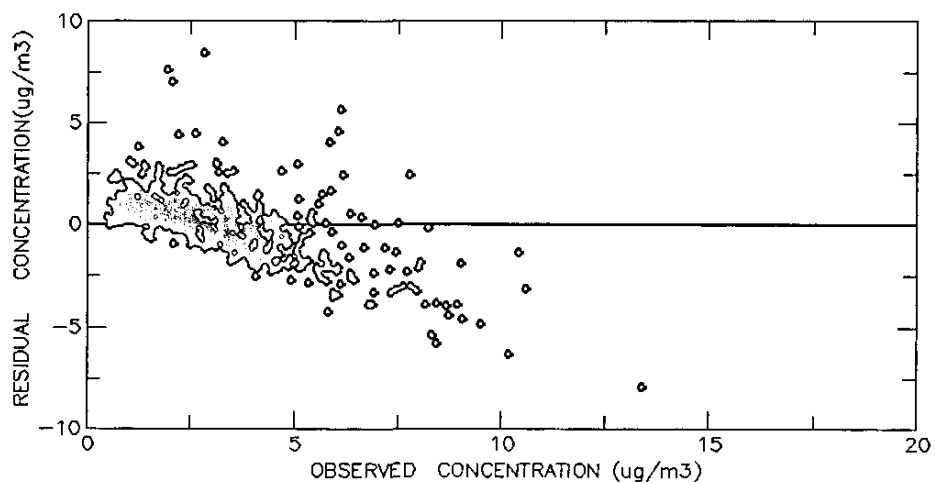
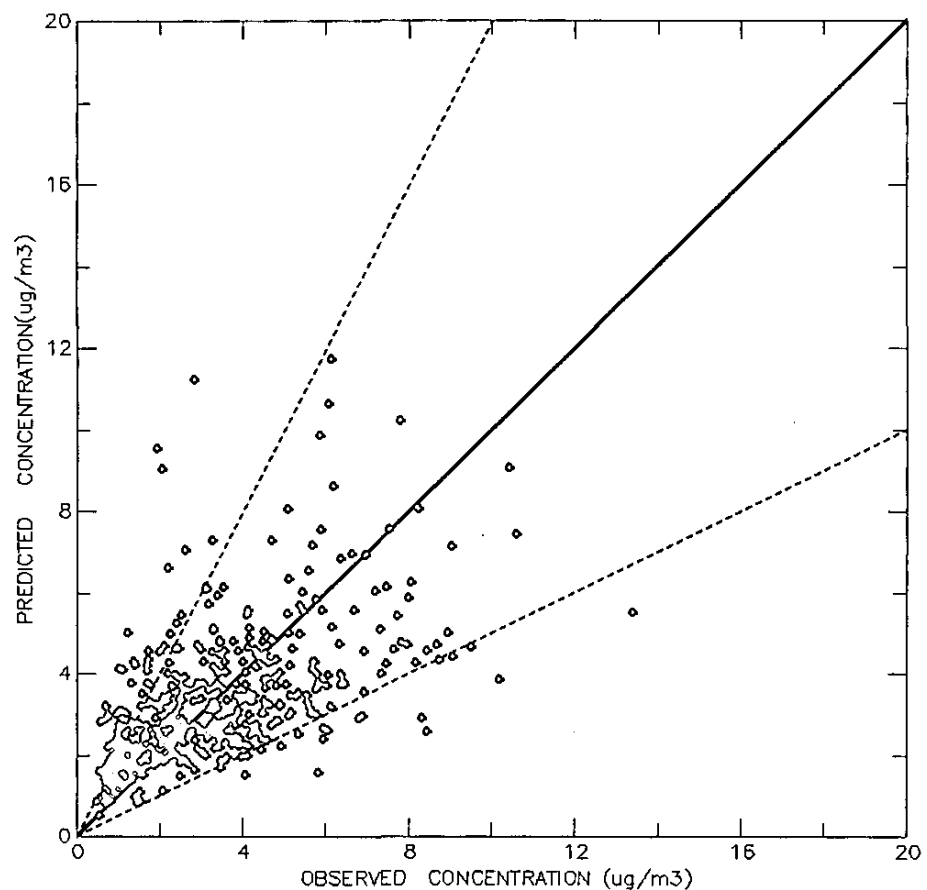


Figure V-10u. Scatter and residual plots of simulated and measured concentrations of elemental carbon.

Hexavalent Chromium
DATA POINTS 496

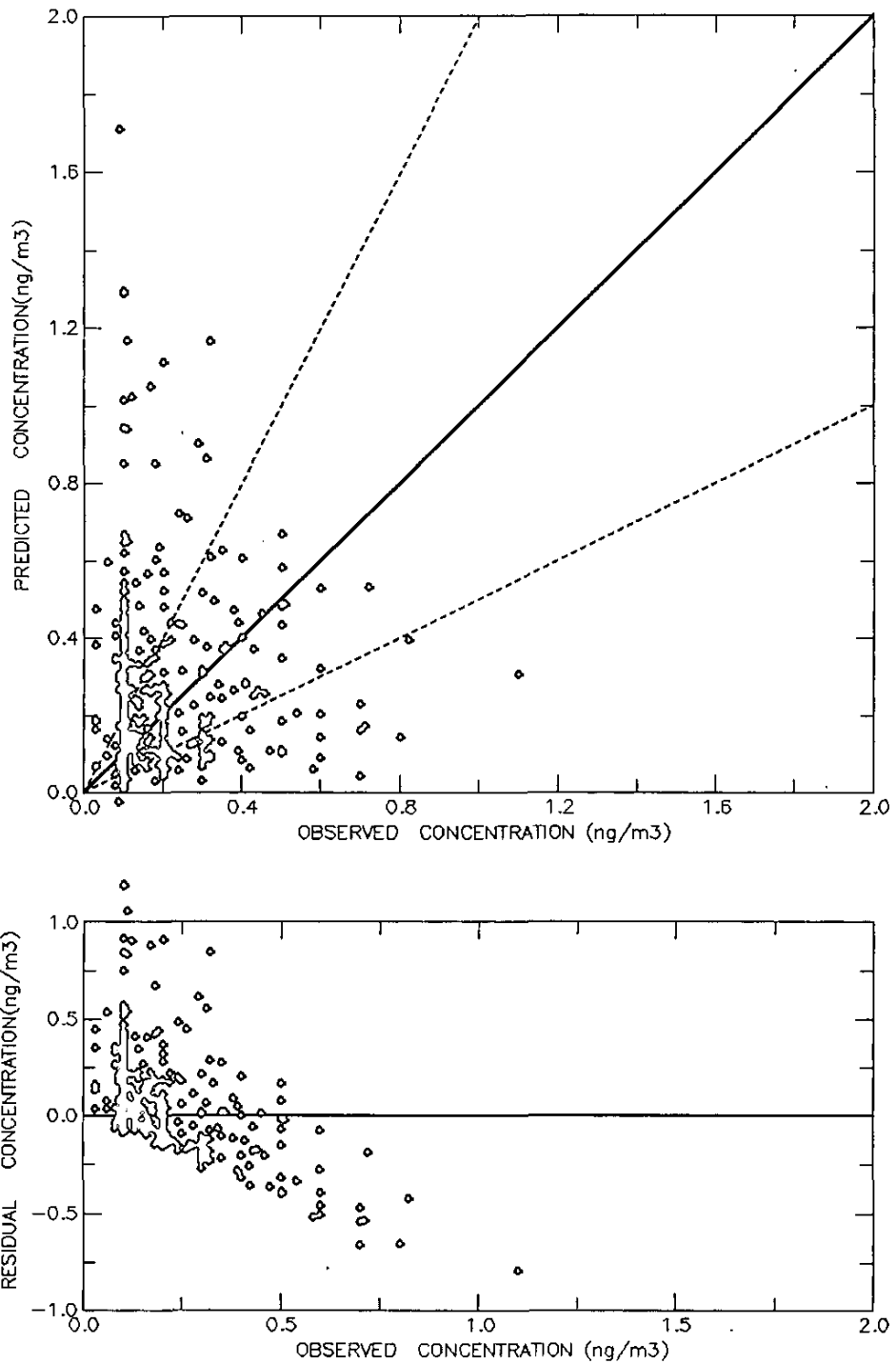


Figure V-10v. Scatter and residual plots of simulated and measured concentrations of hexavalent chromium.

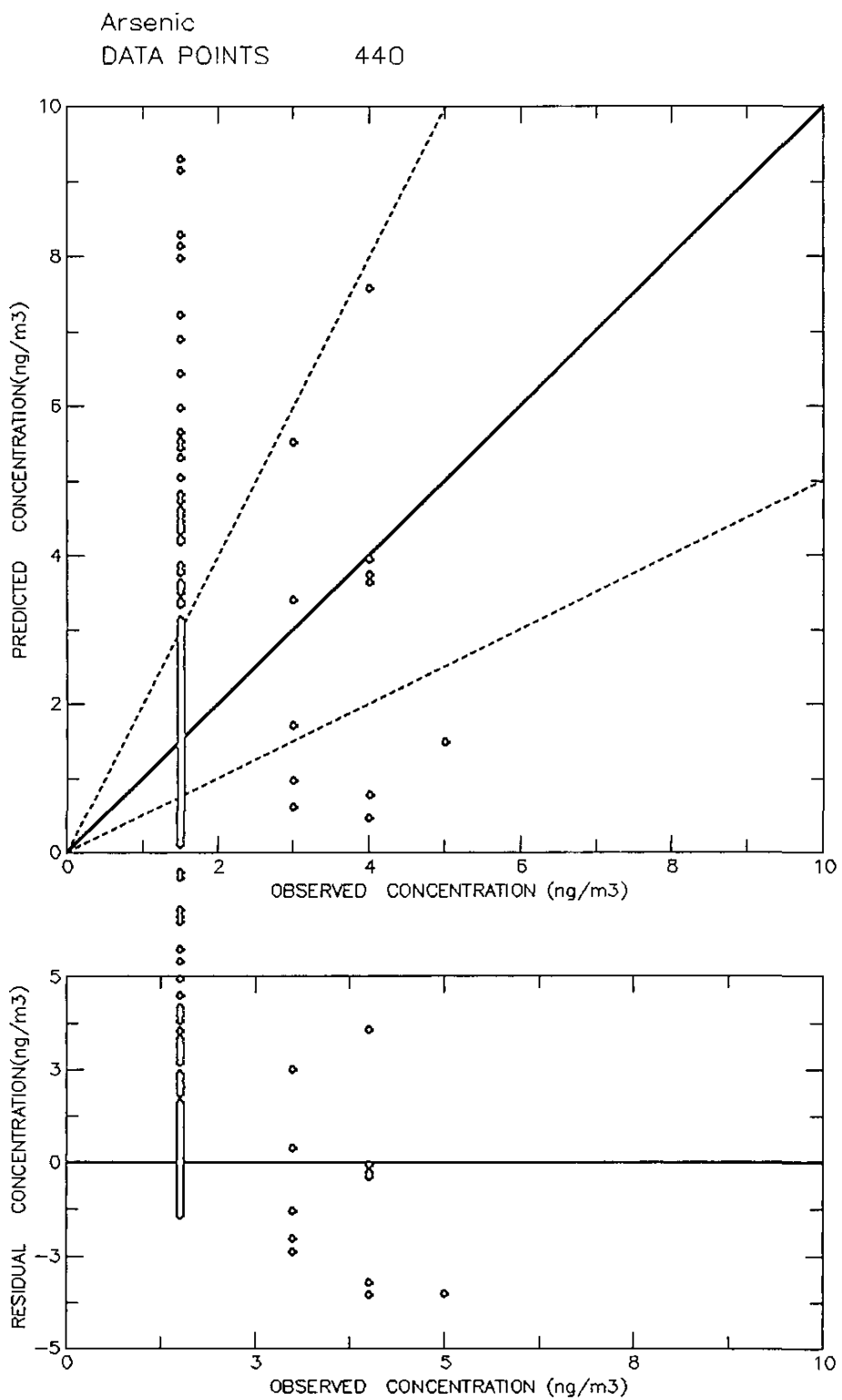


Figure V-10w. Scatter and residual plots of simulated and measured concentrations of arsenic.

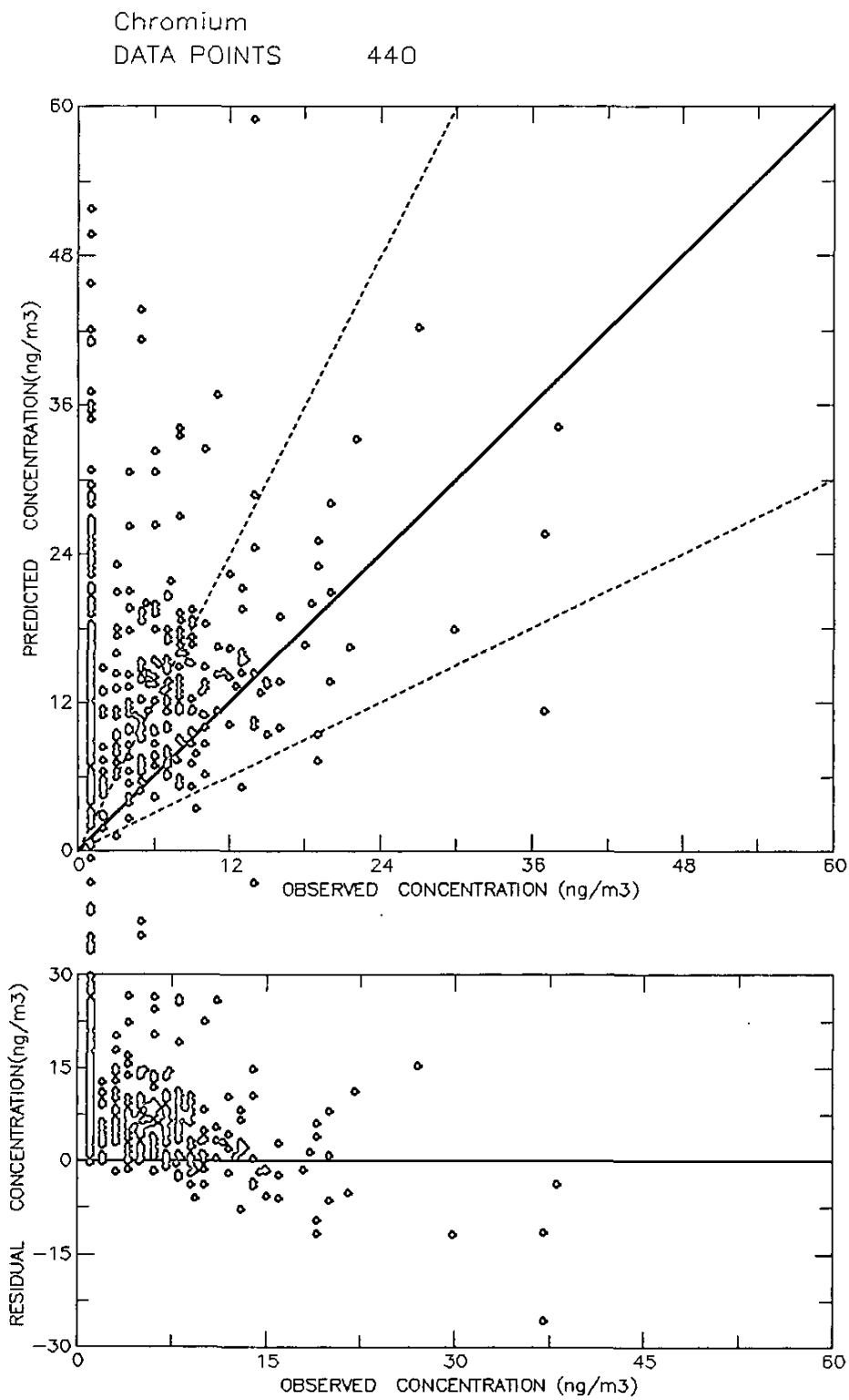


Figure V-10x. Scatter and residual plots of simulated and measured concentrations of chromium.

Lead - Point
DATA POINTS 221

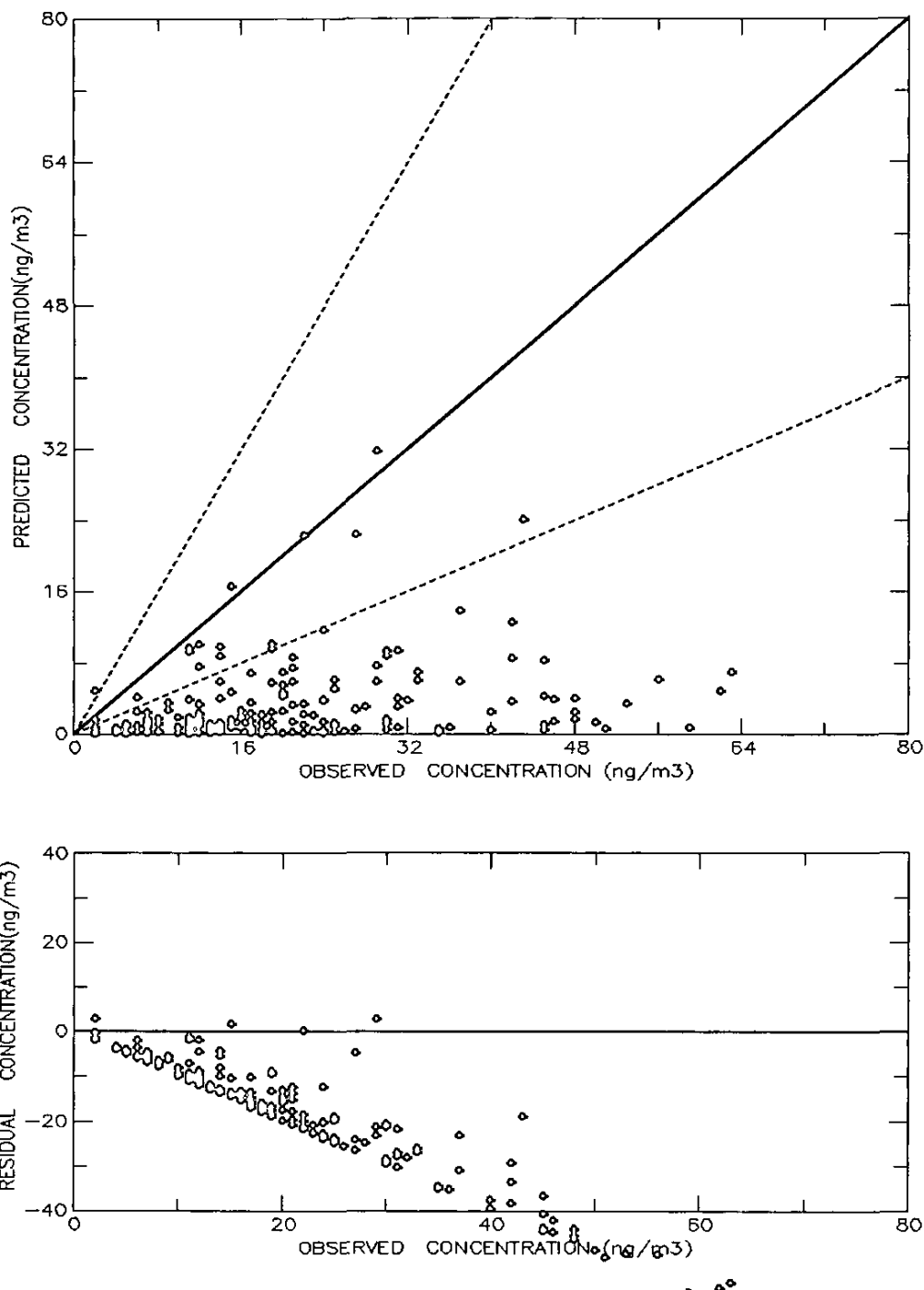


Figure V-10y. Scatter and residual plots of simulated and measured concentrations of point source lead.

Lead - Total
DATA POINTS 221

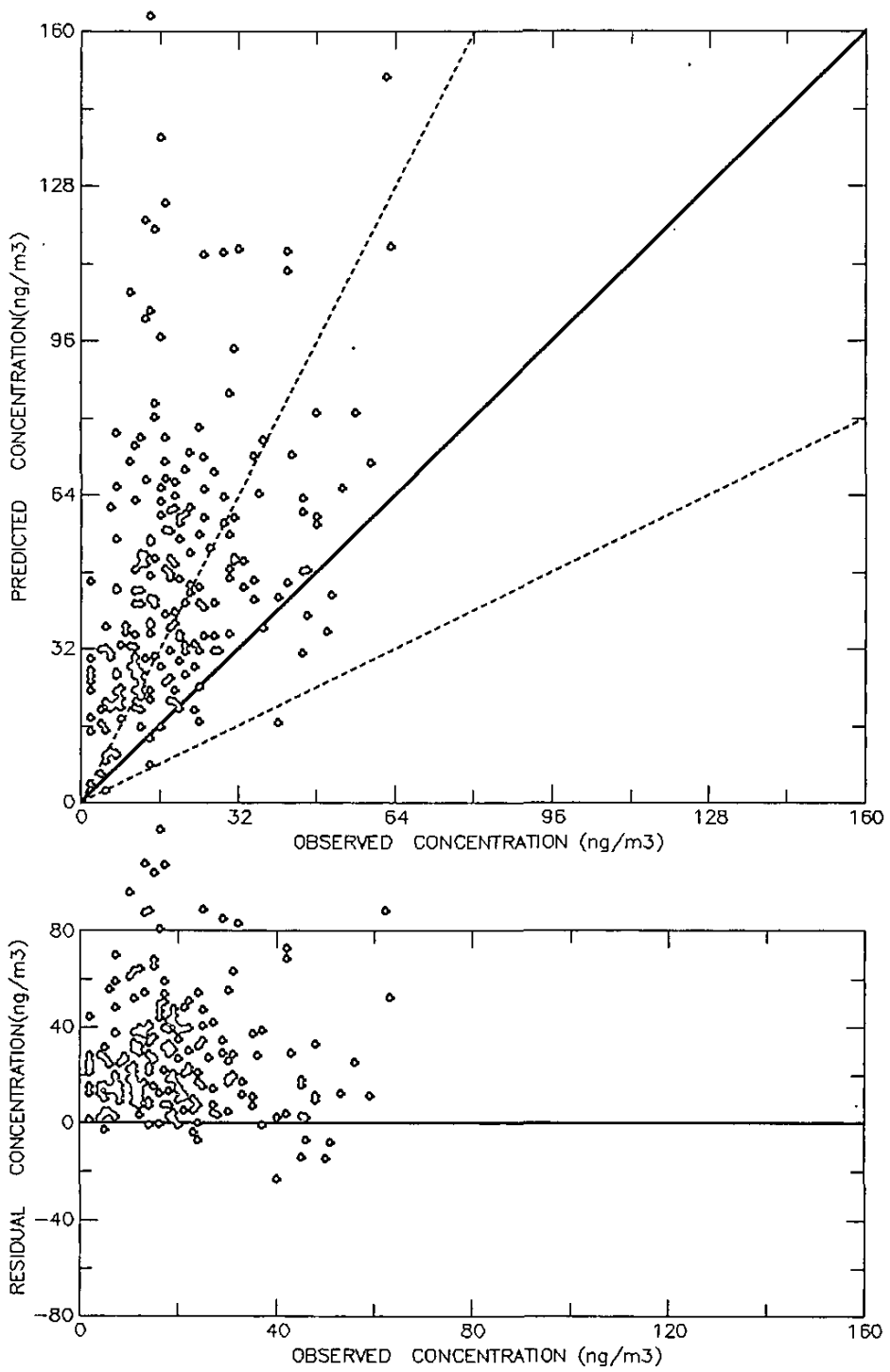


Figure V-10z. Scatter and residual plots of simulated and measured concentrations of total lead.

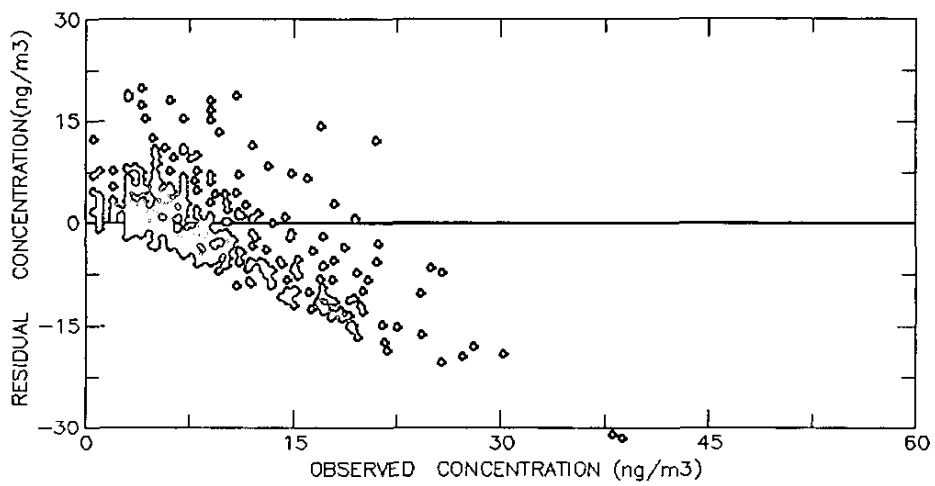
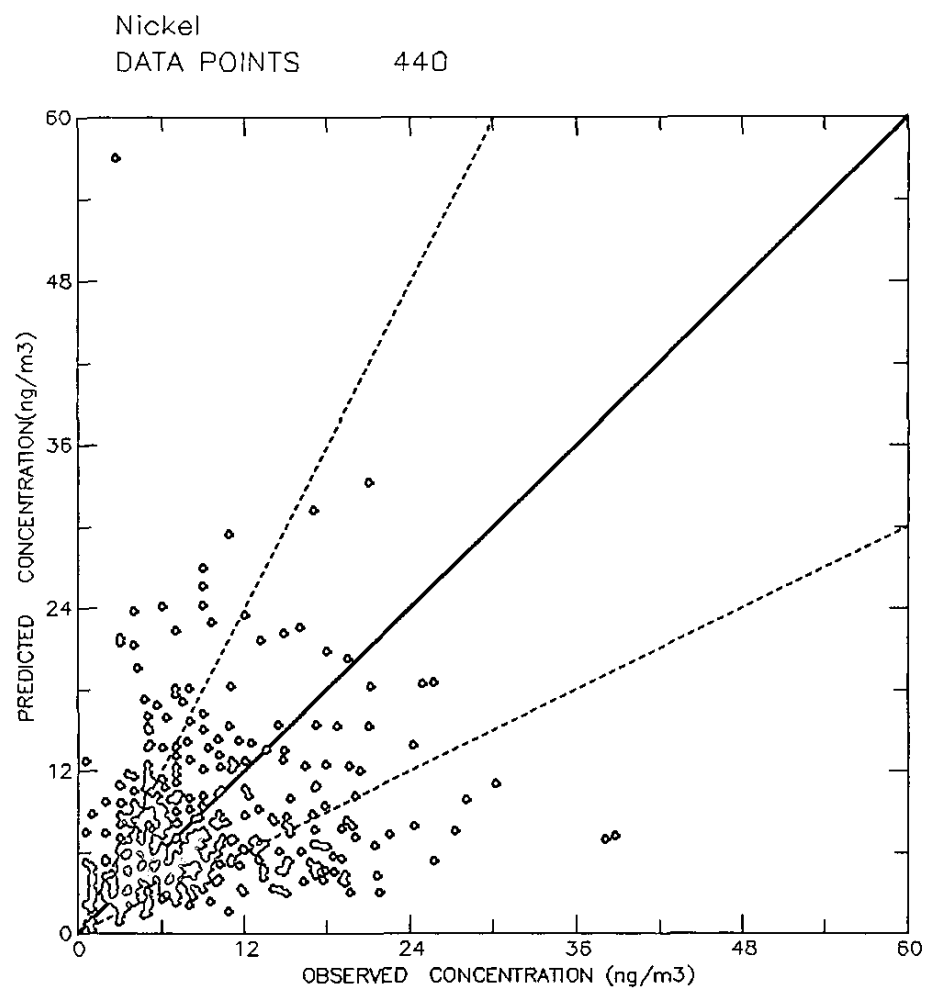


Figure V-10aa. Scatter and residual plots of simulated and measured concentrations of nickel.

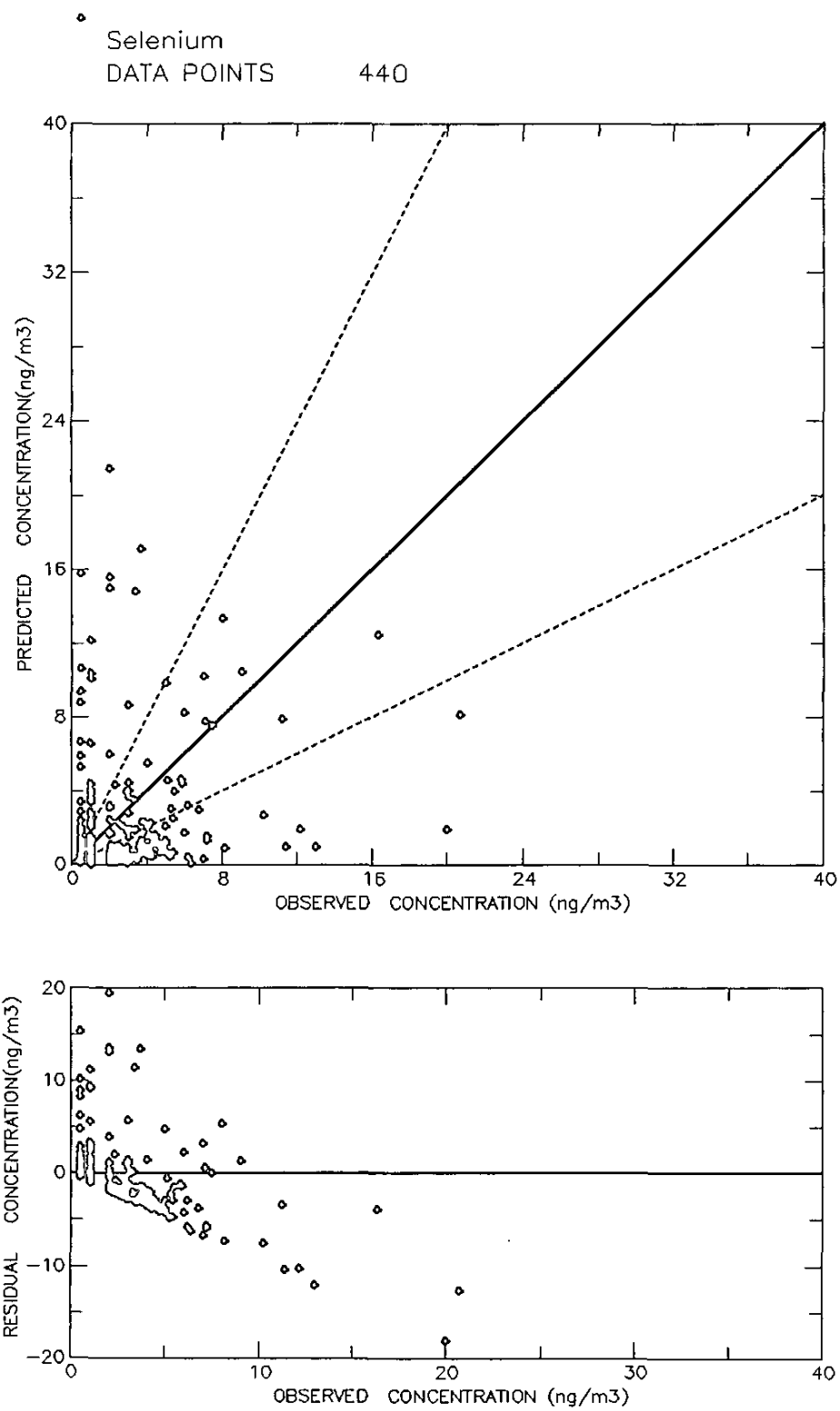


Figure V-10ab. Scatter and residual plots of simulated and measured concentrations of selenium.

Cadmium DATA POINTS

219

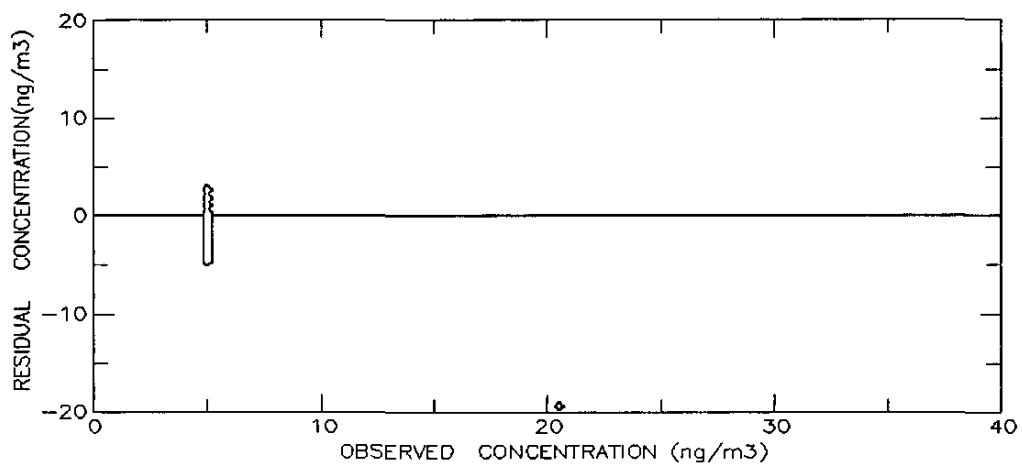
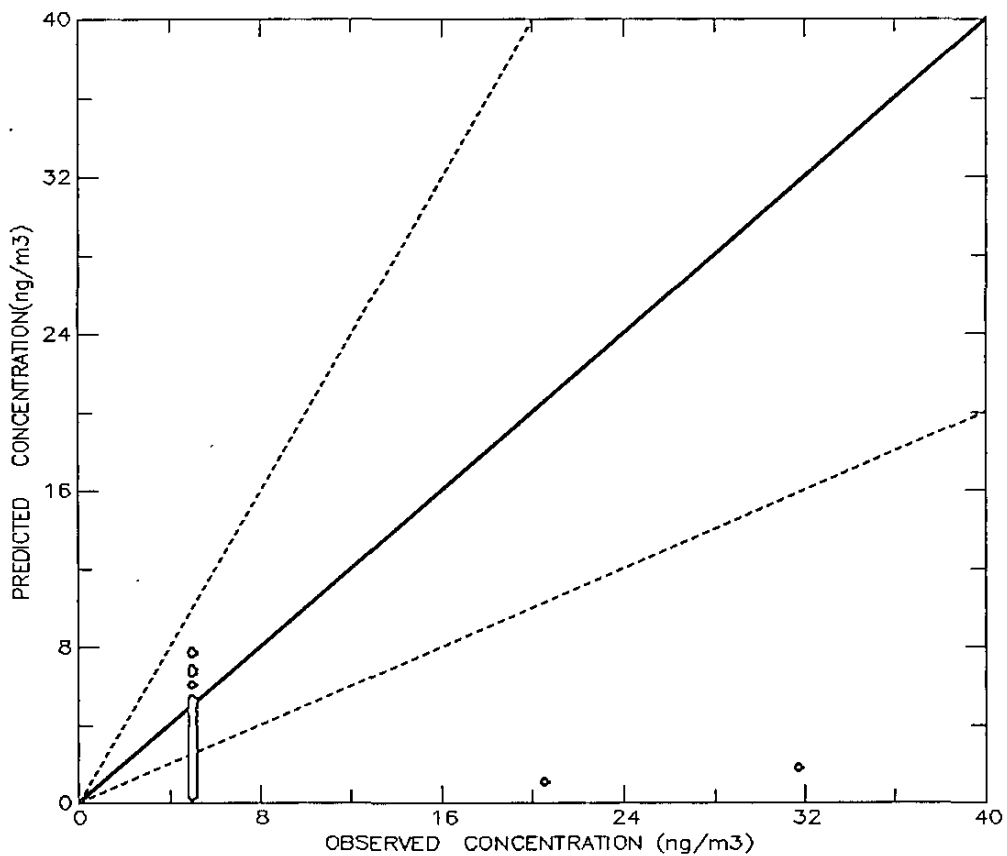


Figure V-10ac. Scatter and residual plots of simulated and measured concentrations of cadmium.

Table V-6. Toxic Compounds Simulated and Measured at the 10 MATES-II Sites

Toxic Compound	Simulated Annual Average ($\mu\text{g}/\text{m}^3$)	Measured Annual Average ($\mu\text{g}/\text{m}^3$)
Benzene	3.13	3.53
1,3Butadiene	0.34	0.79
p-Dichlorobenzene	0.24	0.92
Methylene Chloride	1.08	2.65
Chloroform	0.08	0.24
Perchloroethylene	2.46	1.96
Trichloroethylene	0.26	0.43
Carbon Tetrachloride	0.78	0.65
Ethylene Dibromide	0.01	0.38
Ethylene Dichloride	0.10	0.26
Vinyl Chloride	0.01	0.26
Formaldehyde	5.49	4.82
Acetaldehyde	5.21	3.17
Acetone	2.78	5.00
Methyl Ethyl Ketone	1.72	1.06
Styrene	0.53	1.23
Toluene	12.17	12.98
1,1Dichloroethane	0.03	0.20
Chloromethane	1.24	1.31
Arsenic	1.69	1.56
Elemental Carbon	3.40	3.36
Organic Carbon	5.92	6.43
Chromium	0.01441	0.00487
Hexavalent Chromium	0.00024	0.00018
Cadmium	0.00193	0.00605
Lead (point sources)	0.00292	0.01917
Lead (area sources)	0.04808	0.01917
Nickel	0.00775	0.00872
Selenium	0.00150	0.00197

Model-Estimated Spatial Concentration Fields

Figures V-11a through V-11ad show spatial concentration fields simulated by the UAM for the twenty-nine compounds discussed above and also for particulate emissions from diesel-fueled internal combustion engines. Concentration isopleths for all of the compounds simulated are presented in units of micrograms per cubic meter ($\mu\text{g}/\text{m}^3$) with the exception of the metals, which are presented in nanograms per cubic meter ($\eta\text{g}/\text{m}^3$). The simulated regional maximum and minimum concentrations are listed at the top of the isopleth diagram to provide the range of simulated concentrations.

As seen in Figure V-11, concentration levels vary throughout the Basin proper with higher concentrations generally seen close to their emission sources. For mobile source compounds such as benzene, 1,3 butadiene, and particulates associated with diesel fuels (Figures V-11h V-11c and V-11ad), higher concentration levels are seen along freeways and freeway junctions. In addition, higher concentrations of benzene and 1,3 butadiene are estimated in and around major airports. In particular, benzene and 1,3 butadiene tend to be higher around the Los Angeles International Airport area and in the south central portions of Los Angeles County. In addition, particulate levels (Figure V-11ad) tend to be higher in the south central portions of Los Angeles County and offshore of San Pedro and Long Beach. (Under the current ARB definition of a diesel-fueled internal combustion engines, engines associated with harbor crafts and commercial boats would be included. However, deep sea going vessels would not be considered.)

For perchloroethylene (Figure V-11m), higher concentrations are predicted in the Anaheim area as well as in the San Fernando Valley compared to other areas in the modeling domain. In addition to the higher perchloroethylene levels at Anaheim, high concentration levels of styrene are observed in November 1998 (see Figure V-8n). However, measured styrene levels during the other months are much lower. As seen in the spatial concentration field for styrene (Figure V-11n), model estimated annual values (located six to eight km from the Anaheim site) could be as high as the levels measured at the Anaheim location. This implies that the Anaheim monitoring site may be generally upwind of the sources of styrene.

For several compound, few or no concentration isopleths are depicted on the charts. These compounds, such as carbon tetra chloride (Figures V-11i) have very low emission rates and the simulated concentrations do not vary above the global background levels. For these cases the simulated regional maximum and minimum concentrations are typically within 10 percent, varying only marginally across the modeling domain. For selected compounds falling into this category, a single isopleth will appear along one of the boundaries. This isopleth, as in the case of methyl chloride (Figure V-11a), solely reflects the initial conditions input to the simulation.

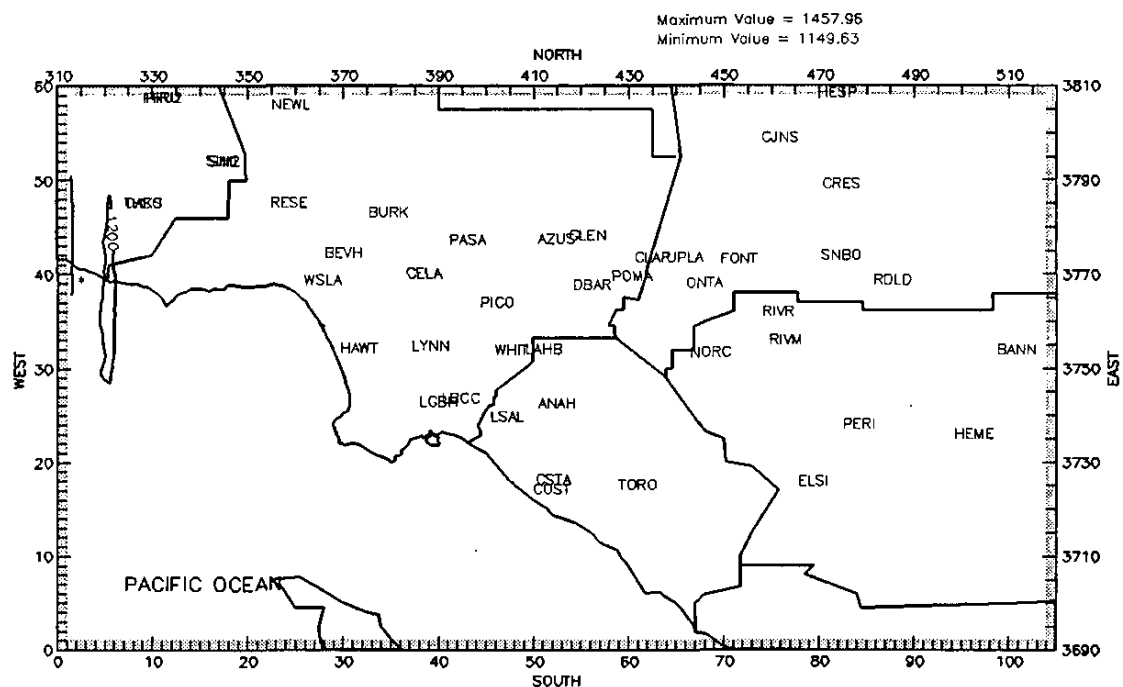


Figure V-11a. Annual average methyl chloride concentrations simulated for the Basin ($\mu\text{g}/\text{m}^3$).

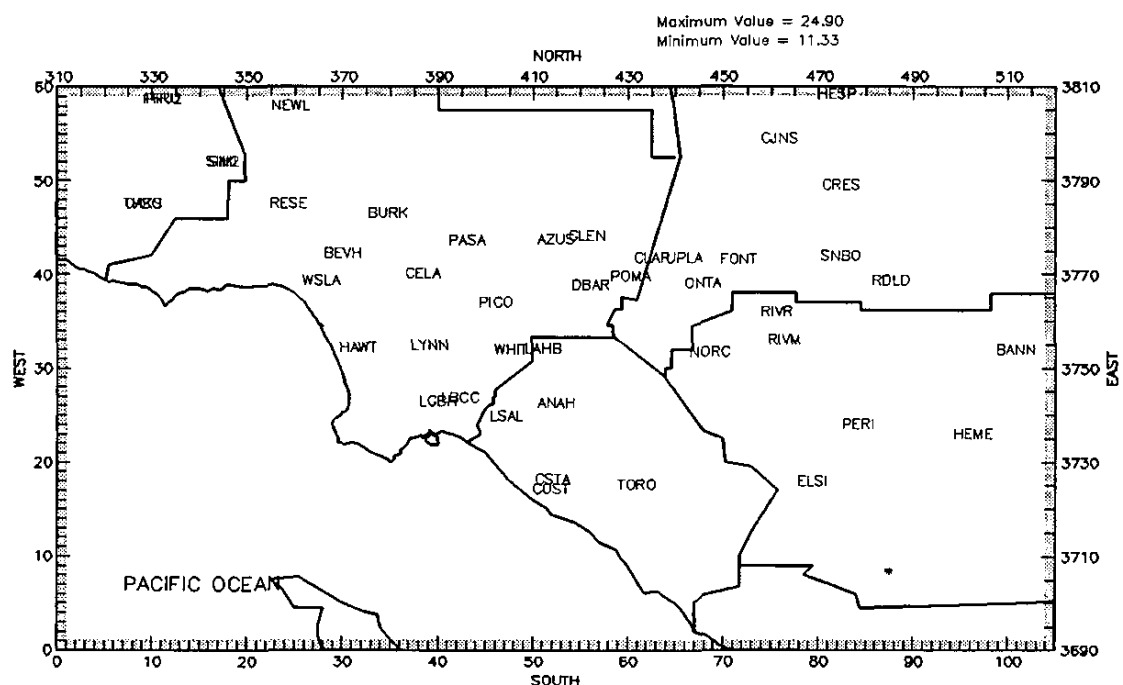


Figure V-11b. Annual average vinyl chloride concentrations simulated for the Basin ($\mu\text{g}/\text{m}^3$).

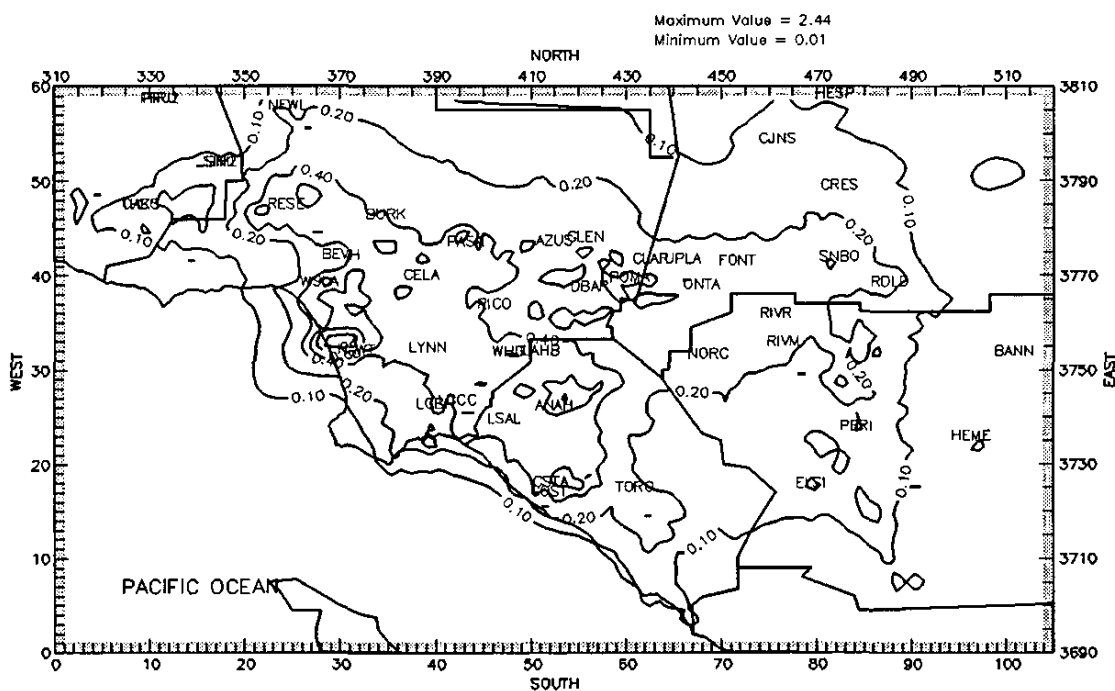


Figure V-11c. Annual average 1,3 butadiene concentrations simulated for the Basin ($\mu\text{g}/\text{m}^3$).

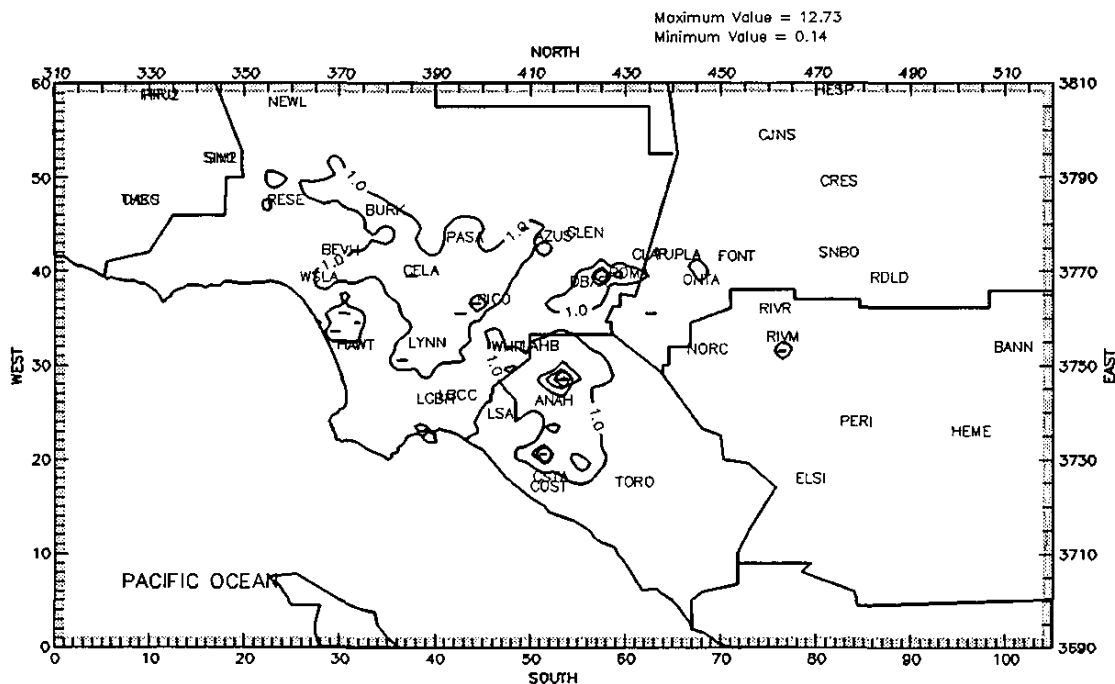


Figure V-11d. Annual average methylene chloride concentrations simulated for the Basin ($\mu\text{g}/\text{m}^3$).

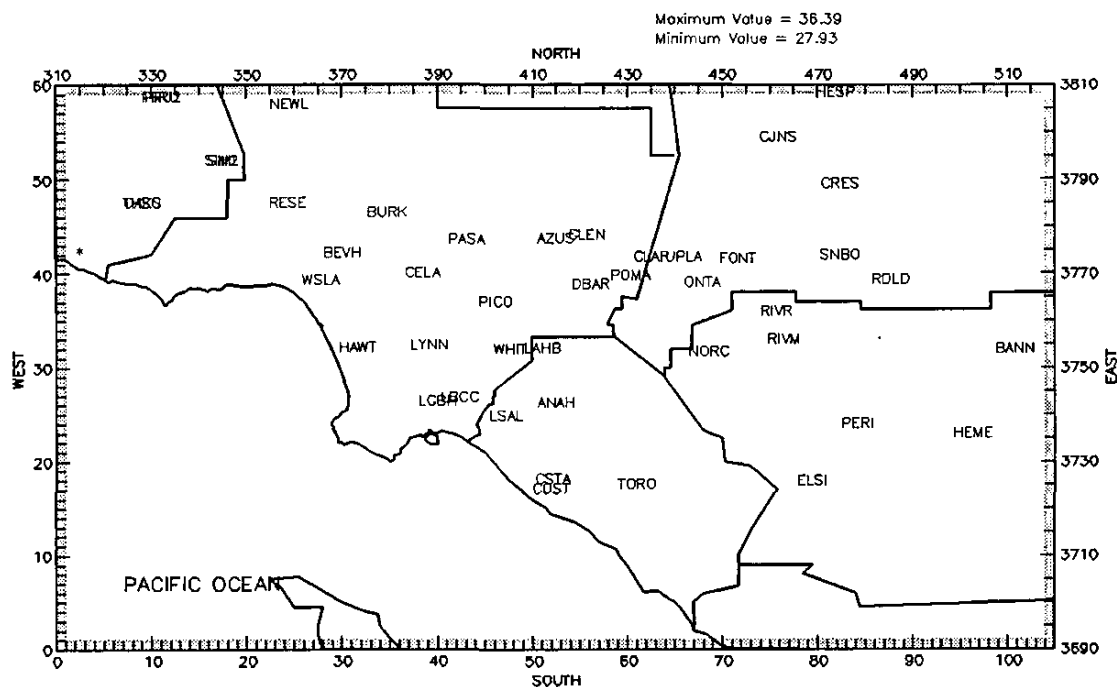


Figure V-11e. Annual average 1,1 dichloroethane concentrations simulated for the Basin ($\mu\text{g}/\text{m}^3$).

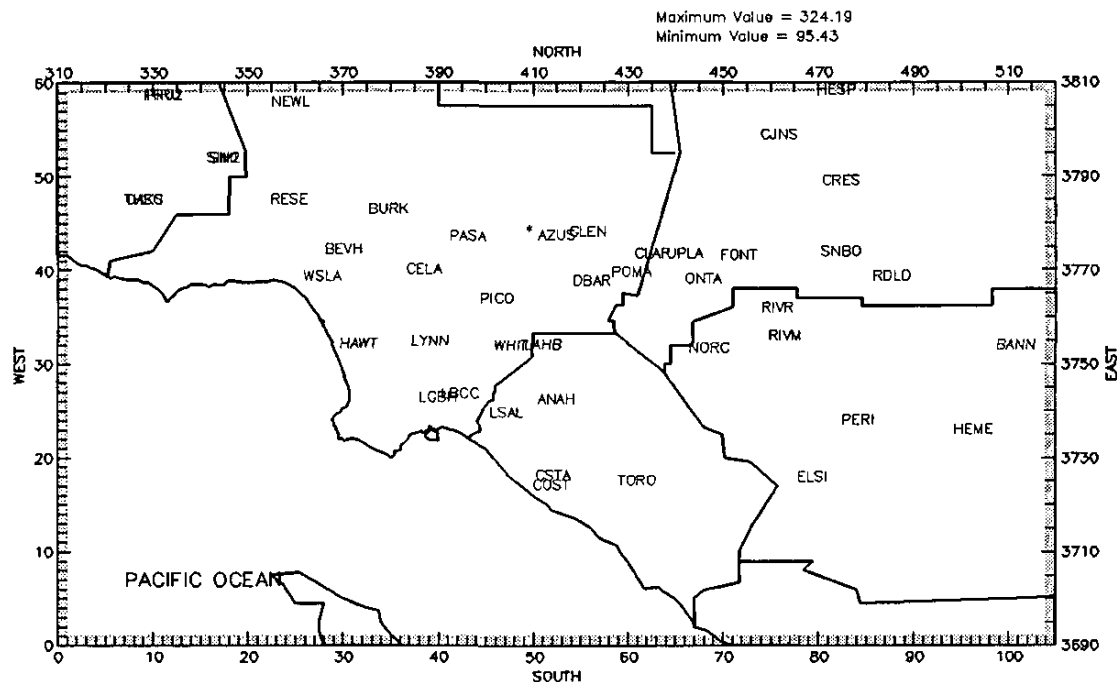


Figure V-11f. Annual average chloroform concentrations simulated for the Basin ($\mu\text{g}/\text{m}^3$).

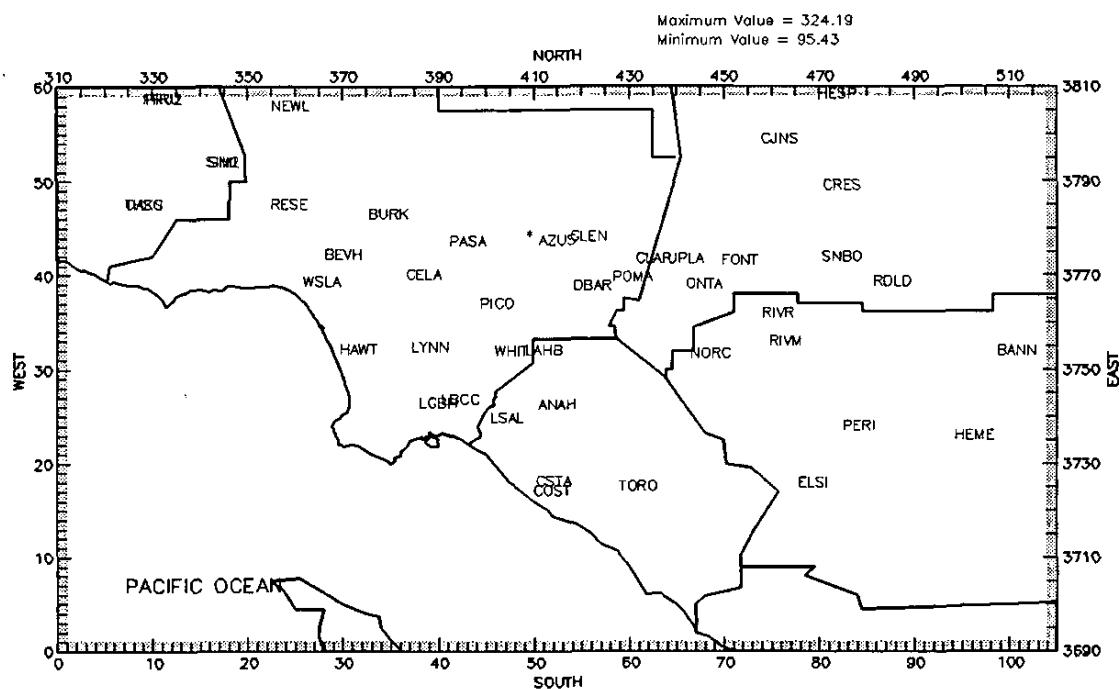


Figure V-11g. Annual average ethylene dichloride concentrations simulated for the Basin ($\mu\text{g}/\text{m}^3$).

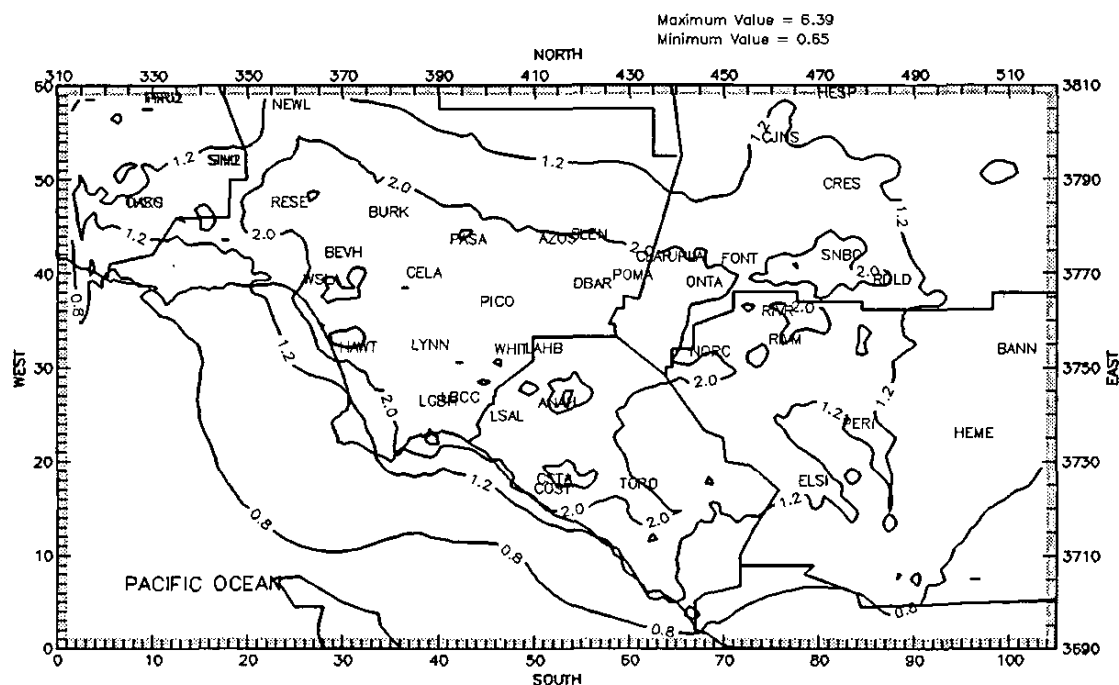


Figure V-11h. Annual average benzene concentrations simulated for the Basin ($\mu\text{g}/\text{m}^3$).

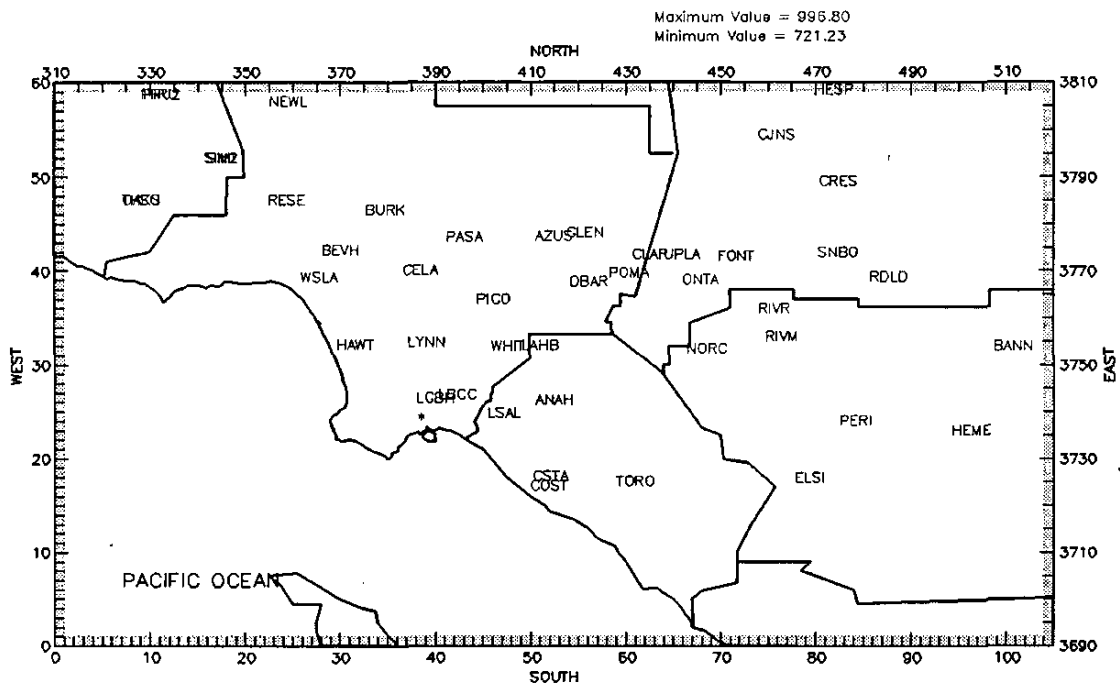


Figure V-11i. Annual average carbon tetrachloride concentrations simulated for the Basin ($\mu\text{g}/\text{m}^3$).

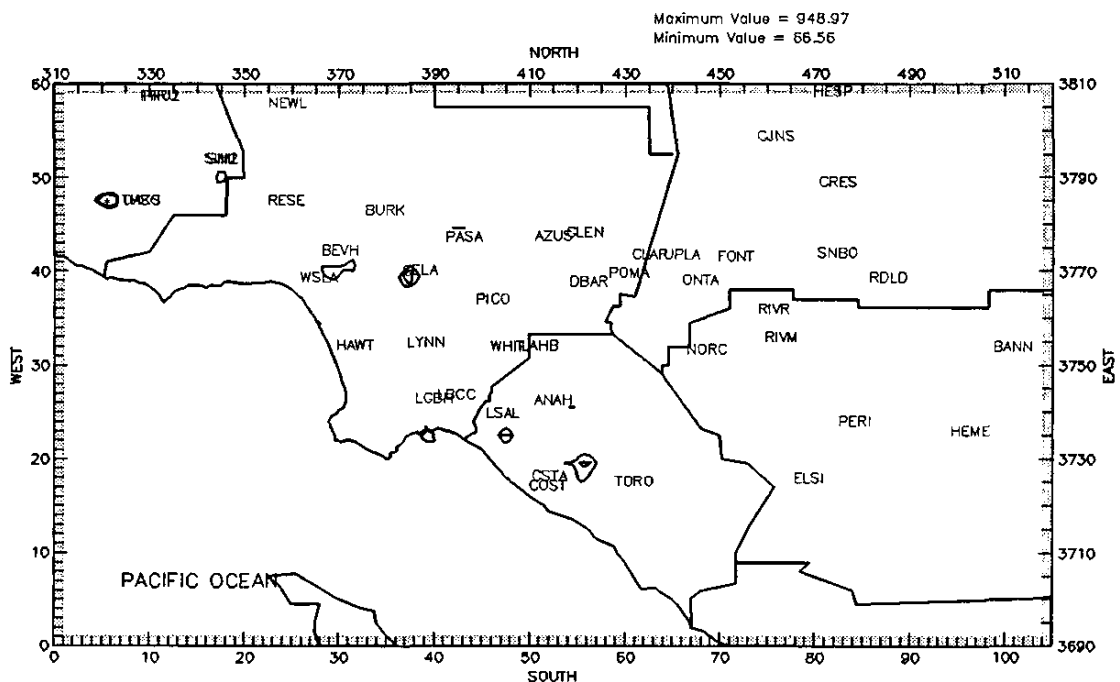


Figure V-11j. Annual average trichloroethene concentrations simulated for the Basin ($\mu\text{g}/\text{m}^3$).

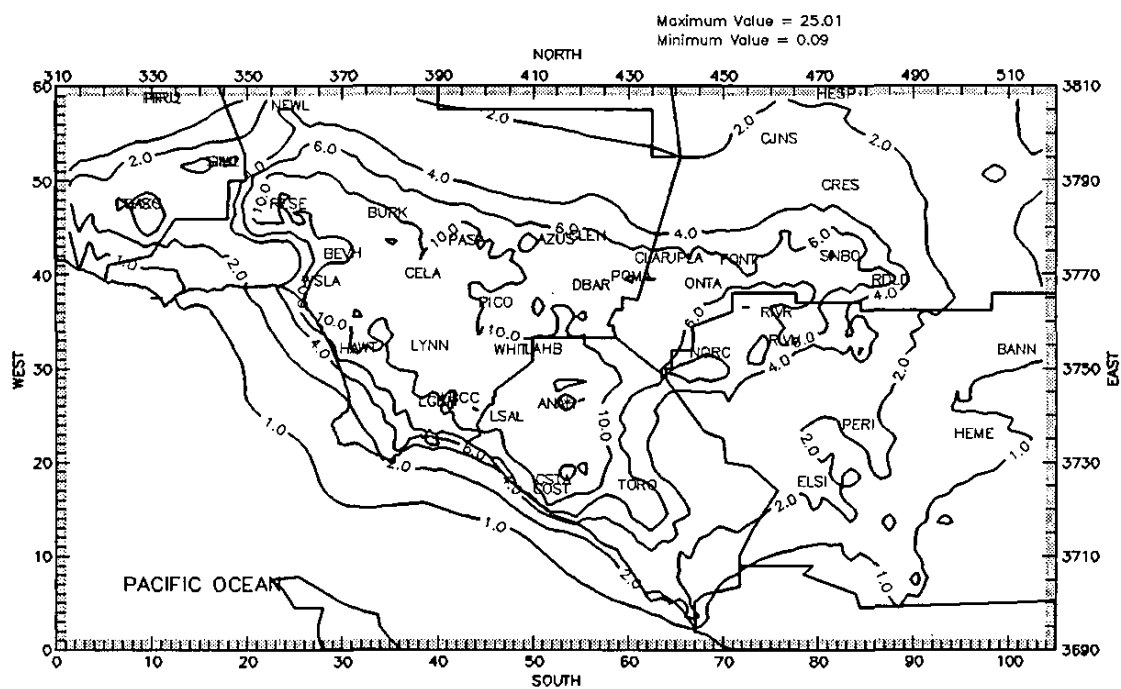


Figure V-11k. Annual average toluene concentrations simulated for the Basin ($\mu\text{g}/\text{m}^3$).

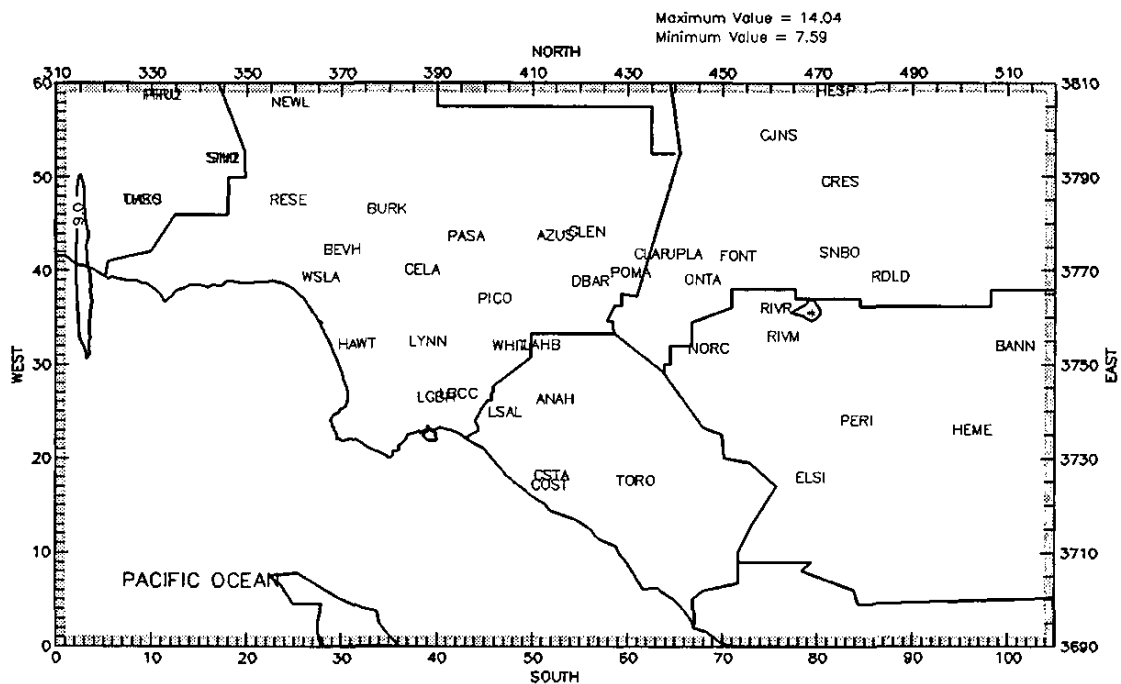


Figure V-11l. Annual average ethylene dibromide concentrations simulated for the Basin ($\mu\text{g}/\text{m}^3$).

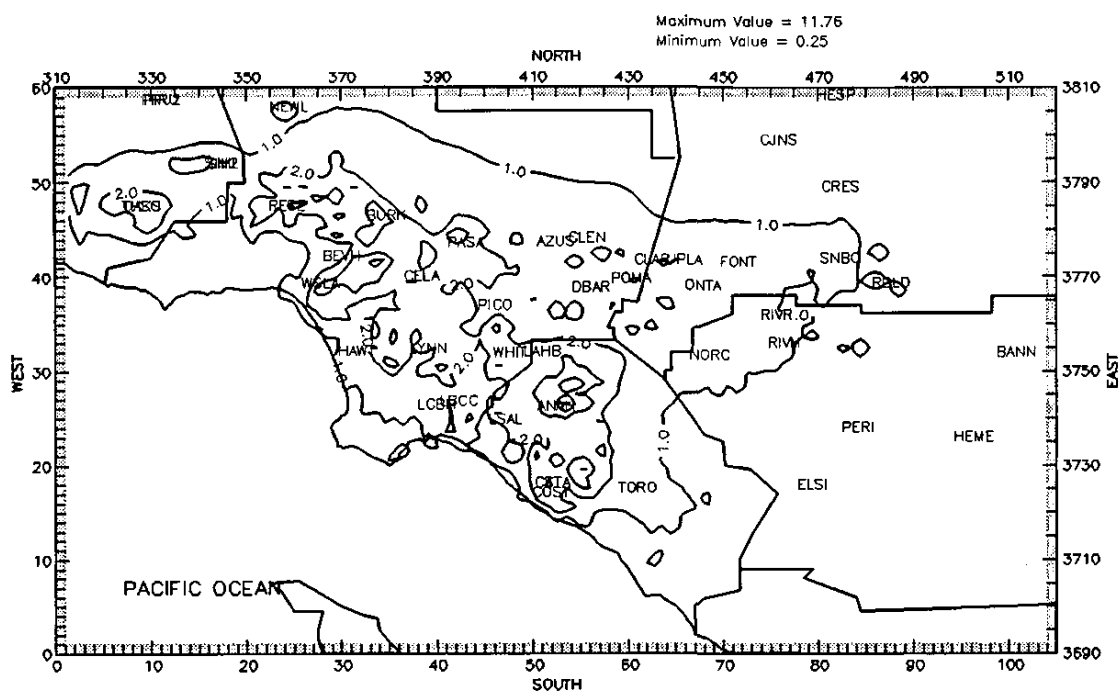


Figure V-11m. Annual average perchloroethylene concentrations simulated for the Basin ($\mu\text{g}/\text{m}^3$).

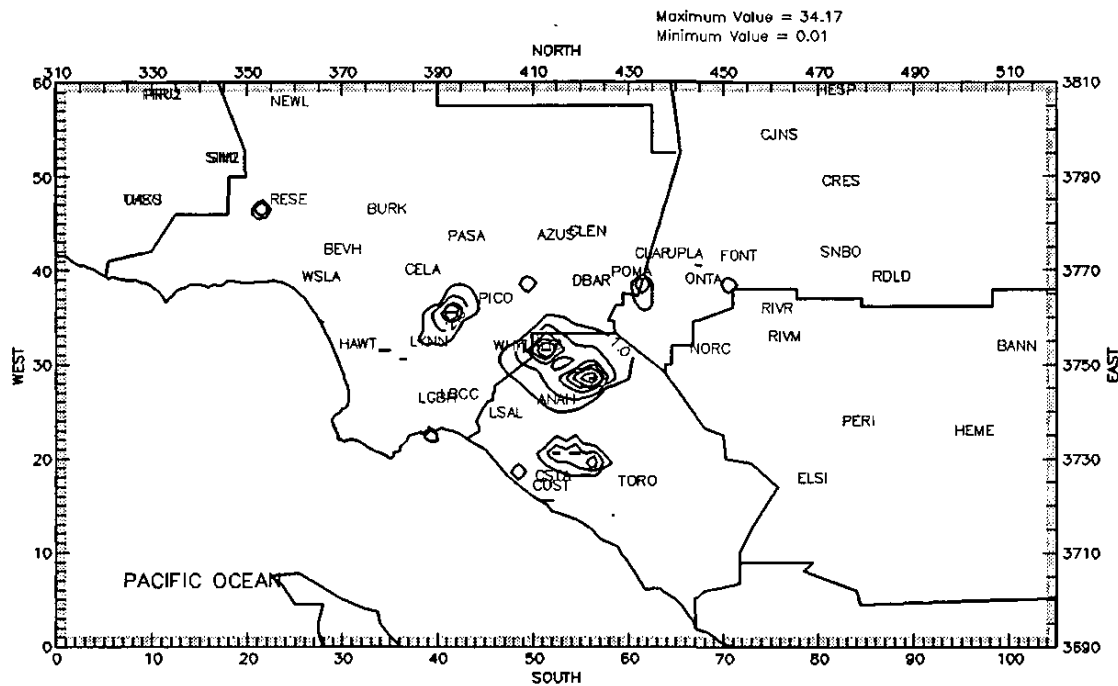


Figure V-11n. Annual average styrene concentrations simulated for the Basin ($\mu\text{g}/\text{m}^3$).

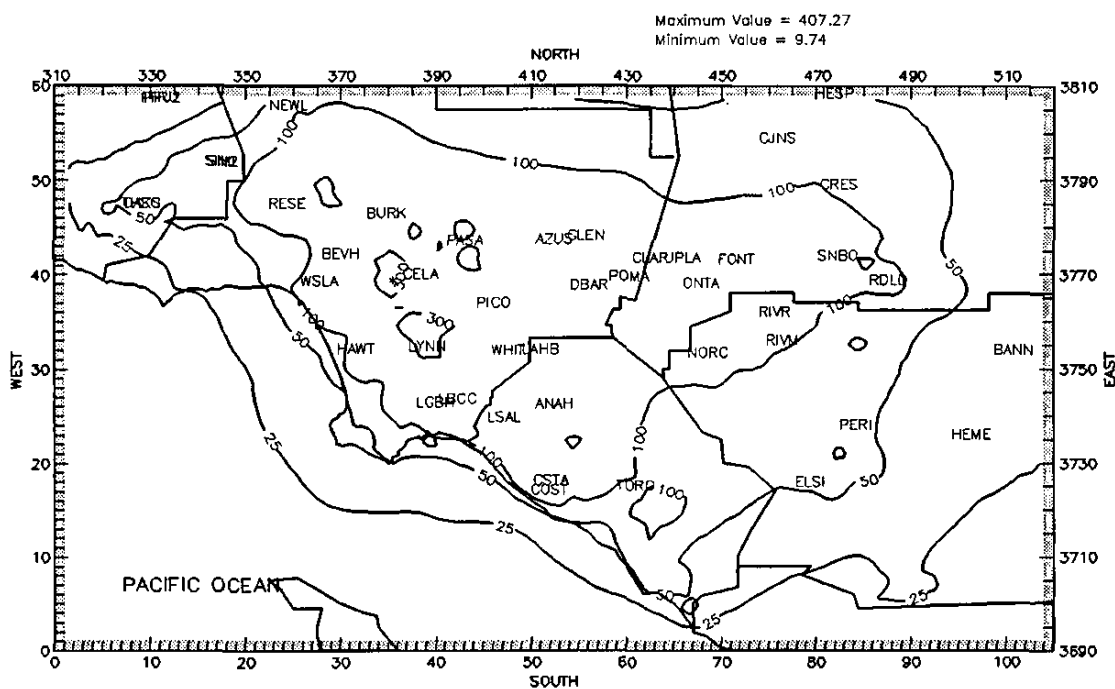


Figure V-11o. Annual average p-dichlorobenzene concentrations simulated for the Basin ($\mu\text{g}/\text{m}^3$).

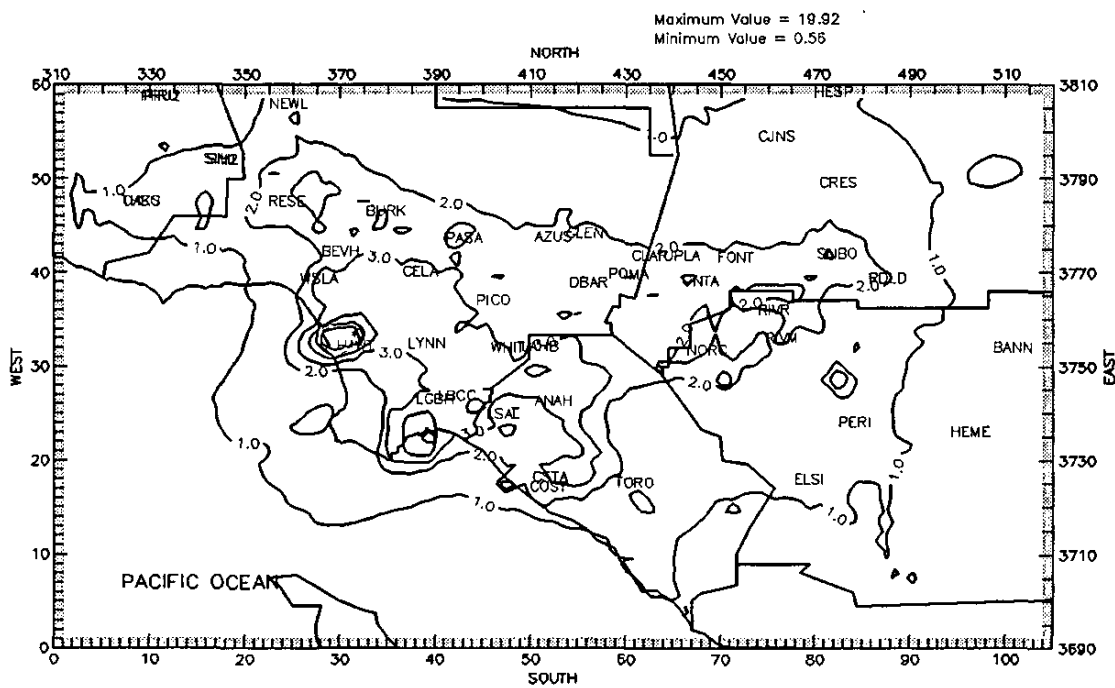


Figure V-11p. Annual average formaldehyde concentrations simulated for the Basin ($\mu\text{g}/\text{m}^3$).

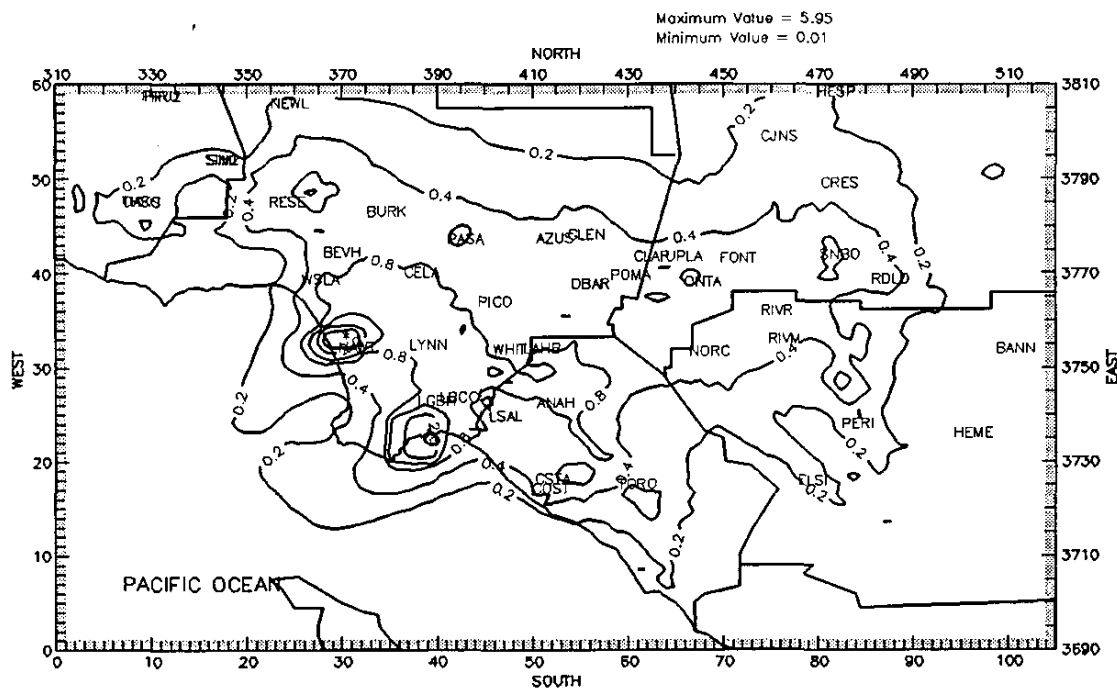


Figure V-11q. Annual average acetaldehyde concentrations simulated for the Basin ($\mu\text{g}/\text{m}^3$).

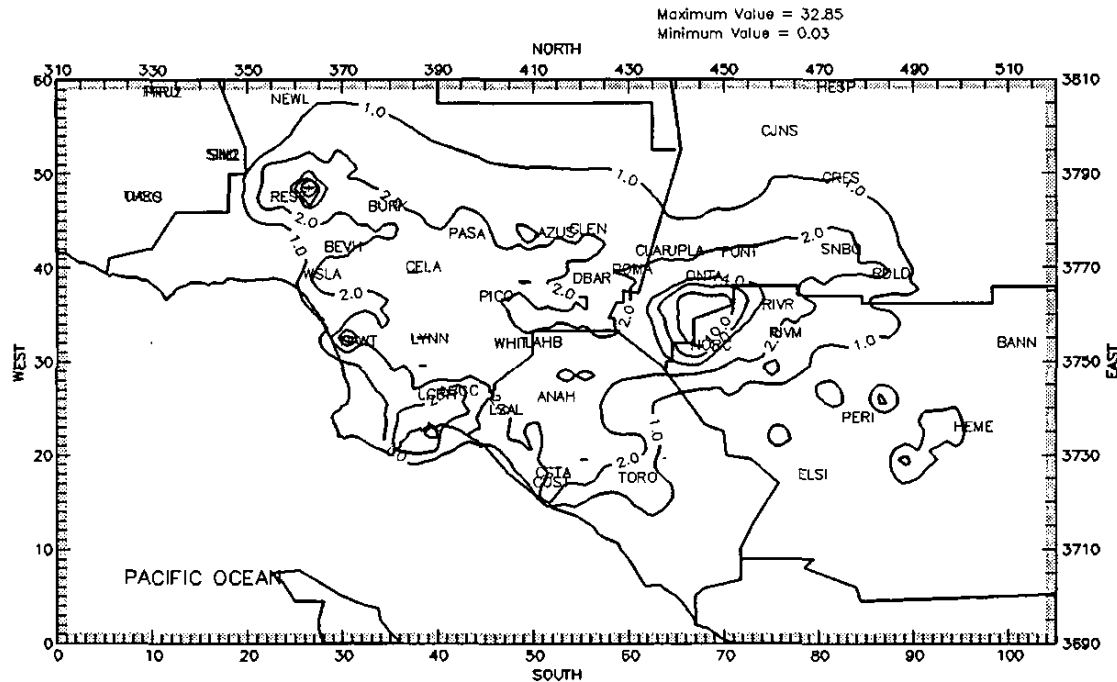


Figure V-11r. Annual average acetone concentrations simulated for the Basin ($\mu\text{g}/\text{m}^3$).

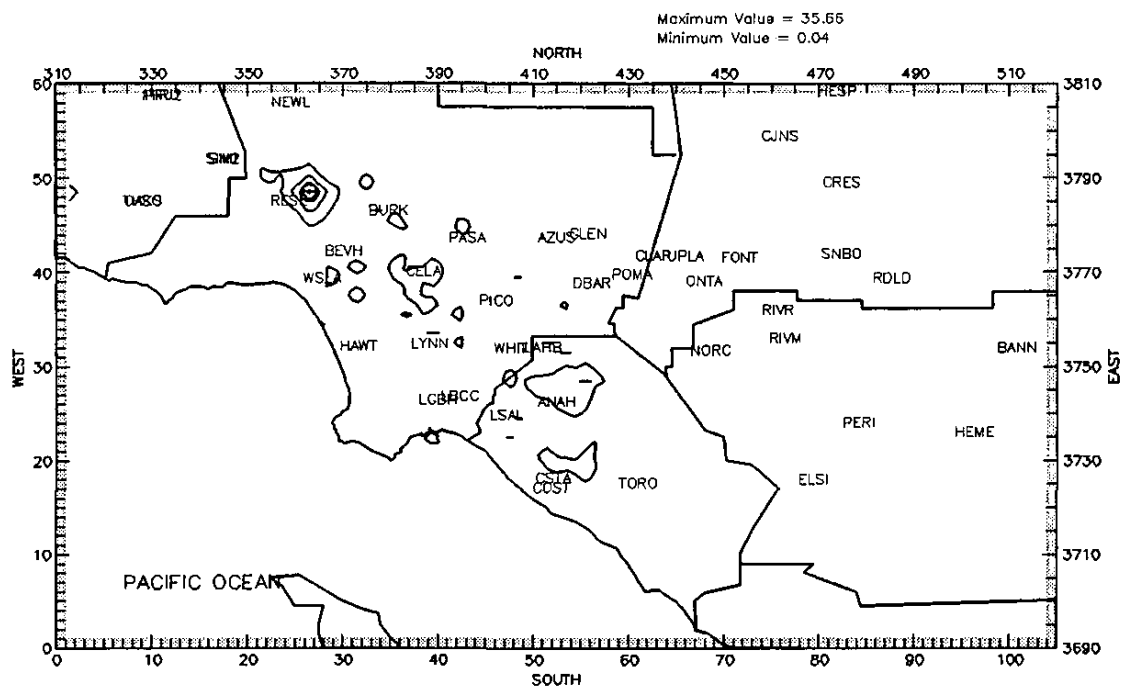


Figure V-11s. Annual average methyl ethyl ketone concentrations simulated for the Basin ($\mu\text{g}/\text{m}^3$).

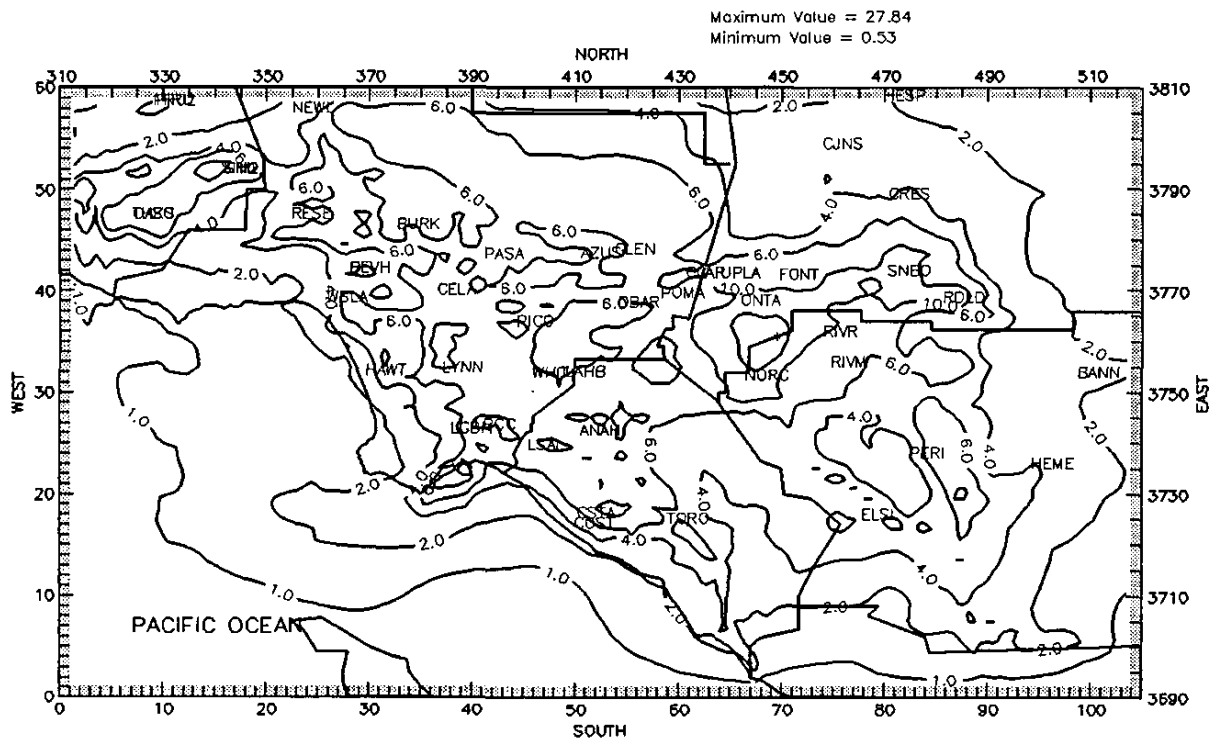


Figure V-11t. Annual average organic carbon concentrations simulated for the Basin ($\mu\text{g}/\text{m}^3$).

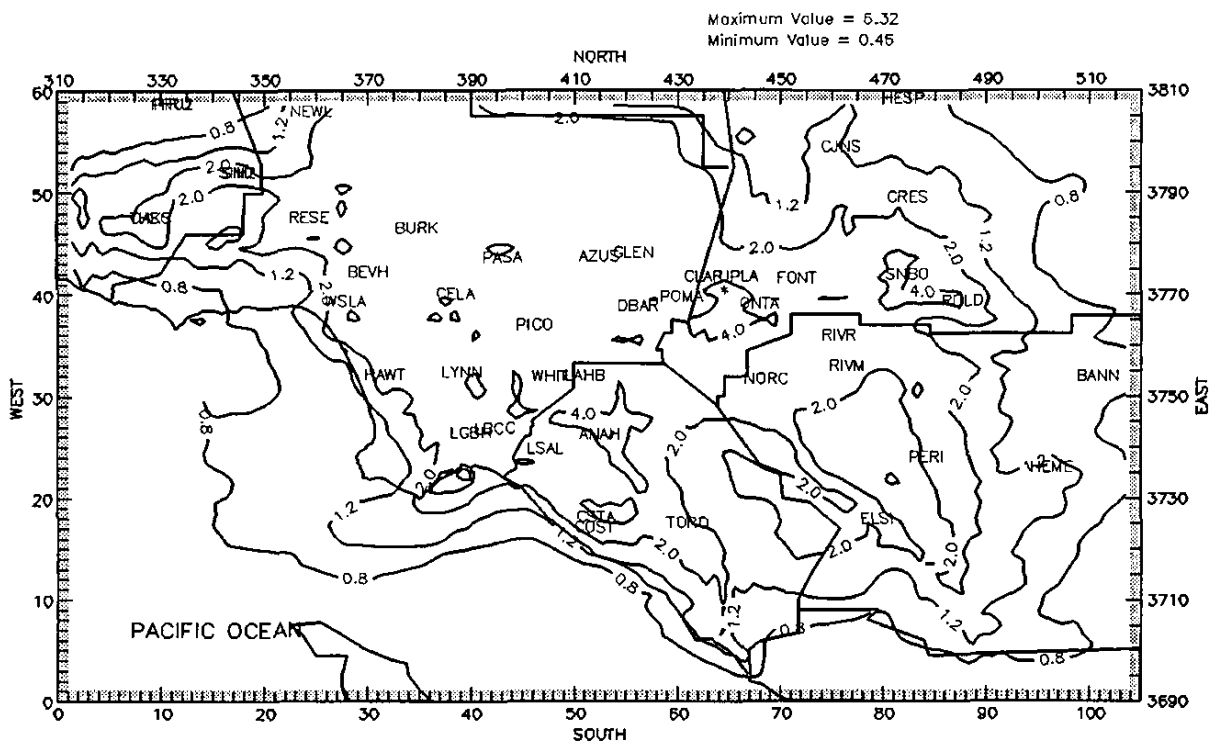


Figure V-11u. Annual average elemental carbon concentrations simulated for the Basin ($\mu\text{g}/\text{m}^3$).

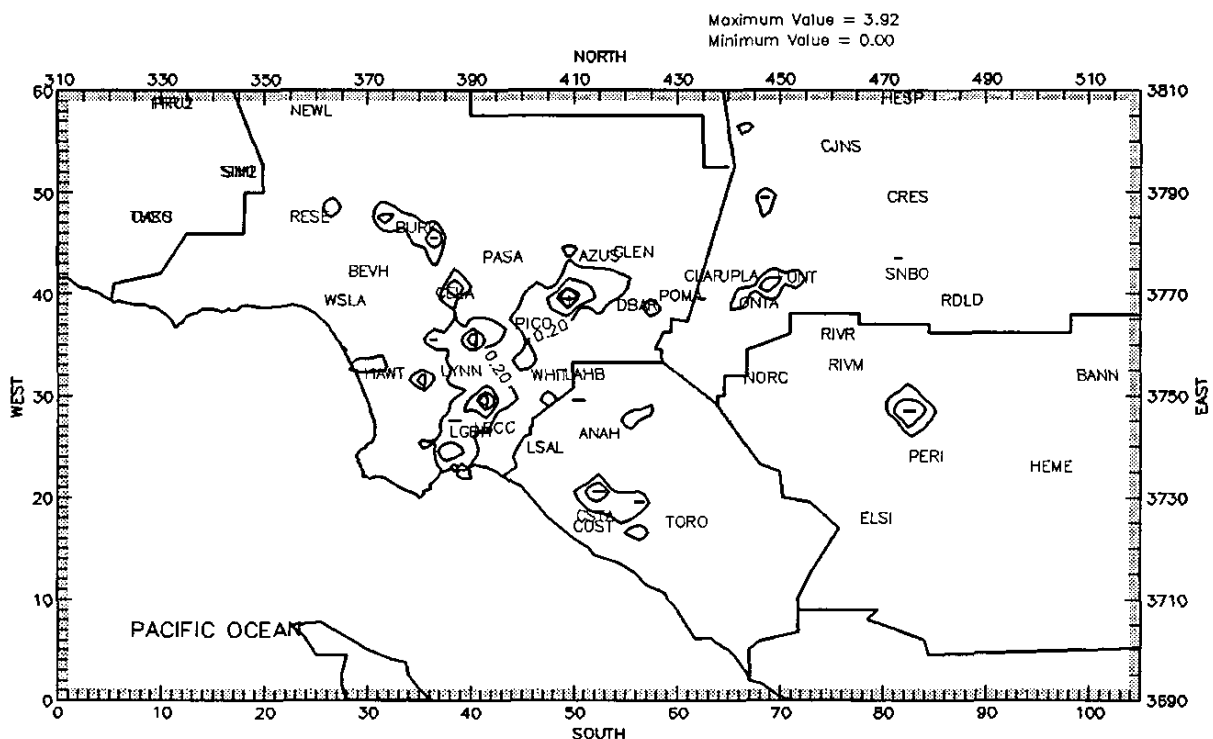


Figure V-11v. Annual average hexavalent chromium concentrations simulated for the Basin (ng/m^3).

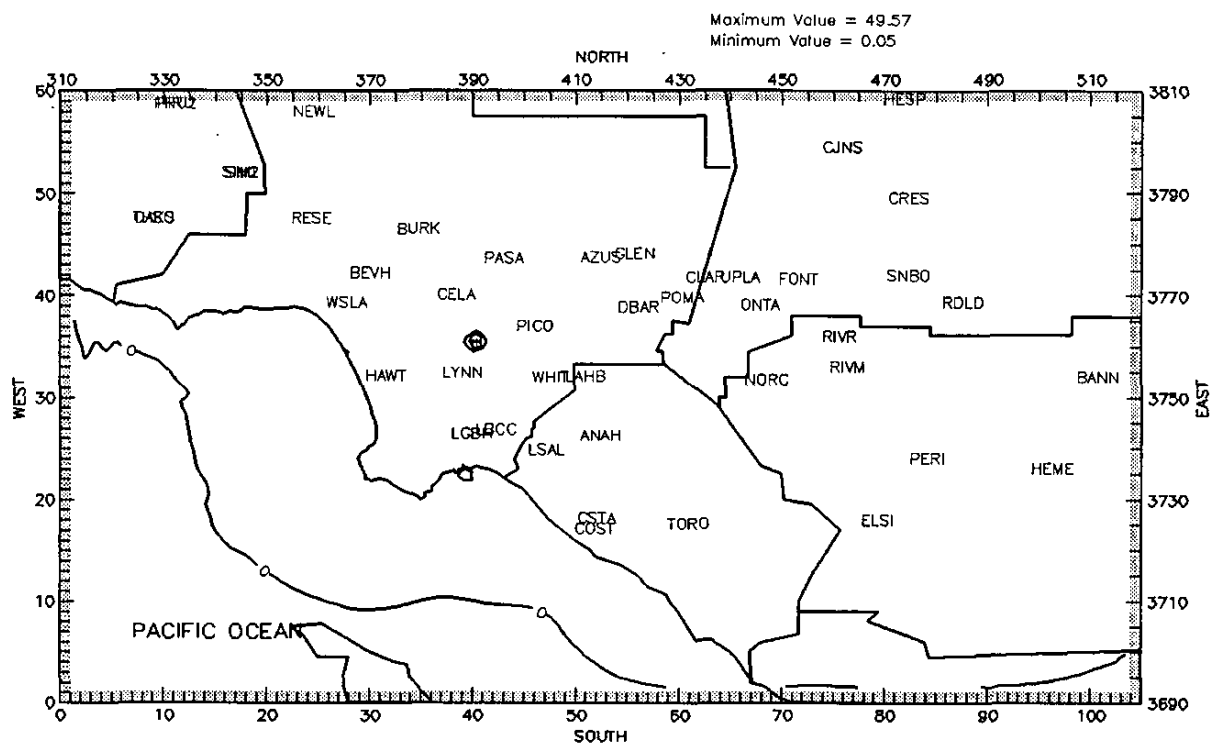


Figure V-11w. Annual average arsenic concentrations simulated for the Basin ($\mu\text{g}/\text{m}^3$).

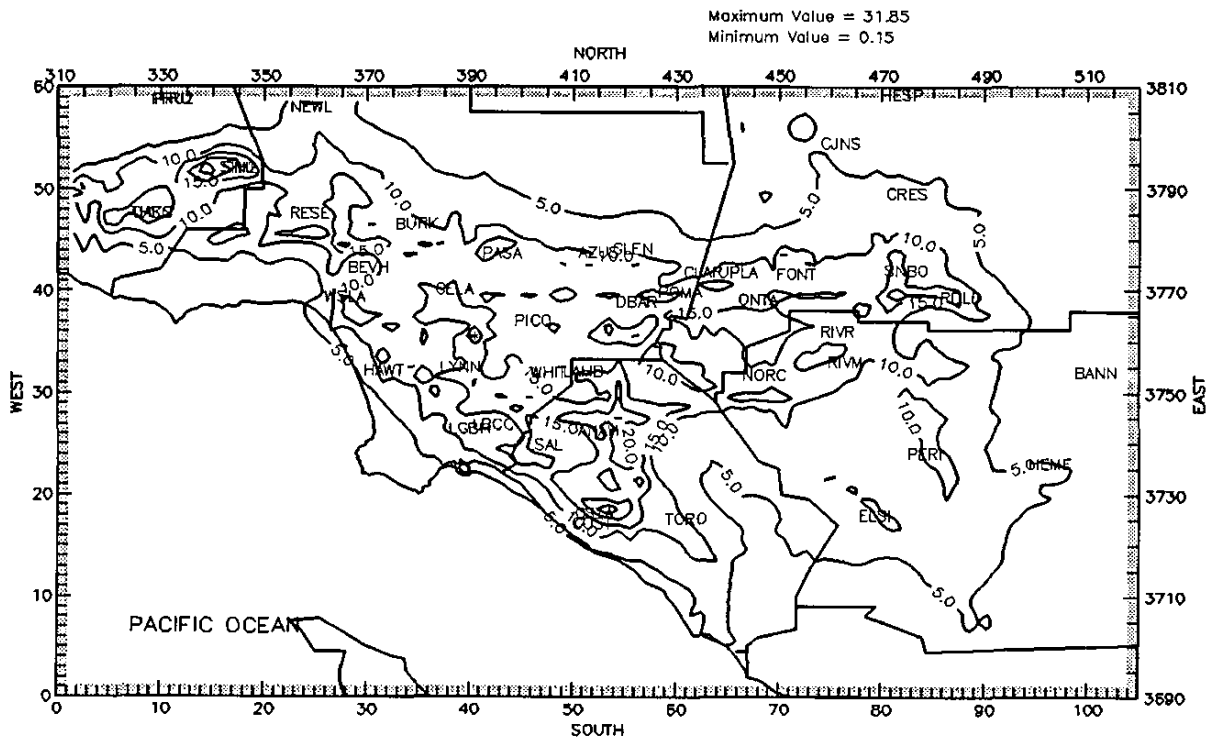


Figure V-11x. Annual average chromium concentrations simulated for the Basin ($\mu\text{g}/\text{m}^3$).

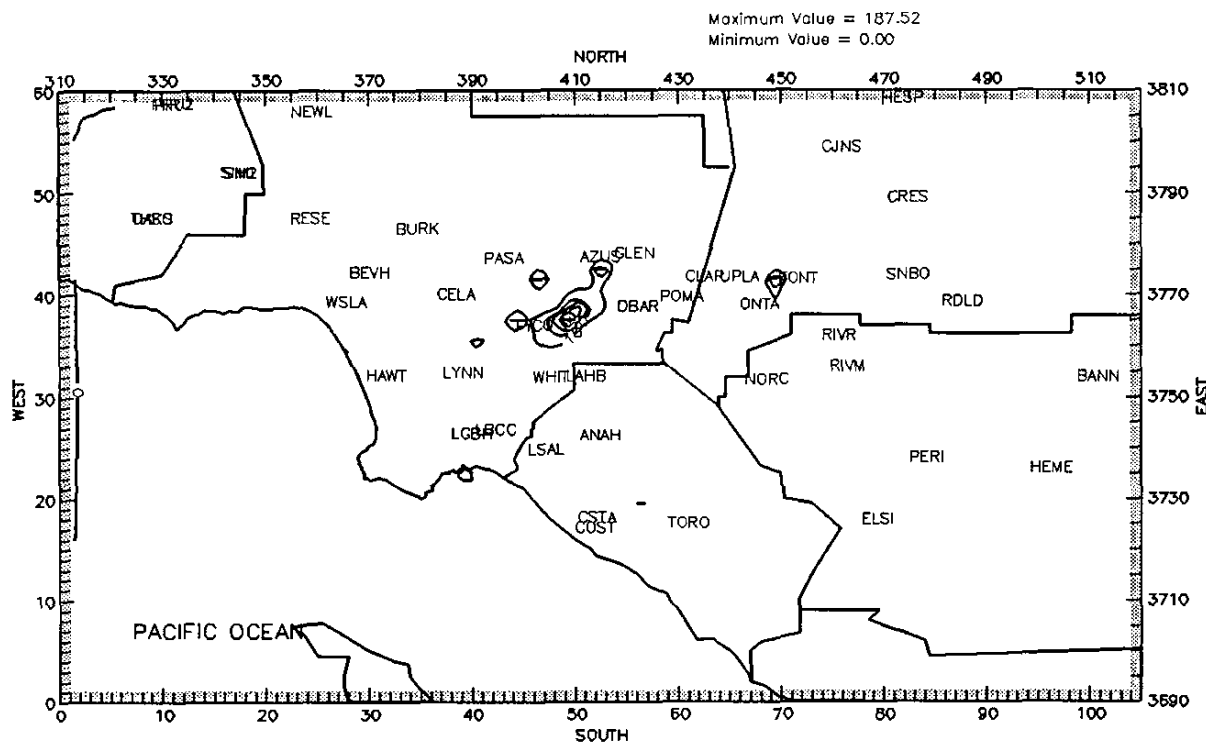


Figure V-11y. Annual average point source lead concentrations simulated for the Basin (ng/m^3).

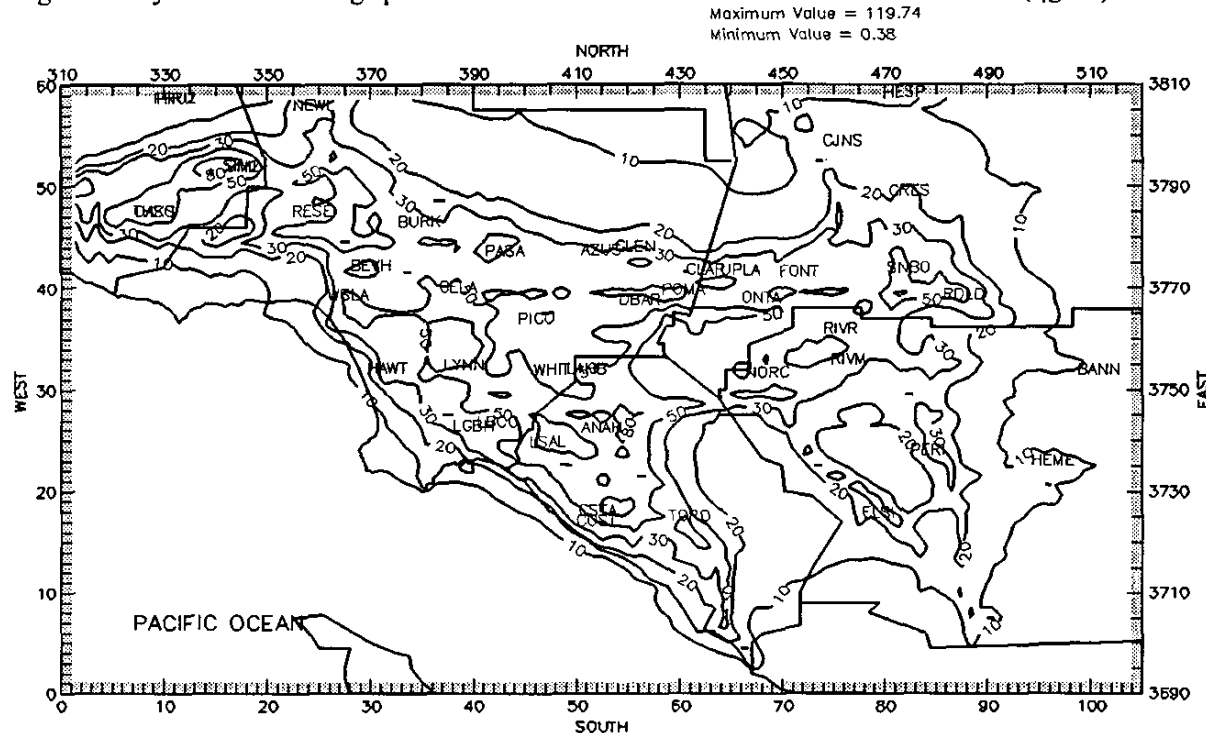


Figure V-11z. Annual average all non-point source lead concentrations simulated for the Basin (ng/m^3).

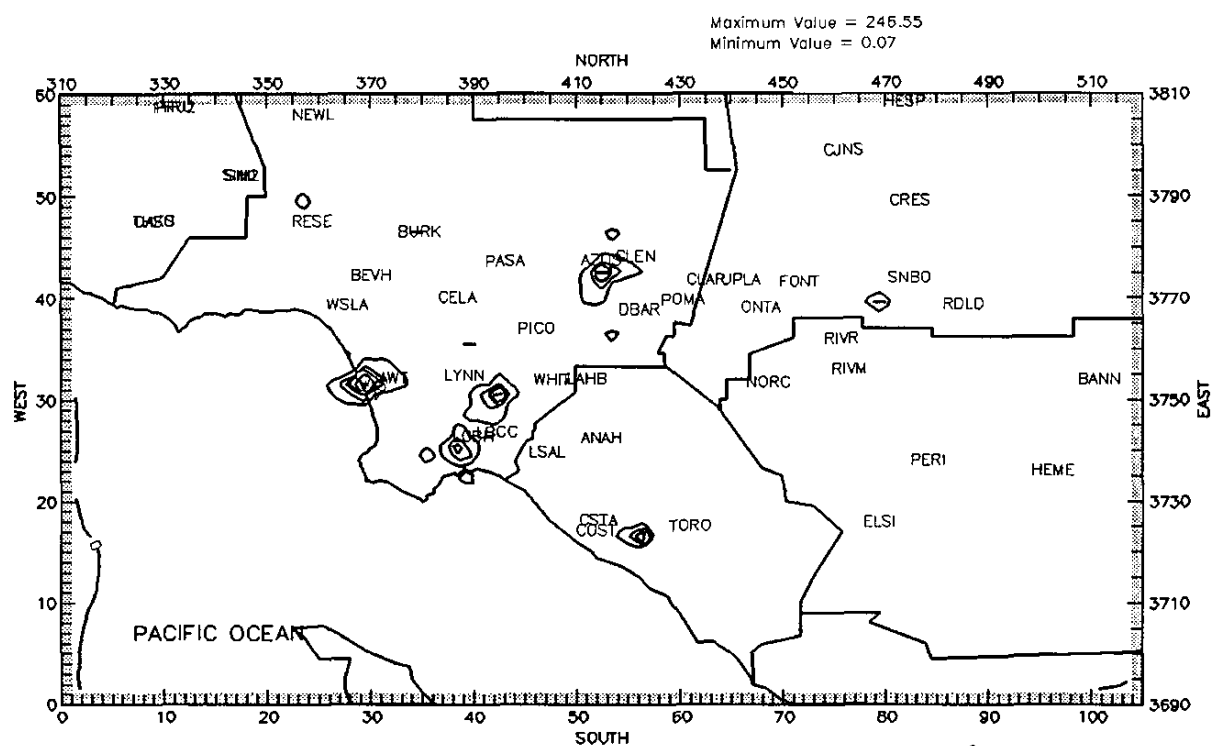


Figure V-11aa. Annual average nickel concentrations simulated for the Basin (ng/m^3).

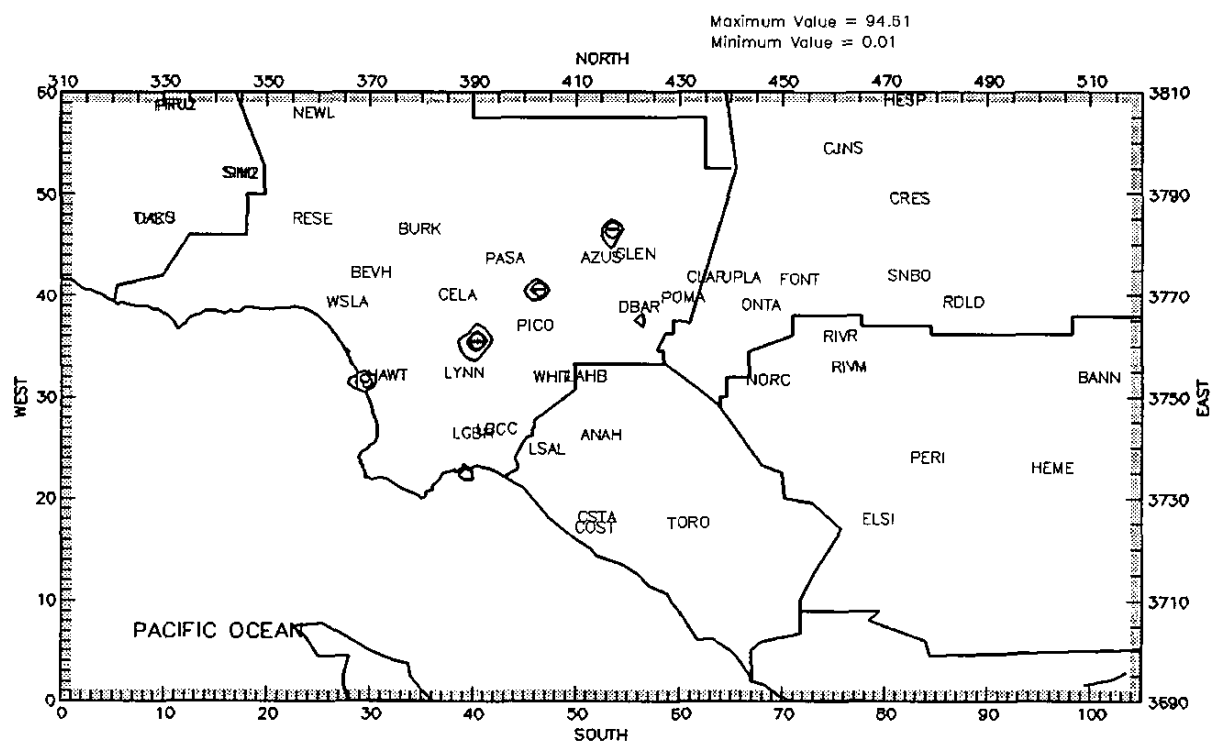


Figure V-11ab. Annual average selenium concentrations simulated for the Basin (ng/m^3).

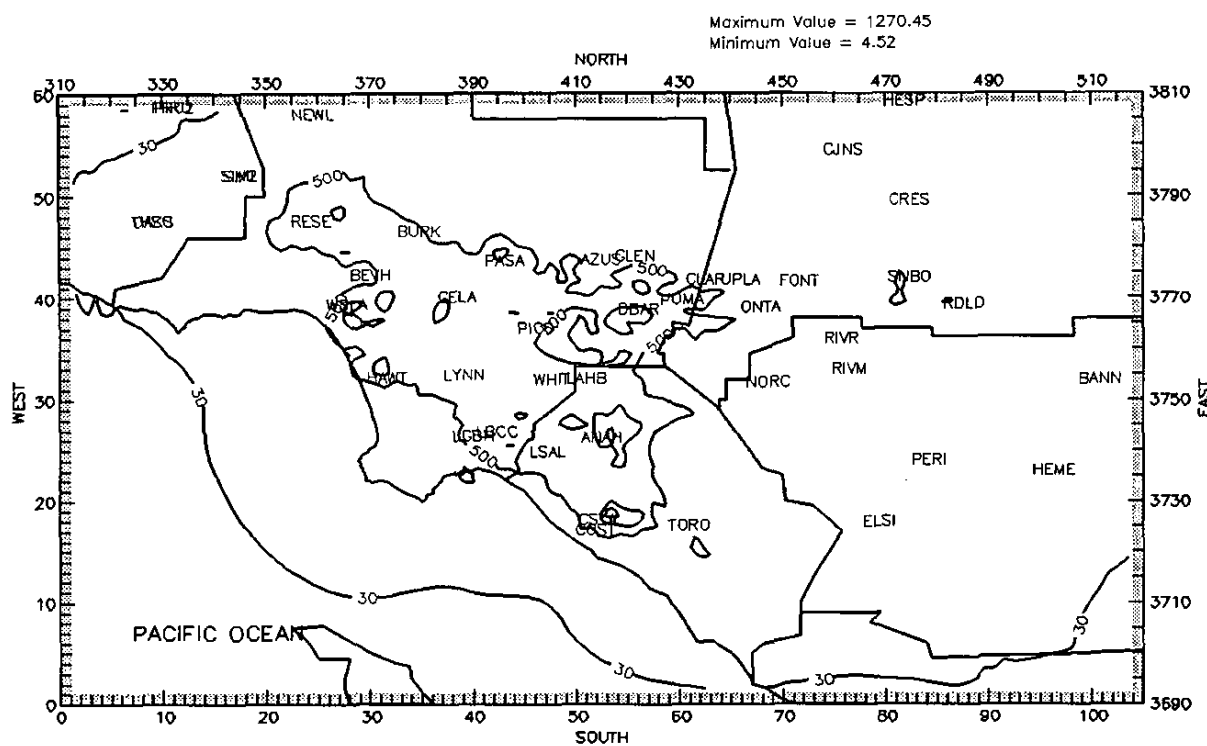


Figure V-11ac. Annual average cadmium concentrations simulated for the Basin (ng/m^3).

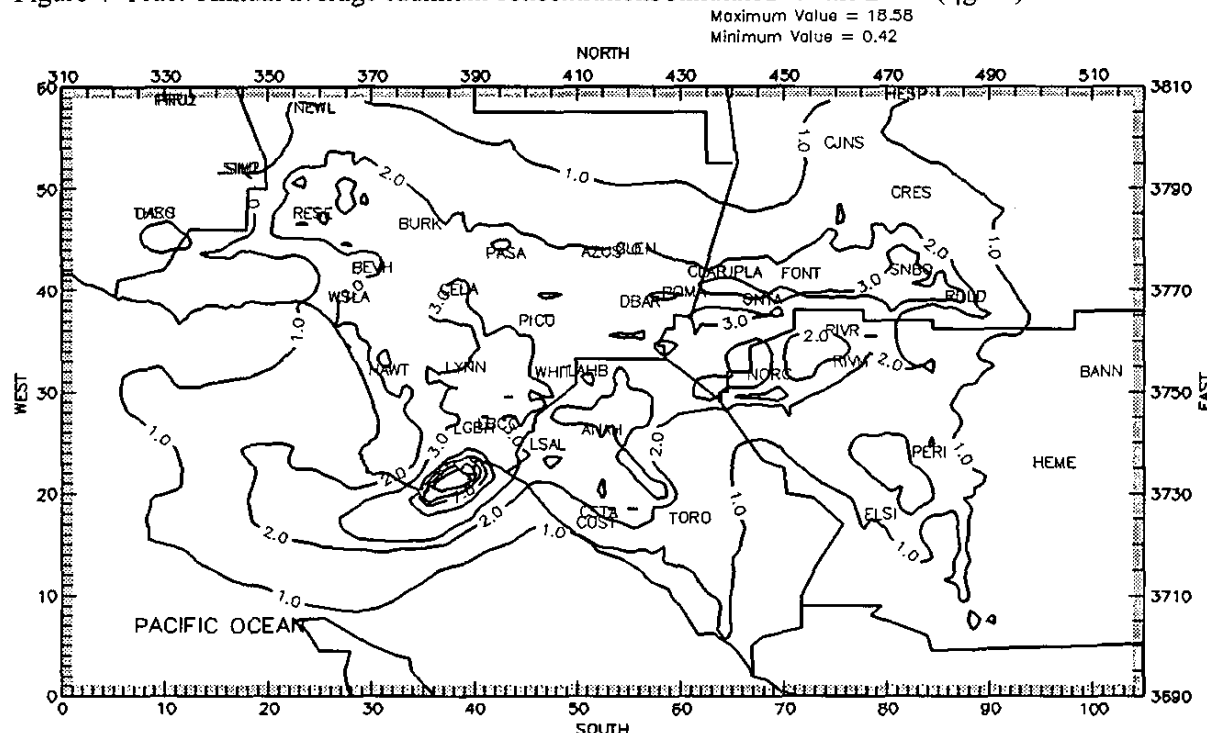


Figure V-11ad. Annual average diesel particulate concentrations simulated for the Basin ($\mu\text{g}/\text{m}^3$).

Risk Assessment Calculations

Based on the spatial concentration fields estimated by the simulation models, risk estimates can be calculated for each grid cell of the modeling domain. There are two approaches for calculating risk [one is weighed by population, the other is using the model estimated concentrations and simply multiplying by the compound's unit risk factor (URF)]. The population weighed risk calculation is more appropriate. However, this assumes that each person is outdoors all of the time. The second approach does not assume any population in the calculation and is more appropriate when comparing with monitored concentrations. As such, both sets of numbers are provided.

Figure V-12 shows the model estimated risk at each grid cell for all modeled compounds with an associated URF. In addition to the total model estimated risk, Figure V-13 shows the risk estimated excluding diesel sources. The cumulative risk averaged over the four counties of the South Coast Air Basin is about 980 in one million when diesel sources are included and about 260 in one million when diesel sources are excluded.

Table V-7 shows the risk for the four counties in the South Coast Air Basin. The average risk levels ranges from 619 to about 1048 in one million with an overall Basin average of about 981 in one million. As seen from Table V-7, Los Angeles County has the highest risk levels followed by Orange and San Bernardino counties. The lowest average risk is estimated in Riverside County.

To compare with the network average risk calculated based on concentrations measured at the ten MATES-II sites modeled concentrations in the grid cells of each of the ten sites are multiplied by their associated URFs (see Table V-8). For comparison purposes to the monitored values, an eight-site average is also provided in Table V-8. (The Wilmington and Compton sites were not included in the average because elemental carbon was not measured at either site). The overall average risk calculated for the ten locations is about 1200 in one million (1182 – for the eight-site average and 1230 for the ten-site average). This value is compared to the eight-site network average value of 1400 in one million based on measured concentrations. This analysis also shows that the average basin risk (determined from the model simulations) may be 16 percent lower than the average risk based on the actual monitoring site data.

Table V-9 summarizes the comparative risk estimated by the annual UAM simulation for the fourteen-microscale monitoring locations where short-term monitoring was conducted. Since the monitoring conducted at the microscale sites was typically of the duration of one month, no attempt was made to estimate annual risk based on the measured data. However, the simulation provides a general profile of the risk estimated for the grid in which the fourteen monitoring sites were located. In general, the fourteen-site average modeled risk was essentially equivalent to the average estimated for the ten fixed sites. In addition, as with the modeled risk at the ten MATES II sites, diesel particulate

accounts for seventy five percent of the total risk, with relative contributions from benzene, 1,3 butadiene and others being approximately the same as the ten-site analysis. Moreover, there exists a variation in the estimated risk across the Basin and within the counties.

This is clearly evident in Orange County where risk ranges from a low of 752 in one million at Costa Mesa to a high of 1521 at the Anaheim microscale site. The spatial variation in risk is highlighted by the differential risk estimated for the Anaheim MATES-II fixed site (approximately 1300 in one million) and the risk calculated for the microscale site. Spatial variations are also seen throughout Los Angeles County where the risk at the coastal Torrance was estimated to be 795 in one million, while at Van Nuys, in the San Fernando Valley was modeled at 1389 in one million. Again, the spatial variation is demonstrated by a risk of 975 in one million at Pacoima, another microscale site located in the San Fernando Valley. Estimated risk for the Riverside and San Bernardino microscale sites are close to the fourteen-site average varying only 100 in one million from the mean.

Maximum Value = 5800.21
Minimum Value = 184.94

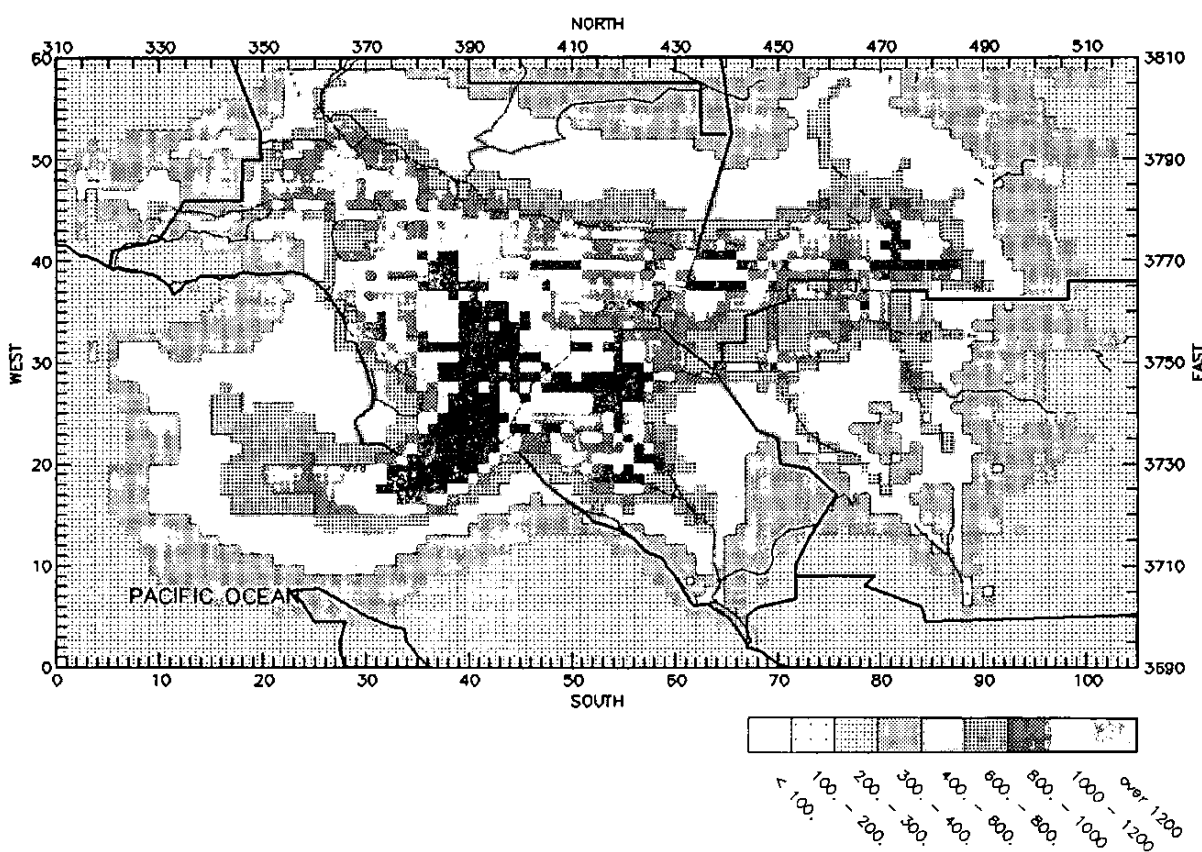


Figure V-12. Model estimated risk for the Basin.
(Number in a million, all sources).

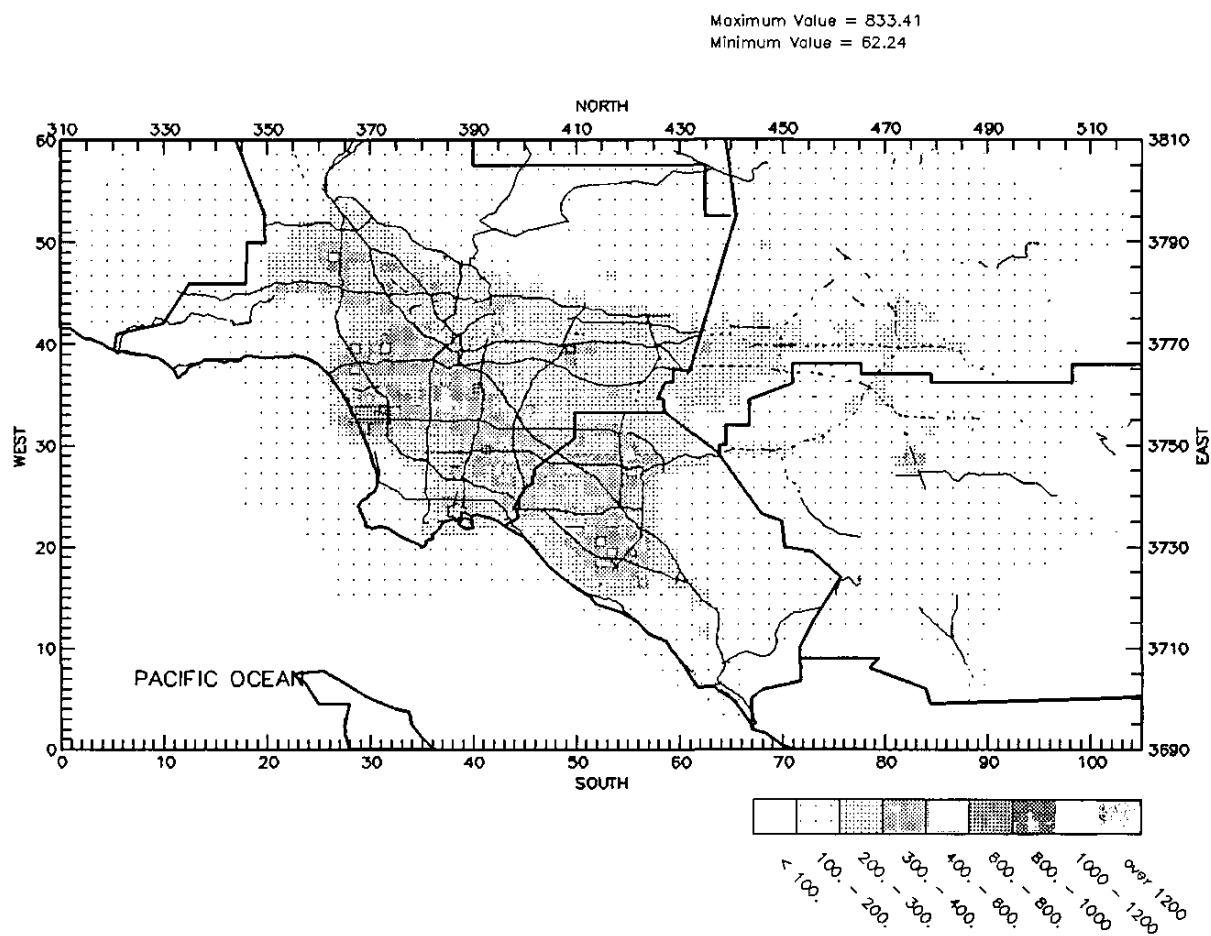


Figure V-13. Model estimated risk for the Basin.
(Number in a million, without diesel sources).

Table V-7. South Coast Air Basin Modeled Risk

	Population	Average Risk (per million)
Los Angeles County	9,305,726	1048
Orange County	2,579,974	940
Riverside County	1,249,554	619
San Bernardino County	1,269,919	926
Basin Total	14,404,993	981

Table V-8. Comparison of the Network Averaged Modeled Risk to Measured Risk at the Ten MATES-II Sites

Location	Benzene	1,3 Butadiene	Other	Diesel	Total
Anaheim	119	87	160	961	1330
Burbank	94	62	162	848	1161
Compton	97	65	146	1001	1302
Fontana	48	20	121	741	939
Huntington Park	89	61	177	875	1195
Downtown L.A.	94	65	170	1182	1505
Long Beach	88	58	138	930	1204
Pico Rivera	77	43	141	872	1131
Rubidoux	57	26	107	786	987
Wilmington	81	46	223	1187	1531
Modeled Average	84	53	155	936	1228
Modeled Average*	83	53	147	898	1181
Monitored Average*	92	118	187	1017	1414

* Eight monitoring site average excluding Wilmington and Compton where elemental carbon was not measured.

Table V-9. Modeled Risk at the Fourteen MATES-II Microscale Monitoring Sites

Location	Benzene	1,3 Butadiene	Other	Diesel	Total
Anaheim	115	82	161	1163	1521
Boyle Heights	95	69	146	999	1309
Corona	66	34	112	1006	1218
Costa Mesa	98	59	123	472	752
Hawthorne	143	346	262	995	1746
Montclair	69	39	136	1148	1392
Norwalk	104	70	149	1089	1412
Pacoima	67	35	119	696	917
Rialto	58	31	112	948	1149
Riverside	66	31	111	901	1109
San Pedro	55	26	109	1122	1312
South El Monte	86	54	157	929	1226
Torrance	55	31	101	608	795
Van Nuys	118	103	288	880	1389
Modeled Average	85	72	149	925	1231

Conclusion

Overall, the UAM and UAM-TOX model perform within ± 50 to 60 percent of measured annual values. However, the model performance varies significantly on short-term averaged concentrations. In addition, given that mobile source emissions are most likely underestimated with the current ARB mobile source emission factor models, the model performance would improve somewhat with the latest versions of the mobile source models.

The spatial concentration fields show that higher concentrations generally occur near their emission sources. Higher concentrations of compounds that are emitted primarily from stationary and area sources tend to be highest within a few kilometers from the source location. Mobile source related compounds such as benzene and 1,3 butadiene tend to be generally high throughout the Basin. However, spatial variations are estimated by the models with higher concentrations occurring along freeway corridors and junctions. In addition, higher levels of mobile source related compounds are estimated near major mobile source activities such as airports and other areas with major industrial activities such as south central Los Angeles County, and the industrial areas of Orange, Riverside, and San Bernardino counties.

References

- DeMarrias, G.A., G.C. Holzworth, and C.H. Hosler. 1965, "Technical Report No. 54, Meteorological Summaries Pertinent to Atmospheric Transport and Dispersion Over Southern California" U.S. Weather Bureau, Department of Commerce, Washington D.C.
- Douglas, S.G., R.C. Kessler, and E. Carr. 1990. "User's Guide for the Urban Airshed Model. Volume III: User's Manual for the Diagnostic Wind Model." EPA Publication No. EPA-450/4-90-007C. U.S. EPA, Research Triangle Park, NC.
- U.S. EPA. 1995. A User's Guide for the CALMET Meteorological Model, EPA-454/B-95-002, U.S. EPA, OAQPS, Research Triangle Park, NC.